Universidade de Aveiro Departamento de Química
2017

TÂNIA EREIRA SINTRA

SÍNTESE DE LÍQUIDOS IÓNICOS MAIS BENIGNOS PARA APLICAÇÕES ESPECÍFICAS

SYNTHESIS OF MORE BENIGN IONIC LIQUIDS FOR SPECIFIC APPLICATIONS

Universidade de Aveiro Departamento de Química
2017

TÂNIA EREIRA SINTRA

SÍNTESE DE LÍQUIDOS IÓNICOS MAIS BENIGNOS PARA APLICAÇÕES ESPECÍFICAS

SYNTHESIS OF MORE BENIGN IONIC LIQUIDS FOR SPECIFIC APPLICATIONS

Tese apresentada à Universidade de Aveiro para cumprimento dos requisitos necessários à obtenção do grau de Doutor em Química, realizada sob a orientação científica do Professor Doutor João Manuel da Costa e Araújo Pereira Coutinho, Professor Catedrático do Departamento de Química da Universidade de Aveiro, e co-orientação da Doutora Sónia Patrícia Marques Ventura, Investigadora Auxiliar no Instituto de Materiais de Aveiro (CICECO), do Departamento de Química da Universidade de Aveiro.

Apoio financeiro através da FCT/MEC, no âmbito do projeto PTDC/ATP-EAM/5331/2014.

Apoio financeiro do POCTI no âmbito do III Quadro Comunitário de Apoio. Co-financiamento do POPH/FSE.

O doutorando agradece o apoio financeiro da FCT no âmbito do III Quadro Comunitário de Apoio (SFRH/BD/85871/2012).

Dedico este trabalho ao nº 128 da Rua 21 de Maio, Antões.

o júri

presidente

Prof. Doutor António Manuel Rosa Pereira Caetano
professor catedrático da Universidade de Aveiro

Prof. Doutor Carlos Alberto Mateus Afonso
professor catedrático da Faculdade de Farmácia da Universidade de Lisboa

Prof. Doutor Artur Manuel Soares da Silva
professor catedrático da Universidade de Aveiro

Prof. Doutora Emília Tojo Suárez
professora associada da Universidade de Vigo, Espanha

Doutora Cristina Silva Pereira
investigadora principal do Instituto de Tecnologia Química e Biológica da Universidade Nova de Lisboa

Doutora Sónia Patrícia Marques Ventura
investigadora auxiliar da Universidade de Aveiro

agradecimentos

Era uma vez um reino vestido de cor-de-rosa…

O rosa que carreguei com orgulho estes 4 anos resulta de múltiplas pinceladas de várias cores, provenientes do arco-íris multidisciplinar que é o Path. Obrigada por toda a generosidade, paciência e conhecimentos transmitidos. Vou levar sempre comigo esta palete de cores. Gostaria de agradecer em particular ao Professor João Coutinho e à Doutora Sónia Ventura por terem orientado os meus traços nesta grande "pintura científica".

Doctor Peter Schulz and Doctor Mikhail Gantman, "danke schön" for all your attention and for your help during my three months in Erlangen.

Neste reino a vivência é produto de muito amor, cumplicidade e dedicação do paizinho João, da mamã Dalita e da nenuca Didi. Obrigada por estarem sempre comigo. Estando eu a falar de reinos, não poderia faltar um princeso, o meu André. Obrigada por estares ao meu lado na governação do reino. Por fim, mas não menos importante, temos os restantes habitantes do mesmo: os avozinhos, os Sintras e os amigos. Obrigada por rechearem os meus dias de sorrisos.

A história continua…

… que venham as próximas aventuras!

palavras-chave

Líquidos iónicos, ajustabilidade, síntese, antioxidantes, seletores quirais, hidrótopos, tensioactivos, magnéticos, anião per-fluoro-*tert*-butóxido, ecotoxicidade.

resumo

Nas últimas décadas, os líquidos iónicos (ILs) têm sido alvo de elevado interesse quer por parte da academia como a nível industrial. Isto deve-se em grande parte às suas propriedades únicas, assim como à possibilidade de, através de uma apropriada combinação dos seus iões, ser possível ajustar as suas propriedades para uma dada aplicação. Assim, os ILs têm vindo a ser considerados uma abordagem inovador para a "Química verde" e para a sustentabilidade. Contudo, a sua solubilidade em água faz com que estes possam facilmente chegar ao ecossistema aquático, podendo representar um perigo para este. O principal objetivo deste trabalho é estudar novos ILs, mais sustentáveis, assim como algumas das suas potenciais aplicações. Assim, foram investigados ILs como sendo antioxidantes, seletores quirais, hidrótopos, surfactantes, compostos magnéticos, assim como novos compostos hidrofóbicos. Para cada classe de ILs, foi estudada a sua síntese, caracterização físico-química e perfil de ecotoxicidade. Os novos ILs antioxidantes preparados neste trabalho foram avaliados quanto à sua solubilidade em água, estabilidade térmica, citotoxicidade e ecotoxicidade. Foram também estudados vários ILs quirais, quer baseados em aniões quirais (derivados de vários aminoácidos e do ácido tartárico), quer em catiões quirais (derivados da quinina, L-prolina e L-valina), no que respeita à sua estabilidade térmica, rotação ótica e ecotoxicidade. Além disso, foi avaliado o impacto de diferentes estruturas químicas dos ILs, assim como da sua concentração, na solubilidade de fármacos com reduzida solubilidade em água, a fim de analisar o seu comportamento enquanto hidrótopos cataniónicos.

Entre as estruturas mais hidrofóbicas referidas neste trabalho estão vários ILs com natureza surfactante e um IL hidrofóbico baseado no anião per-fluoro-*tert*-butóxido. Relativamente aos ILs com carácter surfactante, foram preparados ILs pertencentes à família dos imidazólios, amónios quaternários e fosfónios, sendo posteriormente avaliados quanto à sua natureza de agregação, propriedades térmicas, ecotoxicidade, e à sua capacidade em promover disrupção celular. Por sua vez, o IL baseado no anião per-fluoro-*tert*-butóxido foi estudado relativamente às suas propriedades físicas, tais como a sua densidade, viscosidade e tensão superficial, assim como à sua toxicidade. Por fim, 24 ILs magnéticos foram preparados conjugando o catião colínio com diferentes aniões magnéticos ($[FeCl_4]^-$, $[MnCl_4]^{2-}$, $[CoCl_4]^{2-}$ and $[GdCl_6]^{3-}$), sendo seguidamente avaliados quanto à sua ecotoxicidade.

Visando o desenho racional de novos ILs, foi desenvolvido um modelo preditivo QSAR, onde foram utilizandos os dados de ecotoxicidade medidos neste trabalho. As previsões deste modelo relativamente à não toxicidade de um certo número de novos ILs foram testadas com êxito através da síntese destes compostos e posterior avaliação da sua ecotoxicidade utilizando o bioensaio Microtox.

keywords

Ionic liquids, designer solvents, synthesis, antioxidants, chiral selectors, hydrotropes, surface-active, magnetics, per-fluoro-*tert*-butoxide anion, ecotoxicity.

abstract

Due to their unique properties, ionic liquids (ILs) have attracted an increased scientific and industrial attention in the last decades. The possibility of tailoring their properties for a specific task by the adequate combination of their ions, makes these ionic compounds good candidates for a wide range of different applications. Actually, ILs have been described as an innovative approach to the “Green Chemistry” and sustainability principles. However, their solubility in water allows their easy access to the aquatic compartment, which makes them potentially hazardous compounds to aquatic organisms. The main goal of this work is to study new, more environmental friendly, IL structures and their main applications. ILs as antioxidants, chiral selectors, hydrotropes, surface-active compounds, with magnetic properties, as well as, new hydrophobic compounds are investigated. The synthesis, physico-chemical characterization and ecotoxicity profile were studied for the various classes of task specific ILs evaluated. New cholinium-based ILs with antioxidant nature were studied regarding their solubility in water, thermal stability, cytotoxicity, and ecotoxicity. Moreover, a large range of chiral ILs (CILs) based on several chiral anions (derived from chiral amino acids and tartaric acid) and chiral cations (based on quinine, L-proline and L-valine), was investigated and their thermal stability, optical rotation and ecotoxicity evaluated. Furthermore, the impact of different ILs structures and concentrations on the solubility of poorly water-soluble drugs was studied, and their role as catanionic hydrotropes investigated.

Among the most hydrophobic structures reported in this work are several surface-active ILs and a hydrophobic IL based on the per-fluoro-tert-butoxide anion. The tensioactive ILs, belonging to the imidazolium, quaternary ammonium and phospholium families were tested in terms of their aggregation behavior, thermal properties, ecotoxicity, and their capacity to promore cell disruption. On the other hand, the per-fluoro-*tert*-butoxide-based IL was evaluated regarding its physical properties, such as density, viscosity, and surface tension and toxicity. Finally, 24 magnetic ILs belonging to the cholinium family and using $[FeCl_4]^-$, $[MnCl_4]^{2-}$, $[CoCl_4]^{2-}$ and $[GdCl_6]^{3-}$ as anions were investigated and their ecotoxicity evaluated.

Aiming at the rational design of ILs, a predictive QSAR model was developed with our help, and using ecotoxicity data measured in this work. The predictions of this model concerning the non-toxicity of a number of novel ILs were successfully tested by synthesizing these compounds and evaluating their toxicity using the Microtox bioassay.

Contents

List of Figures ii
List of Schemes v
List of Tables vi
Nomenclature viii
Abbreviations viii
Symbols xii
Chapter 1 - General Introduction 1
1.1 General Context 3
1.1.1 Synthesis of Ionic Liquids 5
1.1.2 Physicochemical properties of ILs 18
1.1.3 Ecotoxicity of ILs 33
1.2 Scope and objectives 36
Chapter 2 - Ionic Liquids with Antioxidant Character 39
Chapter 3 - Ionic Liquids as Chiral Selectors 61
Chapter 3.1 – Ionic liquids with chiral anion 65
Chapter 3.2 – Ionic liquids with chiral cation 77
Chapter 4 - Ionic Liquids as Catanionic Hydrotropes 87
Chapter 5 - Ionic Liquids with Surfactant Nature 107
Chapter 6 - Magnetic Ionic Liquids 125
Chapter 7 - Hydrophobic Ionic Liquids 141
Chapter 8 - More Biocompatible Ionic Liquids - Predictive QSAR Models 155
Final Remarks and Future Work 179
List of Publications 185
References 189

List of Figures

Figure 1.1. Some common cations and anions used in the preparation of ILs. 3

Figure 1.2. Description of the most common steps applied in the synthesis of ILs. 6

Figure 1.3. Melting temperatures for a series of $[C_nC_1im][PF_6]$. 19

Figure 1.4. Structure of a 1-methyl-3-octadecylimidazolium cation showing the relevant structural regions with impact on the melting points.[110] 20

Figure 1.5. Schematic representation of the distillation process for protic and aprotic ILs.[161] For protic ILs, a dynamic equilibrium exists between the ionic and dissociated forms: $[BH]^+X^-$ (l) ⇆ B (l) + HX (l) ⇆ B (g) + HX (g). Green circles represent the cations, blue circles represent the anions and the remaining coloured circles represent neutral molecules. For the gaseous phase over the aprotic IL, the representation is purely schematic and has no implication for the actual degree of aggregation. 27

Figure 1.6. Solubility of $[PF_6]$-based ILs in water (expressed in mole fraction) as function of the IL molar volume at 298.15 K.[187] 30

Figure 1.7. Schematic representation of the work layout. 37

Figure 2.1. IC_{50} values ($\mu mol \cdot L^{-1}$) and respective standard deviations, after 30, 90, and 120 min of exposure to DPPH. 51

Figure 2.2. EC_{50} values ($mmol \cdot L^{-1}$) determined after 5, 15, and 30 min of *V. fischeri* exposure. The error bars correspond to 95% confidence level limits. 54

Figure 2.3. Viability of Raw 264.7 and HaCaT cells assessed as the normalized response of treated cells to untreated controls, measured by the metabolic conversion of resazurin. The data shown represents the dose−response curves of Raw 264.7 cells to (A) $[N_{1,1,1,2(OH)}][Gal]$ EC_{50} 835.8 μM and gallic acid EC_{50} 590.7 μM; and (C) $[N_{1,1,1,2(OH)}][Caf]$ EC_{50} 2336 μM and caffeic acid EC_{50} 1996 μM; and HaCaT cells to (B) $[N_{1,1,1,2(OH)}][Gal]$ EC_{50} 303.5 μM and gallic acid EC_{50} 267.1 μM; and (D) $[N_{1,1,1,2(OH)}][Caf]$ EC_{50} 1794 μM and caffeic acid EC_{50} 1803 μM. 56

Figure 2.4. Effect of cholinium-based salts and their respective acids on the NO production in macrophages for concentrations of 10, 50, and 100 μM. The results are expressed as the amount of NO produced by the control cells maintained in a culture medium. LPS at a concentration of 1 $\mu g \cdot mL^{-1}$ was used as a positive control. Each value

represents the average value and the respective standard deviation obtained from 3 independent experiments (*p < 0.05, **p < 0.01, ****p < 0.0001). 57

Figure 2.5. Effect of NAC, BAY, PDTC, cholinium-based salts and their respective acids (at 100 μM and 50 μM) on the inhibition of LPS-induced NO production in macrophages. The results are expressed as the amount of NO produced relatively to cells treated with 1 μg.mL^{-1} of LPS. Each value represents the average value and the respective standard deviation obtained from 3 independent experiments (****p < 0.0001: LPS vs LPS + treatment). 58

Figure 3.1. Acronym and chemical structures of the CILs studied..... 69

Figure 3.2. Density as a function of the temperature for CILs: [$N_{1,1,1,2(OH)}$]$_2$[L-Glu] (▰), [$N_{1,1,1,2(OH)}$][D-Phe] (✳),[$N_{1,1,1,2(OH)}$][L-Phe] (O), [$N_{4,4,4,4}$][L-Pro] (◢),[$N_{4,4,4,4}$][L-Val] (◆). 72

Figure 3.3. Viscosity as a function of the temperature for CILs: [$N_{1,1,1,2(OH)}$]$_2$[L-Glu] (▰), [$N_{1,1,1,2(OH)}$][D-Phe] (✳),[$N_{1,1,1,2(OH)}$][L-Phe] (O), [$N_{4,4,4,4}$][L-Pro] (◢),[$N_{4,4,4,4}$][L-Val] (◆). 73

Figure 3.4. Refractive index as a function of temperature for CILs: [$N_{1,1,1,2(OH)}$]$_2$[L-Glu] (▰), [$N_{1,1,1,2(OH)}$][D-Phe] (✳),[$N_{1,1,1,2(OH)}$][L-Phe] (O), [$N_{4,4,4,4}$][L-Pro] (◢),[$N_{4,4,4,4}$][L-Val] (◆). 73

Figure 3.5. EC_{50} values (mmol·L^{-1}) determined after 5, 15, and 30 min of exposure time towards the *V. fischeri* bacteria. The error bars correspond to 95% confidence level limits. 75

Figure 3.6. Chemical structures and acronym of all ILs with chiral cation here synthesized. 83

Figure 3.7. The partial 19F NMR spectra of CILs under study and the racemic Mosher's acid salt complex. 84

Figure 4.1. Chemical strutures of (a) ibuprofen, (b) naproxen and (c) caffeine. 92

Figure 4.2. Chemical structure of the ILs and salts studied as hydrotopes. 95

Figure 4.3. Impact of the IL concentration on the solubility of caffeine in aqueous solution of (●) [C_4C_1im][$N(CN)_2$]; and naproxen in aqueous solutions of (■) [$N_{1,1,1,2(OH)}$][Sal] and (◆) [$N_{1,1,1,2(OH)}$][Van]. Line is guide for the eye. 96

Figure 4.4. Impact of the IL concentration on the solubility of ibuprofen in aqueous solutions of (■) [C_4C_1im][$N(CN)_2$], (○) [C_4C_1py][$N(CN)_2$], (▲) [C_4C_1im][SCN], (✕)

[$P_{4,4,4,4}$]Cl, (●) [C_4C_1im]Br, (◆) [C_4C_1pip]Cl and (△) [C_4C_1pyrr]Cl, in order to evaluate the MHC. Lines are guides for the eye. 97

Figure 4.5. Impact of the hydrotrope concentration on the solubility of (a) ibuprofen and (b) naproxen in aqueous solutions of (●) [$N_{1,1,1,2(OH)}$][Van], (◆) [$N_{1,1,1,2(OH)}$][Gal], (■) [C_4C_1im][$N(CN)_2$], (✕) Na[Benz], (▲) [C_4C_1py][$N(CN)_2$], (●) [C_4C_1im][SCN], (◆) [$P_{4,4,4,4}$]Cl, (■) [C_4C_1im][CF_3SO_3], (▲) [C_4C_1im][TOS], (-) Na[$N(CN)_2$], (●) Na[TOS], (●) [$N_{4,4,4,4}$]Cl, (◆) [$N_{1,1,1,2(OH)}$][Sal], (■) [C_4C_1im]Br, (+) [C_4C_1py]Cl, (+) [C_4C_1pip]Cl, (✳) [C_4C_1mim]Cl, (▲) [$N_{(Bz),1,1,2(OH)}$]Cl, (-) [C_4C_1pyrr]Cl, (✕) [$N_{1,1,1,2(OH)}$]Cl, (▲) Na[SCN] and (▲) urea. S and S_0 represent the solubility of the drug in aqueous solution of the hydrotrope and in water, respectively. Lines are guides for the eye. 98

Figure 4.6. K_{Hyd} values of the chloride-based ILs for ibuprofen (blue stripes), naproxen (blue) and caffeine (orange spots). 101

Figure 4.7. K_{Hyd} values for ibuprofen (blue stripes) and naproxen (blue) using tosylate-, thiocyanate- and dicyanamide-based hydrotropes. 101

Figure 4.8. K_{Hyd} values of the [C_4C_1im]-based ILs for ibuprofen (blue stripes), naproxen (blue) and caffeine (orange spots). 102

Figure 4.9. K_{Hyd} values for ibuprofen (blue stripes) and naproxen (blue) using sodium- and cholinium-based hydrotropes. 104

Figure 4.10. Impact of the logK_{ow} value of each biomolecule on the hydrotropy constant of the (●) [C_4C_1im][$N(CN)_2$], (○) [C_4C_1py][$N(CN)_2$], (▲) [C_4C_1im][TOS], (□) Na[TOS], (◆) [C_4C_1im]Br, (■)[C_4C_1im][CF_3SO_3] and (✕)[C_4C_1pyrr]Cl. Lines are guides for the eye. 104

Figure 5.1. Chemical structures and acronyms of the SAILs synthesized in this work. 117

Figure 5.2. EC_{50} values (μM) determined towards *V. fischeri* after 5, 15 and 30 minutes of exposure. The error bars correspond to 95 % confidence level limits. 121

Figure 5.3. Results of fluorescence intensity describing the release of GFP to extracellular medium using aqueous solutions of SAILs, with a concentration of 100 mM (except for *, with 25 mM). 122

Figure 5.4. Influence of the IL concentration (mM) in GFP release to extracellular medium. 123

Figure 6.1. Cations and anions used in the design of the MILs studied in this work. 131

Figure 6.2. The effect of the alkyl chain length on the ecotoxicity of the series $[N_{1,1,n,2(OH)}][M]$, where *n* is the number of carbons and M represents the metal anion. The experimental data presented for the bromide anion (Br) can be checked elsewhere.[232] 135

Figure 6.3. The effect of the alkyl chain length on the ecotoxicity of the series $[N_{1,n,2(OH),2(OH)}][M]$, where *n* is the number of carbons and M represents the metal anion. 137

Figure 6.4. The effect of the number of hydroxyethyl groups in the cations on the ecotoxicity of the MILs. The number 1, 2 and 3 represent $[N_{1,1,6,2(OH)}]$, $[N_{1,6,2(OH),2(OH)}]$ and $[N_{6,2(OH),2(OH),2(OH)}]$ cations, respectively. The experimental data presented for the bromide anion (Br) can be checked elsewhere.[232] 138

Figure 7.1. Schematic preparation of IL $[C_4C_1im][Pftb]$..... 147

Figure 7.2. FTIR spectra of the novel synthesized IL and the starting material. $[C_4C_1im][Pftb]$, solid line; per-fluoro-*tert*-butanol, dashed-line; $[C_4C_1im][OAc]$, dotted-line. 148

Figure 7.3. ^{1}H (a), ^{13}C (b), and ^{19}F (c) spectra of $[C_4C_1im][Pftb]$ in DMSO-d_6 produced from route 1. 150

Figure 7.4. Thermogravimetric analysis of $[C_4C_1im][Pftb]$. Heating rate 5 $K{\cdot}s^{-1}$. 151

Figure 8.1. Synthesis scheme and chemical structure of the morpholinium-based ILs synthesized specifically for this study. 166

Figure 8.2. Scatter plot of the observed *versus* computed (consensus from models 1, 2, 3) toxicity values of ILs. 173

List of Schemes

Scheme 1.1. Synthesis of ILs with alkyl sulfate anions by the quaternization method.[45] 7

Scheme 1.2. Scheme representative of the parallel and competing reactions (a) alkylation and (b) elimination. 8

Scheme 1.3. Synthesis of ILs using a zwitterion agent. 10

Scheme 1.4. Equilibria series for the reaction between the $[C_2C_1im]Cl$ and $AlCl_3$ 10

Scheme 1.5. Anion exchange through the carbene methodology applied in the preparation of ILs. 14

Scheme 1.6. Synthesis of two ILs by simultaneous ion exchange.[103] 17

Scheme 1.7. Synthesis scheme for the transesterification reaction exemplified for a tetraalkylammonium system.[104] 17

Scheme 1.8. Synthesis of alkylsulfonate esters and their use to prepare ammonium alkanesulfonates. 18

Scheme 1.9. Protic-IL formation through proton transfer from a Brønsted acid (HA) to a Brønsted base (B). 26

Scheme 2.1. Synthesis scheme and chemical structure of the cholinium-based salts prepared. 50

Scheme 3.1. Synthesis scheme followed to prepare the quinine-based CILs. 78

Scheme 3.2. Synthesis scheme followed to prepare the L-proline-based CILs. 79

Scheme 3.3. Synthesis scheme followed to prepare the L-valine-based CILs. 80

List of Tables

Table 1.1. Description of some ILs prepared by the anion metathesis reaction. 13

Table 2.1. Thermal properties of the synthesized cholinium-based salts, namely the melting temperature (T_{fus}) and temperature of decomposition (T_d). 52

Table 2.2. Water solubility of the synthesized salts and of the corresponding acids (mmol·L^{-1}) at 25 °C, with the respective standard deviations. 53

Table 3.1. The optical rotations, $[\alpha]^{20}_D$, of CILs and respective starting materials, amino acids/tartaric acid. 70

Table 3.2. Thermal properties of the synthesized CILs and respective starting materials, amino acids/tartaric acid, namely the melting temperature (T_{fus}) and temperature of decomposition (T_d). 70

Table 3.3. Chemical shift difference of the CF_3 signals of racemic Mosher's acid sodium salt in the presence of 0.5 M of each CIL under study. Duplicate measurements were carried out. 85

Table 4.1. K_{Hyd} values for the several hydrotropes analysed in the solubility of ibuprofen, naproxen and caffeine at (303.1 ± 0.5) K. 99

Table 5.1. Physical properties of the SAILs synthetized in this work. 118

Table 5.2. Thermal properties of the synthetized SAILs, namely the thermal transition (T_{tr}), melting temperature (T_{fus}) and temperature of decomposition (T_d). 120

Table 6.1. EC_{50} values ($mg \cdot L^{-1}$) for MILs under study after 5 minutes of exposure to the luminescent marine bacteria *V. fischeri*, with the respective 95% confidence limits (in brackets). 132

Table 6.2. EC_{50} values ($mg \cdot L^{-1}$) for MILs under study after 15 minutes of exposure to the luminescent marine bacteria *V. fischeri*, with the respective 95% confidence limits (in brackets). 133

Table 6.3. EC_{50} values ($mg \cdot L^{-1}$) for MILs under study after 30 minutes of exposure to the luminescent marine bacteria *V. fischeri*, with the respective 95% confidence limits (in brackets). 134

Table 6.4. The impact of the magnetic anion on the ecotoxicity of the MILs, according to EC_{50} values (μM) after 30 minutes of exposure towards *V. fischeri*. 138

Table 7.1. Physical properties and toxicity of the novel IL $[C_4C_1im][Pftb]$ at 298 K. 152

Table 8.1. Predictive QSAR models developed using the ecotoxicity values of ILs to *V. fischeri*. Here, $n_{training}$=213, n_{test}=92. 168

Table 8.2. Predictive quality of the models for the true external validation set (n=8) employing classic metrics and MAE based criteria. 172

Table 8.3. The experimental and predicted ecotoxicity values for the true external set obtained from best model (with the lowest DModX value) and consensus approach. ... 173

Table 8.4. Predicted ecotoxicity values of the designed ILs towards *V. fischeri* determined using the best model (model with the lowest DModX value) and the consensus approach. 175

Table 8.5. Experimental ecotoxicity values of the selected synthesized ILs. 175

Nomenclature

Abbreviations

ABS	Aqueous Biphasic Systems
API	Active Pharmaceutical Ingredient
BAY	NF-*κ*b Inhibitors
CILs	Chiral Ionic Liquids
CMC	Critical Micellar Concentration
DAD	Diode Array Detector
DNA	Deoxyribonucleic Acid
DPPH	2,2-Diphenyl-2-Picrylhydrazyl
DSC	Differential Scanning Calorimetry
ETA	Extended Topochemical Atom
FDA	Food and Drug Administration
FTIR	Fourier Transform Infrared
GFA	Genetic Function Approximation
GFP	Green Fluorescent Protein
HPLC	High-Performance Liquid Chromatography
ILs	Ionic Liquids
KF	Karl Fischer
LLE	Liquid-Liquid Extraction
LPS	Lipopolysaccharide
MHC	Minimum Hydrotrope Concentration
MILs	Magnetic Ionic Liquids
MLR	Multiple Linear Regression
NAC	*N*-Acetyl Cysteine
NF-*κ*B	Nuclear Factor *κ*-Light-Chain-Enhancer of Activated B Cells
NMR	Nuclear Magnetic Resonance
OECD	Organization For Economic Cooperation And Development
PLS	Partial Least Squares
QSAR	Quantitative Structure-Activity Relationships
QTMS	Quantum Topological Molecular Similarity
REACH	Registration, Evaluation, Authorization And Restriction of Chemicals
ROS	Reactive Oxygen Species
rpm	Revolutions per Minute
SAILs	Surface Active Ionic Liquids
TGA	Thermogravimetric Analysis
UV	Ultraviolet

Chemicals

$Ag[BF_4]$	Silver Tetrafluoroborate
$Ag[CB_{11}H_{12}]$	Silver Carba-*Closo*-Dodecaborate

$Ag[CF_3CO_2]$	Silver Trifluoroacetate
$Ag[N(CN)_2]$	Silver Dicyanamide
$Ag[NO_2]$	Silver Nitrite
$Ag[NO_3]$	Silver Nitrate
Ag[OAc]	Silver Acetate
$Ag_2[SO_4]$	Silver Sulfate
$AlCl_3$	Aluminium Chloride
$AlEtCl_2$	Ethylaluminum Dichloride
BCl_3	Boron Trichloride
$CF_3SO_3CH_3$	Methyl Trifluoromethansulfonate
DMSO	Dimethylsulfoxide
Et_3N	Triethylamine
$FeCL_3$	Iron(III) Chloride
$HAuCl_4$	Chloroauric Acid
HBF_4	Tetrafluoroboric Acid
HBr	Hydrobromic Acid
HCl	Hydrochloric Acid
HI	Hydroiodic Acid
HPF_6	Hexafluorophosphoric Acid
K[Ace]	Potassium Acesulfamate
$K[CF_3(CF_2)_3SO_3]$	Potassium Perfluoro-*N*-Butylsulfonate
KOH	Potassium Hydroxide
$Li[NTf_2]$	Bis(Trifluoromethane)Sulfonimide Lithium Salt
Na[Benz]	Sodium Benzoate
$Na[BF_4]$	Sodium Tetrafluoroborate
$Na[N(CN)_2]$	Sodium Dicyanamide
$Na[NO_3]$	Sodium Nitrate
Na[Sac]	Sodium Saccharinate
Na[SCN]	Sodium Thiocyanate
Na[TOS]	Sodium Tosylate
NaH	Sodium Hydride
$[NH_4][BF_4]$	Ammonium Tetrafluoroborate
$[NH_4][CF_3SO_3]$	Ammonium Trifluoromethanesulfonate
$[NH_4][PF_6]$	Ammonium Hexafluorophosphate
PTDC	Pyrrolidine Dithiocarbamate
$SnCl_2$	Tin(II) Chloride

Ionic Liquid Cations

$[C_2C_1im]^+$	1-Ethyl-3-methylimidazolium
$[C_3C_1im]^+$	1-Methyl-3-propylimidazolium
$[C_4C_1im]^+$	1-Butyl-3-methylimidazolium
$[C_6C_1im]^+$	1-Hexyl-3-methylimidazolium
$[C_8C_1im]^+$	1-Methy-3-octylimidazolium

$[C_1C_{14}Im]^+$	1-Methyl-3-tetradecylimidazolium
$[C_{1(OH)}C_1im]^+$	1-Hydroxymethyl-3-methylimidazolium
$[C_4C_1C_1im]^+$	1-Butyl-2,3-dimethylimidazolium
$[C_{14}Im\text{-}6\text{-}C_{14}Im]^{2+}$	3,3´-(1,6-Hexanedyl)bis(1-tetradecylimidazolium)
$[C_3C_1py]^+$	3-Methyl-1-propylpyridinium
$[C_4C_1py]^+$	1-Butyl-3-methylpyridinium
$[C_8C_1py]^+$	4-Methyl-1-octylpyridinium
$[C_{2(OH)}py]^+$	1-Hydroxyethylpyridinium
$[C_3C_1pyrr]^+$	1-Methyl-1-propylpyrrolidinium
$[C_4C_1pyrr]^+$	1-Butyl-1-methylpyrrolidinium
$[iC_4C_1pyrr]^+$	1-Isobutyl-1-methylpyrrolidinium
$[C_8C_1pyrr]^+$	1-Methyl-1-octylpyrrolidinium
$[C_4C_{3(CN)}pyrr]^+$	1-Butyl-1-cyanopropylpyrrolidinium
$[C_3C_1pip]^+$	1-Methyl-1-propylpiperidinium
$[C_4C_1pip]^+$	1-Butyl-1-methylpiperidinium
$[P_{4,4,4,4}]^+$	Tetrabutylphosphonium
$[P_{1,1,1,14}]^+$	Trimethyltetradecylphosphonium
$[N_{4,4,4,4}]^+$	Tetrabutylammonium
$[N_{1,1,1,14}]^+$	*N,N,N*-Trimethyl-*N*-tetradecylammonium
$[N_{1,1,10,14}]^+$	*N*-Decyl-*N,N*-dimethyl-*N*-tetradecylammonium
$[N_{1,1,14,14}]^+$	*N,N*-Dimethyl-*N,N*-ditetradecylammonium
$[N_{1,1,14}\text{-}6\text{-}N_{1,1,14}]^{2+}$	*N,N*'-Bis(tetradecyldimethyl)-1,6-hexanediammonium
$[N_{1,1,1,2(OH)}]^+$	(2-Hydroxyethyl)trimethylammonium
$[N_{1,1,2,2(OH)}]^+$	(2-Hydroxyethyl) ethyl dimethylammonium
$[N_{1,1,6,2(OH)}]^+$	Hexyl (2-hydroxyethyl) dimethylammonium
$[N_{1,1,8,2(OH)}]^+$	(2-Hydroxyethyl) dimethyl octylammonium
$[N_{1,1,12,2(OH)}]^+$	Dodecyl (2-hydroxyethyl) dimethylammonium
$[N_{1,4,2(OH),2(OH)}]^+$	Butyl di(2-hydroxyethyl) methylammonium
$[N_{1,6,2(OH),2(OH)}]^+$	Hexyl di(2-hydroxyethyl) methylammonium
$[N_{6,2(OH),2(OH),2(OH)}]^+$	Hexyl tri(2-hydroxyethyl) ammonium
$[N_{(Bz),1,1,2(OH)}]^+$	Benzyldimethyl(2-hydroxyethyl)ammonium
$[2\text{-}HDEA]^+$	(2-Hydroxydiethyl)ammonium
$[C_1C_1C_1Pro]^+$	*N,N*-Dimethyl-L-proline methyl ester
$[C_2C_2C_2Pro]^+$	*N,N*-Diethyl-L-proline ethyl ester
$[C_1Qui]^+$	1-Methyl quininium
$[C_1C_1C_1Val]^+$	*N,N,N*-Trimethyl-L-valinolium
$[Mor]^+$	Morpholinium
$[C_2C_1mor]^+$	*N*-Ethyl-*N*-methylmorpholinium
$[C_3C_1mor]^+$	*N*-Methyl-*N*-propylmorpholinium
$[C_{2(OH)C1}mor]^+$	*N*-Hydroxyethyl-*N*-methylmorpholinium

Ionic Liquid Anions

Cl^-	Chloride

Br^-	Bromide
I^-	Iodide
$[AlCl_4]^-$	Aluminium tetrachloride
$[Al_2Cl_7]^-$	Dialuminum heptachloride
$[Al_3Cl_{10}]^-$	Trialuminum decachloride
$[PF_6]^-$	Hexafluorophosphate
$[NO_3]^-$	Nitrate
$[NO_2]^-$	Nitrite
$[BF_4]^-$	Tetrafluoroborate
$[NTf_2]^-$	Bis(trifluoromethylsulfonyl)imide
$[CF_3SO_3]^-$	Trifluoromethanesulfonate
$[CF_3CO_2]^-$	Trifluoroacetate
$[CF_3(CF_2)_3SO_3]^-$	Perfluoro-n-butylsulfonate
$[(CF_3CF_2SO_2)_2N]^-$	Bis(pentafluoroethylsulfonyl)imide
$[N(CN)_2]^-$	Dicyanamide
$[C(CN)_3]^-$	Tricyanomethanide
$[CB_{11}H_{12}]^-$	Carba-*closo*-dodecaborate
$[Ace]^-$	Acesulfamate
$[Sac]^-$	Saccharinate
$[AuCl_4]^-$	Tetrachloroaurate
OH^-	Hydroxide
$[DCTA]^-$	4,5-Dicyano-1,2,3-triazolate
$[SO_4]^{2-}$	Sulfate
$[C_1SO_4]^-$	Methyl sulfate
$[C_2SO_4]^-$	Ethyl sulfate
$[C_8SO_4]^-$	Octyl sulfate
$[C_{10}SO_4]^-$	Decyl sulfate
$[C_1(OC_2)_2SO_4]^-$	Diethyleneglycol monomethylethersulfate
$[FAP]^-$	Tris(pentafluoroethyl)trifluorophosphate
$[N(FSO_2)_2]^-$	Bis(fluorosulfonyl)imide
$[C_nF_{2n+1}BF_3]^-$	Perfluoloalkyltrifluoroborate
$[ClO_4]^-$	Perchlorate
$[C_4C_4PO_4]^-$	Dibutyl phosphate
$[Gal]^-$	Gallate
$[Sal]^-$	Salicylate
$[Caf]^-$	Caffeate
$[Van]^-$	Vanillate
$[Syr]^-$	Syringate
$[Ell]^{2-}$	Ellagate
$[L\text{-}Pro]^-$	L-Prolinate
$[L\text{-}Phe]^-$	L-Phenylalaninate
$[D\text{-}Phe]^-$	D-Phenylalaninate
$[L\text{-}Val]^-$	L-Valinate
$[L\text{-}Ala]^-$	L-Alaninate
$[L\text{-}Arg]^-$	L-Argininate

$[L\text{-}Glu]^{2-}$	L-Glutamate
$[L\text{-}Tar]^{2-}$	L-Tartrate
$[D\text{-}Tar]^{2-}$	D-Tartrate
$[BES]^{-}$	2- (Bis(2-hydroxyethyl)amino)ethanesulfonate
$[MOPSO]^{-}$	2-Hydroxy-3-morpholinopropanesulfonate
$[CAPSO]^{-}$	3-(Cyclohexylamino)-2-hydroxypropanesulfonate
$[SCN]^{-}$	Thiocyanate
$[TOS]^{-}$	Tosylate
$[FeCl_4]^{-}$	Iron tetrachloride
$[MnCl_4]^{2-}$	Manganese tetrachloride
$[CoCl_4]^{2-}$	Cobalt tetrachloride
$[GdCl_6]^{3-}$	Gadolinium hexachloride
$[Pftb]^{-}$	Per-fluoro-*tert*-butoxide
$[For]^{-}$	Formate
$[OAc]^{-}$	Acetate
$[Pr]^{-}$	Propionate
$[i\text{But}]^{-}$	Isobutyrate
$[But]^{-}$	Butyrate
$[Pe]^{-}$	Pentanoate

Symbols

T	Temperature
R^2	Correlation Coefficient
x	Mole Fraction
wt %	Weight Fraction Percentage
σ	Standard Deviation
K_{ow}	1-Octanol-Water Partition Coefficient
η	Viscosity
ρ	Density
n_D	Refractive Index
γ	Surface Tension
$[\alpha]^{20}_D$	Optical Rotation
EC_{50}	Concentration Yielding a 50% of Bioluminescence Inhibition of *V. fischeri*
IC_{50}	Concentration of the Antioxidant Needed to Scavenge 50% of the DPPH
AA(%)	DPPH Radical Scavenging Activity
S/S_0	Solubility Enhancement
K_{Hyd}	Hydrotropy Constant
$\triangle\delta$	Chemical Shift Difference

Chapter 1 - General Introduction

1.1 General Context

In the past few years, ionic liquids (ILs) became one of the hottest research areas in the chemistry field attracting a lot of academic and industrial interest.[1] By definition, ILs are liquids entirely composed of ions, usually large organic cations and organic or inorganic anions, with melting points lower than 100 °C, since one or both ions have a dispersed charge and their asymmetry making difficult their development in an ordered crystalline structure.[2] The increasing attention devoted to ILs is largely justified by their unique properties, such as their negligible vapour pressure, high chemical and thermal stability, their non-flammability, high ionic conductivity, wide electrochemical potential window and high solvation ability. Furthermore, these ionic compounds are considered as ‘‘*designer solvents*’’ due to their tuneable properties, which means that they can be designed for a specific purpose by the selection of the adequate cation/anion combination (see Figure 1.1 where some of the most common cations and anions are represented).[3] Some reviews[4,5] have highlighted the industrial applications of ILs as an innovative approach to Green Chemistry and Sustainability.

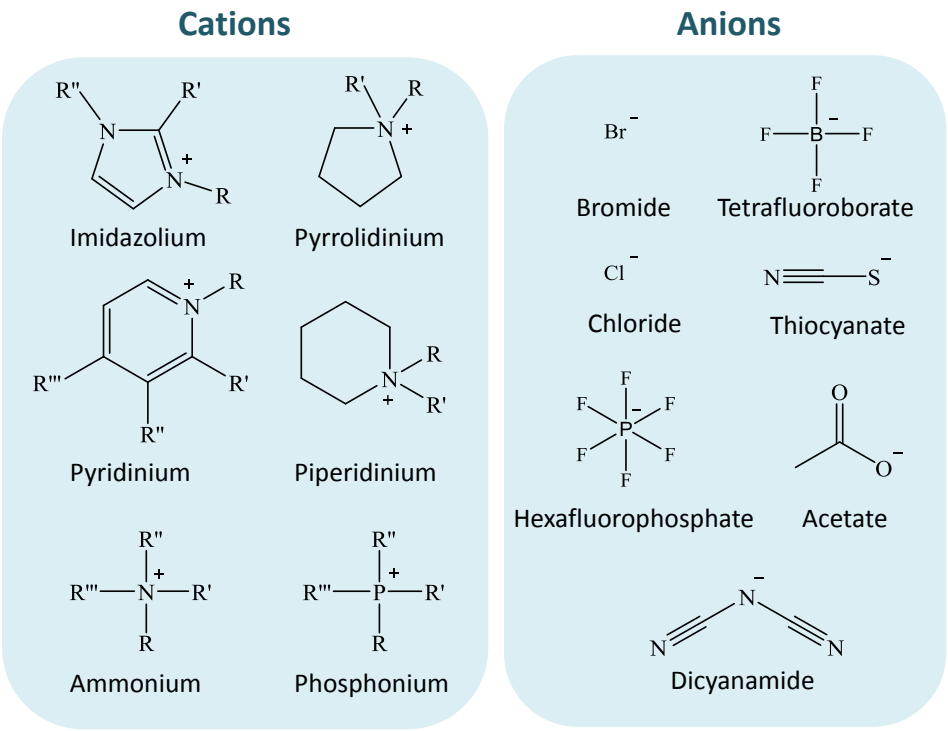

Figure 1.1. Some common cations and anions used in the preparation of ILs.

Due to their negligible vapour pressure, ILs have been considered as a promising "green" substitute for organic solvents. However, this is not enough to assure that these compounds can be labeled as "green" solvents. Actually, even the most hydrophobic ILs present some solubility in water.[6–9] As a result, this is the most likely medium through which ILs could be released into the environment. Moreover, properties that brought them into the focus of industrial interest, namely the high chemical and thermal stability, may also promote them to become sources of potential environmental hazards, particularly regarding their toxicity and biodegradability.

Although ILs are not yet widely used in industrial applications, the continued development and further use of these solvents may lead to accidental discharges, promoting, in consequence, aquatic contaminations. The deficient information and uncertainty surrounding their environmental impact is one of the barriers to their widespread industrial application and international registration. One of the principles of Green Chemistry aims at the reduction of the environmental toxicity of chemical compounds used in industrial processes or product formulations. Legislation concerning this subject is nowadays more stringent in Europe as REACH (Registration, Evaluation, Authorization and Restriction of Chemicals)[10] requires the registration of new commercial chemicals and holds the suppliers responsible for their products. Nowadays, ILs have shown to be useful in a large number of applications, namely as solvent in organic chemistry (homogeneous catalysis,[11] Heck reaction,[12,13] or Suzuki reaction[14]), inorganic synthesis,[15] biocatalysis,[11,16,17] biomass conversion[16] and polymerization.[18] Furthermore, ILs have shown potential for the separation of gases, for example to remove water or CO_2 from natural gas,[19] and in the extraction of small impurities, such as traces of naphthalene or even ethanol.[20] These ionic compounds can also be applied in engineering processes, as heat transfer fluids, azeotrope-breaking liquids and lubricants, as well as new materials, such as electrolytes, liquid crystals, supported ionic liquid membranes, gas chromatography columns, plasticizers, surfactants, antimicrobial and embalming agents, anticorrosion coatings and electropolishing agents.[21] Recently, biological applications have emerged, such as media for DNA,[22] protein solubilisation[23] and biomolecule purification.[24,25] In addition, ILs have demonstrated high potential for the pharmaceutical

industry in the fields of pharmaceutical drug delivery,[26,27] active pharmaceutical ingredient (API) formulation[28,29] and chiral resolution.[30]

Since ILs can be designed to be task-specific for a given application and are seen as an innovative approach to sustainable chemistry,[31] they are no longer confined to academic ivory towers, they are already present in a range of commercial products and processes.[1] In this context, the ILs' synthesis, characterization in terms of their physicochemical and toxicological properties and main applications are rapid growing areas of interest.

1.1.1 Synthesis of Ionic Liquids

The first IL was obtained, almost occasionally, in 1914, during the World War I, by Paul Walden when testing new explosives for the replacement of nitroglycerin.[32] By the neutralization of ethylamine with concentrated nitric acid it was possible to synthesize what is now considered by many as the first IL, the ethylammonium nitrate, with a melting point of 12 °C.[32] In the 1930s, Graenacher[33] suggested a process for the preparation of cellulose solutions by heating cellulose in a liquid *N*-alkylpyridinium or *N*-arylpyridinium chloride salt, in the presence of a nitrogen-containing base such as pyridine. That finding seems to have been treated as a novelty of little practical value because the ILs were, at the time, somewhat unknown.[33] Some years after, ILs appeared again after the World War II in 1948, being applied in mixtures of aluminum chloride (III) and 1-ethylpyridinium bromide for the electrodeposition of aluminium.[34,35] Nevertheless, only in the last decades, stable ILs were developed and the research in this field increased exponentially with a variety of ILs synthesized and applications being proposed.

The synthesis of ILs can be generally divided into two steps; 1) the synthesis of the desired cation and 2) the anion exchange using the desired cation, as illustrated in Figure 1.2. In some specific cases only the first step is required, as with the formation of ethylammonium nitrate. On the other hand, the desired cation can be commercially available at reasonable cost, most commonly as a halide salt, thus requiring only the anion exchange reaction. The formation of the cations may be carried out either *via* protonation with a free acid or by quaternization of an amine, phosphine or sulfide,

commonly using a haloalkane or dialkylsulfates. The anion exchange reactions of ILs can be divided into two distinct categories, the direct reaction of halide salts with Lewis acids, and the formation of ILs *via* anion metathesis.

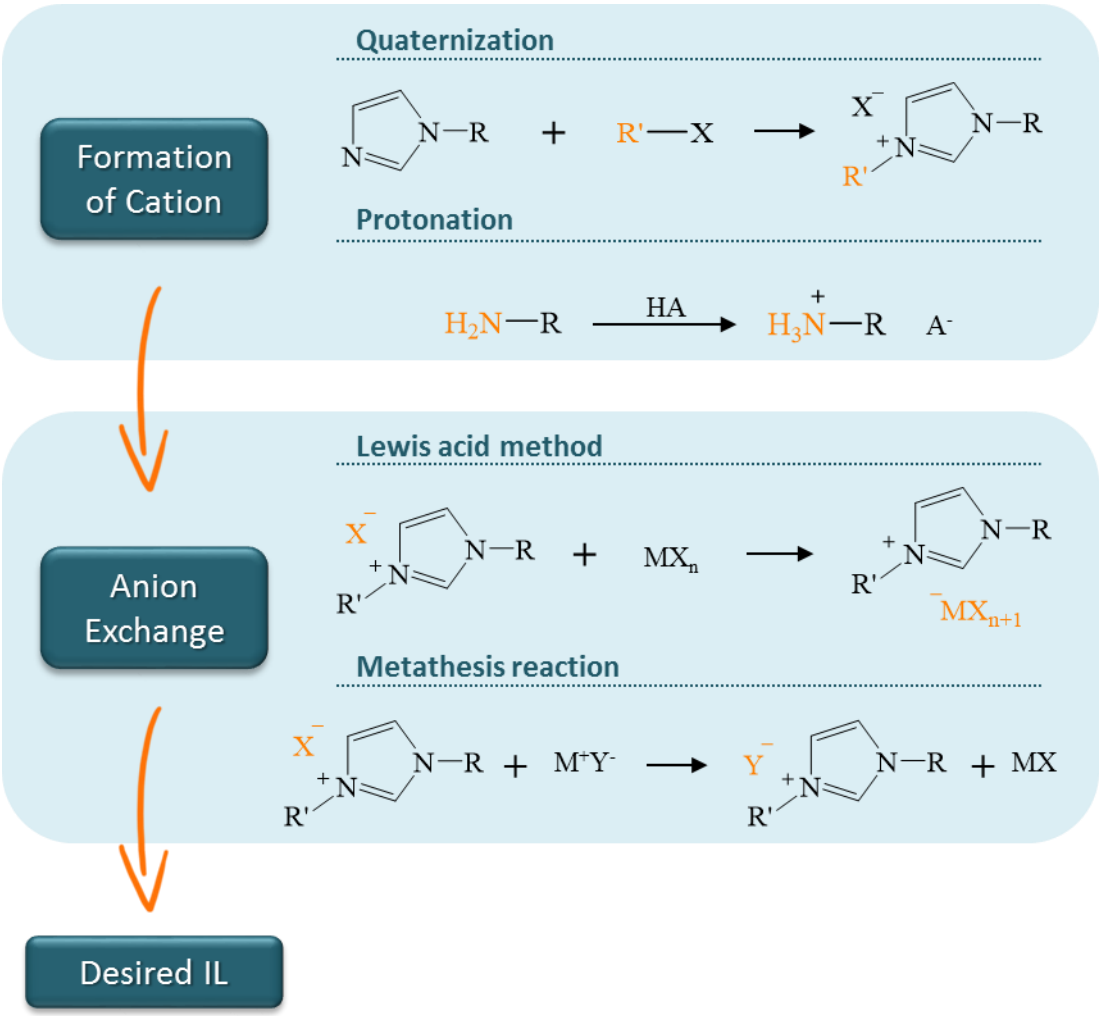

Figure 1.2. Description of the most common steps applied in the synthesis of ILs.

Synthesis of the cations

The protonation of suitable starting materials (generally amines and phosphines) still represents the simplest method for the formation of such materials, but unfortunately, it can only be used for a small range of useful salts.[36,37] The possibility of decomposition *via* deprotonation severely limits the use of such salts and in this context, more complex

methods are required. The quaternization of an amine or phosphine is the principal method to form the corresponding organic cation of the desired ionic liquid. The most common starting materials are 1-alkylimidazoles,[38] but other amines such as pyridine,[38,39] isoquinoline,[40] 1-alkylpyrrolidine,[41] and trialkylamines[42] can also be applied. In general, the reaction may be carried out using haloalkanes (chloroalkanes, bromoalkanes and iodoalkanes, but not floroalkanes) as well as using a alkyl derivative containing a good leaving group (methyl or ethyl triflate,[43] methyl trifluoroacetate,[43] alkyl tosylates[44]). Holbrey *et al.*[45] have also reported the preparation of ILs with alkyl sulfate anions using this methodology. Dimethyl sulfate or diethyl sulfate were applied in the preparation of a range of alkylimidazolium ILs that were, in many cases, liquid at room temperature, as displayed in Scheme 1.1.

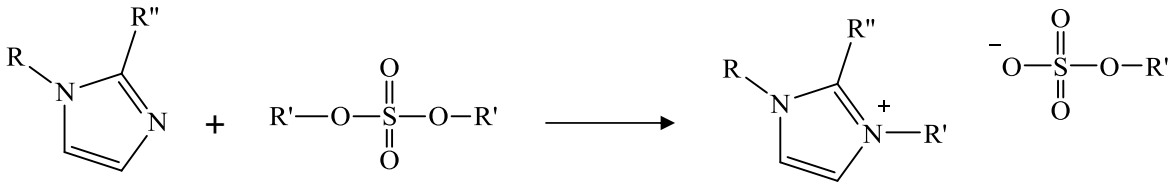

Scheme 1.1. Synthesis of ILs with alkyl sulfate anions by the quaternization method.[45]

In general, the quaternization reactions are quite simple: the amine (or phosphine) is mixed with the desired alkylating agent, being then the mixture stirred and heated. The reaction temperature and time are the two main conditions, extremely dependent on the alkylating agent employed. Considering the haloalkanes, the reaction conditions required become steadily more gentle in the order Cl < Br < I, as expected for nucleophilic substitution reactions. For example, it is typically necessary to heat 1-methylimidazole with chloroalkanes to about 80 °C for 2 - 3 days, to ensure the complete reaction, while the equivalent reaction with bromoalkanes is usually complete within 24 hours at lower temperatures (ca. 50 - 60 °C). The reaction with iodoalkanes can often be carried out at room temperature, but the iodide salts formed are light-sensitive, requiring protection from the light. The reactivity of the haloalkanes normally decreases with the increase in the alkyl chain length. In general, the excellent leaving group ability of the triflate and

tosylate, methylsulfate and ethylsulfate anions also allows the quaternization reaction to take place at room temperature. However, it is important that these reactions are carried out under an inert atmosphere, as the alkyl triflates, tosylates, dimethylsulfate and diethylsulfate are extremely sensitive to hydrolysis.[46] Many alkylating agents used are known to be highly toxic and carcinogenic, so precautions must be taken into account during their handling. Therefore, a small excess of nucleophile is necessary to avoid traces of the alkylating agent in the product. The synthesis can be carried solvent free (when the reagents are liquids and mutually miscible) or using a solvent in which the product is immiscible. This nucleophilic substitution is highly exothermic, which can lead to parallel reactions.[47,48] The overheating of the reaction solution can also promote a stronger formation of elimination products from the competing reaction (Scheme 1.2). Hence, the reaction is usually carried out in solution, being the reactants usually slowly added at 0 °C to prevent hot spots. This procedure has been a trend over the years aiming to reduce the temperature required to perform the reactions and to extend the reaction time.

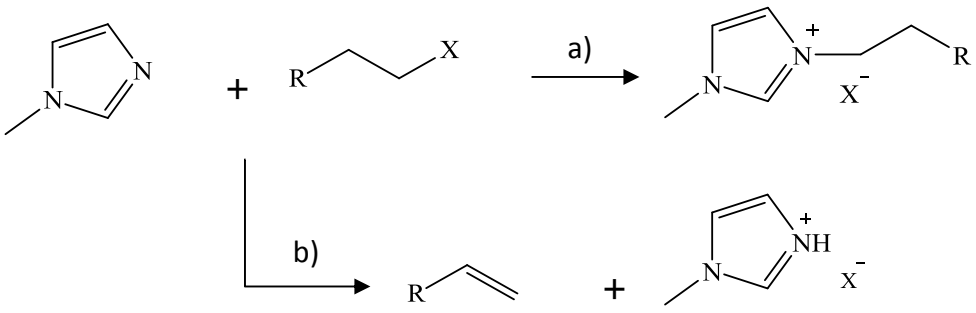

Scheme 1.2. Scheme representative of the parallel and competing reactions (a) alkylation and (b) elimination.

If the overheating is avoided, this approach allows preparing the desired ionic liquid without side products. At the end of the reaction it is only necessary to ensure that all the remaining starting materials are removed either by washing the product with a suitable solvent or by evaporation under vacuum.[46]

The thermal reaction has been used in most of ionic liquid synthesis reported in literature, being easily adaptable to large-scale processes, and providing high yields of products of acceptable purity with relatively simple methods.[46] An alternative approach involves the use of microwave irradiation.[49] Although the reactions using microwaves can be conducted with shorter reaction times, the difficulty in controlling the reaction conditions, especially the generation of hot spots, promotes a higher variability of the products formed.[50] The ultrasound technique has also been employed at this stage of the synthesis, with excellent yields, with lower reaction time and at lower temperatures, when compared with the conventional heating and stirring.[51] Here, the authors also reported that the product salts were purer than those synthesized by the conventional method. These results probably arise from the more efficient mixing achieved with the use of ultrasounds, leading to faster reactions and preventing the formation of hot spots, particularly when the mixture becomes more viscous. Continuously operating micro-reactor systems were already tested. The results show that their use constitutes an appreciable improvement over a batch system for the alkylation step, allowing a production rate of 9.3 kg of 1-butyl-3-methylimidazolium bromide, $[C_4C_1im]Br$, *per* day.[47]

By far, the most common starting material used nowadays is the 1-methylimidazole. This is readily available at a reasonable cost, and provides access to a great number of cations of interest. However, there is only a limited range of other *N*-substituted imidazole compounds commercially available and the majority is relatively expensive. Nevertheless, it is possible to prepare *N*-substituted imidazole compounds by reaction between the imidazole and a strong base, such as NaH, followed by an alkylation. A wider range of *C*-substituted imidazole compounds is commercially available, and the combination of these with distinct alkylating agents allows the formation of many different possible starting materials. Furthermore, distinct methodologies have been described in order to prepare ILs with specific alkyl chains, such as the synthesis of chiral ILs with amino acid-derivate alkyl chains.[52] Another way to directly obtain functionalized ILs is through the ring opening of sultones (Scheme 1.3). From this reaction results zwitterions which generally have high melting points. These zwitterions can react with acidic species or salts in the presence of water to form the corresponding IL.[53,54]

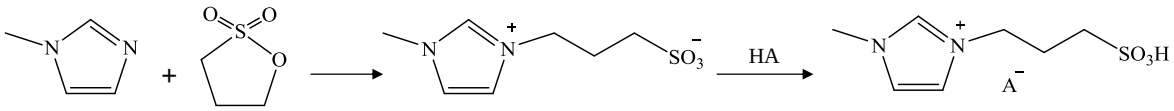

Scheme 1.3. Synthesis of ILs using a zwitterion agent.

Anion exchange

As previously mentioned, the anion-exchange reactions of ILs can be performed by the direct reaction of halide salts with Lewis acids or by anion metathesis. The formation of ILs by treatment of a quaternary halide salt (with the desired cation) with a Lewis acid, has dominated the first years of this field.[55] Generally, this reaction results in the formation of more than one anion species, depending on the relative proportions of the starting materials added. The electrolytes formed by combining aluminium chloride ($AlCl_3$) with 1-ethyl-3-methylimidazolium chloride ($[C_2C_1im]Cl$) have been considered as the most promising electrolytes for the electrolytic extraction and recycling of aluminium, being their equilibria series illustrated in Scheme 1.4.[56]

1. $[C_2C_1im]Cl + AlCl_3 \rightleftharpoons [C_2C_1im][AlCl_4]$
2. $[C_2C_1im][AlCl_4] + AlCl_3 \rightleftharpoons [C_2C_1im][Al_2Cl_7]$
3. $[C_2C_1im][Al_2Cl_7] + AlCl_3 \rightleftharpoons [C_2C_1im][Al_3Cl_{10}]$

Scheme 1.4. Equilibria series for the reaction between the $[C_2C_1im]Cl$ and $AlCl_3$.

$AlCl_3$-$[C_2C_1im]Cl$ ionic liquid displays adjustable Lewis acidity over a wide range of the molar ratio of $AlCl_3$ to $[C_2C_1im]Cl$.[57] When the molar ratio of $AlCl_3$ / $[C_2C_1im]Cl$ is less than 1, only the equilibrium (1) needs to be considered, and the IL has a basic nature (Lewis base). On the other hand, when the molar ratio of $AlCl_3$ / $[C_2C_1im]Cl$ is greater than 1, equilibrium reactions (2) and (3) are predominant and an acidic IL is formed (Lewis acid). The chloroaluminates are not the only ILs prepared using this methodology. Other Lewis acids have been employed, namely $AlEtCl_2$,[58] BCl_3,[59] $SnCl_2$[60] and $FeCl_3$.[61]

The most common method for the preparation of such liquids is simply the mix of the Lewis acid and the halide salt, with the IL being formed by the contact of both starting materials. In general, this reaction is quite exothermic, being important the cooling of the mixture vessel. Moreover, it should also be taken into consideration the addition of one component to the other in small portions to allow the adequate dissipation of the heat. The reaction should be carried out in a drybox due to the water-sensitive nature of most of the starting materials and the ionic liquid produced.[46]

Finally, ILs with distinct anions can also be prepared by metathesis of the halide salt with a metal or an ammonium salt or the conjugated acid of the required anion. The main disadvantage of these reactions is the difficulty to obtain the desired IL without impurities, which is more pronounced for hydrophilic than hydrophobic ILs. For hydrophobic ILs this reaction can be done in aqueous solution, with the product being separated during the reaction, while the halide salts (or impurities) generated remain dissolved in the aqueous phase.[62] Usually, this procedure involves the preparation of a salt aqueous solution with the desired cation, followed by the addition of an acid or a salt (usually a metal or an ammonium) with the corresponding anion. Where available, the use of a free acid is more prudent, as it leaves only HCl, HBr or HI as the by-product, being these easily removed from the final product by washing the final mixture with water. The washing should be continued until the aqueous residues are neutral, as traces of acid can cause the decomposition of the IL over time. Here, it is recommended that these reactions are carried out with cooling of the halide salt in an ice bath, as the addition of a strong acid to an aqueous solution is often exothermic. When the free acid is unavailable or inconvenient to use, it can be substituted by alkali metals or ammonium salts. At this point, it is advisable to check for the presence of halide anions in the washing solutions, for example, by testing it with a silver nitrate solution.[46] The high viscosity of some ILs makes difficult an efficient washing step, even though the presence of water results in a considerable reduction of this parameter. As a result, a number of authors have recently recommended the prior dissolution of these liquids in water-immiscible organic solvents (e.g. dichloromethane) before the washing step.

For hydrophilic ILs, the metathesis is usually performed in a water-immiscible organic solvent.[63] The resulting mixture is then filtered and the filtrate washed with water to remove any residual halide salt. The higher the miscibility of the IL in water, the less effective this process is, leading to either low yields or even the halide contamination of the IL.[64] Usually, the solubility of ILs in water is affected by the anion nature as well as by the alkyl chain length, *i.e.* the elongation of the alkyl chain promotes the decrease of the solubility. In this context, the synthesis of ILs with short chains cannot be sufficiently effective using the metathesis method, being necessary to find an alternative route for this type of synthesis. In 1992, Wilkes and Zaworotko[62] reported the first preparation of air- and water-stable ILs based on 1,3-dialkylmethylimidazolium cations by the metathesis reaction between $[C_2C_1im]I$ and a range of silver salts ($Ag[NO_3]$, $Ag[NO_2]$, $Ag[BF_4]$, Ag[OAc] and $Ag_2[SO_4]$) in methanol or in an aqueous methanol solution. This work represented a milestone in the creation of so called "second generation" ILs, and the method applied remains one of the most efficient for the synthesis of hydrophilic ILs, but it is obviously limited by the high cost of the silver salts and the large amount of by-products generated.[62] Two years later, it was reported the preparation of $[C_2C_1im][PF_6]$ from the reaction of $[C_2C_1im]Cl$ and HPF_6 in aqueous solution.[65] Over the past few years, an enormous variety of anion exchange reactions has been reported for the preparation of distinct ILs. Table 1.1 shows a representative selection of the commonly used and more eccentric examples of ILs synthesized.[46] The application of ultrasound-assisted techniques for the metathesis reaction of $[NH_4][PF_6]$ or $[NH_4][BF_4]$, using $[C_4C_1im]Cl$ in acetone, has been shown to lead to less coloured ILs in a shorter period of time than the same reaction with conventional stirring (500 rpm at room temperature).[66]

An alternative approach to the "classical" metathesis involves the use of an ion-exchange resin. This procedure consists of passing a salt solution with the desired cation through a column impregnated with the ion-exchange resin (with the desired anion), and the subsequent elimination of the eluent at vacuum. During the process, the anion of the ion-exchange resin is equilibrated with the anion present in the solution, which passes through the column. These processes are reversible and, for the success of the exchange technique, the preference of the ion-exchange resin for the counter ion of the salt (with

the desired cation) must be as high as possible when compared with its affinity for its initial counter ion. In general, the ion-exchange resin has a high affinity for ions with small volume and high valence and polarizability. When the difference between the affinities is not pronounced, an increase in the concentration of the starting material used in the solution together with several passes through the column can be effective in achieving the complete exchange of the anions.[46] ILs prepared by ion-exchange resins also contain notable amounts of remaining halides or other initial anions that have not been fully exchanged. However, the content of metal cations is often reduced when compared with the direct metathesis methods.[67]

Table 1.1. Description of some ILs prepared by the anion metathesis reaction.

IL	**Anion *source***	**References**
[cation][PF_6]	HPF_6	38,63
[cation][BF_4]	HBF_4, [NH_4][BF_4], Na[BF_4]	63,64,68
[cation][NTf_2]	Li[NTf_2]	43,63,69–71
[cation][CF_3SO_3]	$CF_3SO_3CH_3$, [NH_4][CF_3SO_3]	43,72
[cation][OAc]	Ag[OAc]	62
[cation][CF_3CO_2]	Ag[CF_3CO_2]	62
[cation][$CF_3(CF_2)_3SO_3$]	K[$CF_3(CF_2)_3SO_3$]	43
[cation][NO_3]	Ag[NO_3], Na[NO_3]	43,63,73
[cation][$N(CN)_2$]	Ag[$N(CN)_2$]	74
[cation][$CB_{11}H_{12}$]	Ag[$CB_{11}H_{12}$]	75
[cation][Ace]	K[Ace], Ag[Ace]	69,76,77
[cation][Sac]	Na[Sac], Ag[Sac]	76,77
[cation][$AuCl_4$]	$HAuCl_4$	78

The acid-base neutralization can also be used to achieve the exchange of the anions when the difference between the affinities is not significant. In this case, the ion-exchange material would be employed to exchange ions with OH^- and subsequently, with the acid of the ion desired.[79] Surprisingly and to date, only a few reports were described in literature on the use of ion-exchange resins for the large scale preparation of ILs. One exception is the work reported by Lall *et al.*[80] regarding the conversion of a series of

polyammonium halide salts into phosphate-based ILs. Wasserscheid and Keim[81] suggested that this might be an ideal method for the preparation of ILs at high purity levels, being the use of such resin materials patented in what concerns their application in the production of $[C_2C_1im][DCTA]$ from $[C_2C_1im]Br$.[82] More recently, electrodialysis has been applied to the anion exchange of $[C_2C_1im]$-based ILs.[83] In the electrodialysis processes, both cation and anion exchange membranes are applied, which have to be passed by the IL cation and the initial anion. To overcome the transport limitations of this technique caused by the size of the cation, the Donnan dialysis has been suggested, where only the small anions exchange by an anion-selective membrane. This diffusion dialysis has been applied successfully to prepare 1-ethyl-3-methylimidazolium acetate, formate and hydroxide from 1-ethyl-3-methylimidazolium chloride.[67]

The anion exchange can also be done using carbenes, highly reactive molecules that possess a lone pair of electrons on the carbon atom. The synthesis of ILs by this method may be accomplished by the reaction of *N*-heterocyclic carbenes with an acid (Scheme 1.5). Carbenes of imidazole derivatives can be prepared from an imidazolium halide in the presence of a strong base, as sodium hydride in dimethylsulfoxide (DMSO). Once generated, these carbenes can be used to obtain the corresponding imidazolium salts by reaction with the protonated form of the desired anion. This method allows obtaining ILs without halides as contaminants.[84]

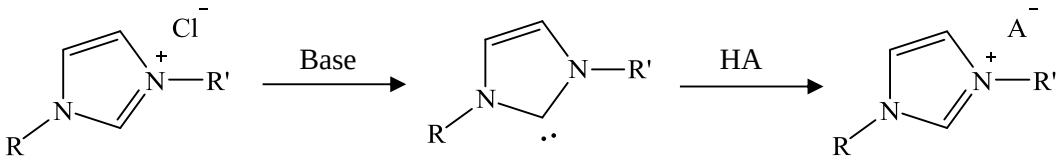

Scheme 1.5. Anion exchange through the carbene methodology applied in the preparation of ILs.

Another alternative method to the "classical" metathesis reactions to prepare ILs, is the neutralization of $[C_nC_nim]OH$ with the acid corresponding to the desired anion. The ILs belonging to the group $[C_nC_nim]OH$ can be prepared by the reaction of water with a carbene or by the addition of KOH in an ethanol solution to another solution of $[C_nC_nim]X$

in ethanol, where X is an halide. The filtration of the solid formed (KX) allows to obtain the [$C_nC_n$im]OH in solution.[85] Due to low solubility of the potassium halides in ethanol, the halogen content in the synthesized ILs using KOH was found between 0.17% and 0.69%, much lower than that observed by the "classical" metathesis reactions in two steps.[85] In fact, the neutralization of the [cation]OH with the acid containing the target anion is a popular method to form the corresponding anion of the desired IL. This methodology has been used for the synthesis of distinct ILs, namely ILs with amino acid-based anions or carboxylic acid-based anions.[86]

Choline (or cholinium), an essential nutrient usually grouped within the vitamin B complex,[87] has been attracting considerable attention as a very good candidate for combination with bio-derived anions to produce "greener" and more "benign" ILs. In 2007, Hu et al.[88] reported the synthesis of the first IL composed of choline and an amino acid, the choline prolinate, [$N_{1,1,1,2(OH)}$][L-Pro]. This IL was obtained from the choline chloride and L(-)-proline through a simple and green route (ion exchange and neutralization). Since then, a wide range of choline-based ILs containing amino acids as the anion have been described, namely those based on alanine,[89–91] serine,[89] glycine,[90,91] phenylalanine,[90,91] threonine,[90] histidine,[90] glutamine,[91] methionine,[91] arginine[91] and cysteine.[91] Fukaya et al.[92] have contributed with the first steps in the incorporation of carboxylic acids (acetic, glycolic, benzoic, propionic, tiglic, succinic, malic, tartaric, maleic, and fumaric acid) as anions to promote the synthesis of new cholinium-based ILs. After that, there is a large number of publications reporting the same approach, including other carboxylic acids such as, the butyric,[93] hexanoic,[93] pivalic,[93] lactic,[94,95] citric,[95] formic,[96] oxalic,[97] cyclopentyl acetic,[98] 3-cyclohexyl propionate,[98] salicylic,[98] levulinic[94] acids. The neutralization reaction has been an important tool to develop new ILs for some specific applications. As an example, Demberelnyamba et al.[99] have reported the synthesis of choline-based ILs with a more exotic anion, purpurin-18 photosensitizer, for possible use in Photodynamic Therapy. Recently, Taha and co-authors have developed self-buffering and biocompatible ILs for biotechnological applications, in which the anions are derived from biological buffers (Good's buffers) and combined, not only with cholinium, but also with imidazolium, ammonium and phosphonium cations.[100–102]

Zgonnik and co-workers[103] have reported a new approach to obtain ILs, what they call "IL ion cross-metathesis" (Scheme 1.6). This procedure involves the mixture of two ILs whose ions have different hydrophilic/hydrophobic nature. The first IL used is hydrophobic, with a hydrophobic anion and a hydrophilic cation. The second IL is hydrophilic, with a hydrophilic anion and a hydrophobic cation. The addition of water into the ILs mixture leads to the formation of a biphasic system, where the hydrophobic ions form the hydrophobic phase and the hydrophilic ions gather in water. Furthermore, this eco-friendly biphasic system seems to be able to induce chiral recognition. When the chiral ion of the chiral IL (the (*RR*)-tartrate moiety) was exposed to a racemic counter-ion (the protonated form of (*R/S*)-pipecoloxylidide), the tartate dicarboxylate anion moves to water layer, choosing preferentially the (*S*)-enantiomer of pipecoloxylidide as its counter-cation. The best results showed an enantiomeric excess (ee) of 30%.[103]

A structural change on the anion constitutes another approach in the synthesis of ILs. As an example, through a transesterification reaction with the appropriate alcohol, it is possible to increase the alkyl chain length on the alkylsulfate anion. In this process, an alcohol with long alkyl chain reacts with an IL with an alkylsulfate anion in the presence of an acid catalyst (Scheme 1.7). The alcohol used in this reaction should be extremely dry, otherwise the presence of water may cause the hydrolysis of the starting alkylsulfate, leading to the formation of hydrogensulfate. In order to shift the equilibrium of the transesterification reaction towards the desired products, the short chain alcohols formed during the reaction (usually methanol or ethanol) must be efficiently removed.[104]

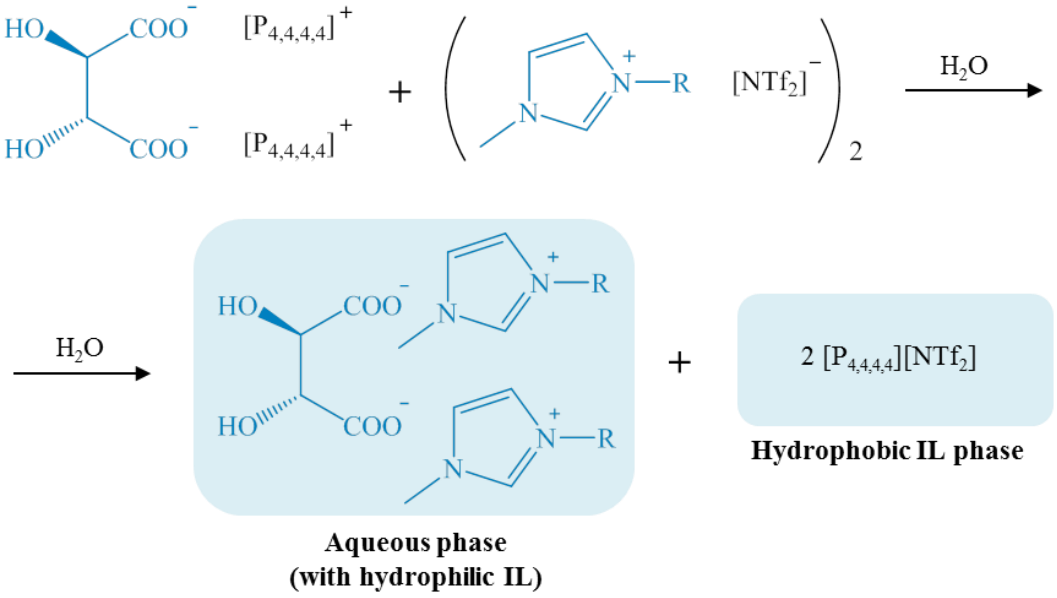

Scheme 1.6. Synthesis of two ILs by simultaneous ion exchange.[103]

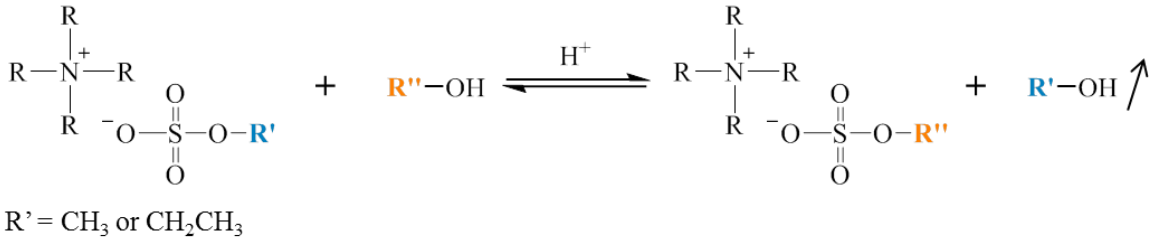

Scheme 1.7. Synthesis scheme for the transesterification reaction exemplified for a tetraalkylammonium system.[104]

Another approach used for the synthesis of ILs with non-available anions and used for the synthesis of ILs with alkylsulfonate anions with chains of different lengths, is the preparation of alkanesulfonate esters by the reaction between an alcohol and an alkylsulfonyl chloride with the desired alkyl chain in presence of triethylamine (Et_3N). For this purpose, the solution of alkylsulfonyl chloride in dichloromethane is added to the solution of alkanol and triethylamine in dichloromethane. This addition step should be done slowly, maintaining the temperature below 0°C. In this reaction, the triethylammonium chloride was formed and then removed by filtration, being the solvent removed by heating at low pressure. Alkanesulfonate ester is obtained as a liquid, which

should be purified by fractional distillation.[105] This kind of alkanesulfonate ester has been applied in the synthesis of imidazolium-[105] and quaternary ammonium-[106] based ILs. Scheme 1.8 illustrates the synthesis of alkylsulfonate esters and their use to prepare ammonium-based ILs.

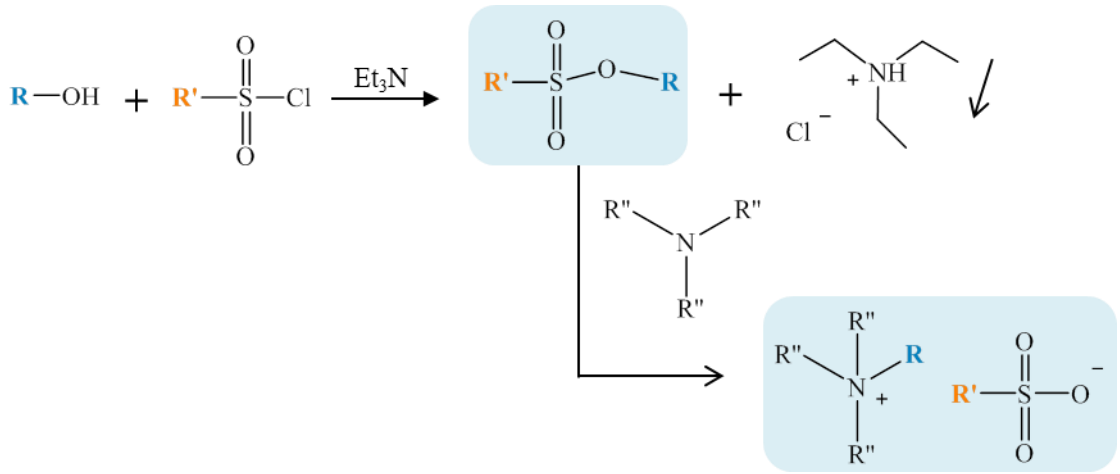

Scheme 1.8. Synthesis of alkylsulfonate esters and their use to prepare ammonium alkanesulfonates.

1.1.2 Physicochemical properties of ILs

ILs are an emerging class of novel materials with a diverse set of interesting properties. These properties can be tailored by the judicious choice of the cation, anion and alkyl chains in type, length and functionalization. With a wide palette of available anions and cations to create a vast range of ILs, and knowing how their structures affect their physicochemical properties, it will be possible in the near future to design an IL with the desired properties for specific applications, which makes ILs as "*designer solvents*".

Melting Points

By definition, the solid-liquid transition temperatures of ILs are lower than 100 °C. In fact, most ILs described in literature are also liquid at room temperature. The most efficient method for measuring the transition temperatures is by differential scanning calorimetry

(DSC). Other methods have been used, including cold-stage polarizing microscopy, Nuclear Magnetic Resonance (NMR), and X-ray scattering. According to the technique employed it is common to obtain quite different results.[107] In contrast to the conventional organic solvents, most ILs show wide liquid ranges, and thus, their use as solvents may be extended over wide temperature ranges. Some reviews suggest that the melting point of ILs results from a subtle balance of cation and anion symmetry, flexibility of chains in the ions, size of the ions, and charge dispersion.[107,108] A well-known trend in the 1-alkyl-3-methylimidazolium [$C_nC_1$im] cation family is the melting point reduction with the increase in the alkyl chain length up to n < 8. With n > 8, the compounds exhibit an increase in the melting point, which is attributed to inter-chain hydrophobic packing and the subsequent formation of bilayer-type structures.[109,110] This behaviour can be seen in Figure 1.3, where it is shown the melting points for a series 1-alkyl-3-methylimidazolium hexafluorophosphate ([$C_nC_1$im][PF_6]) ILs, being the melting point highly dependent on the alkyl chain length.[38,109,110] This V-shaped trend depicted in Figure 1.3, was also observed for the [NTf_2][111] and [BF_4][64] imidazolium series.

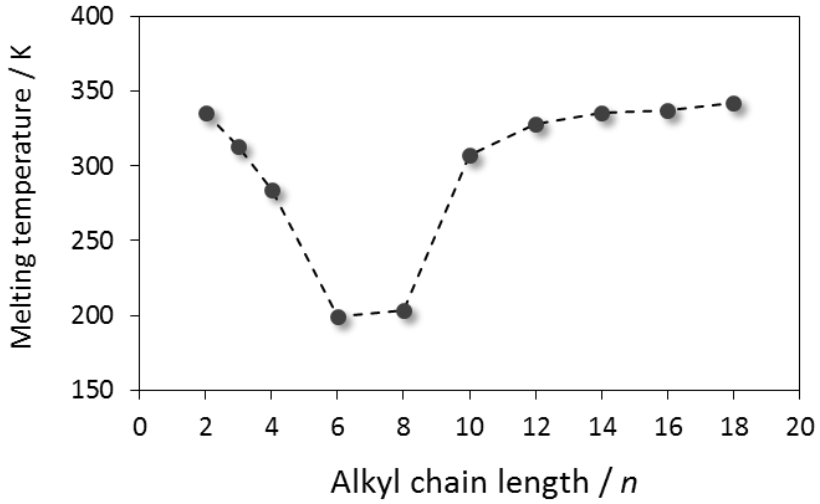

Figure 1.3. Melting temperatures for a series of [$C_nC_1$im][PF_6].

This trend was rationalized in terms of the cationic structure, as depicted in Figure 1.4. Here, it can be observed that at 4Å, the charge-rich region is located on the imidazolium

ring, at 5.5Å it is situated the symmetry-breaking region responsible for the decrease in the melting point, and from 12Å it is positioned the hydrophobic region that increases the IL melting point due to van der Waals interactions.[110] On the other hand, for most of the pyrrolidinium salts, the minimum melting point occurs for alkyl chain lengths of either *n* = 3 or 4.[112] Furthermore, an increased melting point is observed with the branching of the substituent alkyl chain and/or the addition of some particular functional groups. For example, the replacement of a methylene by an ether group results in a lower melting point due to the repulsion effects on an impaired electron pair. On the other hand, the addition of electron-acceptor groups conjugated, for example, with the pyridinium ring results in higher melting points.[81] Recently, Rodrigues et al.[113] have explored the *n* vs. iso isomerization effect on the thermophysical properties of ILs, and concluded that the iso-alkyl pyrrolidinium IL, [iC$_4$C$_1$pyrr][NTf$_2$], present higher melting temperature than the *n*-alkyl isomer.

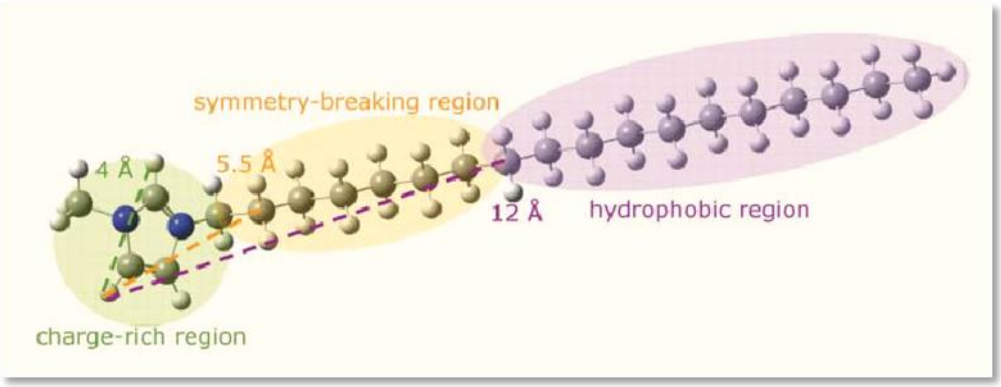

Figure 1.4. Structure of a 1-methyl-3-octadecylimidazolium cation showing the relevant structural regions with impact on the melting points.[110]

As mentioned above, the symmetry of the ions plays an important role in the melting point of ILs. Actually, a high cation symmetry tends to produce ILs with a higher melting point.[114] With regard to impact of the conformational flexibility, higher flexibility leads to lower melting points. Many occurrences of conformational flexibility have been reported, including crystallographic analysis considering systems where the less energetically

preferred conformation crystallizes, such as the *cis*-conformation for the [NTf_2] anion,[115] the twisted/half-chair ring disorder for [$C_nC_1$pyrr] salts[116] and the *cis*-conformation considering [$C_nC_1$im] alkyl chains.[117] These effects may contribute to the lower lattice energies and lower melting points.

Other factors such as, the crystalline structure, shape, conformational equilibria, and also other interactions, namely π-π stacking, hydrogen bonds and van der Waals forces, must be taken into account in order to explain the melting point.[107,118] Finally, a greater charge delocalization results in lower melting points,[119] which can be explained by the decrease of the intermolecular interactions' strength. Interesting melting point trends are also observed with slight modification of ions. For example, changes in the cation's central atom have a significant effect on the melting point, being observed that ammonium-based ILs present higher melting temperatures than the corresponding phosphonium structures.[120]

Decomposition Temperature

Melting and decomposition temperatures are two of the most remarkable properties for ILs, especially for their application as solvents, because they determine the liquidus range of these ionic compounds. Given its negligible pressures the upper operating limit of an IL is given by its thermal decomposition. Many thermal stability measurements are done by thermogravimetric analysis (TGA), more specifically ramped temperature analysis (also called as step-tangent or dynamic analysis) with the most common heating rates being 10 °C min^{-1} and 20 °C min^{-1}.[109,121,122] In general, the thermal stability range of ILs is large and the decomposition temperatures of some ILs may be above 400 °C.[19] In most cases, decomposition occurs with complete mass loss and volatilization of the component fragments. Grimmett et al.[123] have studied the decomposition of imidazolium halides and identified the degradation pathway as E2 elimination of the *N*-substituent.

The thermal stability of the ILs is mainly dependent on the anion nature. Considering the most common anions used in the ILs synthesis, the decomposition temperatures decrease following the order: $[(CF_3CF_2SO_2)_2N]^-$ > $[NTf_2]^-$ > $[CF_3SO_3]^-$ > $[BF_4]^-$ ≈ $[PF_6]^-$ > Br^- > Cl^-, so that

ILs containing weakly coordinating anions are most stable at high temperatures.[124] It is clear that halides significantly reduce the thermal stability, since they possess both a relatively high nucleophilic and basic character. Although the effect of the cation nature or alkyl chain length is less obvious considering the decomposition temperatures, the effect of some cations has been reported.[107,125,126] In general, it has been shown that pyrrolidinium ILs are more temperature resistant than their imidazolium, pyridinium and non-cyclic tetraalkyl ammonium, in that order.[127–130] Furthermore, some works demonstrated a significant influence of the alkyl chain length of the cation on the thermal stability of ILs. Generally, increasing the alkyl chain length decreases the thermal stability, being this observed for imidazolium ILs with the Cl^-,[109] $[PF_6]^-$,[131,132] or $[NTf_2]^-$ anions.[109,133]

Viscosity

The viscosity of a fluid arises from the internal friction of the fluid, and it is externally manifested as the resistance of the fluid to its natural flow. This physical property is of utmost importance from the industrial point of view, being essential for the design of process units, engineering fluids, and for process simulation and optimization, because the viscosity strongly affects the flow behaviour and the transport phenomena, being one of the physical properties mostly studied, along with density.[134–139] The viscosities of many ILs are strongly dependent upon temperature.[140]

In general, ILs are more viscous than most organic fluids commonly used in the chemical industry.[134] The viscosity of ILs vary widely depending on the type of cation and anion, ranging at least from 6 - 7600 mPa at 20°C and atmospheric pressure.[141] Their high viscosity can be considered as a disadvantage for some industrial applications because it would negatively affect those processes, such as pumping, mixing, stirring, combined heat and mass transfer operations. However, it can be favourable in other situations, namely when ILs are utilized as lubricants. Nevertheless, viscosity may be fine-tuned through an adequate cation/anion combination leading to the range of viscosity desired for each application.

The viscosity of ILs is highly dependent on the structure and interactions between their ions, namely electrostatic, van der Waals and hydrogen bonding forces. However, the relationship between the IL structure and their viscosity is still not entirely clear. Literature suggests that several factors can contribute to the high viscosity, such as the ions form, the charge density, the contribution of other interactions and conformational changes in the alkyl chains.[142] For example, the delocalization of the charge on the anion, such as through fluorination, decreases the viscosity by weakening the hydrogen bond forces.[143] Gardas and Coutinho[134] have analysed the viscosity dependence of several ILs with their structure showing that, with the same cation ($[C_4C_1im]^+$, $[C_4C_1py]^+$, $[C_4C_1pyrr]^+$), the viscosity increases with the anion type, following the trend: $[NTf_2]^-$ < $[CF_3SO_3]^-$ < $[BF_4]^-$ < $[C_2SO_4]^-$ < $[C_1SO_4]^-$ < $[PF_6]^-$ < $[OAc]^-$ < Cl^-. In the same work, it was also reported that for ILs with a common anion ($[NTf_2]^-$) and similar alkyl chain length (butyl) on the cation, the viscosity increases following the order: imidazolium < pyridinium < pyrrolidinium.[134] The ILs with lowest viscosities are based on $[N(CN)_2]^-$, $[N(FSO_2)_2]^-$, $[C_nF_{2n+1}BF_3]^-$ with n < 4 and $[NTf_2]^-$ anions.[125,134,144] The low viscosity is related to the high flexibility (e.g., for $[NTf_2]^-$) and to the electronic delocalization (e.g.,$[N(CN)_2]^-$).

I general, there is a pronounced increase in viscosity as the alkyl chain in the cation grows, as was reported for imidazolium, pyridinium, alkylammonium, and pyrrolidinium based ILs.[143,145,146] This effect can be explained because of the increase in the van der Waals interactions. However, as previously observed for melting temperature, there seems to be two regions in the viscosity dependency of the alkyl chain that can be relate to the structural segregation occurring in longer alkyl chain ILs.[147] Surprisingly, some ILs with ethyl chains are less viscous with the corresponding ones with methyl chains. This fact may be due to more flexibility of the ethyl chain than that of the methyl group (more conformational degrees of freedom, which may partly compensate the increase of van der Waals interactions).[144] On the other hand, the higher the number of alkyl chains, the higher the viscosity. Gaciño et al.[148] have compared the viscosity data at high pressure of $[C_4C_1C_1im][NTf_2]$ and $[C_4C_1im][NTf_2]$, concluding that the addition of another methyl group on the $[C_4C_1im]^+$ cation leads to a viscosity increase of up to 75%. Some author have investigated the impact of cation symmetry of the ILs on their viscosity. Zheng et al.[149]

observed that the viscosity of the asymmetric imidazolium-based ILs is larger than that found for the symmetric counterparts. Similar behaviour was reported by Rocha et al.[147] The effect of *n* vs. iso isomerization of aromatic and non-aromatic ILs on their viscosities were investigated by Rodrigues et al. The authors have observed a clear differentiation between the aromatic and non-aromatic ILs. While for the aromatic ILs the iso-alkyl ILs presents a higher viscosity than the n-alkyl, the non-aromatic ILs presented the opposite behaviour.[113] Recently, it was reported that the viscosity can be affected by the nature of the cation's central atom. The change of a *P* atom for a *N* leads to a surprising increase in the viscosity of all the IL pairs studied.[120]

Density

Density is perhaps the most easily accessible and unambiguous physical property of ILs. For ILs, typical densities range from 0.96 - 1.65 $g \cdot cm^{-3}$ at 20 °C.[141] The ILs density is temperature dependent, decreasing linearly with increasing temperature.[107] In addition, the impact of impurities on the density is far less important than for the viscosity.

The effect of the cation on the density has been investigated by several authors.[145,150,151] Regueira et al.[152] have reported that the density for $[NTf_2]$-besed ILs decreases in the order: $[C_4C_1im]^+ > [C_4C_1py]^+ > [C_4C_1pyrr]^+$. The trend can be related to the planarity of the aromatic moieties and aromatic interactions. Nevertheless, this trend seems to strongly depend on the anion. For example, Sánchez et al.[145] have reported that for dicyanamide ILs, pyrrolidinium ILs are denser than imidazolium and pyridinium ILs. In general, density decreases by increasing the length of the alkyl chains in the cations or anions.[136] It was reported that with the elongation of the alkyl chain, the density of 3-alkoxymethyl-1-methylimidazolium tetrafluoroborate salts linearly declines.[153] This effect can be explained by the increasing of the dispersive interactions between the aliphatic carbon chains (but also a decreasing of the polar or H-bond interactions) with the increase of chain length, leading to a lower dense packing. The same trend was observed for quaternary ammonium ILs.[154] Some works have suggested that the branching of the alkyl side chain not affect their density significantly.[113,155] As mentioned for both the melting

point and viscosity, the density was also shown to be affected by the cation's central atom. In fact, the authors confirm that for all pairs studied, the ammonium-based ILs have a higher density than the corresponding phosphonium-based ILs.[120]

The anion structure similarly affects the density. Recently, Regueira et al., among other authors, have investigated the effect of the anion structure in the ILs density.[152,156,157] These authors found for densities of $[C_4C_1im]$-based ILs the following trend: $[(CF_3CF_2SO_2)_2N]^-$ > $[NTf_2]^-$ > $[PF_6]^-$ > $[CF_3SO_3]^-$ > $[ClO_4]^-$ > $[CF_3CO_2]^-$ > $[C_1SO_4]^-$ > $[BF_4]^-$ > $[C_1(OC_2)_2SO_4]^-$ > $[NO_3]^-$ > $[C_8SO_4]^-$ > $[N(CN)_2]^-$ > $[OAc]^-$ > $[C_4C_4PO_4]^-$ > $[C(CN)_3]^-$. Since the density is related with the ILs molecular weight, the presence of heavy atoms leads to denser ILs. Thus, the replacement of hydrogen atoms by heavier atoms such as fluorine, chlorine or bromine elements leads to an increased density.[158] The molar mass of the anion significantly affects the overall density of ILs. As an example, the imidazolium-based ILs' density increases with the molar mass of the anion, following the order $[BF_4]^-$ < $[CF_3SO_3]^-$ < $[PF_6]^-$ < $[NTf_2]^-$ < $[FAP]^-$.

Volatility and Vapour Pressure

It was claimed for a long time that one of the main characteristics of ILs was their non-volatility, making them known by their non-measurable vapour pressure, hence, they could not be distilled. Nevertheless, some works showed that ILs could be distilled under reduced pressure at high temperatures, although for temperatures closer the ambient condition, their vapour pressure remains almost negligible.[159–161] In this sense, the measurement of their vapour-liquid equilibria properties remains extremely difficult due to their very low volatility and decomposition temperature. The competing effects of fluids decomposition and vaporization make it difficult to measure some properties such as, the enthalpies of vaporization and of course, the vapour pressures.[162]

Considering their volatility, ILs can be divided into two main groups: the protic species (with an acidic proton on the cation) and the aprotic ILs. Considering the protic ILs, which can be easily produced by the combination of a Brønsted acid and a Brønsted base, as depicted in Scheme 1.9, most of them are easily distillable and present high vapour

pressures. These are justified by the proton transfer from the cation to the anion upon vaporization, which leads to the original neutral acid and base species that have, in general, high vapour pressures (Figure 1.5). To obtain protic and distillable ILs, it is necessary to take into account the ionization level of their ion species. To access volatile states, the acidity of the promoter organic acid and the conjugated acid of the base must be sufficiently different, causing thus a sufficient degree of ionization capable of to produce a pure salt in a liquid form.[163] The vaporization of the aprotic ILs occurs by the direct transference of the ions to a gas phase, as depicted in Figure 1.5.[161] It was demonstrated that the vapour pressure of ILs can be very small (<1 Pa) even at temperatures up to 300 °C, which for some ILs is below the decomposition temperature.[162] The main decomposition mechanisms of ILs on distillation are the dealkylation or transalkylation of the cation, which are phenomena favoured by the presence of nucleophilic anions. As a result, anions with low nucleophilicity, such as triflate and $[NTf_2]^-$, leads to more thermally stable ILs than ILs with halides, sulfates or carboxylates anions.[161]

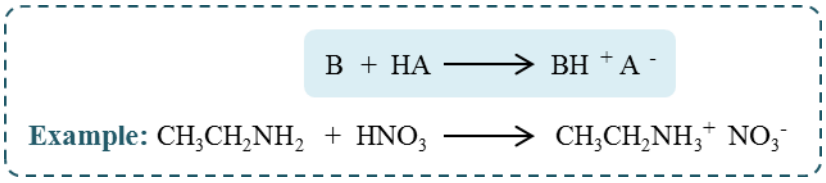

Scheme 1.9. Protic-IL formation through proton transfer from a Brønsted acid (HA) to a Brønsted base (B).

A thermodynamic study concerning the vaporization of an extended series of ILs, $[C_nC_1im][NTf_2]$, have found that their thermodynamic properties of vaporization present a trend shift along the studied series, which are related to a change in the molecular structure of the liquid for compounds larger than $[C_6C_1im][NTf_2]$.[164,165] Recently, Rocha et al.[166] have investigated the cation symmetry effect on the thermodynamic properties of vaporization for the symmetric $[C_{n/2}C_{n/2}im][NTf_2]$ ILs, with *n* = 4, 6, 8, 10, and 12. It was

concluded that the symmetric imidazolium-based ILs present a higher volatility than the asymmetric counterparts, $[C_{n-1}C_1im][NTf_2]$.

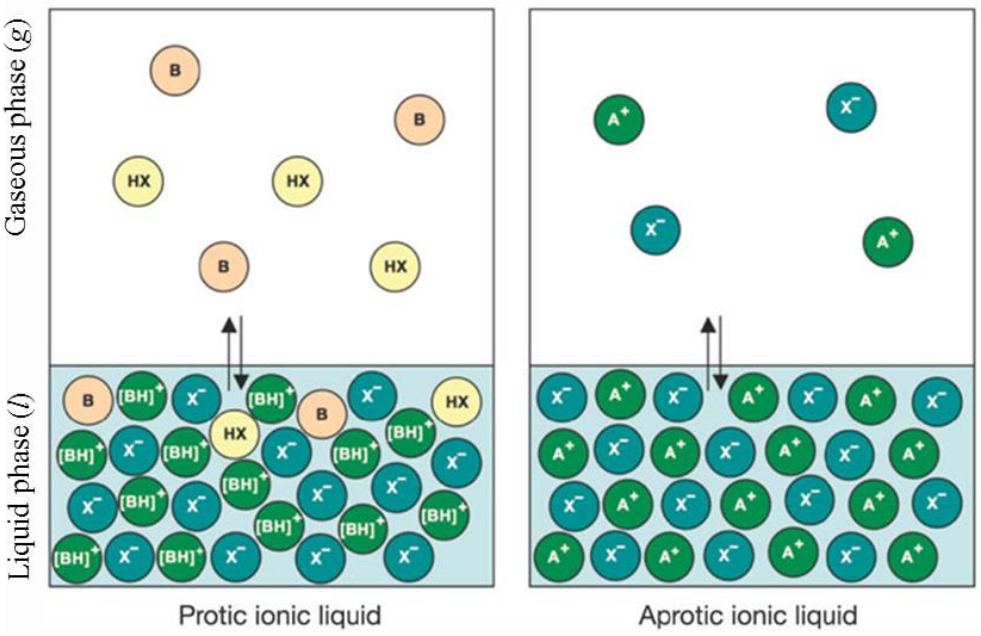

Figure 1.5. Schematic representation of the distillation process for protic and aprotic ILs.[161] For protic ILs, a dynamic equilibrium exists between the ionic and dissociated forms: $[BH]^+X^-$ (l) ⇆ B (l) + HX (l) ⇆ B (g) + HX (g). Green circles represent the cations, blue circles represent the anions and the remaining coloured circles represent neutral molecules. For the gaseous phase over the aprotic IL, the representation is purely schematic and has no implication for the actual degree of aggregation.

Surface tension

The interfacial properties are very important for many industrial applications, namely in the control of the mass transfer efficiency in liquid-liquid and gas-liquid extractions. Furthermore, it should be highlighted that surface tension data are central in research areas related to colloid and interface sciences. Tariq et al.[167] have recently published a critical review on surface tension of ILs. In general, the liquid/air surface tension values of ILs are higher than those of conventional solvents (hexane 18 $mN \cdot m^{-1}$ at 25 °C), but not so high as water (72 $mN \cdot m^{-1}$ at at 25 °C).[154] These larger than usual surface tension data

decrease quite slowly with increasing temperature, a fact that constitutes a fingerprint of their underlying extremely broad liquid ranges.[167]

There is a very strong relation between the anion/cation interaction strength and the ILs surface tension. Moreover, the relative orientation of the cations and the anions at the surface has been postulated as determinant for this property.[168] Actually, the surface tensions of ILs are ruled by the preferential orientation of the alkyl group to the surface. Different types of cations (with long alkyl chain) marginally influence the differentiation of the ILs surface tension, since their surface is very similar to alkanes.[167] In general, the surface tension of ILs decreases with the increase of the cation alkyl chain length.[169–174] Santos et al.[174] showed that the surface tension of ILs decreases with increasing the chain length independently of the chain location (on the cation or anion). However, some authors have mentioned a different behaviour of the surface tension for some ILs conjugated with the $[NTf_2]^-$ anion, i.e. beyond a certain size of the alkyl chains, the surface tension appears constant.[168,175,176] Rodrigues et al.[113] have reported that the aromaticity of the ILs seems to influence this interfacial property. The slight increase of the surface tension from the aromatic to non-aromatic ring ILs should be related to the expected higher cohesive energy of the bulk in the non-aromatic fluids. In the same work, the authors have investigated the effect of *n* vs. iso isomerization, showing that this effect on the surface tension seems to be different for ILs with 5 and 6 atom rings. While the former, the iso isomers, present a lower surface tension, the effect is negligible, or even opposite, for the latter.[113] Considering the anion impact, Freire et al.[170] proposed that this interfacial property decreases for ILs with increased anion size, a conclusion attributed to the higher charge delocalization promoted in larger anions and, therefore, a reduction on the hydrogen bond strength between the anion and cation. However, using a wide range of anions, Martino et al.[177] found no general trend with the anion size.

Electrical Conductivity

Electrical conductivity is an important property of ILs to evaluate their suitability for electrochemical processes, solar power applications, or in lithium batteries. Due to their

ionic composition, it is expected that ILs present a high electrical conductivity. However, their conductivity values are quite low when compared to conventional aqueous electrolyte solutions used in electrochemical applications (40 - 75 $S \cdot m^{-1}$).[178] The low conductivities can be attributed to the available charge, as well as the reduced mobility resulting from the large ions size. Through the appropriate cation/anion combination it is possible to design an ionic liquid with a specific conductivity characteristics. Electrical conductivity of an IL depends on the mobility of its ions, which is influenced by the viscosity, ion size, and the ion association. In general, small ions with little interionic interactions result in high conductivities.[179] Ionic liquid conductivity appears to be only weakly correlated with the size and type of the cation. The increase of the cation size tends to give rise to lower conductivity, most probably due to the lower mobility of the larger cations. The overall trend in conductivity with respect to cation type follows the order: imidazolium ≥ sulfonium > ammonium ≥ pyridinium.[19] The planeness of the imidazolium ring seems to confer a higher conductivity than the tetrahedral arrangement of alkyl groups displayed by the ammonium ILs.[41,180] Considering the imidazolium- and pyrrolidinium-based ILs, the conductivity decreases as the alkyl chain length increases, whereas it increases when ether groups are added to the alkyl chain.[143,181] The correlation between the anion type or size and the ionic liquid conductivity is still not clear.[182–184] As an example, ILs with large anions, such as $[NTf_2]^-$, often exhibit higher conductivities than those with smaller anions, like the $[OAc]^-$.[19]

Water Solubility

The solubility of ILs in water is of significant relevance for both the process design and the evaluation of their environmental impact, being this parameter strongly dependent on both the cation and anion, namely anion nature and cation alkyl side chain length.[185] Indeed, this property is related to the standard Gibbs energies of the transfer of ions constituting the ionic liquid from the ionic liquid phase to water.

Most of ILs present a complete miscibility in water at room temperature. Those that are not completely soluble, seams to display a linear dependence of the logarithm of their

solubility in water with their molar volume.[186–188] As an example, Figure 1.6. depicted that correlation for the [PF_6]-based ILs at 298.15 K.[187] Thus, although the solubility of ILs in water is more strongly dependent on the anion than on the cation, the effect of the cation size is more pronounced, as illustrated through the differences of one order of magnitude when comparing the solubility of [C_4C_1im][PF_6] with [C_8C_1im][PF_6] and even of two orders of magnitude by comparing [C_2C_1im][NTf_2] with [C_8C_1im][NTf_2] in water at 318 K.[189]

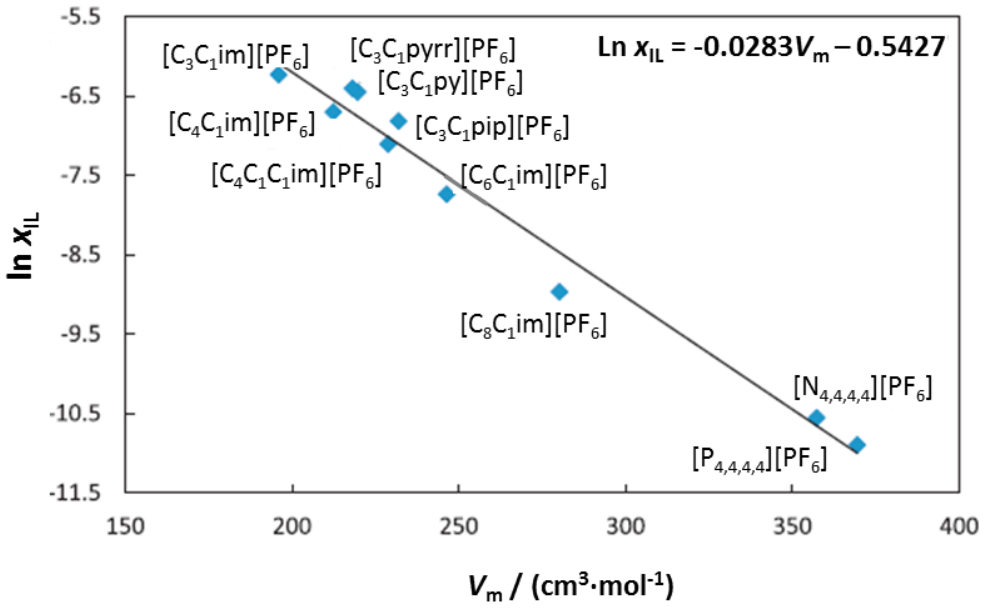

Figure 1.6. Solubility of [PF_6]-based ILs in water (expressed in mole fraction) as function of the IL molar volume at 298.15 K.[187]

In general, the ILs solubility in water decreases with the alkyl side chain length at the cation.[9] Exploring the hydrogen C2 substitution by a methyl group in the imidazolium ring, it can be seen in Figure 1.6 that the [$C_4C_1C_1$im][PF_6] presents a solubility in water between the [C_4C_1im][PF_6] and [C_6C_1im][PF_6] indicating that the hydrogen bonding is not one of the dominant factors in the water solubility.[189] Furthermore, the branching of the cation alkyl chain was observed to increase the ILs solubility in water.[190] In fact, contrary to what is observed for the IL-rich phase,[7] where the solubility of water in ILs largely depends on the

IL availability of electrons for privileged interactions, the solubility of ILs in water is primarily defined by their molar volume and anion hydrophobicity.[6,7,9,189,191,192] Finally, and taking into account the imidazolium-based ILs, it was reported that the solubility decreases following the anion order: $[BF_4]^-$ > $[C(CN)_3]^-$ > $[PF_6]^-$ > $[NTf_2]^-$.[189]

Recently, the scope of ILs as functional fluids has been expanded to include their mixtures with water for multiple applications.[193] Several reviews have focused on the structure and behaviour of ILs clusters in water.[194] ILs bearing long alkyl chains (contain, in general, at least eight carbon atoms) have been considered as a new class of surfactants and named surface active ionic liquids (SAIL). Due to the co-existence of a charged hydrophilic head group and a hydrophobic tail domain, SAILs can exhibit high ability to self-aggregate in water. The understanding of the molecular interface interactions of SAILs in aqueous solutions is a prerequisite for sustainably predicting, controlling, and designing IL properties for application in industrial scale processes.[195] A number of computational and experimental techniques, including molecular dynamics simulations, surface tension and conductivity measurements, potentiometry, UV-Vis spectroscopy, fluorescence probes, NMR spectroscopy, mass spectrometry, isothermal titration calorimetry, light scattering and small-angle X-ray and neutron scattering (SAXS and SANS) have been applied to understand the self-aggregation of SAILs in water.[196–203] The critical micellar concentration (CMC) is a basic parameter of surface chemistry and colloid science that has been largely determined for SAILs in aqueous solution. Several studies showed that the CMC is strongly influenced by the structure of the IL, in particular in terms of the alkyl chain length of the hydrophobic tail unit.[196–198,204–208] As for conventional cationic surfactants, a linear correlation between the number of carbon atoms on the cation alkyl chain and the logarithm of the CMC has been observed. The CMC values decrease significantly with increasing alkyl chain length, indicating that the hydrophobic interactions become stronger as the alkyl chain length increases.[208,209] This linear relationship can be applied for predicting the CMC for a homologous series of linear-single chain amphiphiles at a fixed temperature. The CMC is also dependent on the relative sizes of their hydrophilic and hydrophobic domains. A larger hydrophobic domain results in a lower CMC, and a more hydrophilic domain area leads to a higher CMC.[210]

The introduction of the second alkyl substituent on the imidazolium cations may also play a dominant role in CMC values of ILs. For example, lower CMC values were verified for the ILs with butyl substituents instead of methyl in the imidazolium ring.[211] Wang et al.[212] investigated the influence of the type of ring in the cations on the aggregation behaviour by comparing the CMC values of $[C_8C_1im]Br$, $[C_8C_1py]Br$ and $[C_8C_1pyrr]Br$. The results indicated CMC value increase in the order $[C_8C_1py]Br < [C_8C_1im]Br < [C_8C_1pyrr]Br$.[212] This trend results from a balance among the hydrophobicity of the cations, binding strength of the cations with a given anion, and the steric repulsion between the cations. The aggregates of $[C_8C_1pyrr]Br$ were formed unfavorably due to probably its biggest van der Waals volume, that is, the biggest steric hindrance and the weakest interaction with Br anion. On the other hand, the difference in steric hindrance between $[C_8C_1im]^+$ and $[C_8C_1py]^+$ is small. Therefore, the stronger aggregation of $[C_8C_1py]^+$ is driven by its stronger hydrophobicity.[195]

Gemini ILs are a class of SAILs in which two monomeric surfactant groups (two hydrophilic and two hydrophobic) are coupled together via a spacer. Their CMC values depend on the length of the alkyl linkage chain connecting the two cations, and on the length of the free alkyl substituents. Elongation of the alkyl linkage chain, as well as the free alkyl chain, leads to a linear decrease of the CMC. [211]

As previously mentionated, the nature of ILs anions determines the water solubility of ILs and cation-anion interactions. Therefore, the aggregation of ILs in water is also affected by the nature of their anions. The anion impact on the aggregation of imidazolium ILs in water has been studied by Wang et al.[212] Considering the $[C_8C_1im]^+$ cation, CMC values increase in the order: $[CF_3CO_2]^- < [NO_3]^- < Br^- < Cl^- < [OAc]^-$. This trend is correlated with the Hofmeister series of the anions for cationic surfactants.[213] Although the halogen atoms might lead to a series of environmental problems, most studies reporting SAILs focus on the halogen containing ILs. In the past few years, a number of greener amphiphiles based on the structures of ILs have emerged, such as amino acid-based,[214] alkylcarboxylate-[215] and alkylsulfatebased[216] SAILs free of halogen. Blesic et al.[217] studied the self-aggregation of both neat and aqueous solutions of catanionic SAILs, 1-alkyl-3-imidazolium alkylsulfonate salts ($[C_nC_1im][C_mSO_3]$, n = 8, 10 or 12; m = 1 and n = 4 or 8; m

= 4 or 8). They observed when the amphiphilic character was present on both the cation and anion (n=4 and 8, m=4 and 8), the novel catanionic surfactants exhibited an unanticipated enhanced reduction of surface tension.

Recently, Barycki et al[218] proposed the first QSPR model for predicting the CMC for ILs. In that study, the authors identified the length of cation (the size of the hydrophobic domain), the level of cation's folding/sphericity and anion's size as the structural properties responsible for the process of micelles formation.

Finally, since amphiphilic compounds are capable of interacting with cell membranes and other nonpolar surfaces, both toxicity and biodegradation of those compounds can be directly related to their aggregation nature. Consequently, the CMC provides an important indicator indicator to toxicity and biodegradability of ILs.[219]

1.1.3 Ecotoxicity of ILs

As mentioned before, if large-scale industrial applications for ILs are implemented, their entry to the aquatic environment through accidental spills or as part of liquid effluents is the most probable pathway for creating environmental hazards. Consequently, aquatic toxicology investigations have attracted considerable interest concerning the ILs environmental safety. Despite initial efforts that have been made to offer a preliminary insight into the environmental behaviour of ILs,[220–226] data on their ecotoxicity, biodegradability, bioaccumulation and distribution in different environmental compartments is still scarce, and needs to be expanded to improve the knowledge for the prospective design of safer ILs. Up to now, a broad range of testing models (bacteria, fungi, crustaceans, algae, aquatic plants, mammalian cell lines and vertebrates) has been used to evaluate the toxicity of ILs.[221,223,224,227–229] Here, it is noted that the toxicological effect of the IL depends, not only on their structure, but also on the biological system under evaluation. In what concerns their aquatic toxicity, the most tested trophic levels are decomposers represented by marine bacteria,[228,230–232] producers represented by microalgae[228,233–236] and primary consumers represented by cladocerans.[228,236–238] Toxicity tests with freshwater microalgae and daphnids are highly recommended as part of the

test batteries required for the ecological risk assessment of new and existing chemicals.[239] The standard assay using the luminescent marine bacteria *Vibrio fischeri*, the Microtox® bioassay, is today one of the most widespread toxicological bioassays due to its quick response, simplicity and cost-effective implementation.

Considering the experimental evidence, some trends ruling the IL ecotoxicity have been established. For example, ILs with longer cation alkyl side chains tend to be more ecotoxic ("side-chain effect") until a certain threshold, above this threshold there is no further increment in the IL toxicity ("cut-off effect").[223] There has also been an agreement on the fact that functionalized cations with polar groups tend to produce less toxic ILs, when compared with non-functionalized counterparts as they are more hydrophilic,[240–242] and that the cation is the main driver of toxicity.[71,222,230] With regard to freshwater microalgae, several species have been studied, being concluded that in general, the cation alkyl chain length of the ILs has a pronounced effect towards all these producers. In what concerns the use of cladocerans, *Daphnia magna* is one of the most used daphnids, being of fast reproduction rate and sensitivity to environmental conditions. Literature results suggest that cladocerans are also strongly affected by the alkyl chain length.[243] Concerning the Microtox® bioassay, it has been widely used in the study of the influence of the anion moiety,[230,244,245] cation core[71] and alkyl chain length[231,244] of several ILs with results that are qualitatively in agreement with those carried out for species of higher trophic levels, namely algae and cladocerans. Indeed, it has been shown that the anion moiety can contribute to the (eco)toxic profile of ILs, but the anion presents in general, a much lower impact upon the IL toxicity[223] when compared with the side-chain effect.[240,244] An exception is the $[NTf_2]^-$ anion, since its pronounced negative effect towards different organisms was verified, independently of the cation.[240]

In addition to their chemical structure, there have been attempts at understanding the relationship between the ILs toxicity and other properties, namely their hydrophobicity,[246] lipophilicity,[191,244,247] membrane water partitioning,[247] central atom,[120] and the aromaticity.[228] In general, the IL toxicity increases with the increase in hydrophobicity/lipophilicity, octanol-water partition coefficients and aromaticity. Indeed, some authors have suggested that the enhancement of the hydrophobic/lipophilic

character of the IL cation with the alkyl chain elongation increases the possibility of its interaction with the cell membrane phospholipids and hydrophobic domains of the membrane proteins, promoting the membranes disruption and, consequently, leading to the cell death.[221] Considering the influence of the cation's central atom to the ILs toxicity, it was shown that ammonium-based ILs present lower toxicities than the respective phosphonium congeners, proving that the presence of a phosphorous or a nitrogen as the cation's central atom has a significant impact on the IL toxicity.[71,120] The lower toxicity of the ammonium compounds can be attributed to their lower hydrophobic nature (higher polarities) when compared with their corresponding phosphonium counterparts.[120]

Although it was concluded that the cation aromatic nature plays an important role on the ILs toxicity, the aromatic ILs based on the imidazolium cation are, by far, the most widely studied family.[224] Some recent studies focused on emerging classes of more "biocompatible" ILs, such as cholinium- and ammonium-based ILs.[232,236,248] In fact, non-aromatic ILs promise to be important tools to look for "greener" and more benign ILs.

Apart from a low ecotoxicity, current environmental legislation makes insistent demands for non-persistent chemicals. For chemicals to be considered as "sustainable" or "green", complete and rapid biotic and/or abiotic degradation is a crucial requirement.[10] The influence of ILs' structure on biodegradation potential was intensively studied and it was concluded that the degree of degradation is strongly influenced by the length of the alkyl side-chain, core ring structure and by the presence of functionalized groups (e.g. ester, amide),[249–251] while the impact of the anion structure is less pronounced.[252] For example, Stolte et al.[251] studied biodegradation of 27 ILs with different head groups and attached side-chains and they found that imidazolium ILs proved less degradable than pyridinium, while longer side-chains were more susceptible to biodegradation. A promising design criterion towards achieving biodegradability is the introduction of polar functional groups (e.g. ether, hydroxyl or nitrile functions).[226] Furthermore, different anions such as alkyl sulfates, linear alkyl sulphonates, linear alkylbenzenesulphonates and organic acid salts are recommended with respect to their biodegradability and also from an (eco)toxicological point of view, while the use of typical fluorine-containing anions should be avoided.[245,249,253,254]

The conscious design of ILs and the use of structure-activity relationships are essential tools to deliver safer compounds with enhanced technical performance. During recent years, several authors have developed mathematical models based on the structural features of ILs to predict their toxicity or biodegradability. Most of these models are of the so-called Quantitative Structure-Activity Relationships (QSAR) type and consist of group contribution methods.[255–260261] The development of these models has known some limitations due to the lack of experimental data for some specific families of ILs.

1.2 Scope and objectives

As mentioned above, ILs present a wide variety of interesting properties making them promising alternative solvents for a large range of applications. Furthermore, due to the selection of the adequate cation/anion combination, ILs can be designed to be task-specific for a given application as an innovative approach to sustainable chemistry.[1] In fact, their insignificant vapour pressure reduce the risk of air pollution in comparison to common organic solvents. However, with further development and use of ILs at an industrial level, their release into aquatic environments could cause a severe contamination.[222] In this context, the present work proposes to investigate the synthesis and characterization, through the physicochemical properties determination, and (eco)toxicity of novel ILs from distinct ILs families and some of their potential applications. After a general introduction (Chapter 1), this work is divided considering the studied application/property (Chapter 2-7), as sketched in Figure 1.7.

- Due to the correlation between oxidative stress and a plethora of inflammatory diseases, antioxidants have received an increased attention for incorporation into dermatological products.[262] In this sense, the Chapter 2 proposes the synthesis and characterization of a set of new cholinium-based ILs with antioxidant features in order to develop novel ILs that could be used in the formulation of pharmaceutical/cosmetic products.

- The separation of two enantiomers remains a major challenge for the pharmaceutical industry.[263] Chapter 3 will focus on the synthesis and characterization of

chiral ionic liquids (CILs), based on chiral selectors, in order to develop enantioselective CIL-ABS, for the chiral resolution. For that purpose, CILs with either chiral cation (Chapter 3.1), or chiral anion (Chapter 3.2) were investigated.

- Another challenge in the pharmaceutical industry is the solubilisation of poorly water-soluble drugs, since the therapeutic effectiveness of a drug can be severely limited by its aqueous solubility.[264] In this context, the impact of the ionic liquid chemical structures and their concentration on the solubility of two model, poorly water-soluble, drugs, namely ibuprofen and naproxen, and moderately water-soluble caffeine, were evaluated in Chapter 4.

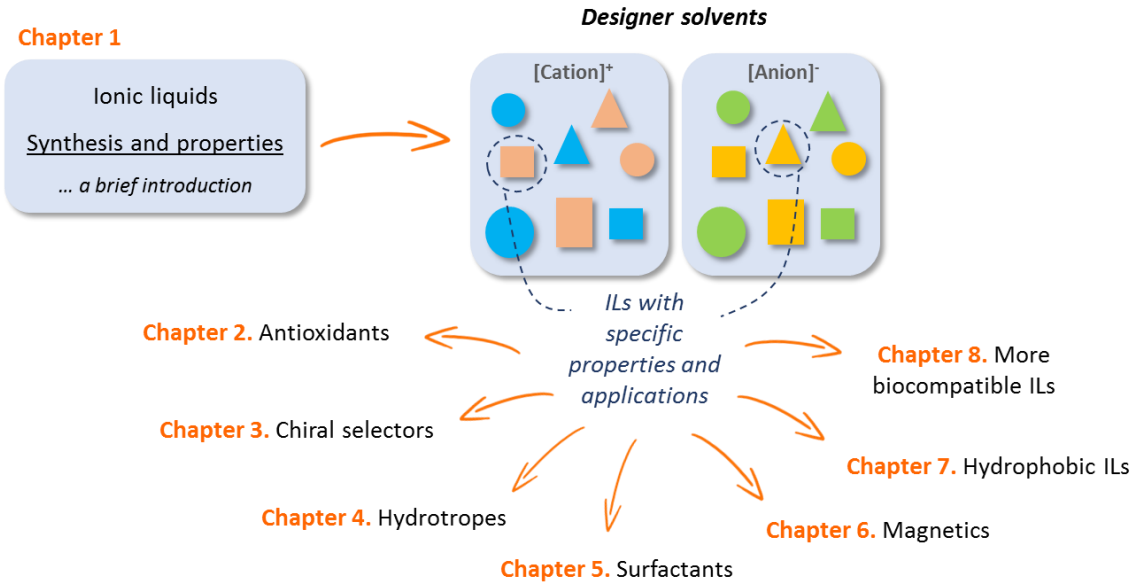

Figure 1.7. Schematic representation of the work layout.

- The potential industrial application of IL-based surfactants, as well as their impact on the environment, is closely dependent on their aggregation behaviour.[204] Although their self-organization in aqueous solutions is currently under investigation by a number of authors, their correlation with ILs structure is limited. In order to address this lack of information, the Chapter 5 proposes the synthesis and characterization of several families of surface-active ILs (meaning ILs with a surfactant nature). Here, imidazolium,

quaternary ammonium and phosphonium-based ILs, containing one or more long alkyl chains in the cation and/or anion were evaluated.

- Magnetic ionic liquids (MILs) are an emerging class of ILs that are inherently paramagnetic. These compounds can be interesting for applications in process and product engineering.[265] Despite the initial efforts carried to get a preliminary insight into the environmental behaviour of MILs, data on their ecotoxicity is still scarce, and needs to be expanded to improve the knowledge for the adequate design of safer MILs. In this context, the Chapter 6 shows the synthesis and ecotoxicological assessment of a series of MILs based on the cholinium derivative cation in combination with $[FeCl_4]^-$, $[MnCl_4]^{2-}$, $[CoCl_4]^{2-}$ and $[GdCl_6]^{3-}$ anions, towards the *Vibrio fischeri* marine bacteria.

- Hydrophobic ILs have been shown to be promising media for the extraction of (bio)molecules and (bio)fuels from aqueous solutions.[266–268] Nevertheless, that class of ILs is still limited. Chapter 7 proposes a simple and atom-economic method to prepare a novel hydrophobic IL with a per-fluoro-*tert*-butoxide anion from hydrophilic ILs, namely $[C_4C_1im][OAc]$ and $[C_4C_1im]Cl$. Furthermore, its thermophysical characterization is reported.

- Finally, and considering the huge number of possible cations and anions combinations, a rational guide for the structural design of ILs is essential in order to prioritize the synthesis of "greener" ILs.[269] Thus, Chapter 8 reports a work on the development of a QSAR model for ecotoxicity prediction of new ILs, done in collaboration with another research group, for which the ILs predicted to be of low toxicity were synthesized and tested to evaluate the validity of the model predictions.

Chapter 2 - Ionic Liquids with Antioxidant Character

Enhancing the Antioxidant Characteristics of Phenolic Acids by Their Conversion into Cholinium Salts

Tânia E. Sintra, Andreia Luís, Samuel N. Rocha, Ana I. M. C. Lobo Ferreira, Fernando Gonçalves, Luís M. N. B. F. Santos, Bruno M. Neves, Mara G. Freire, Sónia P. M. Ventura and João A. P. Coutinho, *ACS Sustainable Chemistry and Engineering*, **2015**, 3, 2558-2565, DOI: 10.1021/acssuschemeng.5b00751.

(In this communication Tânia E. Sintra contributed with synthesis and characterization of cholinium salts, measurement of their antioxidant activity, ecotoxicity and solubility in water, and with the manuscript preparation/writing.)

ABSTRACT

Because of the close relation between oxidative stress and a plethora of inflammatory diseases, antioxidants have received an increased attention for incorporation into dermatological products. Their use and absorption are, however, limited by their low solubility in water-rich formulations. Herein, a set of novel cholinium-based salts, namely dicholinium ellagate and cholinium caffeate, syringate, vanillate, gallate, and salicylate, were synthesized and characterized. Their melting and decomposition temperatures, water solubility, and toxicological, antioxidant, cytotoxicity and pro-/anti-inflammatory activities were addressed. These new salts, exclusively composed of ions derived from natural sources, display a high thermal stability−up to 150 °C. The synthesized compounds are significantly more soluble in water (on average, 3 orders of magnitude higher) than the corresponding phenolic acids. Furthermore, they present not only similar but even higher antioxidant and anti-inflammatory activities, as well as comparable cytotoxicity and lower ecotoxicity profiles than their acidic precursors. Among all the investigated salts, dicholinium ellagate is the most promising synthesized salt when considering the respective antioxidant and anti-inflammatory activities. Because all the synthesized salts

are based on the cholinium cation, they can further be envisaged as essential nutrients to be used in oral drugs.

INTRODUCTION

The human skin is constantly exposed to both endogenous and environmental pro-oxidant agents, leading to the formation of highly noxious reactive oxygen species (ROS). ROS-mediated oxidative damage includes a wide variety of pathological effects, such as DNA modification, lipid peroxidation, as well as the activation of inflammatory pathways. To minimize these deleterious effects, mammalian skin cells have antioxidant defence mechanisms, which comprise enzymatic and non-enzymatic antioxidant agents.[270,271] However, these systems may not be enough to ensure the skin barrier integrity.[262] In this context, antioxidants have found an increased interest as constituents of dermatological pharmaceutical formulations and skin care products.[272,273] In both of these products, there is a preference for antioxidants from natural rather than synthetic sources.[274] Phenolic compounds are the most abundant secondary metabolites of plants, being recognized by their antioxidant and anti-inflammatory properties. These chemical compounds have one or more aromatic rings, with one or more hydroxyl groups directly bonded, and which can donate a hydrogen atom or an electron to a free radical, being thus ideal structures for free radical scavenging. Naturally available phenolic acids include gallic, caffeic, syringic, and vanillic acids, typically present in sources such as fruits and vegetables.[275,276] Nevertheless, the limited aqueous solubility of some of these phenol-based antioxidants represents a major drawback when envisaging their incorporation into water-rich dermatological formulations or for their absorption and transport in body fluids. To overcome this limitation, cholinium-based salts appear as promising candidates if based in compounds with antioxidant features aiming at enhancing their water solubility. The pioneering synthesis of cholinium salicylate ($[N_{1,1,1,2(OH)}][Sal]$) led to an increase in the water solubility (when compared with the salicylic acid precursor), while maintaining its anti-inflammatory, analgesic, and antipyretic properties.[277,278] Actually, $[N_{1,1,1,2(OH)}][Sal]$ is an active pharmaceutical ingredient currently used in various medicinal products, namely Bonjela, Arthropan, and Bucagel.[279]

Cholinium chloride, an essential nutrient, has been receiving considerable attention due to its biocompatible and "non-toxic" nature.[95,280–282] A significant number of cholinium salts has been reported coupled with a wide range of anions, such as amino acid-,[88–91,283] carboxylic acid-,[92–94,98,284] and good's-buffers-based anions.[102] In fact, the anion selection has been carried out according to specific tasks for which cholinium-based salts can be used and have demonstrated an enhanced potential. Distinct applications have been suggested, namely in catalysis,[88] in photodynamic therapy,[99] in electrical and pH-sensitive drug delivery systems,[285] as cross-linking agents for collagen-based materials,[94] as major solvents in the pretreatment and dissolution of biomass,[286] as cosubstrates for microorganisms in the degradation of dyes,[95] and as self-buffering compounds for the extraction and purification of biologically active molecules.[102] Nevertheless, to the best of our knowledge, a wide variety of cholinium-based salts with remarkable antioxidant activities have not been reported hitherto.

In this work, a series of new cholinium-based salts with antioxidant and anti-inflammatory features were synthesized and characterized. Five anions with antioxidant and anti-inflammatory characteristics, namely gallate, caffeate, vanillate, syringate, and ellagate, were conjugated with the cholinium ((2-hydroxyethyl)trimethylammonium) cation. Additionally, $[N_{1,1,1,2(OH)}][Sal]$ was also synthesized by neutralization to compare its antioxidant performance with the new cholinium-based salts studied in this work. The antioxidant activity of these compounds was investigated using the 2,2-diphenyl-2-picrylhydrazyl (DPPH) hydrate radical scavenging assay and compared with the archetypal ascorbic acid, a well-known antioxidant.[287–289] Their physicochemical properties, namely melting point, decomposition temperature, and water solubility, were also assessed, as well as their impact toward *Vibrio fischeri* (*V. fischeri*), a standard marine luminescent bacteria (Microtox assay). Finally, the impact of these novel antioxidant salts on mammalian cells was evaluated. For that purpose, the three cholinium-based salts that have shown a better performance on the DPPH radical scavenging assay were chosen (cholinium gallate, cholinium caffeate, and cholinium ellagate), and their cytotoxicity and pro-/anti-inflammatory activities were evaluated in Raw 264.7 and HaCaT mammalian cell lines.

EXPERIMENTAL SECTION

Materials: Six cholinium-based salts with antioxidant and/or anti-inflammatory properties were synthesized, namely $[N_{1,1,1,2(OH)}][Gal]$, (2-hydroxyethyl)trimethylammonium 3,4,5-trihydroxybenzoate; $[N_{1,1,1,2(OH)}][Sal]$, (2-hydroxyethyl)trimethylammonium 2-hydroxybenzoate; $[N_{1,1,1,2(OH)}][Caf]$, (2-hydroxyethyl)trimethylammonium (E)-3-(3,4-dihydroxyphenyl)acrylate; $[N_{1,1,1,2(OH)}][Van]$, (2-hydroxyethyl)trimethylammonium 4-hydroxy-3-methoxybenzoate; $[N_{1,1,1,2(OH)}][Syr]$, (2-hydroxyethyl)trimethylammonium 4-hydroxy-3,5-dimethoxybenzoate; $[N_{1,1,1,2(OH)}]_2[Ell]$, di((2-hydroxyethyl) trimethyl ammonium) 3,8-dihydroxy-5,10-dioxo-5,10-dihydrochromeno[5,4,3-*cde*]chromene-2,7-bis(olate). Their full name, acronym, and chemical structure are depicted in Scheme 2.1. Cholinium hydroxide ($[N_{1,1,1,2(OH)}]OH$, in methanol solution at 45 wt %), vanillic acid (97 wt % of purity) and DPPH were acquired from Sigma-Aldrich. Syringic (98 wt % of purity) and ellagic (97 wt % of purity) acids were from Alfa Aesar. Salicylic (99 wt % of purity), gallic (99.5 wt % of purity), and caffeic (99 wt % of purity) acids were from Acofarma, Merck and Acros Organics, respectively. Methanol (HPLC grade), acetone (99.9 wt % of purity), and ethyl acetate (99 wt % of purity) were from VWR. The water used was double distilled, passed by a reverse osmosis system and further treated with a Milli-Q plus 185 water purification apparatus. The human keratinocyte cell line HaCaT, obtained from DKFZ (Heidelberg), was kindly supplied by Doctor Eugénia Carvalho (Centre for Neuroscience and Cell Biology, University of Coimbra, Portugal). Raw 264.7 (ATCC number: TIB-71), a mouse macrophage cell line, was kindly supplied by Doctor Otília Vieira (Centre for Neuroscience and Cell Biology, University of Coimbra, Portugal).

Synthesis and Characterization of Cholinium Salts: Six cholinium-based salts were synthesized by the neutralization of $[N_{1,1,1,2(OH)}]OH$ with the respective acid, with a well-known antioxidant/anti-inflammatory character, namely the gallic, vanillic, caffeic, salicylic, syringic, and ellagic acids (Scheme 2.1).[89,90,94] The synthesis of $[N_{1,1,1,2(OH)}]_2[Ell]$ and $[N_{1,1,1,2(OH)}][Gal]$ has already been reported in the literature;[290,291] however, the synthetic route here proposed is more simple. $[N_{1,1,1,2(OH)}]OH$ (1 equiv, 45 wt % in a methanol solution) was added dropwise to the acidic solution in methanol, with a molar excess of 1.1 equiv, at 0 °C, under nitrogen atmosphere. Regarding the $[N_{1,1,1,2(OH)}]_2[Ell]$

synthesis, the [$N_{1,1,1,2(OH)}$]OH was added to the ellagic acid solution in methanol, with a molar ratio of 2:1. The reaction mixture was stirred at room temperature, under nitrogen atmosphere, and protected from light overnight, producing the cholinium salt and water as the byproduct. The solvent and water were then removed under reduced pressure. Moreover, in the synthesis of [$N_{1,1,1,2(OH)}$][Van], [$N_{1,1,1,2(OH)}$][Syr], and [$N_{1,1,1,2(OH)}$][Caf], the unreacted antioxidant acid accumulated in the prepared IL was eliminated with acetone (3 × 20 mL), followed by filtration to remove the cholinium salt (which is in the solid state). The same procedure was adopted for [$N_{1,1,1,2(OH)}$][Gal], only replacing acetone by methanol. In the synthesis of [$N_{1,1,1,2(OH)}$][Sal], the remaining salicylic acid was removed by a liquid−liquid extraction with ethyl acetate (3 × 20 mL).[98] Finally, the residual solvent was removed under reduced pressure and the obtained compound was dried under high vacuum for at least 48 h. The structure of all compounds synthesized was confirmed by ^{1}H and ^{13}C NMR, IR spectroscopy, and elemental analysis, showing a high purity level of all the ionic structures after their synthesis, as reported in the Appendix A.

Thermogravimetric Analysis: The decomposition temperature was determined by TGA. TGA was conducted on a Setsys Evolution 1750 (SETARAM) instrument. The sample was heated in an alumina pan, under a nitrogen atmosphere, over a temperature range of 25−800 °C, and with a heating rate of 10 °C·min^{-1}.

Differential Scanning Calorimetry: Temperatures of melting transition temperature were measured in a power compensation differential scanning calorimeter, PERKIN ELMER model Pyris Diamond DSC, using hermetically sealed aluminium crucibles with a constant flow of nitrogen (50 mL·min^{-1}). Samples of about 15 mg were used in each experiment. The temperature and heat flux scales of the power compensation DSC were calibrated by measuring the temperature and the enthalpy of fusion of reference materials namely benzoic acid, 4-metoxibenzoic acid, triphenylene, naphthalene, anthracene, 1,3,5-triphenylbenzene, diphenylacetic acid, perylene, *o*-terphenyl, and 9,10-diphenylanthracene, at the scanning rate of 2 °C·min^{-1} and flow of nitrogen. Temperatures of the thermal transitions and melting temperature were taken as the onset temperatures.

Water Solubility: The water solubility of cholinium-based salts and of the corresponding antioxidant acids was determined from a saturated aqueous solution. An excess of each compound was added to pure water (≈1 mL), and allowed to equilibrate at constant temperature (25.0 ± 0.5 °C), under constant agitation (750 rpm) for 72 h using an Eppendorf Thermomixer Comfort equipment. After the equilibration time, properly optimized in this work, all samples were centrifuged at 25.0 ± 0.5 °C in a Hettich Mikro 120 centrifuge during 20 min at 4500 rpm. Then, all samples were placed in an air bath equipped with a Pt 100 probe and PID controller at the aforementioned temperature in equilibrium assays during 2 h. To determine the concentration of each cholinium salt and acid, a sample of the aqueous liquid phase was carefully collected, diluted in ultrapure water, and quantified through UV-spectroscopy, using a SHIMADZU UV-1700, Pharma-Spec Spectrometer, at each λ_{max} in the UV region. Their values, as well as the respective calibration curves, are reported in the Appendix A, Table A1. Triplicate measurements were carried out.

DPPH Radical Scavenging Assay: The antioxidant activities of cholinium-based salts and the respective acids, were determined using the 2,2-diphenyl-1-picrylhydrazyl (DPPH) radical scavenging assay.[287–289] The principle of the assay is based on the colour change of the DPPH solution from purple to yellow, as the radical is quenched by the antioxidant. When a solution of DPPH is mixed with a substance that can donate a hydrogen, the reduced form of DPPH is obtained, and the solution which started to be violet turns to be yellow. This change in colour was monitored by visible (vis) spectroscopy at 517 nm. Briefly, 250 μL of a DPPH solution (0.91 mmol·L^{-1}) in methanol was mixed with different volumes (20, 30, 40, 50, 60, 70, and 80 μL) of a stock solution (with a well-known concentration) of each compound and then methanol was added to complete 4 mL (final volume). The samples were kept in the dark for 30, 90, and 120 min at room temperature and then the decrease in the absorbance at 517 nm was measured. The absorbance of the DPPH solution in the absence of the compounds under analysis was also measured as control. Ascorbic acid was used as positive control. DPPH radical scavenging activity, AA(%), was expressed using eq 1:

$$AA(\%) = (A_0 - A_1)/A_0 \times 100 \qquad (1)$$

where A_0 is the absorbance of the control and A_1 is the absorbance of the sample at 517 nm. DPPH scavenging activity is defined by the IC_{50} value: the concentration of the antioxidant needed to scavenge 50% of the DPPH present in the test solution. IC_{50} values were determined from the equations reported in the Appendix A (Table A2) derived from the graphical representation of the scavenging activity against the sample concentration. Triplicate measurements were carried out.

Microtox Assay: To evaluate the ecotoxicity of the cholinium salts synthesized, as well as of the corresponding acids, the Standard Microtox liquid-phase assay was applied. Microtox is a bioluminescence inhibition method based on the bacterium *V. fischeri* (strain NRRL B-11177) luminescence after its exposure to each sample solution at 15 °C. In this work, the standard 81.9% test protocol was followed.[292] The microorganism was exposed to a range of diluted aqueous solutions of each compound (from 0 to 81.9 wt %), where 100% corresponds to a previously prepared stock solution, with a known concentration. After 5, 15, and 30 min of exposure to each aqueous solution, the bioluminescence emission of *V. fischeri* was measured and compared with the bioluminescence emission of a blank control sample. Thus, the corresponding 5, 15, and 30 min EC_{50} values (EC_{50} being the estimated concentration yielding a 50% of inhibition effect), plus the corresponding 95% confidence intervals, were estimated for each compound tested by nonlinear regression, using the least-squares method to fit the data to the logistic equation. Previously to Microtox testing, the amount of water was determined by Karl Fischer (KF) titration using a Metrohom 831 KF coulometric titrator. On the basis of this parameter, the real concentration of each stock solution was corrected, thus obtaining EC_{50} values with higher accuracy.

Evaluation of Cytotoxicity:

Human Keratinocyte Cell Line HaCaT and Raw 264.7. Keratinocytes were cultured in a Dulbecco's Modified Eagle Medium (high glucose) supplemented with 4 mM glutamine, 10% heated inactivated fetal bovine serum, penicillin (100 $U \cdot mL^{-1}$), and streptomycin (100 $\mu g \cdot mL^{-1}$), at 37 °C, in a humidified atmosphere of 95% of air and 5% of CO_2. Raw 264.7 was cultured in an Iscove's Modified Dulbecco's Eagle Medium supplemented with 10% of noninactivated fetal bovine serum, penicillin (100 $U \cdot mL^{-1}$), and streptomycin (100

$\mu g \cdot mL^{-1}$), at 37 °C, in a humidified atmosphere of 95% of air and 5% of CO_2. During the experiments, the cells were periodically monitored by microscope observations in order to detect any morphological change imposed to the cells.

Cytotoxicity Tests of Cholinium-based Salts and the Respective Acids. The cytotoxicity of the cholinium salts and respective acids was determined by exposing HaCaT and Raw 264.7 cells to distinct and increased concentrations of $[N_{1,1,1,2(OH)}][Gal]$, $[N_{1,1,1,2(OH)}][Caf]$, $[N_{1,1,1,2(OH)}]_2[Ell]$, gallic acid, caffeic acid, and ellagic acid (in a range of concentrations between 1 and 5000 μM). The cells were seeded in 96-well plates and incubated for 24 h to allow attachment, thus enabling high-throughput screening. Cholinium salts samples, formulated at various dilutions in full-complement media, were added to the cells. A resazurin solution (10% v/v) was added to the cells during the last 2 and 1 h(s) of incubation for HaCat and Raw 264.7 cells, respectively. After incubation, the absorbance of resorufin (the product of the resazurin reduction) was measured at 570 and 600 nm in a standard spectrophotometer MultiSkan Go (Thermo Fisher Scientific, Waltham, MA, USA). The treated cells were normalized regarding the control (untreated cells). To calculate the EC_{50} values, dose−response curves were fitted with the nonlinear least-squares method using a linear logistic model. The data reported correspond to the average of three biological independent experiments conducted in triplicate for each compound.

Nitric oxide (NO) Measurement: The pro- or anti-inflammatory activity of $[N_{1,1,1,2(OH)}][Gal]$, $[N_{1,1,1,2(OH)}][Caf]$, $[N_{1,1,1,2(OH)}]_2[Ell]$, gallic acid, caffeic acid, and ellagic acid was evaluated in the mouse macrophage cell line Raw 264.7. The production of NO was measured by the accumulation of nitrite in the culture supernatants, using a colorimetric reaction with the Griess reagent. The cells were plated at 3 × 105 cells/well in 48-well culture plates, allowed to stabilize for 12 h, and then incubated with the culture medium (control), or stimulated with 1 $\mu g \cdot mL^{-1}$ of lipopolysaccharide (LPS), or with 1 $\mu g \cdot mL^{-1}$ of LPS in the presence of three concentrations (100, 50, and 10 μM) of $[N_{1,1,1,2(OH)}][Gal]$, $[N_{1,1,1,2(OH)}][Caf]$, $[N_{1,1,1,2(OH)}]_2[Ell]$, ellagic acid, gallic acid, and caffeic acid for 24 h. Briefly, 100 μL of culture supernatants was collected and diluted with equal volume of the Griess reagent [0.1% (w/v) *N*-(1-naphthyl)ethylenediamine dihydrochloride and 1% (w/v)

sulphanilamide containing 5% (w/v) H_3PO_4] during 30 min, in the dark. The absorbance at 550 nm was measured using a standard spectrophotometer MultiSkan Go (Thermo Fisher Scientific, Waltham, MA, USA). Comparisons between multiple groups were performed by One-Way ANOVA analysis, with a Bonferronís Multiple Comparison post-test. Statistical analysis was performed using GraphPad Prism, version 5.02 (GraphPad Software, San Diego, CA, USA). Significance levels are as follows: $*p < 0.05$, $**p < 0.01$, $***p < 0.001$, $****p < 0.0001$.

RESULTS AND DISCUSSION

A set of new cholinium-based salts with antioxidant features were synthesized by the neutralization of $[N_{1,1,1,2(OH)}]OH$ with five distinct acids with antioxidant and anti-inflammatory characteristics, namely the gallic, vanillic, caffeic, syringic, and ellagic acids. By way of comparison, $[N_{1,1,1,2(OH)}][Sal]$ was also prepared. Their full name, acronym and chemical structure are depicted in Scheme 2.1. All cholinium salts were obtained with high purity levels and yield, cf. the Experimental Section.

The antioxidant activity of all novel cholinium-based salts, as well as of their respective precursors, the phenolic acids, was investigated using the DPPH hydrate radical scavenging assay and compared with ascorbic acid, a well-known prototypic antioxidant. DPPH scavenging activity is usually evaluated by the IC_{50} value output, defined as the concentration of a given compound needed to scavenge 50% of DPPH present in the test solution. Taking into account the IC_{50} definition, a lower IC_{50} value reflects a better DPPH radical scavenging activity. The values depicted in Figure 2.1, expressed in $\mu mol \cdot L^{-1}$, reveal that all the synthesized cholinium-based salts present a higher antioxidant activity when compared with the respective acidic precursor. This trend is particularly visible with $[N_{1,1,1,2(OH)}][Van]$ that displays a significantly higher DPPH radical scavenging activity than vanillic acid. Therefore, these novel compounds appear as promising antioxidant candidates since lower amounts of the cholinium salts are required to reach the same antioxidant activity when compared with the respective and traditional phenolic acids currently used. Moreover, since they are coupled to the cholinium cation, they can also

be envisaged as a source of essential nutrients within the vitamin B complex, an outstanding characteristic for use either in dermatological formulations or as oral drugs.

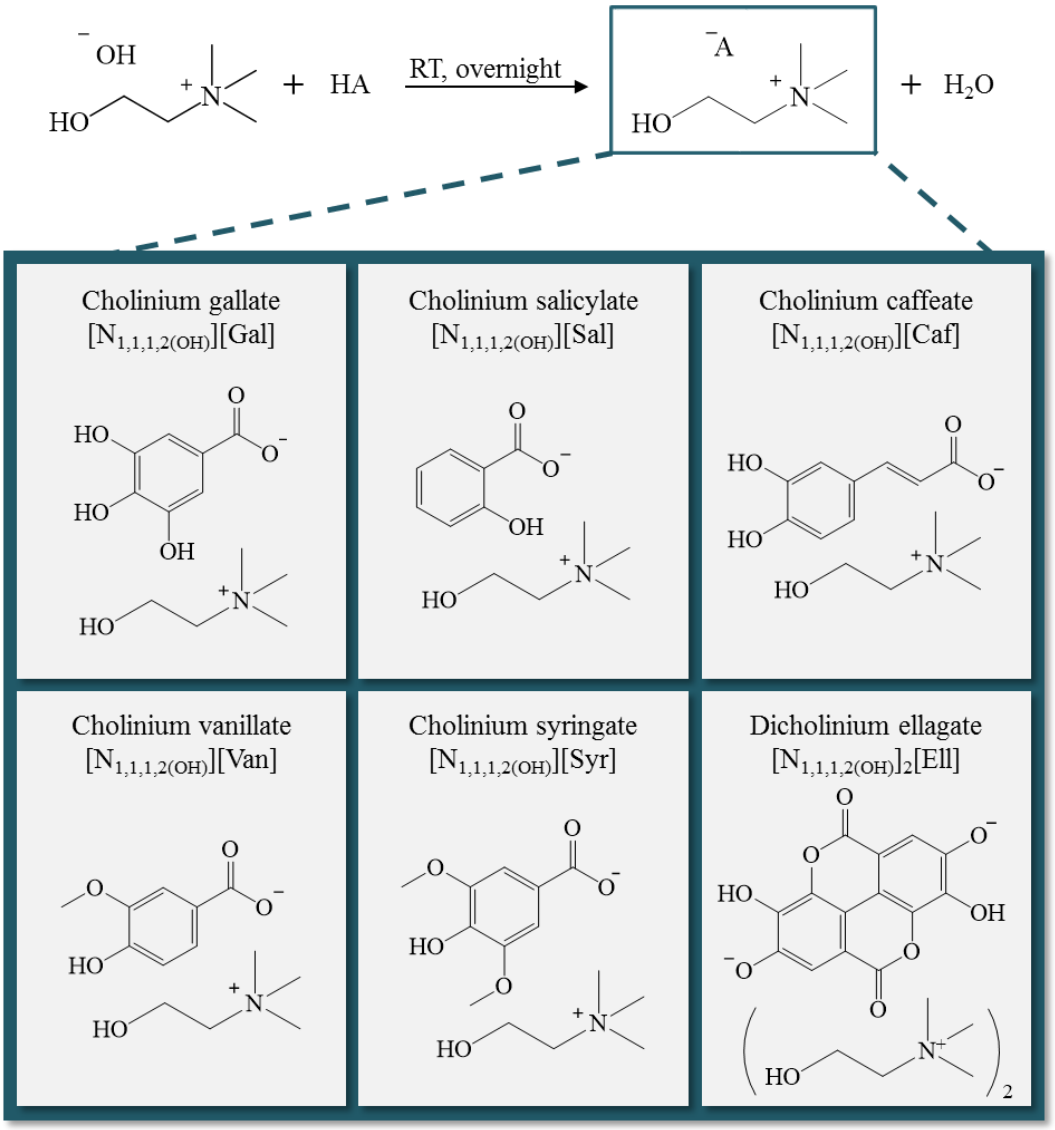

Scheme 2.1. Synthesis scheme and chemical structure of the cholinium-based salts prepared.

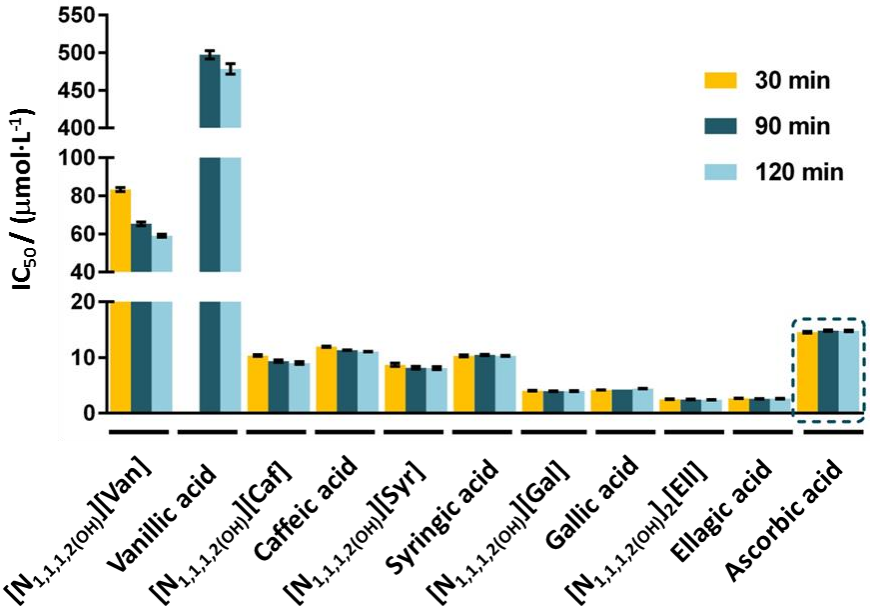

Figure 2.1. IC_{50} values (μmol·L^{-1}) and respective standard deviations, after 30, 90, and 120 min of exposure to DPPH.

The antioxidant activity of $[N_{1,1,1,2(OH)}][Sal]$ and salicylic acid was tested up to a concentration of 1 mg·mL^{-1}, being impossible to determine the IC_{50} value for any of these two compounds. Vanillic acid also requires more time to exert its antioxidant activity, being the IC_{50} only reached after 90 and 120 min of exposure to DPPH. The IC_{50} data (in μg·mL^{-1}), as well as the respective standard deviations, are provided in the Appendix A, Table A3. In general, for the cholinium-based salts synthesized, their antioxidant activity increases in the following order: $[N_{1,1,1,2(OH)}][Van] < [N_{1,1,1,2(OH)}][Caf] \approx [N_{1,1,1,2(OH)}][Syr] < [N_{1,1,1,2(OH)}][Gal] < [N_{1,1,1,2(OH)}]_2[Ell]$; with $[N_{1,1,1,2(OH)}]_2[Ell]$ presenting the highest antioxidant activity.

The physicochemical properties of the antioxidant cholinium salts and respective acids, namely melting point, decomposition temperature and water solubility were additionally addressed. The melting temperatures (T_{fus}), dehydration temperature for the $[N_{1,1,1,2(OH)}][Gal]$, glass transition temperature and cold crystallization temperatures were measured by DSC data and are presented in Table 2.1. The onset temperatures of decomposition (T_d) were further evaluated by TGA, and are reported in Table 2.1.

Table 2.1. Thermal properties of the synthesized cholinium-based salts, namely the melting temperature (T_{fus}) and temperature of decomposition (T_d).

	[$N_{1,1,1,2(OH)}$] [Van]	**[$N_{1,1,1,2(OH)}$] [Caf]**	**[$N_{1,1,1,2(OH)}$] [Syr]**	**[$N_{1,1,1,2(OH)}$] [Gal]**[a]	**[$N_{1,1,1,2(OH)}$]$_2$ [Ell]**	**[$N_{1,1,1,2(OH)}$] [Sal]**[b]
T_{fus} / °C	169	155	150	179	259	38
T_d / °C	186.8	155.0	178.9	185.3	265.0	226.0

	Vanillic acid	**Caffeic acid**	**Syringic acid**	**Gallic acid**	**Ellagic acid**	**Salicylic acid**
T_{fus} / °C	210[c]	191[d]	207[e]	262[f]	287[d]	158[f]
T_d / °C	233.7	218.3	256.4	262.5	472.6	183.9

[a]Dehydration temperature = 140 °C. [b]Glass transition temperature = −56 °C; cold crystallization temperature = −14 °C. [c]Sigma database (http://www.sigmaaldrich.com/portugal.html). [d]Estimated using a group-contribution method.[293] [e]Queimada et al.[294] [f]Mota et al.[295]

From the TGA profiles of the cholinium-based salts prepared, and of the corresponding acids (shown in the Appendix A, Figure A1), as well as from the T_d values reported in Table 2.1, it is possible to conclude that all compounds studied present a high thermal stability, at least up to 150 °C. However, [$N_{1,1,1,2(OH)}$][Caf] and gallic acid decompose immediately after their melting temperatures are reached. Among all the investigated cholinium-based salts, [$N_{1,1,1,2(OH)}$]$_2$[Ell] is the salt with the highest thermal stability (265 °C). Cholinium-based salts also display a slightly lower thermal stability than the respective acids. [$N_{1,1,1,2(OH)}$][Sal] appears as an exception to this pattern since it presents a higher decomposition temperature compared to salicylic acid. Taking into account that the decomposition of cholinium chloride occurs at circa 305 °C,[296] the obtained results show that the anion plays a crucial role in the thermal stability of cholinium salts. Actually, the trend observed in the thermal stability of phenolic acids is similar to that corresponding to cholinium-based salts. In general, the increase in the number of substituents at the benzene ring leads to a decrease of the thermal stability, particularly by the introduction of a methoxy group.

Although depending on the composing anion, it is well-established that cholinium-based salts display, in general, a high solubility in water.[297,298] The water solubility of the antioxidant-cholinium salts was determined and compared with the water solubility of

their corresponding acids at 25 °C. The solubility data and the respective standard deviations are reported in Table 2.2. The values obtained for the phenolic acids are in close agreement with those in the literature.[294,295] The results obtained for the cholinium-based salts demonstrate that these new antioxidant compounds display a solubility in water 3 orders of magnitude (in average) higher than the respective acidic precursors. This feature is certainly a great advantage afforded by these antioxidant salts to be incorporated into more formulations and for a widespread range of applications for which their high water solubility is relevant.

Table 2.2. Water solubility of the synthesized salts and of the corresponding acids ($mmol \cdot L^{-1}$) at 25 °C, with the respective standard deviations.

	Solubility in water ± σ / ($mmol \cdot L^{-1}$)	
Y	**$[N_{1,1,1,2(OH)}][Y]$**	**HY**
Van	3181.40 ± 118.17	10.43 ± 0.30
Caf	2722.47 ± 63.30	3.84 ± 0.04
Syr	2793.71 ± 17.98	7.40 ± 0.02
Gal	2402.27 ± 6.09	71.33 ± 2.70
Ell[a]	622.97 ± 36.98	$1.26 \times 10^{-02} \pm 3.31 \times 10^{-04}$[b]
Sal	completely miscible	15.66 ± 0.14

[a]$[N_{1,1,1,2(OH)}]_2[Ell]$. [b]From Queimada et al.[294]

Albeit a high water solubility of the new ionic compounds can be valuable for their incorporation into dermatological and pharmaceutical formulations, on the other hand, these may lead to an increase on their potential release into aquatic ecosystems. The legislation concerning the (eco)toxicological hazards of several chemical compounds is nowadays more stringent in Europe, and all the new substances should be evaluated a priori by REACH before any industrial-scale application.[10] Standard assays using the luminescent marine bacteria *V. fischeri* are one of the most widespread toxicological bioassays used.[229,248,299,300] The ecotoxicological impact of these cholinium-based salts was evaluated using the standard Microtox acute assay. EC_{50} values ($mg \cdot L^{-1}$), the estimated concentration yielding a 50% of inhibition effect in the microorganism

luminescence, were determined for the cholinium salts and the simple acids after 5, 15, and 30 min of exposure to the bacteria *V. fischeri*: values reported in the Appendix A, Table A4. Considering the obtained results (EC_{50} values at 30 min of exposure time), it is possible to categorize these compounds as non-hazardous substances (EC_{50} > 100 $mg{\cdot}L^{-1}$) according to the limits imposed by the European Legislation for the aquatic compartment.[301] According to Passino's classification,[302] these cholinium-based salts can be classified as (1) "practically harmless" ([$N_{1,1,1,2(OH)}$][Caf], [$N_{1,1,1,2(OH)}$][Syr], and [$N_{1,1,1,2(OH)}$][Sal], with 100 $mg{\cdot}L^{-1}$ < EC_{50} < 1000 $mg{\cdot}L^{-1}$); and as (2) "harmless" ([$N_{1,1,1,2(OH)}$][Van] and [$N_{1,1,1,2(OH)}$][Gal] with EC_{50} > 1000 $mg{\cdot}L^{-1}$).[302] On the opposite, all antioxidant acidic precursors are "moderately toxic" (with 10 $mg{\cdot}L^{-1}$ < EC_{50} < 100 $mg{\cdot}L^{-1}$).[302] Figure 2.2 depicts the EC_{50} data in $mmol{\cdot}L^{-1}$. Their ecotoxicity increases as follows: [$N_{1,1,1,2(OH)}$][Gal] < [$N_{1,1,1,2(OH)}$][Caf] ≈ [$N_{1,1,1,2(OH)}$][Van] < [$N_{1,1,1,2(OH)}$][Syr] < [$N_{1,1,1,2(OH)}$][Sal]; being [$N_{1,1,1,2(OH)}$][Gal] the less toxic and [$N_{1,1,1,2(OH)}$][Sal] the most toxic cholinium-based salts, respectively.

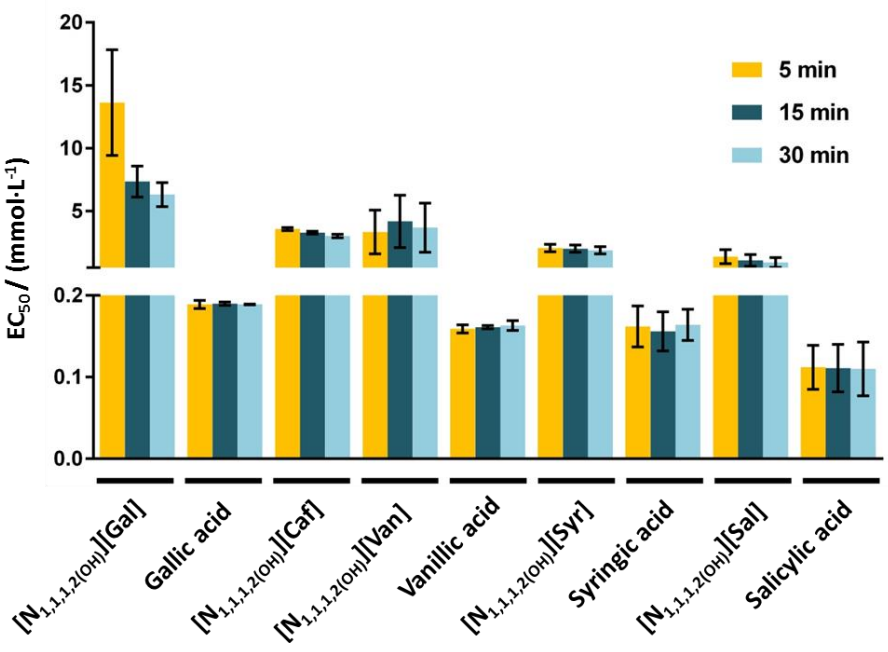

Figure 2.2. EC_{50} values ($mmol{\cdot}L^{-1}$) determined after 5, 15, and 30 min of *V. fischeri* exposure. The error bars correspond to 95% confidence level limits.

The EC_{50} values of $[N_{1,1,1,2(OH)}][Van]$ and $[N_{1,1,1,2(OH)}][Syr]$ suggest that the incorporation of methoxy groups into the aromatic ring increases their ecotoxicity. Even though, in general, all the cholinium-based salts with antioxidant features also display a remarkably lower ecotoxicological impact than their precursors, which further supports their potential use at large-scale applications.

Taking into consideration the high antioxidant activity and/or low ecotoxicity of $[N_{1,1,1,2(OH)}][Gal]$, $[N_{1,1,1,2(OH)}][Caf]$, and $[N_{1,1,1,2(OH)}]_2[Ell]$, these cholinium salts were chosen to further evaluate their in vitro cytotoxicity and anti-inflammatory features, by addressing their impact, as well as of the corresponding acid counterparts, on the capacity of Raw 264.7 (macrophages) and HaCaT (keratinocytes) to metabolize the dye resazurin. Figure 2.3 depicts the EC_{50} data, which represents the concentration of each compound that, for 24 h of exposure, induces a 50% decrease in the cell viability. $[N_{1,1,1,2(OH)}][Gal]$ and gallic acid have similar cytotoxic profiles against Raw 264.7 (EC_{50} 835.8 μM and EC_{50} 590.7 μM, respectively) and HaCaT (EC_{50} 303.5 μM and EC_{50} 267.1 μM, respectively) cell lines. $[N_{1,1,1,2(OH)}][Caf]$ causes a 50% decrease in cell viability at 2336 μM toward the macrophage cells and at 1794 μM for the keratinocytes. These values are of similar magnitude with those found for caffeic acid in macrophage cells (EC_{50} 1996 μM) and keratinocytes (EC_{50} 1803 μM). For $[N_{1,1,1,2(OH)}]_2[Ell]$ and ellagic acid, it was not possible to accurately determine the EC_{50} cytotoxic values due to restrictions regarding their solubility limits in cell culture medium, given that the presence of salts in the cells medium leads to the cholinium salt and acid precipitation. Although the $[N_{1,1,1,2(OH)}]_2[Ell]$ presents a high water solubility, its precipitation was also observed with the addiction of osmotic solution during the Microtox test. For the maximum concentration of $[N_{1,1,1,2(OH)}]_2[Ell]$ achieved (125 μM), it was not observed a decrease in the cell viability.

For all the compounds investigated, the cells survival rate decreases with the increase on the cholinium salt concentration. Overall, the obtained results demonstrate that the antioxidant cholinium-based salts possess cytotoxicity profiles over mammalian cells similar to their parent acids, allowing therefore their safe utilization in products for human healthcare.

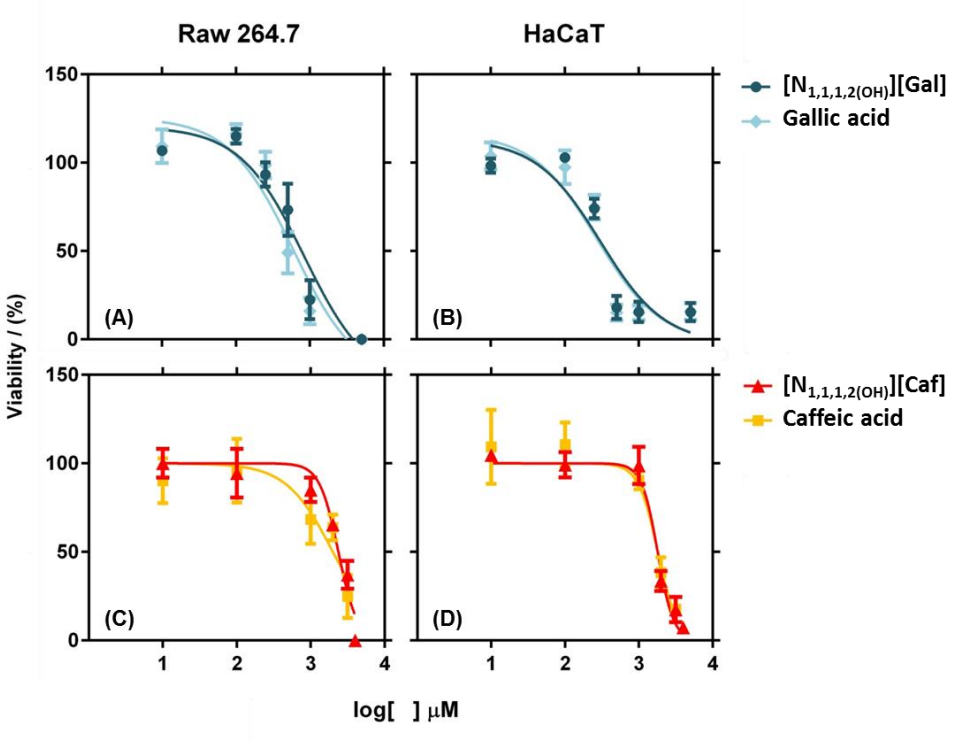

Figure 2.3. Viability of Raw 264.7 and HaCaT cells assessed as the normalized response of treated cells to untreated controls, measured by the metabolic conversion of resazurin. The data shown represents the dose−response curves of Raw 264.7 cells to (A) $[N_{1,1,1,2(OH)}][Gal]$ EC_{50} 835.8 μM and gallic acid EC_{50} 590.7 μM; and (C) $[N_{1,1,1,2(OH)}][Caf]$ EC_{50} 2336 μM and caffeic acid EC_{50} 1996 μM; and HaCaT cells to (B) $[N_{1,1,1,2(OH)}][Gal]$ EC_{50} 303.5 μM and gallic acid EC_{50} 267.1 μM; and (D) $[N_{1,1,1,2(OH)}][Caf]$ EC_{50} 1794 μM and caffeic acid EC_{50} 1803 μM.

In addition to the evaluation of the toxicity profile of the novel cholinium-based salts, it is crucial to ensure that they do not present immunostimulatory abilities when envisaged as novel products for the formulation of human care products. With this goal in mind, we further analysed the effects of $[N_{1,1,1,2(OH)}][Gal]$, $[N_{1,1,1,2(OH)}][Caf]$, $[N_{1,1,1,2(OH)}]_2[Ell]$, and the respective counterpart acids in the production of nitric oxide (NO) by macrophages. The production of NO results from the activation of macrophages and consequent increased expression of nitric oxide synthase, a strong pro-inflammatory mediator closely associated with numerous inflammatory diseases. As shown in Figure 2.4, the three concentrations tested for each compound (100, 50, and 10 μM) barely induce the production of NO in macrophages when compared to a classical proinflammatory

stimulus, such as bacterial LPS. Additionally, the investigated cholinium salts do not present a significant pro-inflammatory activity when compared with the respective acids, indicating thus that the synthesis pathway used in the present work represents a biologically safe modification.

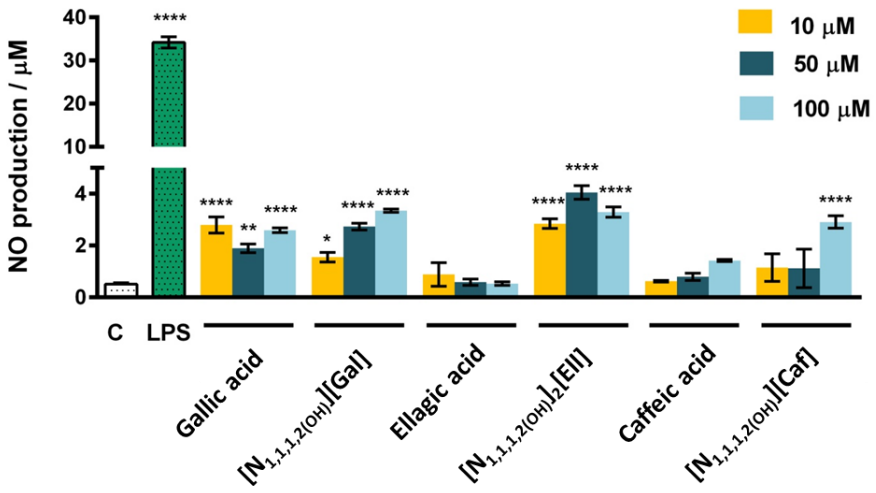

Figure 2.4. Effect of cholinium-based salts and their respective acids on the NO production in macrophages for concentrations of 10, 50, and 100 μM. The results are expressed as the amount of NO produced by the control cells maintained in a culture medium. LPS at a concentration of 1 $\mu g \cdot mL^{-1}$ was used as a positive control. Each value represents the average value and the respective standard deviation obtained from 3 independent experiments (*$p < 0.05$, **$p < 0.01$, ****$p < 0.0001$).

As some antioxidant compounds display also anti-inflammatory activity, we finally addressed whether the synthesized cholinium salts and respective acids can be used in parallel as anti-inflammatory drugs. To this end, an in vitro inflammatory model consisting of Raw 264.7 macrophages stimulated with LPS was used. Cells were pretreated for 1 h with 100 and 50 μM of the cholinium-based salts or their respective acids and then exposed to the strong inflammation activator LPS. The potential anti-inflammatory activities of the studied compounds were evaluated as the effect over the LPS-induced NO production (Figure 2.5). The prototypical anti-inflammatory *N*-acetyl cysteine (NAC)

compound, as well as the nuclear factor κ-light-chain-enhancer of activated B cells (NF-κB) inhibitors, BAY and pyrrolidine dithiocarbamate (PTDC), were also used as positive controls.

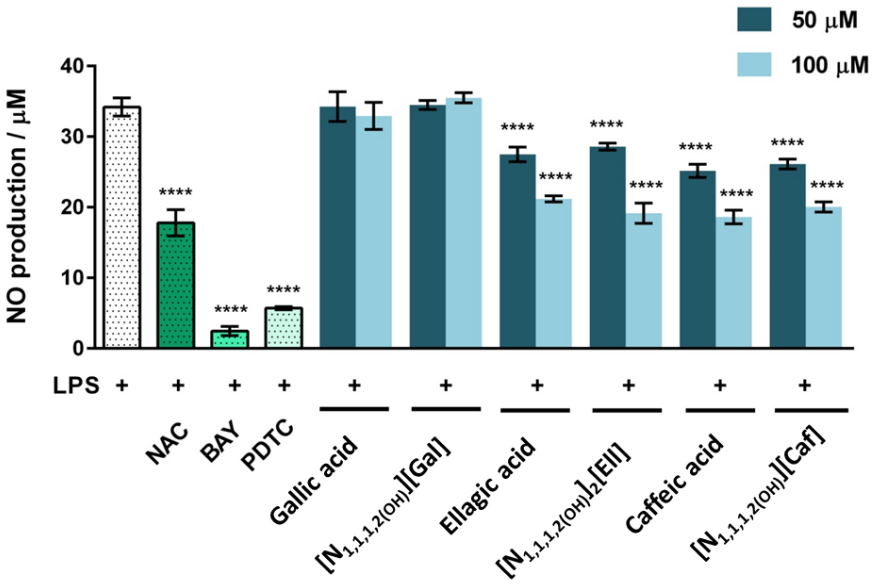

Figure 2.5. Effect of NAC, BAY, PDTC, cholinium-based salts and their respective acids (at 100 μM and 50 μM) on the inhibition of LPS-induced NO production in macrophages. The results are expressed as the amount of NO produced relatively to cells treated with 1 $\mu g.mL^{-1}$ of LPS. Each value represents the average value and the respective standard deviation obtained from 3 independent experiments (****$p < 0.0001$: LPS vs LPS + treatment).

The capacity of the synthesized cholinium-based salts to inhibit the NO production is identical to their parent acids. The compounds with higher anti-inflammatory activity are $[N_{1,1,1,2(OH)}]_2[Ell]$ and $[N_{1,1,1,2(OH)}][Caf]$, which significantly inhibit the LPS-induced NO increase. Their anti-inflammatory effects are, however, smaller than those of BAY and PDTC; yet, of the same order of magnitude of NAC, a well-known antioxidant and anti-inflammatory molecule. It should be highlighted that although the NO production is a common readout in high-throughput screening for anti-inflammatory compounds, it represents only a single parameter that not completely resumes an inflammation pattern. In addition to the NO inhibition, caffeic acid strongly inhibits the production of

prostaglandin E2, leukotrienes, and pro-inflammatory cytokines, such as TNF-α, IL-1β, and IL-6,[303–305] whereas the anti-inflammatory activity of ellagic acid was shown to rely on the decrease of NO, IL-6, TNF-α, IFN-γ, and COX-2.[227,306] Therefore, it is expected that the correspondent cholinium-based salts are also able to maintain these biological effects. On the other hand, we observed that neither $[N_{1,1,1,2(OH)}][Gal]$ nor gallic acid decrease the LPS-induced NO production by macrophages. These results are in accordance with previous reports, where 3,4,5-trihydroxybenzoic acid (gallic acid) was shown to display a limited anti-inflammatory ability, whereas being more effective as an antibacterial and anticancer agent.[307–309]

CONCLUSIONS

Antioxidant cholinium-based salts with outstanding water-solubility and anti-inflammatory activity, exclusively composed of ions derived from natural sources, were synthesized and characterized. All these compounds present a good thermal stability, at least up to 150 °C, with $[N_{1,1,1,2(OH)}]_2[Ell]$ being the cholinium salt with the highest thermal stability (265 °C). The data obtained further reveal that these new cholinium-based salts present not only similar or even higher antioxidant and anti-inflammatory activities, as well as comparable cytotoxicity and lower ecotoxicity profiles than their respective acidic precursors. Considering the $[N_{1,1,1,2(OH)}][Sal]$ and salicylic acid, and although their anti-inflammatory profiles are well reported in the literature, their antioxidant activity was tested up to a concentration of 1 $mg \cdot mL^{-1}$, being impossible to determine the IC_{50} value for any of these two compounds by DPPH Radical Scavenging Assay. Therefore, the five new cholinium-based salts display a significant added-value in terms of antioxidant activity compared with $[N_{1,1,1,2(OH)}][Sal]$. Furthermore, the synthesized compounds are significantly more soluble in water (on average, 3 orders of magnitude higher) than the corresponding acids, rendering thus these new antioxidant and anti-inflammatory cholinium salts as more valuable candidates in the formulation of pharmaceutical/cosmetic products. Finally, $[N_{1,1,1,2(OH)}]_2[Ell]$ seems to be one of the most promising cholinium salts here synthesized in terms of antioxidant and anti-inflammatory activities. Because all synthesized compounds are based on the cholinium cation, they can

also be foreseen as essential nutrients for use in dermatological formulations and oral drugs.

Chapter 3 - Ionic Liquids as Chiral Selectors

Synthesis and characterization of optically active ILs for separation of enantiomers

INTRODUCTION

The differences in the pharmacological activities of enantiomers may result in serious problems in treatment of diseases using racemates. The Food and Drug Administration (FDA) requires chiral drugs to be reported in single isomer form, otherwise the pharmaceutical companies must provide pharmacology and toxicity data for both enantiomers and racemates.[310,311] In order to get single enantiomer drugs, there are three approaches to produce them: chiral pool synthesis (limited by the availability of precursors from natural sources), asymmetric synthesis (requiring specific expensive catalysts) and chiral resolution. Taking into consideration the chiral resolution, the enantiomers separation from a racemic mixture can be achieved by enantioselective liquid-liquid extraction (LLE).[263] This technique has been considered as an attractive technology to get single enantiomers from racemic mixtures in a continuous mode, being easy to scale-up, to use in continuous operation, and of low cost.[312] Nevertheless, the use of water-immiscible organic solvents of high toxicity and volatility and risk of emulsion constrain LLE application. The chiral selector plays a key role in this extraction process. The chiral recognition mechanism follows the "three-point rule" by which chiral recognition requires a minimum of three simultaneous interactions between the chiral selector and the enantiomers, at least one of these interactions being stereochemically dependent.[313] The most used chiral selectors are cyclodextrin derivatives, tartarate derivatives, crown ethers and metal complexes.[312]

Aqueous biphasic systems (ABS) are usually formed as a result of the mutual incompatibility in aqueous solution of two polymers, one polymer and one salt, or two salts above a certain concentration. Since these systems are mainly composed of water they were immediately recognized as biocompatible media for the recovery and purification of (bio)molecules.[24] In 2003, Rogers and co-workers reported the formation

of ABS by the addition of inorganic salts to aqueous solutions of ILs.[314] ILs are a class of solvents that, due to their unique properties, have been proposed in the past few years as alternatives to some hazardous volatile organic compounds.[2] Chiral ionic liquids (CILs) are a subclass of ILs with a chiral moiety at the cation, anion or both. The first CIL reported was the 1-butyl-3-methylimidazolium lactate, by Seddon and co-workers.[315] Afterwards, the synthesis of imidazolium-CILs based on chiral amines (D-α-phenylethylamine) or amino acids (L-alanine, L-leucine, and L-valine) was described by Bao.[316] Since then many examples of CILs were reported and explored for various applications, namely in separation processes where CILs have been used as chiral selectors, background electrolyte additives, chiral ligands and chiral stationary phases in chromatographic and electrophoretic techniques.[317,318] Recently, chiral imidazolium-based ILs naturally derived from carvone[319] and D-xylose[320] have demonstrated excellent enantioselective discrimination of the racemic Mosher's acid salt. In 2015, Wu and co-workers[30,321] reported the preparation of ABS based on CILs and one inorganic salt for the enantiomeric separation of racemic amino acids. In this work, CIL is not only a constituent of the biphasic system as well as the chiral selector.[30,321] These preliminary results show enantioselectivities still limited. In this sense, the purpose of this work is thus to synthesize CILs, based on chiral selector, in order to develop enantioselective CIL-based ABS, for the chiral resolution. For that, two different groups of CILs will be synthetized and characterized: CILs with a chiral anion (Chapter 3.1) or a chiral cation (Chapter 3.2).

Chapter 3.1 – Ionic liquids with chiral anion

Tânia E. Sintra, Samuel N. Rocha, Francisca A. e Silva, Sónia P. M. Ventura and João A. P. Coutinho. *Under preparation*.

(In this work Tânia E. Sintra contributed with the synthesis and characterization of CILs, measurement of their ecotoxicity, and with the manuscript preparation).

ABSTRACT

The adoption by the industry of renewable natural sources as starting materials has become a topic of increasing importance. Natural amino acids and their derivatives provide the most abundant renewable natural chiral pool, and can form an efficient, practical, and facile precursor for the preparation of chiral compounds. In this work, twelve CILs composed of tetrabutylammonium and cholinium cations and several anions naturally derived from different chiral amino acids and the tartaric acid were synthesized and characterized regarding their optical rotation, thermophysical properties and ecotoxicity against the marine bacteria *V. fischeri*.

EXPERIMENTAL SECTION

Materials: Nine tetrabutylammonium-based CILs were synthesized, namely $[N_{4,4,4,4}]$[L-Phe], tetrabutylammonium L-phenylalaninate; $[N_{4,4,4,4}]$[D-Phe], tetrabutylammonium D-phenylalaninate; $[N_{4,4,4,4}]$[L-Val], tetrabutylammonium L-valinate; $[N_{4,4,4,4}]$[L-Ala], tetrabutylammonium L-alaninate; $[N_{4,4,4,4}]$[L-Pro], tetrabutylammonium L-prolinate, $[N_{4,4,4,4}]$[L-Arg], tetrabutylammonium L-argininate; $[N_{4,4,4,4}]_2$[L-Glu], di(tetrabutylammonium) L-glutamate; $[N_{4,4,4,4}]_2$[L-Tar], di(tetrabutylammonium) L-tartrate and $[N_{4,4,4,4}]_2$[D-Tar], di(tetrabutylammonium) D-tartrate. Regarding the cholinium family, three CILs were prepared, namely $[N_{1,1,1,2(OH)}]$[L-Phe], (2-hydroxyethyl)trimethylammonium L-phenylalaninate; $[N_{1,1,1,2(OH)}]$[D-Phe], (2-

hydroxyethyl)trimethylammonium D-phenylalaninate; and $[N_{1,1,1,2(OH)}]_2$[L-Glu], di((2-hydroxyethyl)trimethylammonium) L-glutamate. Their acronym and chemical structures are depicted in Figure 3.1. Tetrabutylammonium hydroxide ($[N_{4,4,4,4}]$OH, in aqueous solution at 40 wt %), (2-hydroxyethyl)trimethylammonium hydroxide ($[N_{1,1,1,2(OH)}]$OH, in methanol solution at 45 wt %), D-phenylalanine (98 wt % of purity), L-phenylalanine (99 wt % of purity) and L-arginine (90 wt % of purity) were acquired from Sigma-Aldrich. D-tartaric acid (99 wt % of purity), L-tartaric acid (ACS reagent grade) and L-proline (99 wt % of purity) were from Acros Organics. L-glutamic acid (99 wt % of purity), L-valine (99 wt % of purity) and L-alanine (99 wt % of purity) were from Riedel de Haen, Fluka and BDH, respectively. Methanol (HPLC grade) and acetonitrile (99.9 wt % of purity) were acquired from VWR. The water used was double distilled, passed by a reverse osmosis system and further treated with a Milli-Q plus 185 water purification apparatus.

Synthesis and Characterization of ILs with chiral anion: Twelve CILs were synthesized by the neutralization of $[N_{4,4,4,4}]$OH or $[N_{1,1,1,2(OH)}]$OH with the respective amino acid/organic acid, namely the L- and D-phenylalanine, L-arginine, L-proline, L-valine, L-alanine, L-glutamic acid and L- and D-tartaric acid. $[N_{4,4,4,4}]$-based CILs were synthesized following literature procedures.[322] Briefly, $[N_{4,4,4,4}]$OH (1 equiv, 40 wt % in aqueous solution) was added dropwise to an aqueous solution of amino acid, with a molar excess of 1.1 equiv, at room temperature. As an exception, in the $[N_{4,4,4,4}]_2$[L-Glu] and $[N_{4,4,4,4}]_2$[L-/D-Tar] synthesis, the $[N_{4,4,4,4}]$OH was added to the acidic solution with a molar ratio of 2:1. The reaction mixture was stirred at 60 °C, and protected from light for 2 hours, producing the respective CIL and water as the byproduct. The water was then removed under reduced pressure. The resultant residue was dissolved in acetonitrile and filtered to remove the unreacted amino acid. Finally, the acetonitrile was removed under reduced pressure and the obtained compound was dried under high vacuum for at least 48 h. $[N_{1,1,1,2(OH)}]$-based CILs were prepared according to the procedure reported by Santis et. al.[323] Briefly, $[N_{1,1,1,2(OH)}]$OH (1 equiv, 45 wt % in methanol solution) was added dropwise to an aqueous solution of amino acid, with a molar excess of 1.1 equiv, at 0 °C, and under nitrogen atmosphere. Regarding the $[N_{1,1,1,2(OH)}]_2$[L-Glu] synthesis, the $[N_{1,1,1,2(OH)}]$OH was added to the L-glutamic acid in aqueous solution, with a molar ratio of 2:1. The reaction mixture

was stirred overnight, at room temperature, under nitrogen atmosphere, and protected from light. The solvents were then removed under reduced pressure. Acetonitrile/methanol (9:1, v/v) was then added under vigorous stirring in order to precipitate the excess of amino acid. The mixture was left stirring overnight and the excess of amino acid was then filtered off. Finally, the acetonitrile and methanol were removed under reduced pressure and the obtained compound was dried under high vacuum for at least 48 h. The water mass fraction of the CILs was determined by coulometric Karl Fischer titration (Metrohm, model 831) and it was verified to be less than 0.05 wt %. The structure of all compounds synthesized was confirmed by ^{1}H and ^{13}C NMR spectroscopy, showing a high purity level of all the ionic structures after their synthesis, as reported in Appendix B.

Thermogravimetric Analysis: The decomposition temperature was determined by TGA. TGA was conducted on a Setsys Evolution 1750 (SETARAM) instrument. The sample was heated in an alumina pan, under a nitrogen atmosphere, over a temperature range of 25−800 °C, and with a heating rate of 10 °C·min^{-1}.

Differential Scanning Calorimetry: The melting temperatures were measured in a DSC, Hitachi DSC7000X, using hermetically sealed aluminium crucibles with a constant flow of nitrogen (50 mL·min^{-1}). The equipment was previously calibrated using a reference material, indium (99 wt % of purity), with a scanning rate of 2 °C·min^{-1}. Each sample (10 mg) was submitted to three cycles of cooling and heating at 2 °C·min^{-1}. The standard uncertainty of temperature is ± 2 °C.

Density and viscosity: Measurements of density, ρ, and dynamic viscosity, η, in the temperature ranging from 20 to 80 °C and at atmospheric pressure (≈ 0.1 MPa) were performed using an automated Stabinger viscometer (Anton Paar, model SVM3000). The standard uncertainty of temperature and density, and the relative uncertainty of dynamic viscosity are within 0.02 °C, 5 x 10^{-4} g·cm^{-3} and 0.35%, respectively. The viscometer used as well as the methodology applied for the density and viscosity measurements of the ILs studied were validated in previous works.[324–326]

Refractive Index: The refractive index, n_D, was carried out at a wavelength of 589 nm using an automated refractometer (Anton Paar, model Abbemat 500), in the temperature range from 20 to 80 °C and at atmospheric pressure, with a scanning rate of 10 °C·min^{-1}. The maximum temperature deviation is 0.01 °C, whereas the maximum uncertainty of the refractive index measurements is ± 4 x 10^{-5} with 95% confidence. The equipment accuracy and the measurement methodology were previously established.[324–326]

Optical rotation: The optical rotation of the synthesized CILs was carried out at 589 nm using a polarimeter JASCO P-2000 and a cylindrical glass cell CG3-100 3.5 x 100 mm (1mL), at room temperature.

Microtox Assay: To evaluate the ecotoxicity of the CILs synthesized, the Standard Microtox liquid-phase assay was applied. This test is described in detail in the Experimental Section of Chapter 2.

RESULTS AND DISCUSSION

In this work, a series of CILs were prepared by the combination of anions that occurs naturally in nature, such as amino acids and tartaric acid, with tetrabutylammonium and cholinium cations. All CILs were obtained with high purity levels and yield, cf. the Experimental Section. Their optical rotation, melting and decomposition temperatures, and ecotoxicity were addressed. Additionally, the physical properties such as density, viscosity and refractive index were measured for $[N_{4,4,4,4}]$[L-Val], $[N_{4,4,4,4}]$[L-Pro], $[N_{1,1,1,2(OH)}]_2$[L-Glu] and $[N_{1,1,1,2(OH)}]$[L/D-Phe] at atmospheric pressure and in the temperature ranging from 20 to 80 °C.

The optical rotations (Table 3.1), $[\alpha]^{20}_D$, for all of CILs and respective amino acids here reported were measured in aqueous solution (anion concentration of 20 mg·mL^{-1}). In general, the magnitude of the optical rotation is smaller than that of the respective amino acid. The obtained results are in agreement with literature, as shown in Table 3.1.[322] Among all the studied CILs, $[N_{4,4,4,4}]$[L-Pro] is the CIL with the highest magnitude of the optical rotation (-33.10). On the other hand, $[N_{4,4,4,4}]$[L/D-Phe], $[N_{4,4,4,4}]$[L-Ala] and $[N_{1,1,1,2(OH)}]$[L/D-Phe] are the CILs with lower magnitude of the optical rotation. While

[$N_{4,4,4,4}$][L-Ala] retains the low optical activity presented by L-alanine, the phenylalanine-based CILs show a much lower optical rotation when comparted with L-phenylalanine. Finally, the replacement of the tetrabutylammonium for the cholinium cation seems to have no influence on the optical rotation of CILs here studied.

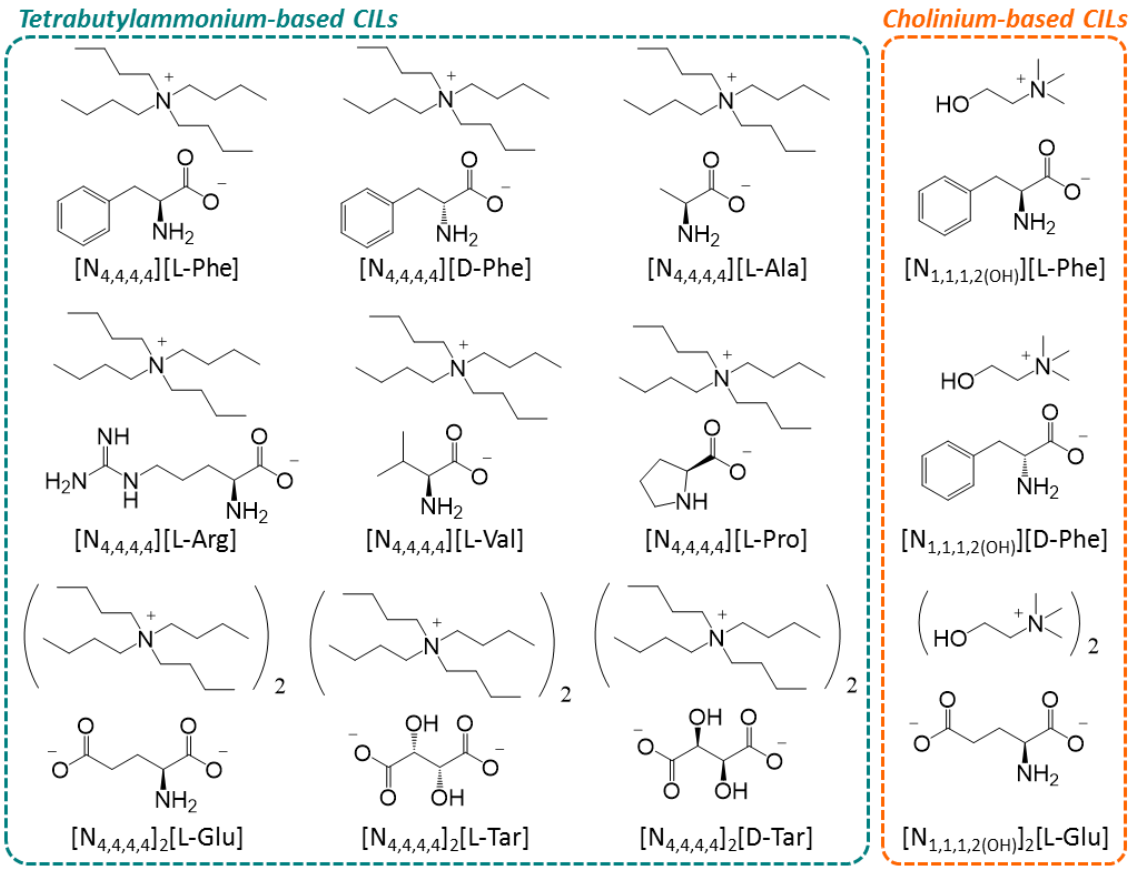

Figure 3.1. Acronym and chemical structures of the CILs studied.

The melting temperatures (T_{fus}) and the onset temperatures of decomposition (T_d) were measured by DSC and TGA, respectively, and are presented in Table 3.2. From the TGA profiles of the CILs prepared (shown in the Appendix B, Figures B1 and B2), as well as from the T_d values reported in Table 3.2, it is possible to conclude that all CILs studied present a high thermal stability, at least up to 166 °C.

Table 3.1. The optical rotations, $[\alpha]^{20}_{D}$, of CILs and respective starting materials, amino acids/tartaric acid.

	$[\alpha]^{20}_{D}$ / here measured	$[\alpha]^{20}_{D}$ / literature[a]		$[\alpha]^{20}_{D}$
$[N_{4,4,4,4}]$[L-Phe]	-0.85 ± 0.04	-0.83	**L-Phe**	-34.34 ± 0.69
$[N_{4,4,4,4}]$[D-Phe]	0.91 ± 0.05	n.a.	**D-Phe**	33.51 ± 0.65
$[N_{4,4,4,4}]$[L-Val]	4.12 ± 0.25	4.10	**L-Val**	5.45 ± 0.11
$[N_{4,4,4,4}]$[L-Ala]	0.83 ± 0.06	1.65	**L-Ala**	1.30 ± 0.03
$[N_{4,4,4,4}]$[L-Pro]	-33.10 ± 2.08	-28.49	**L-Pro**	-86.18 ± 1.79
$[N_{4,4,4,4}]$[L-Arg]	9.35 ± 0.20	n.a.	**L-Arg**	11.50 ± 0.24
$[N_{4,4,4,4}]_2$[L-Glu]	2.12 ± 0.18	1.86	**L-Glu**	11.25 ± 0.06
$[N_{4,4,4,4}]_2$[L-Tar]	8.68 ± 0.75	11.08	**L-Tar**	15.17 ± 0.30
$[N_{4,4,4,4}]_2$[D-Tar]	-8.79 ± 0.76	-11.22	**D-Tar**	-15.07 ± 0.31
$[N_{1,1,1,2(OH)}]$[L-Phe]	-0.82 ± 0.03	n.a.	**-**	-
$[N_{1,1,1,2(OH)}]$[D-Phe]	0.61 ± 0.02	n.a.	**-**	-
$[N_{1,1,1,2(OH)}]_2$[L-Glu]	3.70 ± 0.19	n.a.	-	-

n.a. - not available; [a]Allen et al.[322]

Table 3.2. Thermal properties of the synthesized CILs and respective starting materials, amino acids/tartaric acid, namely the melting temperature (T_{fus}) and temperature of decomposition (T_d).

	T_{fus} / °C	T_d / °C		T_{fus} / °C [a]
$[N_{4,4,4,4}]$[L-Phe]	95	190	**L-Phe**	275
$[N_{4,4,4,4}]$[D-Phe]	95	190	**D-Phe**	275
$[N_{4,4,4,4}]$[L-Val]	-46	181	**L-Val**	295
$[N_{4,4,4,4}]$[L-Ala]	71	184	**L-Ala**	314
$[N_{4,4,4,4}]$[L-Pro]	n.d.	188	**L-Pro**	228
$[N_{4,4,4,4}]$[L-Arg]	79	200	**L-Arg**	222
$[N_{4,4,4,4}]_2$[L-Glu]	123	166	**L-Glu**	205
$[N_{4,4,4,4}]_2$[L-Tar]	74	194	**L-Tar**	170
$[N_{4,4,4,4}]_2$[D-Tar]	74	199	**D-Tar**	170
$[N_{1,1,1,2(OH)}]$[L-Phe]	n.d.	222	**-**	-
$[N_{1,1,1,2(OH)}]$[D-Phe]	n.d.	220	**-**	-
$[N_{1,1,1,2(OH)}]_2$[L-Glu]	5	199	**-**	-

n.d. - not determined; [a]ChemSpider database (http://www.chemspider.com; at January 6th, 2017)

Among the investigated CILs, $[N_{1,1,1,2(OH)}]$[L-Phe] is the IL with the highest thermal stability (222 °C). Considering the tetrabutylammonium family, the obtained results show that the anion assumes an important contribution to the thermal stability of the CILs, as observed in cholinium antioxidants in Chapter 2. Moreover, the pairs of enantiomers $[N_{4,4,4,4}]$[L-Phe]/$[N_{4,4,4,4}]$[D-Phe], $[N_{4,4,4,4}]_2$[L-Tar]/$[N_{4,4,4,4}]_2$[D-Tar] and $[N_{1,1,1,2(OH)}]$[L-Phe]/ $[N_{1,1,1,2(OH)}]$[D-Phe] present similar T_d values, as well as comparable $T_{fus,}$ meaning that their chirality does not seem to influence these thermal properties. Regarding the cation influence on the T_d, it is possible conclude that cholinium cation leads to a CILs with higher thermal stability when compared to the respective tetrabutylammonium-based CIL. On the contrary, Lee et al.[326] have reported an opposite behaviour, namely for the LIs $[N_{4,4,4,4}]$[BES] (269 °C)/$[N_{1,1,1,2(OH)}]$[BES] (227 °C), $[N_{4,4,4,4}]$[MOPSO] (268 °C)/ $[N_{1,1,1,2(OH)}]$[MOPSO] (231 °C) and $[N_{4,4,4,4}]$[CAPSO] (270 °C)/$[N_{1,1,1,2(OH)}]$[CAPSO] (214 °C), where the tetrabutylammonium family present higher thermal stability. Since the amino acids and tartaric acid decompose immediately after their melting temperatures,[327,328] it is possible to conclude that CILs display a slightly lower thermal stability than the respective amino acids. The tartaric-based CILs appears as an exception to this pattern since they present a higher decomposition temperature than tartaric acid.

The experimental density data for $[N_{4,4,4,4}]$[L-Val], $[N_{4,4,4,4}]$[L-Pro], $[N_{1,1,1,2(OH)}]_2$[L-Glu] and $[N_{1,1,1,2(OH)}]$[L/D-Phe] are depicted in Figure 3.2 and reported in Appendix B, Table B1. The density of these CILs decreases with the increase of the temperature. In addition, the density of the investigated CILs increases in the following order: $[N_{4,4,4,4}]$[L-Val] < $[N_{4,4,4,4}]$[L-Pro] < $[N_{1,1,1,2(OH)}]$[L/D-Phe] < $[N_{1,1,1,2(OH)}]_2$[L-Glu]. The higher density of $[N_{1,1,1,2(OH)}]_2$[L-Glu] can be related to the presence of two cations in its structure. Moreover, cholinium-based CILs with shorter alkyl side chain seem to have higher densities than the tetrabutylammonium family, which is in agreement with previous results reported in literature.[326] The experimental viscosity data for $[N_{4,4,4,4}]$[L-Val], $[N_{4,4,4,4}]$[L-Pro], $[N_{1,1,1,2(OH)}]_2$[L-Glu] and $[N_{1,1,1,2(OH)}]$[L/D-Phe] are depicted in Figure 3.3 and reported in Appendix B, Table B1. In contrast to density, a temperature increase has a dramatic impact on the dynamic viscosity. The viscosity of the studied CILs decreases drastically when increasing the temperature. Thus, the density of the investigated CILs

increases in the following order: $[N_{4,4,4,4}][L\text{-Val}] \approx [N_{4,4,4,4}][L\text{-Pro}] < [N_{1,1,1,2(OH)}][L\text{-Phe}] < [N_{1,1,1,2(OH)]2}][L\text{-Glu}] < [N_{1,1,1,2(OH)}][D\text{-Phe}]$. The high viscosity difference observed between $[N_{1,1,1,2(OH)}][D\text{-Phe}]$ and $[N_{1,1,1,2(OH)}][L\text{-Phe}]$ (93775 and 14731 mPa·s, respectively, at 25 °C) is an unexpected but an interesting behaviour that should be better studied in a future work. In addition, the cholinium-based CILs here investigated present higher viscosity than the tetrabutylammonium family. This can be attributed to the presence of a hydroxyl group at the alkyl side chain of the cholinium cation, resulting in the increase of the liquid intermolecular forces and, thus, making cholinium-based CILs more viscous. In fact, the ILs viscosity is essentially governed by the strength of their van der Waals interactions and their capacity to form hydrogen bonds.[124]

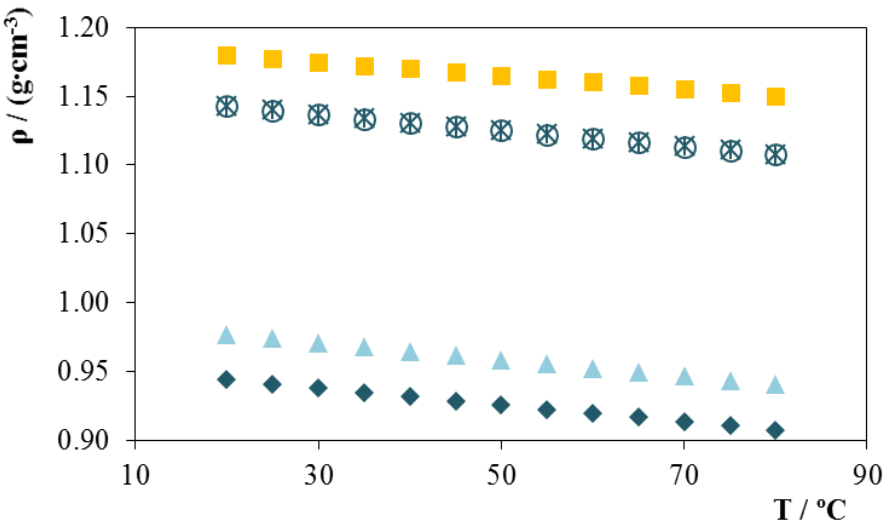

Figure 3.2. Density as a function of the temperature for CILs: $[N_{1,1,1,2(OH)}]_2[L\text{-Glu}]$ (■), $[N_{1,1,1,2(OH)}][D\text{-Phe}]$ (✳),$[N_{1,1,1,2(OH)}][L\text{-Phe}]$ (O), $[N_{4,4,4,4}][L\text{-Pro}]$ (▲),$[N_{4,4,4,4}][L\text{-Val}]$ (◆).

The refractive index can be used to assess the electronic polarizability of a molecule and can provide useful information when studying the forces between molecules or their behaviour in solution.[329] The refractive indices as a function of temperature for CIls are depicted in Figure 3.4 and reported in Appendix B, Table B1. A linear decrease with temperature was observed. In addition, the refractive index of the investigated CILs increases in the following order: $[N_{4,4,4,4}][L\text{-Val}] < [N_{4,4,4,4}][L\text{-Pro}] < [N_{1,1,1,2(OH)}]_2[L\text{-Glu}] <$

[$N_{1,1,1,2(OH)}$][L/D-Phe]. As previous reported, the refractive index of an IL depends on the nature of both the cation and anion.[324,325]

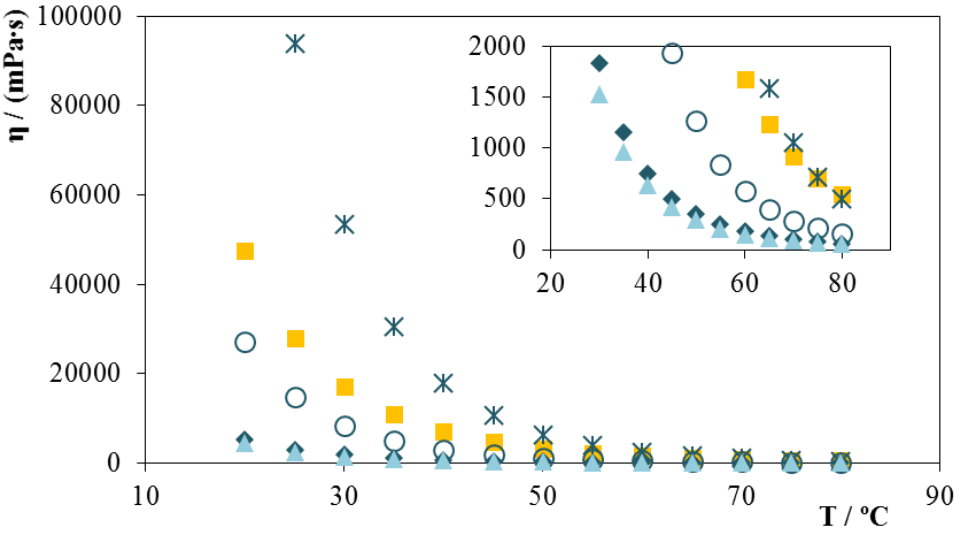

Figure 3.3. Viscosity as a function of the temperature for CILs: [$N_{1,1,1,2(OH)}$]$_2$[L-Glu] (■), [$N_{1,1,1,2(OH)}$][D-Phe] (✳),[$N_{1,1,1,2(OH)}$][L-Phe] (○), [$N_{4,4,4,4}$][L-Pro] (▲),[$N_{4,4,4,4}$][L-Val] (◆).

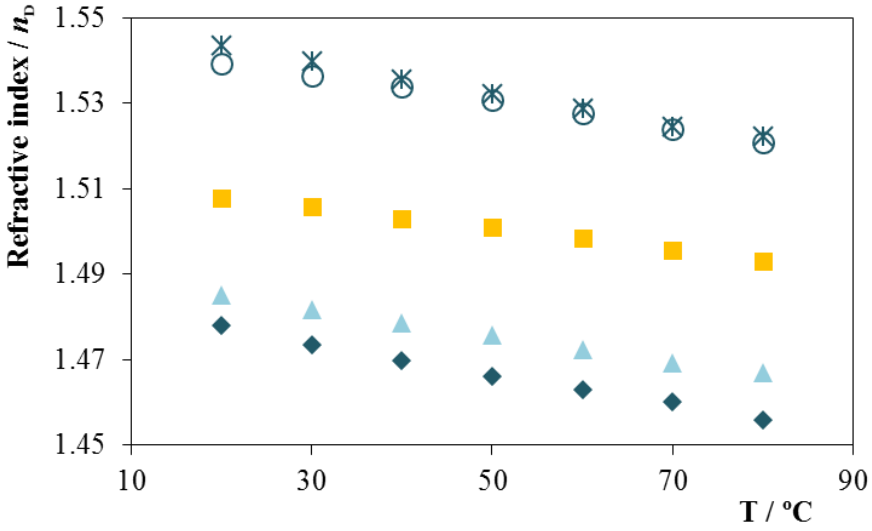

Figure 3.4. Refractive index as a function of temperature for CILs: [$N_{1,1,1,2(OH)}$]$_2$[L-Glu] (■), [$N_{1,1,1,2(OH)}$][D-Phe] (✳),[$N_{1,1,1,2(OH)}$][L-Phe] (○), [$N_{4,4,4,4}$][L-Pro] (▲),[$N_{4,4,4,4}$][L-Val] (◆).

Considering that these CILs were prepared in order to develop enantioselective CIL-ABS for the chiral resolution, their high solubility in water is crucial for their incorporation into the ABS. Nevertheless, and as discussed in the previous chapters, their solubility in water can lead to an environmental problem if they happen to be toxic to the organisms inhabiting aquatic ecosystems. In this context, the ecotoxicological impact of these CILs was evaluated using the standard Microtox acute assay. EC_{50} values ($mg \cdot L^{-1}$), the estimated concentration yielding a 50% of luminescence inhibition of the bacteria *V. fischeri*, were determined for each CIL after 5, 15, and 30 min of exposure to the marine bacteria, and reported in the Appendix B, Table B2. In general, the exposure time had little or no impact on the ecotoxicity of the studied compounds. $[N_{4,4,4,4}]_2$[L/D-Tar] appears as an exception to this pattern, since it presents a higher toxicity for the highest exposure time, which can be related to the necessity of long periods of time for the toxic mechanism to occur.[248] In order to contemplate the entire toxic effect, only the EC_{50} values obtained after 30 min of exposure were considered for further discussion.

Taking into consideration the EC_{50} values at 30 min of exposure time, with the exception of $[N_{4,4,4,4}]$[L/D-Phe], $[N_{4,4,4,4}]$[L-Ala] and $[N_{4,4,4,4}]$[L-Arg] which belongs to the category "acute 3" ($10 < EC_{50} 100$ $mg \cdot L^{-1}$), the remaining CILs can be classified as non-hazardous substances ($EC_{50} > 100$ $mg \cdot L^{-1}$), according to the the European Legislation for the aquatic ecosystems.[301] According to Passino's classification, the CILs here investigated can be categorized as: (1) "moderately toxic" ($[N_{4,4,4,4}]$[L/D-Phe], $[N_{4,4,4,4}]$[L-Ala] and $[N_{4,4,4,4}]$[L-Arg], with $10 < EC_{50} < 100$ $mg \cdot L^{-1}$) and "practically harmless" (the remaining CILs, with $100 < EC_{50} < 1000$ $mg \cdot L^{-1}$). Figure 3.5 shows the EC_{50} data of the CILs in $mmol \cdot L^{-1}$, being possible to rank their ecotoxicity according to the following tendency (30 min of exposure): $[N_{1,1,1,2(OH)}]$[L-Phe] < $[N_{1,1,1,2(OH)}]_2$[L-Glu] ≈ $[N_{4,4,4,4}]_2$[L-Tar] < $[N_{4,4,4,4}]_2$[D-Tar] < $[N_{1,1,1,2(OH)}]$[D-Phe] < $[N_{4,4,4,4}]$[L-Pro] ≈ $[N_{4,4,4,4}]$[L-Val] < $[N_{4,4,4,4}]$[L-Ala] < $[N_{4,4,4,4}]$[D-Phe] ≈ $[N_{4,4,4,4}]_2$[L-Glu] < $[N_{4,4,4,4}]$[L-Arg] ≈ $[N_{4,4,4,4}]$[L-Phe]; with $[N_{1,1,1,2(OH)}]$[L-Phe] presenting the lowest ecotoxicity. Considering the tetrabutylammonium-based CILs here studied, it is possible to infer the impact of the insertion of an aromatic ring into the anion, namely comparing $[N_{4,4,4,4}]$[L-Ala] with $[N_{4,4,4,4}]$[L-Phe]. The results obtained suggest that the introduction of an aromatic system into the anion increases the

ecotoxicity of CILs as shown by the EC_{50} values ($[N_{4,4,4,4}][L\text{-}Ala]$: 0.27 mmol·L^{-1}; $[N_{4,4,4,4}][L\text{-}Phe]$: 0.21 mmol·L^{-1}). Hou et al.[330] have reported a similar behaviour for cholinium-based ILs. On the other hand, the insertion of a branched side chain into the anion leads to lower ecotoxicity, as shown by the EC_{50} values of $[N_{4,4,4,4}][L\text{-}Val]$ and $[N_{4,4,4,4}][L\text{-}Ala]$ (0.33 and 0.27 mmol·L^{-1}, respectively). In addition, CILs where the amino acid side chains contained basic functional groups, e.g. $[N_{4,4,4,4}][L\text{-}Arg]$, exhibited high toxicity, which is in close agreement with that indicated by Hou et al.[330]

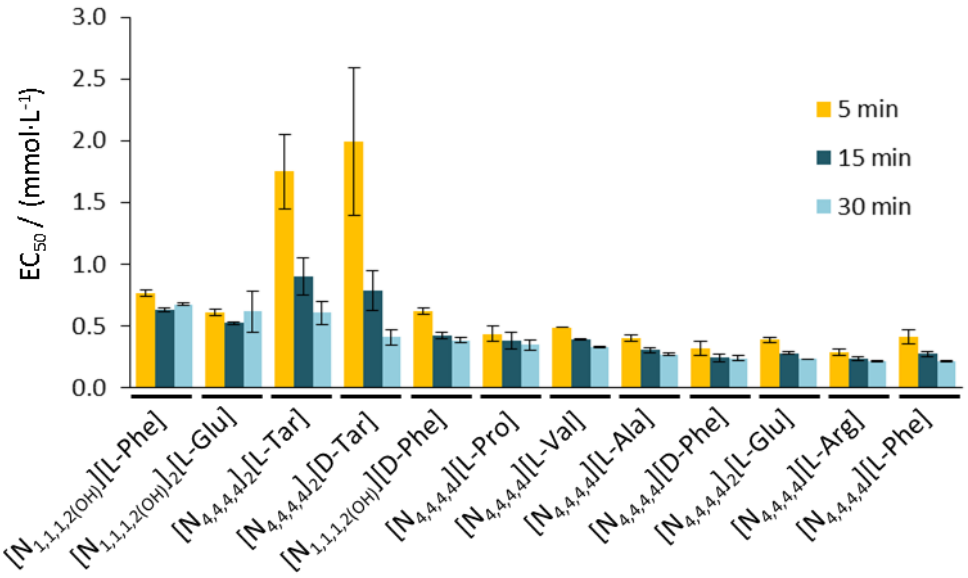

Figure 3.5. EC_{50} values (mmol·L^{-1}) determined after 5, 15, and 30 min of exposure time towards the *V. fischeri* bacteria. The error bars correspond to 95% confidence level limits.

The impact of the chirality on the ecotoxicity of the CILs was evaluated through the pairs of enantiomers $[N_{4,4,4,4}]_2[L\text{-}Tar]/[N_{4,4,4,4}]_2[D\text{-}Tar]$, $[N_{1,1,1,2(OH)}][L\text{-}Phe]/[N_{1,1,1,2(OH)}][D\text{-}Phe]$ and $[N_{4,4,4,4}][L\text{-}Phe]/[N_{4,4,4,4}][D\text{-}Phe]$. Considering the two first pairs, the L-enantiomer presents lower ecotoxicity, as shown by the EC_{50} values ($[N_{4,4,4,4}]_2[L\text{-}Tar]$: 0.61 mmol·L^{-1}, $[N_{4,4,4,4}]_2[D\text{-}Tar]$: 0.41 mmol·L^{-1}, $[N_{1,1,1,2(OH)}][L\text{-}Phe]$ 0.67 mmol·L^{-1} and $[N_{1,1,1,2(OH)}][D\text{-}Phe]$: 0.38 mmol·L^{-1}). However, an opposite behaviour was observed for $[N_{4,4,4,4}][L\text{-}Phe]/[N_{4,4,4,4}][D\text{-}Phe]$ pair, with the D-enantiomer presenting a slightly less toxicity ($[N_{4,4,4,4}][L\text{-}Phe]$: 0.21 mmol·L^{-1} and $[N_{4,4,4,4}][D\text{-}Phe]$: 0.24 mmol·L^{-1}). Finally, the cation

nature impact of the CILs on their ecotoxicity towards the *V. fischeri* was evaluated using the $[L/D\text{-}Phe]^-$ and $[L\text{-}Glu]^-$ anions. As showed in Figure 3.5, the results obtained suggest that cholinium-based CILs present lower toxicity than the corresponding tetrabutylammonium CIL.

CONCLUSION

In this work, a series of CILs composed of tetrabutylammonium and cholinium cations and several anions derived from different natural chiral amino acids and the tartaric acid were synthesized and their thermophysical properties investigated in detail at atmospheric pressure. In addition, their ecotoxicity towards the bioluminescent marine bacteria *V. fischeri* was assessed. The CILs synthesized exhibit a high thermal stability, at least up to 166 °C. Furthermore, they present low ecotoxicity being in general considered as "practically harmless". The physical properties including density, viscosity, and refractive index as a function of temperature were measured for $[N_{4,4,4,4}][L\text{-}Val]$, $[N_{4,4,4,4}][L\text{-}Pro]$, $[N_{1,1,1,2(OH)}]_2[L\text{-}Glu]$ and $[N_{1,1,1,2(OH)}][L/D\text{-}Phe]$ at atmospheric pressure and in the temperature ranging from 20 to 80 °C. These results suggest that the cation imposes a pronounced effect on the density and viscosity of CILs studied. Surprisingly, the chirality of CILs with the anion derived from phenylalanine ($[N_{1,1,1,2(OH)}][L/D\text{-}Phe]$) seems to strongly influence their viscosity. Finally, these data can contribute to the understanding of the cation/anion structure-property relationship of CILs focused on their potential applications as chiral selector.

Chapter 3.2 – Ionic liquids with chiral cation

Tânia E. Sintra, Peter Schulz, Sónia P. M. Ventura and João A. P. Coutinho. *Under preparation*.

(In this work Tânia E. Sintra contributed with synthesis and characterization of CILs and with the manuscript preparation).

ABSTRACT

Eight CILs directly derived from the 'chiral pool' were synthesized and characterized. According to their chiral cations, three different groups of CILs were prepared, namely based on quinine, L-proline and L-valine. After having successfully established their synthesis, the enantiomeric recognition ability of CILs was evaluated. For that, the diastereomeric interactions between a racemic mixture of Mosher's acid sodium salt and each CIL were studied using ^{19}F-NMR spectroscopy. The remarkable chemical shift dispersion induced by some CILs demonstrates their potential application in chiral resolution.

EXPERIMENTAL SECTION

Materials: Eight CILs based on chiral selector were synthesized, namely [C_1Qui]I, 1-methyl quininium iodide; [C_1Qui][C_1SO_4], 1-methyl quininium methylsulfate; [C_1Qui][NTf_2], 1-methyl quininium bis(trifluoromethylsulfonyl)imide; [$C_1C_1C_1$Pro]I, *N,N*-dimethyl-L-proline methyl ester iodide; [$C_1C_1C_1$Pro][C_1SO_4], *N,N*-dimethyl-L-proline methyl ester methylsulfate; [$C_2C_2C_2$Pro]Br, *N,N*-diethyl-L-proline ethyl ester bromide; [C_1,C_1,C_1Val]I *N,N,N*-trimethyl-L-valinolium iodide and [C_1,C_1,C_1Val][C_1SO_4], *N,N,N*-trimethyl-L-valinolium methylsulfate. Quinine (98 wt % of purity), iodomethane (99 wt % of purity), dimethyl sulfate (99 wt % of purity), bis(trifluoromethane)sulfonimide lithium salt (99 wt % of purity), dichloromethane anhydrous (99.8 wt % of purity), ethanol (99.8 wt % of

purity), acetone (HPLC grade), potassium carbonate (99 wt % of purity), L-proline (99 wt % of purity), bromoethane (98 wt % of purity), acetonitrile (99.8 wt % of purity), chloroform (99 wt % of purity), L-valine (98 wt % of purity), tetrahydrofuran anhydrous (99.9 wt % of purity), sodium borohydride (99 wt % of purity), sulfuric acid (99.9 wt% of purity), methanol (99 wt % of purity), ethyl acetate (99.8 wt % of purity), potassium hydroxide (90 wt % of purity), formic acid (98 wt % of purity), formaldehyde (37 wt % in water solution), hydrochloric acid (37 wt % in water solution) and Mosher's acid (97 wt % of purity) were acquired from Sigma-Aldrich®.

Synthesis and Characterization of ILs with chiral cation: Considering the chiral cation, three different groups of CILs were prepared: (I) quinine-, (II) L-proline- and (III) L-valine-based CILs (Scheme 3.1, Scheme 3.2 and Scheme 3.3). The chemical structures and acronym of all CILs synthesized are depicted in Figure 3.6. The structure of all compounds synthesized was confirmed by ^{1}H and ^{13}C NMR spectroscopy, and when appropriate, by the 2D ^{1}H-^{13}C HMQC and ^{1}H-^{1}H Cosy NMR sequences, showing a high purity level of all the ionic structures after their synthesis, as reported in the Appendix B.

I) Quinine-based CILs

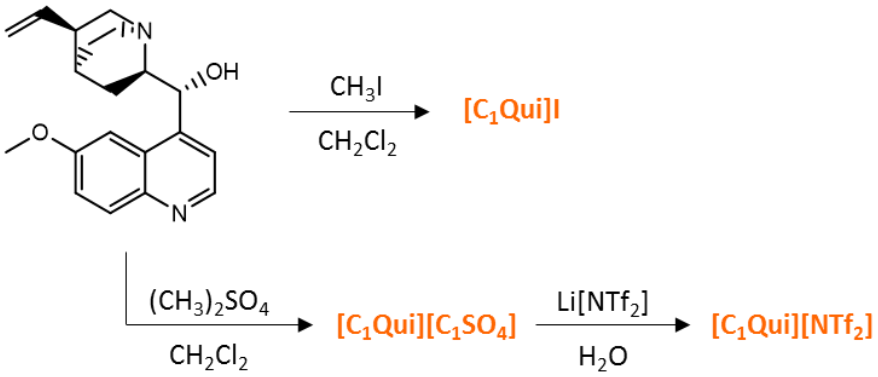

Scheme 3.1. Synthesis scheme followed to prepare the quinine-based CILs.

1-Methyl quininium iodide, $[C_1Qui]I$, was prepared by the dropwise addition of 1.4 mL of iodomethane (22.3 mmol), in a dichloromethane solution, to a solution of quinine (6.9 g, 21.3 mmol) in dichloromethane, at 0 °C and under an inert atmosphere. The reaction mixture was stirred overnight at room temperature, under inert atmosphere. The obtained solid was filtrated, washed with acetone, and recrystallized in ethanol. Finally, the residual solvent was removed under reduced pressure and the obtained compound was dried under high vacuum for at least 48 h, affording $[C_1Qui]I$ as a pale yellow solid (6.7 g, 68% yield). 1-Methyl quininium methylsulfate, $[C_1Qui][C_1SO_4]$, was obtained in a very similar manner as $[C_1Qui]I$, using the dimethyl sulfate as the alkylating agent. $[C_1Qui][C_1SO_4]$ was obtained as a white solid (66% yield). 1-Methyl quininium bis(trifluoromethylsulfonyl)imide, $[C_1Qui][NTf_2]$, was prepared by adding an aqueous solution of 8.0 g (17.7 mmol) $[C_1Qui][C_1SO_4]$ to an aqueous solution of 5.3 g (18.6 mmol) $Li[NTf_2]$ leading to the precipitation of $[C_1Qui][NTf_2]$. The final IL was washed three times with 40 mL water. Finally, the residual water was removed under high vacuum for at least 48 h, affording $[C_1Qui][NTf_2]$ as a white solid (8.7 g, 79% yield).

II) L-Proline-based CILs

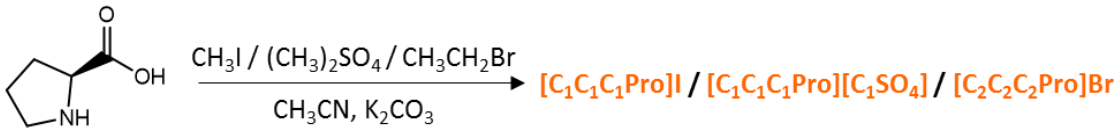

Scheme 3.2. Synthesis scheme followed to prepare the L-proline-based CILs.

In order to prepare *N,N*-dimethyl-L-proline methyl ester iodide, $[C_1C_1C_1Pro]I$, potassium carbonate (5.8 g, 42.0 mmol) was added into the mixture of L-proline (4.8 g, 42.0 mmol) and acetonitrile (70 ml). After stirring the mixture for 1h at room temperature, 5.5 mL of iodomethane (88.3 mmol) was added dropwise at 0 °C, under an inert atmosphere. The reaction mixture was stirred overnight at room temperature, under inert atmosphere. Then, the solid was filtered off, and the resulting liquid was concentrated under reduced

pressure. The light yellow solid crude was washed with chloroform, filtered, and the liquid phase concentrated under reduced pressure, obtaining a viscous yellow oil. The obtained oil was solubilized and crystallized in ethanol. Finally, the residual solvent was removed under high vacuum for at least 48 h, affording $[C_1C_1C_1Pro]I$ as a white solid (1.2 g, 15% yield). To prepare *N,N*-dimethyl-L-proline methyl ester methylsulfate, $[C_1C_1C_1Pro][C_1SO_4]$, potassium carbonate (4.8 g, 34.7 mmol) was added to the mixture of L-proline (4.0 g, 34.7 mmol) and acetonitrile (70 ml). After stirring the mixture for 1h at room temperature, 10 mL of dimethyl sulfate (106.0 mmol) were added dropwise at 0 °C, under inert atmosphere. The reaction mixture was stirred overnight at room temperature, under inert atmosphere. Then, the solid was filtered off, and the resulting liquid was concentrated under reduced pressure. Then, the obtained pale yellow liquid was washed with ethyl acetate (3 x 10 mL). Finally, the residual ethyl acetate was removed under reduced pressure, followed by high vacuum for at least 48 h, affording $[C_1C_1C_1Pro][C_1SO_4]$ as pale yellow liquid (7.2 g, 76% yield). In order to obtain *N,N*-diethyl-L-proline ethyl ester bromide, $[C_2C_2C_2Pro]Br$, potassium carbonate (4.8 g, 34.7 mmol) was added into the mixture of L-proline (4.0 g, 34.7 mmol) and acetonitrile (70 ml). After stirring the mixture for 1h at room temperature, 8 mL of bromoethane (107.7 mmol) was added dropwise at 0°C, under an inert atmosphere. The reaction mixture was stirred at 70 °C for 2 days in an inert atmosphere. After filtering, the resulting liquid was concentrated under reduced pressure. Then, the obtained pale yellow solid was washed with ethyl acetate (3 x 10 mL). Finally, the residual ethyl acetate was removed under reduced pressure, followed by high vacuum for at least 48 h, affording $[C_2C_2C_2Pro]Br$ as a white solid (3.3 g, 34% yield).

III) L-Valine-based CILs

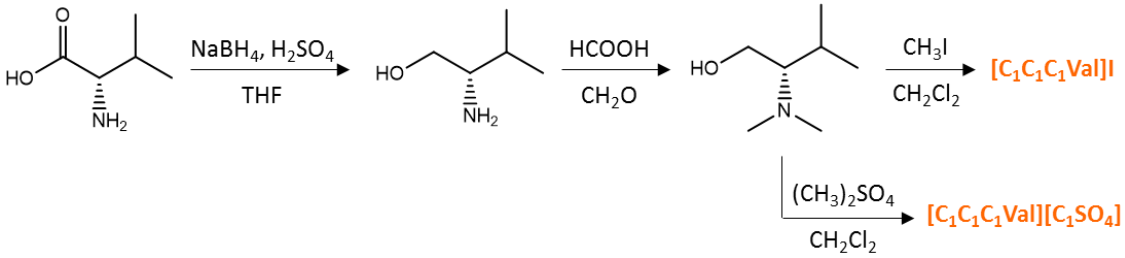

Scheme 3.3. Synthesis scheme followed to prepare the L-valine-based CILs.

L-Valinol, L-2-amino-3-methyl-1-butanol, was obtained by reduction of L-valine, as described in literature.[331] L-Valine (31.0 g, 264.6 mmol) was added to a stirred suspension of sodium borohydride (25.0 g, 661.5 mmol) in tetrahydrofuran (250 mL). The flask was immersed in an ice-water bath, and a solution of fresh concentrated sulfuric acid (17.5 mL, 330.8 mmol) in ether was added dropwise at such a rate as to maintain the reaction mixture below 20 °C (addition time approximately 3h). The reaction mixture was stirred at room temperature overnight, and then 50 mL of methanol were added carefully to destroy the BH_3 in excess. The mixture was concentrated to c.a. 100 mL and 5 N of potassium hydroxide (250 mL) was added. After removing the tetrahydrofuran and methanol under reduced pressure, the mixture was heated at reflux for 3 h (110 °C). The turbid aqueous mixture was cooled and filtered. The filtrate and the washings were combined and diluted with additional water (50 mL). The dichloromethane extraction (4 x 250 mL) followed by evaporation of the solvent left a yellow liquid, which was distilled to yield 15.5 g (57%) of a colourless solid. The *N,N*-dimethylvalinol was synthesized by reductive alkylation of primary amine of L-valinol using the well-known Eschweiler-Clark reaction.[332,333] For that, 30 mL of formic acid (795.0 mmol) were slowly added to an aqueous solution of L-valinol (15.5 g, 150.3 mmol) at 0 °C. The formaldehyde solution (35 mL of 37% wt in a water solution, 470.1 mmol) was added to the resulting solution. The flask was connected to a reflux condenser and heated to 95 °C. A vigorous evolution of CO_2 begins after 2-3 minutes, at which time the flask was removed from the oil bath until the gas evolution notably subsides (15 – 20 min) and then heated at 100 °C overnight. After the solution has been cooled, 70 mL of 4 N hydrochloric acid was added and the solution evaporated to dryness under reduced pressure. The pale yellow liquid was dissolved in 30 mL of water, and the organic base was liberated by the addition of 70 mL of 9 N of potassium hydroxide. The upper organic phase was separated, and the aqueous phase (lower phase) was extracted with dichloromethane (3 x 50 mL). The organic base and the dichloromethane extracts were combined, followed by evaporation of the solvent that left a pale yellow liquid, which was distilled to yield 12.8 g (65%) of a colourless liquid. *N,N,N*-Trimethyl-L-valinolium iodide, $[C_1C_1C_1Val]I$,[333] was prepared by the dropwise addition of 3.0 mL of iodomethane (48.0 mmol), in a dichloromethane solution, to a

solution of *N,N*-dimethylvalinol (6.0 g, 45.7 mmol) in dichloromethane, at 0 °C and under an inert atmosphere. The reaction mixture was stirred overnight at room temperature, under inert atmosphere. The obtained solid was filtered and the residual solvent removed under high vacuum for at least 48 h, affording $[C_1C_1C_1Val]I$ as white solid (11.3 g, 90% yield). *N,N,N*-Trimethyl-L-valinolium methylsulfate, $[C_1C_1C_1Val][C_1SO_4]$, was prepared by dropwise addition of 4.0 mL of dimethyl sulfate (43.2 mmol), in a dichloromethane solution, to a solution of *N,N*-dimethylvalinol (5.4 g, 41.1 mmol) in dichloromethane, at 0 °C and under an inert atmosphere. The reaction mixture was stirred overnight at room temperature, under inert atmosphere. Dichloromethane was removed under reduced pressure and the obtained colorless liquid was dried under high vacuum for at least 48 h, affording $[C_1C_1C_1Val][C_1SO_4]$ as colorless liquid (9.3 g, 88% yield).

Chiral discrimination ability: After the successful synthesis of the target CILs, the chiral discrimination ability was evaluated by studying the diastereomeric interaction between each CIL and the racemic Mosher's acid sodium salt. For that, each CIL (0.5 M) was dissolved in CD_2Cl_2 (0.5 mL) and stirred with 4 drops of a saturated aqueous solution of racemic Mosher's acid sodium salt (2.0 M). After stirring, the mixture was allowed to equilibrate overnight at room temperature, aiming at the complete separation of the coexisting phases. At this point, the lower organic rich-phase was carefully separated and analysed using ^{19}F NMR spectroscopy. The differentiation of the diastereomers was easily visible *via* the different shift of the CF_3 group in Mosher's acid carboxylate.

Racemic Mosher's acid sodium salt was synthesized by stirring racemic Mosher's acid (1.0 g mg, 4.3 mmol) with an equimolar amount of NaOH (170.8 mg, 4.3 mmol) in 50 ml H_2O for 1 h and subsequent evaporation of the solvent.

RESULTS AND DISCUSSION

In this work, a series of CILs naturally derived from chiral compounds, namely quinine, L-proline and L-valine, were prepared and characterized. Their acronym and chemical structure are depicted in Figure 3.6. All CILs were obtained with high purity levels and yield, cf. the Experimental Section.

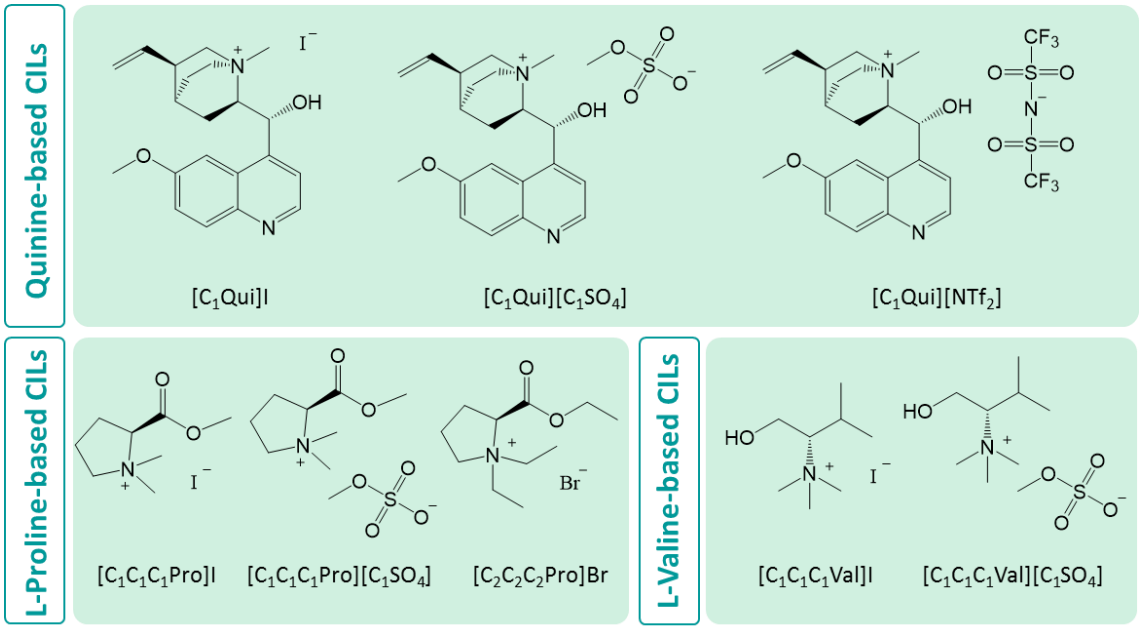

Figure 3.6. Chemical structures and acronym of all ILs with chiral cation here synthesized.

Due to its recognized application as chiral selector,[334–338] quinine, a natural alkaloid, was selected to incorporate three CILs here studied. The synthesis of $[C_1Qui]I$ was already described in literature;[339] however to the best of our knowledge, $[C_1Qui][C_1SO_4]$ and $[C_1Qui][NTf_2]$ have not been reported hitherto. Since amino acids have both a carboxylic acid residue and an amino group in a single molecule, they can be used as either anions or cations. In the present work, three L-proline- and two L-valine-based CILs were prepared and characterized. L-Proline is a representative amino acid with the chiral centre in the pyrrole ring, so the CILs derived from it cannot be racemized easily.[340] While the synthesis of $[C_1C_1C_1Pro]I$ and $[C_2C_2C_2Pro]Br$ reported in literature comprises two steps, esterification and *N*-alkylation,[340] the synthetic route here proposed is simpler, being one-pot synthesis. The L-valine-based ILs here reported were readily obtained from this branched-chain amino acid in a three step synthesis: reduction of L-valine, Eschweiler-Clark reaction, followed by *N*-alkylation.[341] Zhao et al.[342] have already reported the preparation of $[C_1C_1C_1Val]I$ by using a similar procedure. To the best of our knowledge, the synthesis of $[C_1C_1C_1Pro][C_1SO_4]$ and $[C_1C_1C_1Val][C_1SO_4]$ have not been reported hitherto.

After having successfully established their synthesis, the enantiomeric recognition ability of CILs was evaluated. For that, the diastereomeric interactions between a racemic mixture of Mosher's acid sodium salt and each CILs were studied using ^{19}F-NMR spectroscopy. The split of the signal related to the CF_3-group of the racemic Mosher's acid sodium salt indicates the chiral discrimination properties of CILs. As presented in Figure 3.7, quinine- and valine-based CILs and $[C_1C_1C_1Pro]I$ show good splitting of the CF_3 signal of racemic Mosher's acid sodium salt, while in the case of $[C_1C_1C_1Pro][C_1SO_4]$ and $[C_2C_2C_2Pro]Br$ no splitting was observed. The chemical shift difference of the CF_3 signals of racemic Mosher's acid sodium salt in presence of CILs are summarized in Table 3.3. The remarkable chemical shift dispersion induced by some of the CILs demonstrates their potential application in chiral resolution.

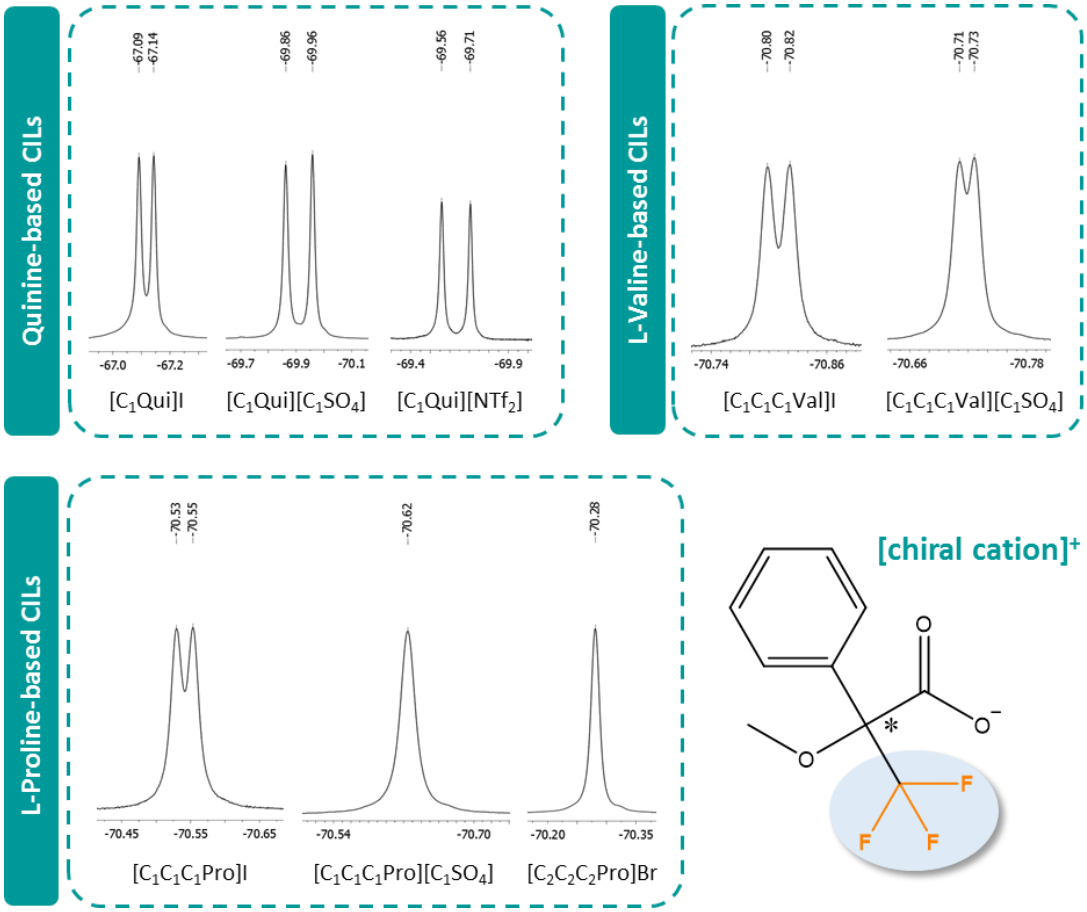

Figure 3.7. The partial 19F NMR spectra of CILs under study and the racemic Mosher's acid salt complex.

Table 3.3. Chemical shift difference of the CF_3 signals of racemic Mosher's acid sodium salt in the presence of 0.5 M of each CIL under study. Duplicate measurements were carried out.

	$\Delta\delta^{R/S}$ (Hz)	
CILs	**Rep 1**	**Rep 2**
$[C_1Qui]I$	19.4	22.5
$[C_1Qui][C_1SO_4]$	36.3	32.7
$[C_1Qui][NTf_2]$	55.4	54.1
$[C_1C_1C_1Pro]I$	9.0	6.6
$[C_1C_1C_1Pro][C_1SO_4]$[a]	NS	NS
$[C_2C_2C_2Pro]Br$[a]	NS	NS
$[C_1C_1C_1Val]I$	8.8	7.9
$[C_1C_1C_1Val][C_1SO_4]$	10.4	10.1

[a]NS - no splitting observed for the CF_3 signal.

Chapter 4 - Ionic Liquids as Catanionic Hydrotropes

Enhanced Dissolution of Drugs Using Ionic Liquids as Catanionic Hydrotropes

Tânia E. Sintra, Sónia P. M. Ventura and João A. P. Coutinho. *Under preparation*.

(In this communication Tânia E. Sintra contributed with all the experimental measurements and with the manuscript preparation/writing.)

ABSTRACT

The therapeutic effectiveness of a drug largely depends on its bioavailability, and thus ultimately on its aqueous solubility. Hydrotropes are compounds able to enhance the solubility of hydrophobic substances in aqueous media being thus extensively used in the formulation of drugs and personal care products. Recently, ILs were reported as a powerful class of catanionic hydrotropes. In this work, the impact of the ionic liquid chemical structures and their concentration on the solubility of two model, poorly water-soluble drugs, namely ibuprofen and naproxen, and moderately water-soluble caffeine, were evaluated and compared with the performance of conventional hydrotropes. The results obtained clearly evidence the exceptional capacity of ILs to enhance the solubility of the most hydrophobic ibuprofen and naproxen. Cholinium vanillate and cholinium gallate seem to be the most promising ILs for the ibuprofen and naproxen solubilisation, where an increase in the solubility of up to 130-fold was observed with IL concentrations of circa 0.7 mol·kg^{-1}. Furthermore, the results suggest that there is a general correlation between the enhanced solubility, as expressed in terms of the hydrotropy constant, and the drug/biomolecule hydrophobicity.

INTRODUCTION

The solubilisation of poorly water-soluble drugs has been a very important issue in the screening of new drugs as well as in their formulation. It was reported that more than 40% of the failures in the development of new drugs have been attributed to poor biopharmaceutical properties, including poor water solubility. In fact, the therapeutic effectiveness of a drug can be severely limited by its aqueous solubility.[264] Among the various techniques employed to enhance the aqueous solubility of poorly water-soluble drugs, such as the use of surfactants, salt forms and alteration of pH, the hydrotropic solubilisation is one of the most studied due to its simplicity and efficiency.[343] Moreover, hydrotropes present, in general, low toxicity and low bioaccumulation potential due to their low octanol-water partition coefficients.[344] The term hydrotropic agent was first introduced by Neuberg in 1916.[345] By definition, hydrotropes are compounds capable to substantially increase the solubility of hydrophobic substances in water. Conventional hydrotropes are typically composed of a hydrophobic aromatic ring with an anionic group (hydrophilic part) where ammonium, calcium, potassium or sodium act as counter ions.[346] The cationic hydrotropes are a minority, an example being the salts of aromatic amines (procaine hydrochloride).[347] Although these compounds present an amphiphilic nature, they are not surfactants. Actually, due to their short hydrophobic moiety, hydrotropes have a weak tendency to self-aggregate in water and therefore do not form micelles, nor do they present a CMC.[348] Despite the large number of reviews addressing the hydrotropy, its mechanism of action is not yet clearly understood.[343,349,350] Three main hypotheses have been proposed in order to explain the hydrotropic-mediated solubilisation. Some authors justify this phenomenon with the formation of a complex between the solute and the hydrotrope.[351,352] On the other hand, some works suggest that the hydrotropes may change the solvent structure around the solute and can be therefore considered as structure makers or breakers.[353,354] In recent years, co-aggregation of the solute with the hydrotropes above a minimum hydrotrope concentration (MHC) has been proposed as the main mechanism behind the enhanced solubility.[355–358] The MHC of a hydrotrope is considered as a measure of the stability of its

aggregation form relatively to its monomeric form. Thus, the lower the MHC, the greater is the hydrotope stability.[343]

During the last years the application of ILs was extended from solvents in "green" chemistry to pharmaceutical application with the ultimate aim to improve the API dissolution, solubility and bioavailability and to prevent polymorphism.[29,359–366] Recently, ILs were reported as a promising class of catanionic hydrotropes since both the IL cation and anion may contribute to enhance the solubility of hydrophobic compounds in aqueous solution.[367] The aqueous solutions of ILs showed a much higher capacity to solubilize the two antioxidants studied than any of the pure solvents, with a solubility enhancement of up to 40-fold.[367] Rengstl and co-authors had already shown the capacity of the short chain choline carboxylates to act as hydrotropes for Disperse Red 13, a hydrophobic dye.[368] In this context, ILs appear as promising candidates to enhance the aqueous solubility of hydrophobic drugs by the selection of the adequate cation/anion combinations.

The present work proposes to investigate the effect of the ionic liquid chemical structures and their concentration on the solubility of two model poorly water-soluble drugs, namely ibuprofen and naproxen, whose chemical structures are shown in Figure 4.1. These two anti-inflammatory drugs belong to BCS Class II (BCS 2), which is characterized by a low solubility and high permeability. To achieve an acceptable absorption after oral administration, APIs should present both, enough aqueous solubility and permeability through gastrointestinal mucosa.[369] Therefore, a solubility improvement is a powerful formulation strategy for compounds of this class to optimize their biopharmaceutical profiles.[369,370] In order to evaluate the impact of the hydrophobic/hydrophilic nature of biomolecules on the hydrotropicity induced by ILs, the present study was further extended to caffeine, a central nervous system stimulant with moderate water-solubility, whose chemical structure is also depicted in Figure 4.1.

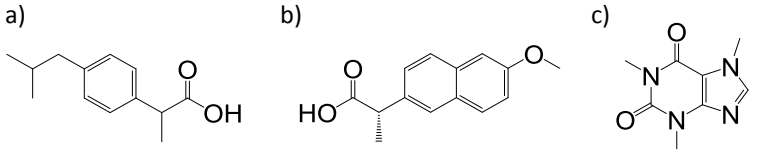

Figure 4.1. Chemical strutures of (a) ibuprofen, (b) naproxen and (c) caffeine.

EXPERIMENTAL SECTION

Materials: In this work, eighteen ILs were investigated in terms of their capacity to enhance the solubility in water of two hydrophobic drugs, namely 1-butyl-3-methylimidazolium trifluoromethanesulfonate, $[C_4C_1im][CF_3SO_3]$; 1-butyl-3-methylimidazolium thiocyanate, $[C_4C_1im][SCN]$; 1-butyl-3-methylimidazolium methylsulfate, $[C_4C_1im][C_1SO_4]$; 1-butyl-3-methylimidazolium tosylate, $[C_4C_1im][TOS]$; 1-butyl-3-methylimidazolium bromide, $[C_4C_1im]Br$, 1-butyl-3-methylimidazolium chloride, $[C_4C_1im]Cl$; 1-butyl-3-methylimidazolium dicyanamide, $[C_4C_1im][N(CN)_2]$; 1-butyl-3-methylpyridinium dicyanamide, $[C_4C_1py][N(CN)_2]$; 1-butyl-3-methylpyridinium chloride, $[C_4C_1py]Cl$; 1-butyl-1-methylpiperidinium chloride, $[C_4C_1pip]Cl$; 1-butyl-1-methylpyrrolidinium chloride, $[C_4C_1pyrr]Cl$, tetrabutylammonium chloride, $[N_{4,4,4,4}]Cl$, tetrabutylphosphonium chloride, $[P_{4,4,4,4}]Cl$; cholinium chloride, $[N_{1,1,1,2(OH)}]Cl$; benzyldimethyl(2-hydroxyethyl)ammonium chloride, $[N_{(Bz),1,1,2(OH)}]Cl$; cholinium gallate, $[N_{1,1,1,2(OH)}][Gal]$; cholinium vanillate, $[N_{1,1,1,2(OH)}][Van]$ and cholinium salicylate, $[N_{1,1,1,2(OH)}][Sal]$. The imidazolium-, pyridinium-, piperidinium- and pyrrolidinium-based ILs were purchased from Iolitec. $[N_{4,4,4,4}]Cl$, $[N_{1,1,1,2(OH)}]Cl$ and $[N_{(Bz),1,1,2(OH)}]Cl$ were obtained from Sigma-Aldrich. $[P_{4,4,4,4}]Cl$ was kindly offered by Cytec Industries Inc. Finally, $[N_{1,1,1,2(OH)}][Gal]$, $[N_{1,1,1,2(OH)}][Van]$ and $[N_{1,1,1,2(OH)}][Sal]$ were synthesized according to literature.[366] The chemical structure of these three compounds was confirmed by ^1H and ^{13}C NMR, showing the high purity level of all the ionic structures after their synthesis. The remaining ILs used have a stated supplier purity of at least 98 wt %, which were further checked by their ^1H and ^{13}C NMR spectra. Sodium benzoate, Na[Benz] (99.0 wt % pure), was supplied by Panreac; sodium thiocyanate, Na[SCN] (98.0 wt % pure) was supplied by Fluka; sodium tosylate, Na[TOS] (95.0 wt % pure), was from TCI; and sodium dicyanamide,

$Na[N(CN)_2]$ (96.0 wt % pure) and urea (99.5 wt % pure) were from Sigma-Aldrich. Ibuprofen (98.0 wt % pure) and naproxen (99.0 wt % pure) were supplied by Sigma-Aldrich. Caffeine anhydrous (99.0 wt % pure) was from Fluka. The mobile phase used in the HPLC analysis was composed of ammonium acetate, (99.99 wt % pure) and acetic acid, (99.99 wt % pure), both from Sigma-Aldrich, HPLC grade acetonitrile from HiPerSolv Chromanorm® and ultrapure water, which was double distilled, passed by a reverse osmosis system and further treated with a Milli-Q plus 185 water purification apparatus. The ionic structure of all ILs and salts studied are depicted in Figure 4.2. The filters used during the filtration steps were syringe filters (0.45 μm) and regenerated cellulose membrane filters (0.45 μm), acquired at Specanalitica and Sartorius Stedim Biotech, respectively.

Solubility of pharmaceutical drugs: Each drug (ibuprofen, naproxen and caffeine) was added in excess to the IL aqueous solutions, pure water or pure IL. Then, it was equilibrated in an air oven at (303.15 ± 0.5) K, under constant agitation (750 rpm) and an equilibration time of 72h, using an Eppendorf Thermomixer Comfort equipment. The equilibration conditions were previously optimized. After the saturation was achieved, all samples were centrifuged at (303.15 ± 0.5) K during 20 minutes at 4500 rpm, using a Hettich Mikro 120 centrifuge. Then, the procedure was adjusted according to the quantification method used for each drug. As regards the ibuprofen and naproxen, the samples of the liquid phase were collected and filtered using syringe filters, in order to remove all solids particles in suspension. The saturated solution was diluted in a mixture of acetonitrile and ultrapure water in a volumetric ratio of 30 : 70, when required, and the amount of ibuprofen and naproxen was quantified by HPLC-DAD (HPLC Elite LaChrom, VWR Hitachi, with a diode array detector l-2455), using an analytical method previously developed by our group.[371] DAD was set to measure the amount of ibuprofen and naproxen at 230 nm and 270 nm, respectively, using calibration curves previously established, reported in the Appendix C, Table C1. Triplicates were performed for each assay. For the caffeine quantification, after centrifugation, the samples were put into an air bath equipped with a Pt 100 probe and a PID controller at (303.15 ± 0.5) K during 2h. After this equilibration time, the samples of the liquid phase were carefully collected and

diluted in ultrapure water. The amount of caffeine was then quantified by UV-spectroscopy using a SHIMADZU UV-1700, Pharma-Spec spectrometer at a wavelength of 273 nm, using a calibration curve previously determined, as reported in the Appendix C, Table C1. In all samples, the same compositions of ILs aqueous solutions, without caffeine, were used as control samples. Triplicates were performed for each assay.

RESULTS AND DISCUSSION

In order to evaluate the hydrotropic capability of ILs for drugs, the solubility of ibuprofen, naproxen and caffeine were determined in several aqueous solutions of ILs, with various concentrations, and compared with the results obtained with conventional hydrotropes. The values obtained for the solubility of ibuprofen, naproxen and caffeine in water at (303.15 ± 0.50) K were (37.54 ± 0.93) $mg \cdot L^{-1}$, (31.85 ± 0.87) $mg \cdot L^{-1}$ and (23.09 ± 1.36) $g \cdot L^{-1}$, respectively, being in good agreement with literature (21.0 $mg \cdot L^{-1}$, 15.9 $mg \cdot L^{-1}$ and 21.6 $g \cdot L^{-1}$, respectively, at 298.15 K).[372] All the solubility data, as well as the respective standard deviations, are presented in Appendix C (Tables C2, C3 and C4). Aiming at studying the effect of the IL concentration, the solubility of naproxen in aqueous solutions of $[N_{1,1,1,2(OH)}][Sal]$ and $[N_{1,1,1,2(OH)}][Van]$, and caffeine in aqueous solution of $[C_4C_1im][N(CN)_2]$ were determined at (303.1 ± 0.5) K in the whole concentration range, from pure water to aqueous saturated solutions of these ILs. Figure 4.3 shows the solubility enhancement (S/S_0) as a function of IL concentration, where S and S_0 represent the solubility of each drug in the aqueous solutions of the hydrotropes and in pure water, respectively. The results obtained clearly demonstrate the capacity of aqueous solutions of IL to enhance the solubility of the drugs here studied, when compared to pure water or pure IL. In fact, an increase in the solubility of up to 600-fold was observed, confirming the exceptional capacity of ILs to act as hydrotropes.

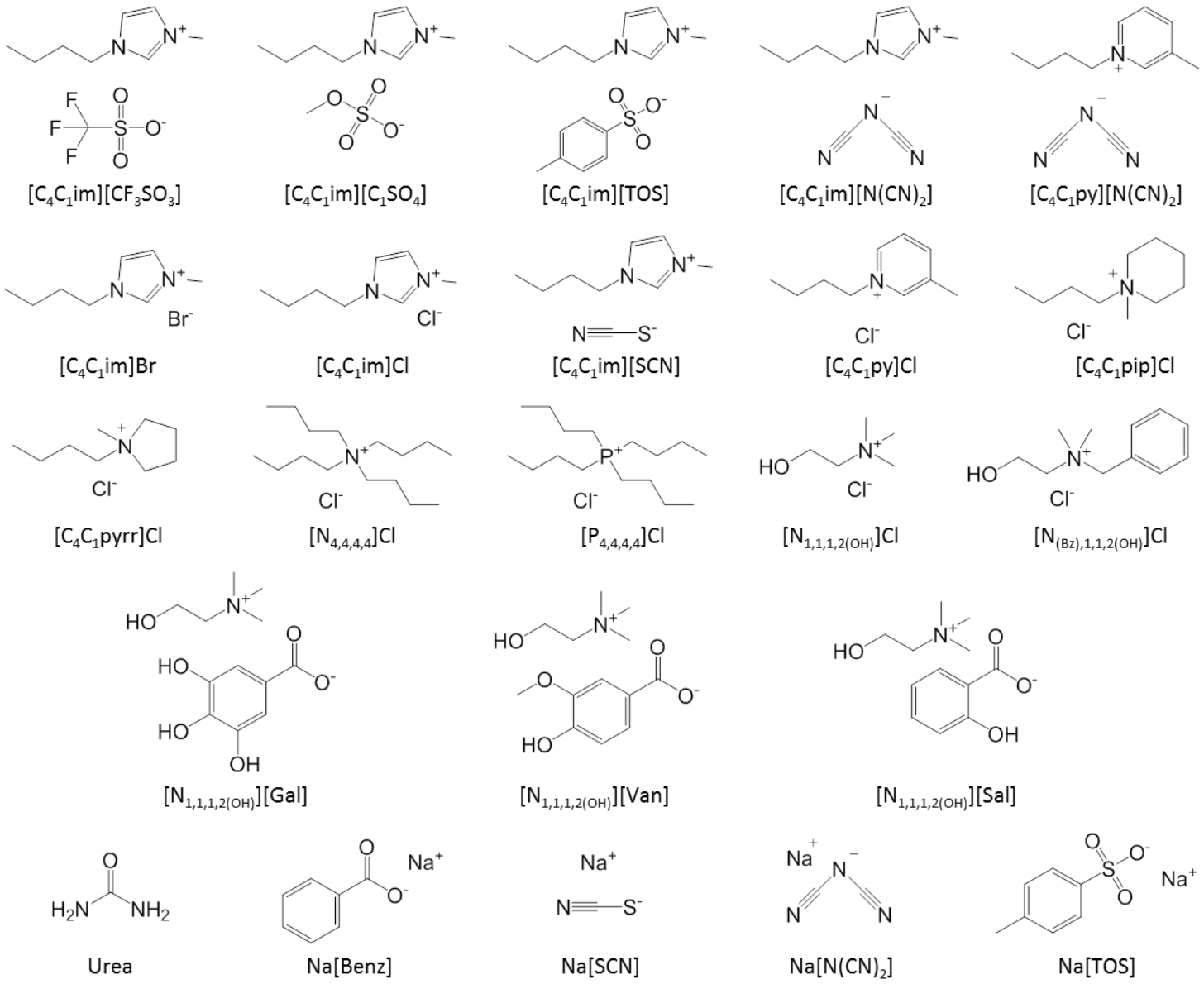

Figure 4.2. Chemical structure of the ILs and salts studied as hydrotopes.

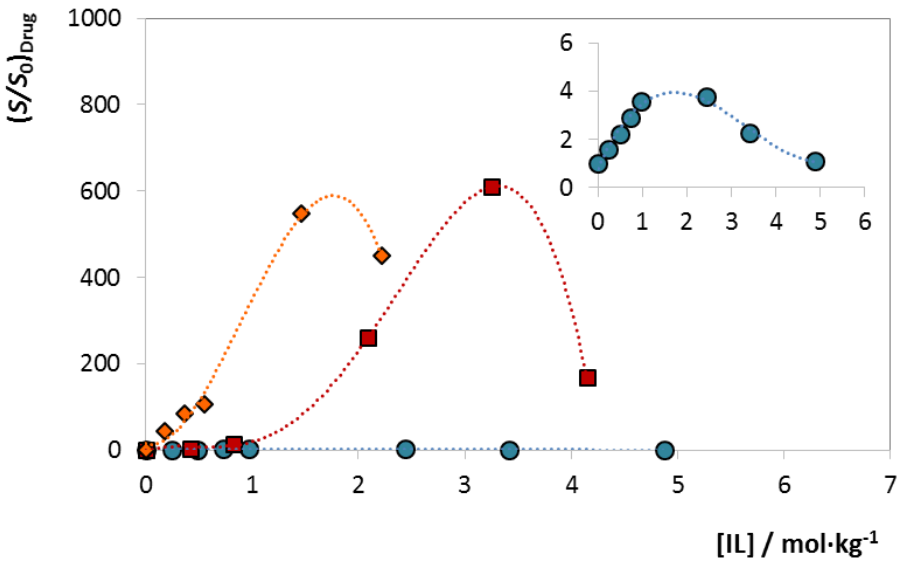

Figure 4.3. Impact of the IL concentration on the solubility of caffeine in aqueous solution of (●) $[C_4C_1im][N(CN)_2]$; and naproxen in aqueous solutions of (■) $[N_{1,1,1,2(OH)}][Sal]$ and (◆) $[N_{1,1,1,2(OH)}][Van]$. Line is guide for the eye.

Minimum hydrotrope concentration (MHC) is the lowest concentration of hydrotrope required for the solubility of a certain compound in water to start increasing significantly, being used in the interpretation of the hydrotropic behavior.[343] In order to investigate the MHC for $[C_4C_1im][N(CN)_2]$, $[C_4C_1py][N(CN)_2]$, $[C_4C_1im][SCN]$, $[P_{4,4,4,4}]Cl$, $[C_4C_1im]Br$, $[C_4C_1pip]Cl$ and $[C_4C_1pyrr]Cl$, the solubility of ibuprofen was measured in aqueous solution with hydrotrope concentrations between 0.02 and 1.3 $mol_{Hyd}·kg_{water}^{-1}$. Unlike the sudden change in the solubility associated with MHC, the results reported in Figure 4.4 show a continuous variation in the solubility of ibuprofen. The same behaviour was observed for naproxen, as reported in Appendix C (Figure C1). These results are in good agreement with some previous works.[367,373–375] In fact, although the MHC concept has been extensively accepted in the academia, recently authors have been questioning this concept and relate it with less accurate experimental measurements (such as due to the presence of impurities) and with an incorrect interpretation of the experimental data.[375–377]

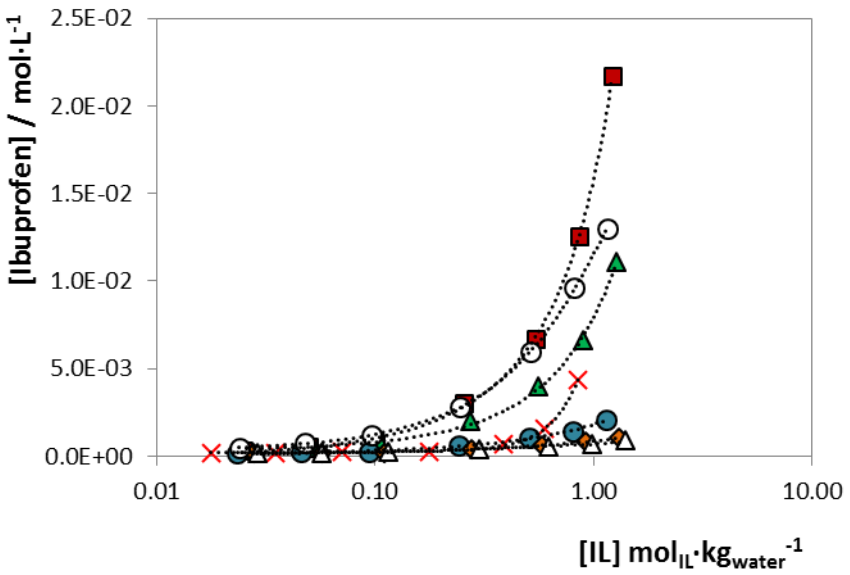

Figure 4.4. Impact of the IL concentration on the solubility of ibuprofen in aqueous solutions of (■) $[C_4C_1im][N(CN)_2]$, (○) $[C_4C_1py][N(CN)_2]$, (▲) $[C_4C_1im][SCN]$, (✕) $[P_{4,4,4,4}]Cl$, (●) $[C_4C_1im]Br$, (◆) $[C_4C_1pip]Cl$ and (△) $[C_4C_1pyrr]Cl$, in order to evaluate the MHC. Lines are guides for the eye.

The set of ILs here investigated was chosen to evaluate the influence of the anion nature and cation core upon its capacity to enhance the solubility of the drugs studied. The results of the influence of ILs, as well as some common hydrotropes, on the solubility enhancement of ibuprofen and naproxen are presented in Figure 4.5. The results for caffeine are depicted in the Appendix C (Figure C2). In agreement with what was previously reported,[367] the results show that both the IL cation and anion may contribute to enhance the solubility of the poorly water-soluble drugs (ibuprofen and naproxen). Furthermore, their performance as hydrotropes is much superior to that of conventional hydrotropes and salting-in inducing salts (urea, Na[Benz], Na[TOS), Na[SCN], $Na[N(CN)_2]$). The performance for caffeine solubility enhancement, for both ILs and salts, is however low. Reasons for this will be discussed below. In order to obtain a quantitative assessment of the influence of the ILs chemical structure on the solubility enhancement, the solubility data was correlated with the hydrotrope concentration using the modified Setschenow equation below:

$$S/S_0 = 1 + K_{Hyd} \times C_{Hyd} \qquad (2)$$

where S and S_0 are the solubility (mol·L^{-1}) of the drug in the hydrotrope aqueous solution and in pure water, respectively, C_{Hyd} is the concentration of hydrotrope in aqueous solution (mol$_{Hyd}$·kg$_{water}^{-1}$). The hydrotropy constants, K_{Hyd}, and the respective standard deviations, were estimated for each hydrotrope and listed in Table 4.1.

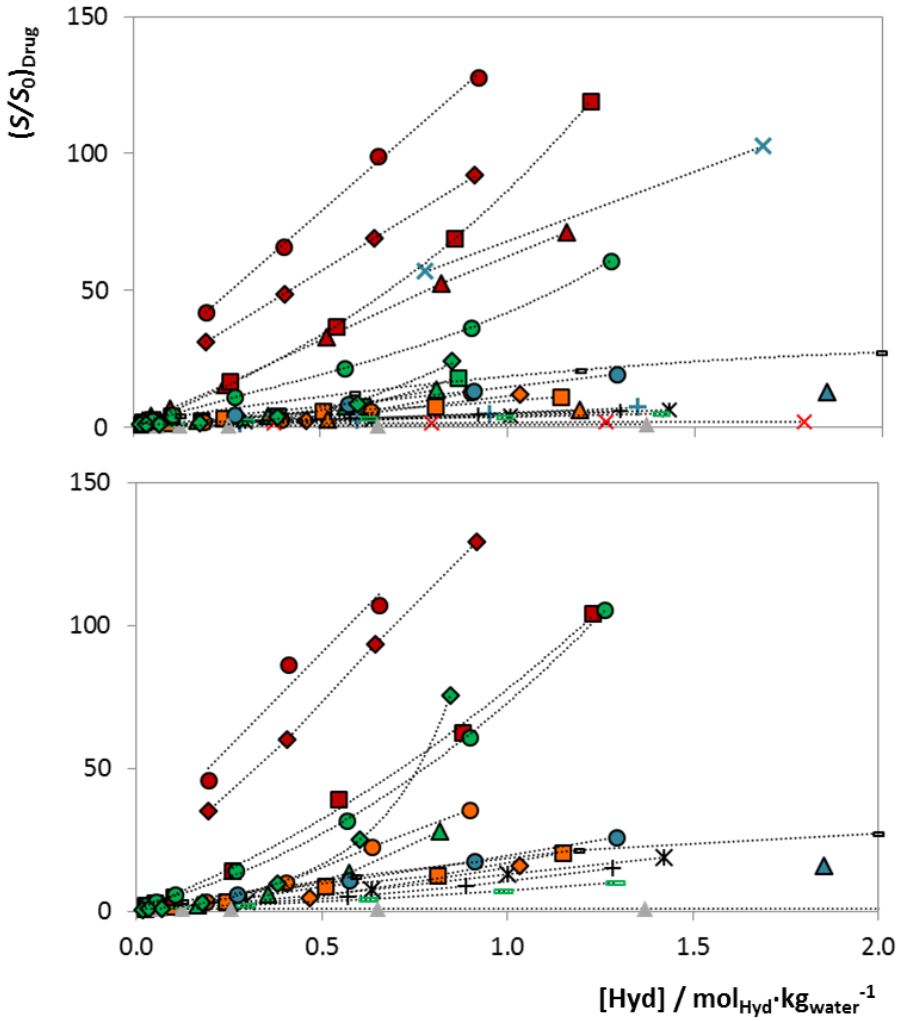

Figure 4.5. Impact of the hydrotrope concentration on the solubility of (a) ibuprofen and (b) naproxen in aqueous solutions of (●) [$N_{1,1,1,2(OH)}$][Van], (◆) [$N_{1,1,1,2(OH)}$][Gal], (■) [C_4C_1im][$N(CN)_2$], (✕) Na[Benz], (▲) [C_4C_1py][$N(CN)_2$], (●) [C_4C_1im][SCN], (◆) [$P_{4,4,4,4}$]Cl, (■) [C_4C_1im][CF_3SO_3], (▲) [C_4C_1im][TOS], (▪) Na[$N(CN)_2$], (●) Na[TOS], (●) [$N_{4,4,4,4}$]Cl, (◆) [$N_{1,1,1,2(OH)}$][Sal], (■) [C_4C_1im]Br, (+) [C_4C_1py]Cl, (+) [C_4C_1pip]Cl, (✳) [C_4C_1mim]Cl, (▲) [$N_{(Bz),1,1,2(OH)}$]Cl, (▪) [C_4C_1pyrr]Cl, (✕) [$N_{1,1,1,2(OH)}$]Cl, (▲) Na[SCN] and (▲) urea. S and S_0 represent the solubility of the drug in aqueous solution of the hydrotrope and in water, respectively. Lines are guides for the eye.

Table 4.1. K_{Hyd} values for the several hydrotropes analysed in the solubility of ibuprofen, naproxen and caffeine at (303.1 ± 0.5) K.

	K_{Hyd} (kg_{water} mol_{Hyd}^{-1}) ± σ		
Hydrotrope	Ibruprofen	Naproxen	Caffeine
$[C_4C_1im][N(CN)_2]$	87.161 ± 5.027	77.445 ± 3.344	2.182 ± 0.036
$[C_4C_1im][SCN]$	43.411 ± 1.739	74.128 ± 4.448	1.831 ± 0.132
$[C_4C_1im][CF_3SO_3]$	15.714 ± 2.900		1.957 ± 0.065
$[C_4C_1im][TOS]$	13.839 ± 1.435	27.457 ± 4.180	2.772 ± 0.352
$[C_4C_1im]Br$	8.993 ± 0.175	16.134 ± 0.538	0.496 ± 0.014
$[C_4C_1im]Cl$	3.646 ± 0.117	12.248 ± 0.530	0.167 ± 0.019
$[C_4C_1im][C_1SO_4]$			0.706 ± 0.038
$[C_4C_1py][N(CN)_2]$	61.499 ± 0.423		4.307 ± 0.312
$[C_4C_1py]Cl$	4.184 ± 0.421		0.172 ± 0.069
$[C_4C_1pip]Cl$	3.834 ± 0.117	10.123 ± 0.752	-0.126 ± 0.047
$[C_4C_1pyrr]Cl$	3.002 ± 0.138	6.762 ± 0.253	-0.101 ± 0.005
$[P_{4,4,4,4}]Cl$	19.971 ± 3.467	64.508 ± 11.316	0.613 ± 0.118
$[N_{4,4,4,4}]Cl$	10.721 ± 1.885	35.064 ± 3.505	0.794 ± 0.204
$[N_{1,1,1,2(OH)}][Van]$	145.891 ± 7.762	179.187 ± 16.959	
$[N_{1,1,1,2(OH)}][Gal]$	104.983 ± 5.835	142.707 ± 3.401	
$[N_{1,1,1,2(OH)}][Sal]$	56.782 ± 8.986	41.881 ± 3.361	
$[N_{1,1,1,2(OH)}]Cl$	0.710 ± 0.068		-0.295 ± 0.048
$[N_{(Bz),1,1,2(OH)}]Cl$	4.349 ± 0.407		
$Na[N(CN)_2]$	14.580 ± 1.232	14.738 ± 1.268	
Na[TOS]	13.995 ± 0.295	18.846 ± 0.385	
Na[SCN]	-0.085 ± 0.026	0.104 ± 0.031	2.267 ± 0.217
Na[Benz]	62.478 ± 4.370		3.975 ± 0.397
Urea	5.941 ± 0.185	7.313 ± 0.369	

This constant can be considered as a measure of the effectiveness of a hydrotrope, in other words, the higher the constant, the higher its capacity to increase the solubility of a given compound in water. The ability of the various ILs and salts to act as a hydrotropes for ibuprofen increase in the following order: Na[SCN] < $[N_{1,1,1,2(OH)}]Cl$ < $[C_4C_1pyrr]Cl$ < $[C_4C_1im]Cl$ < $[C_4C_1pip]Cl$ < $[C_4C_1py]Cl$ < $[N_{(Bz),1,1,2(OH)}]Cl$ < Urea < $[C_4C_1im]Br$ < $[N_{4,4,4,4}]Cl$ < $[C_4C_1im][TOS]$ < Na[TOS] < $Na[N(CN)_2]$ < $[C_4C_1im][CF_3SO_3]$ < $[P_{4,4,4,4}]Cl$ < $[C_4C_1im][SCN]$ < $[N_{1,1,1,2(OH)}][Sal]$ < $[C_4C_1py][N(CN)_2]$ < Na[Benz] < $[C_4C_1im][N(CN)_2]$ < $[N_{1,1,1,2(OH)}][Gal]$ <

$[N_{1,1,1,2(OH)}][Van]$. A similar order was observed for naproxen: Na[SCN] < $[C_4C_1pyrr]Cl$ < Urea < $[C_4C_1pip]Cl$ < $[C_4C_1im]Cl$ < $Na[N(CN)_2]$ < $[C_4C_1im]Br$ < Na[TOS] < $[C_4C_1im][TOS]$ < $[N_{4,4,4,4}]Cl$ < $[N_{1,1,1,2(OH)}][Sal]$ < $[P_{4,4,4,4}]Cl$ < $[C_4C_1im][SCN]$ < $[C_4C_1im][N(CN)_2]$ < $[N_{1,1,1,2(OH)}][Gal]$ < $[N_{1,1,1,2(OH)}][Van]$. As regards the caffeine, the hydrotropic effect follows the order: $[N_{1,1,1,2(OH)}]Cl$ < $[C_4C_1pip]Cl$ < $[C_4C_1pyrr]Cl$ < $[C_4C_1im]Cl$ < $[C_4C_1py]Cl$ < $[C_4C_1im]Br$ < $[P_{4,4,4,4}]Cl$ < $[C_4C_1im][C_1SO_4]$ < $[N_{4,4,4,4}]Cl$ < $[C_4C_1im][SCN]$ < $[C_4C_1im][CF_3SO_3]$ < $[C_4C_1im][N(CN)_2]$ < Na[SCN] < $[C_4C_1im][TOS]$ < Na[Benz] < $[C_4C_1py][N(CN)_2]$.

In order to evaluate the effect of the IL cation on the solubility of these drugs, a series of chloride-based ILs was studied and presented in Figure 4.6. The set of IL cations analysed includes aromatic ($[C_4C_1im]^+$ and $[C_4C_1py]^+$), cyclic non-aromatic ($[C_4C_1pyrr]^+$ and $[C_4C_1pip]^+$), non-cyclic non-aromatic ($[N_{4,4,4,4}]^+$, $[P_{4,4,4,4}]^+$ and $[N_{1,1,1,2(OH)}]^+$) and non-cyclic with a benzene ring ($[N_{(Bz),1,1,2(OH)}]^+$) compounds. Among the cations investigated in the chloride-based IL series, $[N_{4,4,4,4}]Cl$ and $[P_{4,4,4,4}]Cl$ presented the higher increase in the solubility of both drugs studied in this work. The remaining IL cations showed a significant hydrotropic activity for ibuprofen and naproxen, with the exception of the $[N_{1,1,1,2(OH)}]Cl$. Regarding the caffeine, while $[C_4C_1im]Cl$ and $[C_4C_1py]Cl$ seems to present only a small hydrotropic effect, $[N_{1,1,1,2(OH)}]Cl$, $[C_4C_1pyrr]Cl$ and $[C_4C_1pip]Cl$ have a negative effect on its solubility. The π-π interactions has been used in the past to explain the formation of solute-hydrotrope complexes, and thus the hydrotropic effect.[351,352,378] However, the results obtained support the idea that these interactions (between the aromatic drug and the aromatic cation core) are not the dominant driving forces behind the hydrotropic behaviour, since the best results were obtained for non-cyclic non-aromatic ILs, in agreement with other authors.[354,367,379,380]

The influence of the IL cation on the hydrotropic constant was further evaluated using the tosylate, thiocyanate and dicyanamide anions, as depicted in Figure 4.7. With the exception of tosylate-based hydrotropes that present similar hydrotropic effect, the replacement of sodium cation by an imidazolium or pyridinium cation leads to a remarkable enhancement in the solubility of ibuprofen and naproxen. On the other hand, the hydrotropy constants of Na[SCN] and $[C_4C_1im][SCN]$ are low and quite similar for caffeine, (2.267 and 1.831 $kg_{water}{\cdot}mol_{Hyd}^{-1}$, respectively). These results reinforce the idea

that there is no universal hydrotropic agent able to solubilize all hydrophobic drugs[349] but instead, the hydrotropic effect may be quite solute specific.

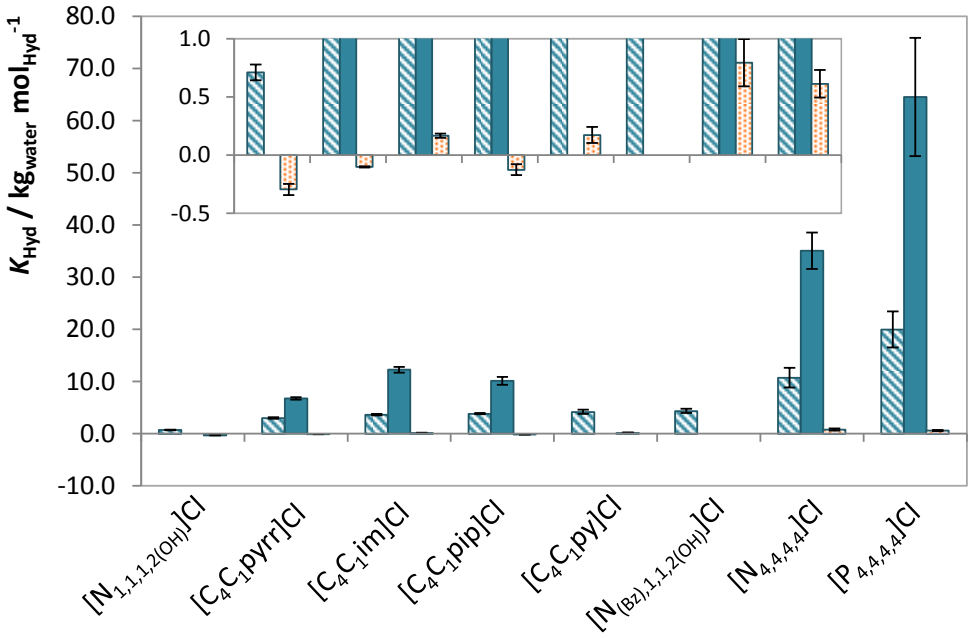

Figure 4.6. K_{Hyd} values of the chloride-based ILs for ibuprofen (blue stripes), naproxen (blue) and caffeine (orange spots).

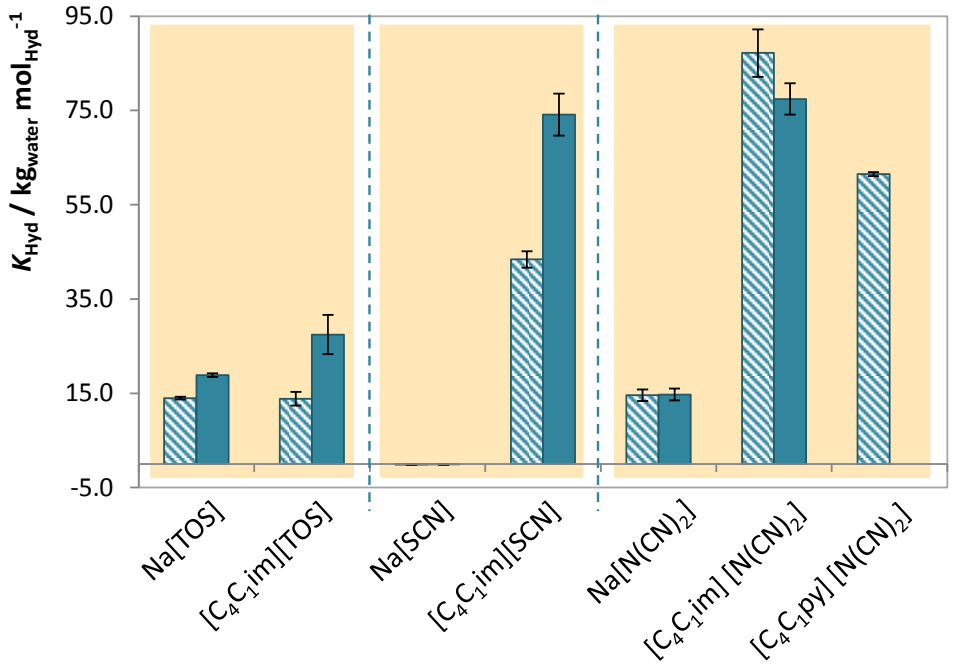

Figure 4.7. K_{Hyd} values for ibuprofen (blue stripes) and naproxen (blue) using tosylate-, thiocyanate- and dicyanamide-based hydrotropes.

In order to evaluate the influence of the IL anion on the solubility of drugs here studied, a series of $[C_4C_1im]^-$, $[N_{1,1,1,2(OH)}]^-$ and sodium-based hydrotropes was investigated and presented in Figure 4.8 and Figure 4.9. The set of IL anions analysed covers halogens (Br^- and Cl^-), nitriles ($[SCN]^-$ and $[N(CN)_2]^-$), sulfate ($[C_1SO_4]^-$), sulfonates ($[CF_3SO_3]^-$ and $[TOS]^-$), fluorinated ($[CF_3SO_3]^-$) and aromatic ($[Benz]^-$) with a phenyl group ($[Van]^-$, $[Gal]^-$ and $[Sal]^-$). As previously mentioned, the conventional hydrotropes are usually anionic compounds composed of an aromatic ring substituted by an anionic group, such as sulfate, sulfonate, or carboxylate group. Considering the $[C_4C_1im]$-based IL series, $[C_4C_1im][N(CN)_2]$ and $[C_4C_1im][SCN]$ presented the highest hydrotropic activity for ibuprofen and naproxen, as depicted in Figure 4.8. The same trend on the enhanced solubility of this set of IL anions was observed for ibuprofen and naproxen, being the halogens those that present the lowest hydrotropic efficiency. Regarding the caffeine, only a residual effect was observed for the range of IL anions studied.

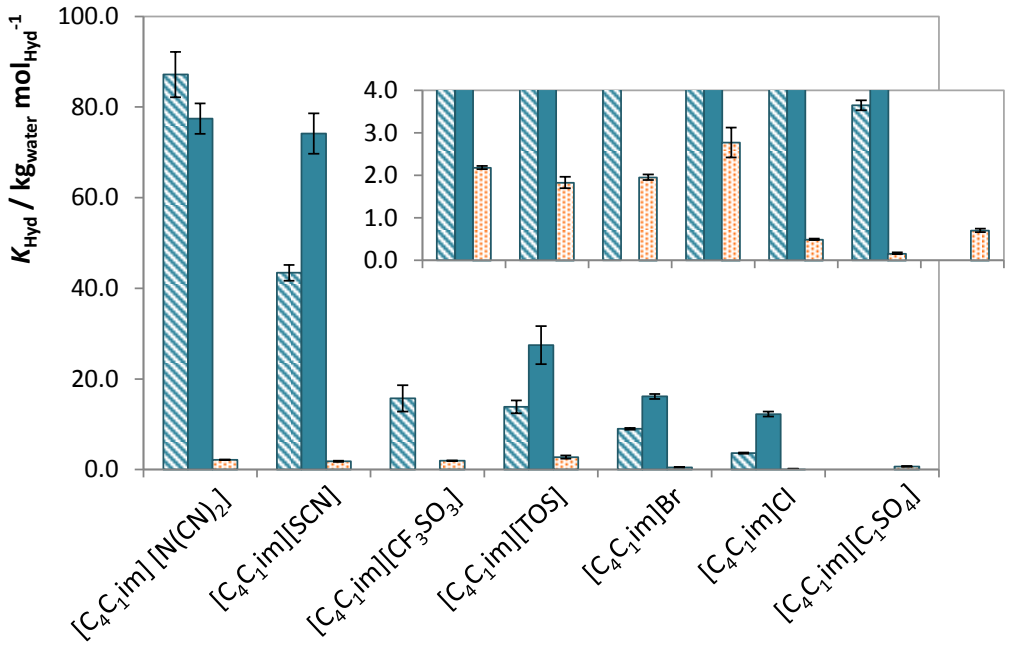

Figure 4.8. K_{Hyd} values of the $[C_4C_1im]$-based ILs for ibuprofen (blue stripes), naproxen (blue) and caffeine (orange spots).

Although dicyanamide and thiocyanate present an outstanding hydrotropic activity when conjugated with the $[C_4C_1im]^+$ cation, the same behaviour was not observed when these were combined with the sodium cation (Figure 4.9). These results support the idea that both anion and cation may contribute to the hydrotropic phenomenon in a synergistically manner.[367] It should be noted that the replacement of chloride anion by dicyanamide, when conjugated with $[C_4C_1py]^+$ cation, leads to a significant enhancement in the solubility of ibuprofen and caffeine. Among the sodium-based hydrotropes studied in this work, sodium benzoate was the most effective in terms of the hydrotropic effect for ibuprofen. Since this compound is a well-known hydrotrope, this result was expected.[350] As regards the $[N_{1,1,1,2(OH)}]$-based IL series, cholinium vanillate and cholinium gallate are the most promising ILs for the ibuprofen solubilisation, and have indeed the higher hydrotropy constant values of all hydrotropes studied in this work. These remarkable results can be justified by the presence of a phenyl group in their structure.[346] This premise was also verified for another phenolic anion studied, namely salicylate anion. It is also worth mentioning that both cholinium vanillate and gallate present similar antioxidant activity and cytotoxicity profiles when compared with the respective phenolic acids currently used in the therapeutic, rendering these hydrotropes as valid and valuable candidates in the formulation of pharmaceutical/cosmetic products.[366]

The increase in solubility of hydrophobic solutes depends not only on the nature of the hydrotrope but also on the nature of the solute. As shown in Table 4.1, the hydrotropic efficiency of the studied compounds is much higher on the solubility of ibuprofen and naproxen than on the solubility of caffeine, with the exception of the Na[SCN]. Considering their distinct solubilities in water, these results suggest that the hydrotropic solubilisation may be more effective for the most hydrophobic solutes. In an attempt to investigate this hypothesis, the logarithmic value of the 1-octanol-water partition coefficients ($\log K_{ow}$) for these three drugs (3.84, 2.99, -0.55 for ibuprofen, naproxen and caffeine, respectively), as well as two antioxidants (1.22 and 0.72 for vanillin and gallic acid, respectively), were estimated using the ChemSpider database (accessed at January 6th, 2017). The hydrotropy constants for vanillin and gallic acid were estimated according to the solubility data reported previously by our group and by using equation 2.[367] As

reported in Figure 4.10, it seems that there is a general correlation between the K_{Hyd} ($kg_{water}.mol_{Hyd}^{-1}$) estimated and the log$K_{ow}$ values of the molecules studies. In general, the results suggest that there is an increase of the hydrotropic effect with the compounds hydrophobicity.

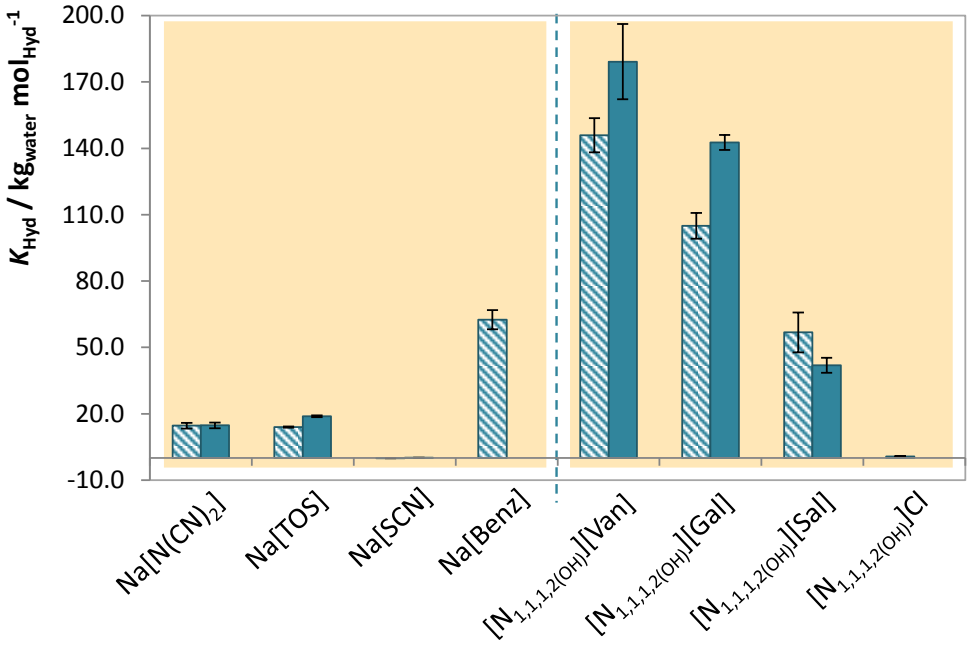

Figure 4.9. K_{Hyd} values for ibuprofen (blue stripes) and naproxen (blue) using sodium- and cholinium-based hydrotropes.

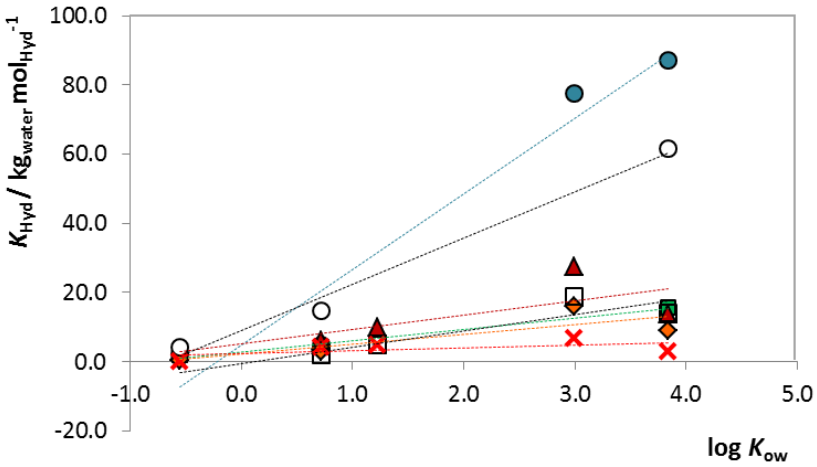

Figure 4.10. Impact of the logK_{ow} value of each biomolecule on the hydrotropy constant of the (●) $[C_4C_1im][N(CN)_2]$, (○) $[C_4C_1py][N(CN)_2]$, (▲) $[C_4C_1im][TOS]$, (□) Na[TOS], (◆) $[C_4C_1im]Br$, (■)$[C_4C_1im][CF_3SO_3]$ and (✕)$[C_4C_1pyrr]Cl$. Lines are guides for the eye.

CONCLUSION

The results reported in this work clearly evidence the outstanding ability of ILs to act as hydrotropes for ibuprofen and naproxen. Furthermore, the cation and anion may synergistically contribute to the hydrotropic phenomenon, which makes them powerful catanionic hydrotropes. Considering the chloride-based IL series, the $[N_{4,4,4,4}]Cl$ and $[P_{4,4,4,4}]Cl$ have presented the higher increase in the solubility of the all drugs studied. On the other hand, considering the 1-butyl-3-methylimidazolium family, dicyanamide and thiocyanate anions were the best hydrotropic solubilizing agents. Nevertheless, cholinium vanillate and cholinium gallate seem to be the most promising ILs for the ibuprofen solubilisation, where an increase in the solubility of up to 125- and 95-fold was observed, respectively, only with IL concentrations around 0.7 M. Similar results were obtained for naproxen. It should be noted that these two cholinium-based ILs have analogous antioxidant activity and cytotoxicity profiles when compared with the respective phenolic acids currently used in the therapeutic, meaning that these hydrotropes are promising candidates in the formulation of drugs and personal care products. Finally, the increase in solubility of hydrophobic solutes depends not only on the nature of hydrotrope but also on the solute hydrophobicity.

Chapter 5 - Ionic Liquids with Surfactant Nature

Synthesis and characterization of new surface active ionic liquids with capacity to promote cell disruption of Escherichia coli

Tânia E. Sintra, Miguel Vilas, Margarida Martins, Sónia P. M. Ventura, Ana I. M. C. Lobo Ferreira, Luís M. N. B. F. Santos, Fernando Gonçalves, Emilia Tojo and João A. P. Coutinho.
Under preparation.

(In this communication Tânia E. Sintra contributed with characterization of SAILs, measurement of theirs aggregation and thermal properties, their ecotoxicity, and with the manuscript preparation.)

ABSTRACT

The self-aggregation of ILs in aqueous solution represents an important key to a variety of applications. Twelve SAILs, based on imidazolium, ammonium and phosphonium cations and containing one or more long alkyl chains in the cation and/or anion, were synthetized and characterized. The aggregation behaviour of these SAILs in water, as well as their adsorption at solution/air interface, were studied using surface tension and conductivity. Their thermal properties were characterized, namely the melting point and decomposition temperature by DSC and TGA, respectively. Furthermore, the toxicity of these ILs was evaluated in what concerns the effect of different structural features using the marine luminescent bacteria *V. fischeri*. Finally, their ability to induce cell disruption of *Escherichia coli* and, consequently, to release the intracellular green fluorescent protein (GFP) was investigated.

INTRODUCTION

ILs are a class of low melting point ionic compounds, which have attracted increasing attention as media for performing distinct reactions.[381–385] These compounds possess high thermal stabilities and negligible vapor pressures at room temperature, making them a promising alternative to conventional solvents. Moreover, due to their amphiphilic nature they can dissolve a wide range of compounds and can be structurally tailored for specific applications by choosing the appropriate anion-cation combination.[4,367] A number of ILs containing long alkyl chain substituents (typically larger that octyl chains) have been reported to be surface active. These ionic compounds are currently termed as SAILs and are attracting a great deal of interest in classical colloid and surface chemistry research.[386–388] As the conventional surfactants, SAILs have the capacity to self-aggregate in aqueous media above the CMC.[196] Due to their tunable structure, these compounds allow to design many new families and types of surfactants. A number of analytical applications have emerged in separation science regarding the use of SAILs, not only as solubilization media for proteins,[389] but also in analytical techniques, namely chromatography or electrophoresis,[390–393] in biocatalysis[394] and also in extractive and preconcentration techniques.[395,396] The potential industrial application of SAILs, as well as their impact on the environment, is closely dependent on their self-assembly behavior and aggregate structure in aqueous solution.[204] Thus, the study of the aggregation behavior of these compounds in water is of high importance. The amphiphilic structure of ILs in water began to be intensively studied in 2004.[199,200,202,211,397] A significant amount of research has focused on the study of the aggregation behavior of alkylimidazolium ILs. Sirieix-Plénet and co-authors described the self-aggregation of 1-decyl-3-methylimidazolium bromide ($[C_{10}C_1im]Br$) at low concentrations, and the CMC value was estimated to be 0.04 M by using potentiometric and conductimetric studies. The author also observed that at higher concentrations it adopts a fairly complex structure with interpenetrated domains of the water and electrolyte.[199] Bowers and co-authors reported the aggregation behavior in aqueous solution of three ILs, namely 1-butyl-3-methylimidazolium tetrafluoroborate $[C_4C_1im][BF_4]$, 1-methyl-3-octylimidazolium chloride $[C_8C_1im]Cl$ and 1-methyl-3-octylimidazolium iodide $[C_8C_1im]I$, by using surface tension,

conductivity and small-angle neutron scattering (SANS) measurements. The CMC values were estimated for these three ILs, being approximately 0.1 M for $[C_8C_1im]$-based ILs and 0.8 M for $[C_4C_1im][BF_4]$. SANS data allowed for the proposition that the short chain $[C_4C_1im][BF_4]$ system can best be modeled as a dispersion of polydisperse spherical aggregates, whereas the $[C_8C_1im]I$ solutions can be modeled as a system of regularly sized near-spherical charged micelles above the CMC.[200] Miskolczy et al.[202] studied aggregation of ILs with *n*-octyl alkyl chain by measuring conductivity, turbidity and using a solvatochromic probe. 1-Butyl-3-methylimidazolium octyl sulfate ($[C_4C_1im][C_8SO_4]$) was found to form micelles above 0.031 M. In contrast, $[C_8C_1im]Cl$ produced an inhomogeneous solution of larger aggregates.[202] Baltazar et al.[211] investigated eighteen different mono- and dicationic (or gemini) imidazolium bromide ILs using surface tension measurements. The results showed a correlation between substituted alkyl chain length and the CMC value for mono and dicationic ILs. Furthermore, mono cationic imidazolium ILs generally have lower CMC values than dicationic imidazolium ILs, and longer alkyl linkage chain connecting the two imidazolium rings were found to slightly decrease the CMC values.[211] Brown et al. reported a series of IL-based surfactants composed of tetraalkylammonium cations and common surfactant anions (derived from dodecyl sulfate and aerosol-OT) as alternatives to imidazolium-based systems, being claimed as cheaper and environmentally more benign.[398] More recently, a series of mono- and dicationic ammonium bromide ILs were synthetized an studied by Özdil and co-workers.[399] The results showed that the absence of the spacer group may confer relatively low flexibility to the molecules, with potential implications on the interfacial properties, namely, on micellization.[399] Phosphonium-based ILs with long alkyl chains have also shown a great potential as surfactants, namely in separation science.[392] Although the phenomena of IL self-organization in aqueous solutions are currently under investigation by a number of authors, their correlation with ILs structure is limited.[198,205,207,399] This lack of information may compromise their potential industrial application.

The present work reports the synthesis and characterization of several families of ILs with a surfactant nature, namely imidazolium, quaternary ammonium and phosphonium,

containing one or more long alkyl chains in the cation and/or anion. As a result, cationic, gemini, and catanionic ILs will be prepared, as illustrated in Figure 5.1. The structures of these ILs will be confirmed by ^{1}H and ^{13}C NMR. The aggregation behavior of these SAILs in water, as well as their adsorption at solution/air interface, will be studied using surface tension and conductivity. Their thermal properties will be characterized, namely the melting point and decomposition temperature by DSC and TGA, respectively. Moreover, the ecotoxicity of the entire set of ILs prepared will be tested in what concerns the effect of different structural features, in particular the cation core, anion nature, and cation and anion alkyl chain lengths. For that purpose, several Microtox® test assays will be performed using the marine luminescent bacteria *V. fischeri*.[292] Finally, the ILs obtained will be studied in order to understand their capacity to promote cell disruption of *Escherichia coli* cells, as a possible application.

EXPERIMENTAL SECTION

Materials: Twelve IL-based surfactants were synthesized, namely $[N_{1,1,1,14}]Br$, *N,N,N*-trimethyl-*N*-tetradecylammonium bromide; $[N_{1,1,1,14}]Cl$, *N,N,N*-trimethyl-*N*-tetradecylammonium chloride; $[P_{1,1,1,14}]Br$, trimethyltetradecylphosphonium bromide; $[N_{1,1,1,14}][C_1SO_4]$, *N,N,N*-trimethyl-*N*-tetradecylammonium methylsulfate; $[C_1C_{14}Im]Br$, 1-methyl-3-tetradecylimidazolium bromide; $[N_{1,1,14,14}]Br$, *N,N*-dimethyl-*N,N*-ditetradecylammonium bromide; $[N_{1,1,14,14}]Cl$, *N,N*-dimethyl-*N,N*-ditetradecylammonium chloride; $[N_{1,1,10,14}]I$, *N*-decyl-*N,N*-dimethyl-N-tetradecylammonium iodide; $[C_{14}C_{14}Im]Br$, 1,3-ditetradecylimidazolium bromide; $[N_{1,1,14}\text{-}6\text{-}N_{1,1,14}]Br_2$, *N,N*'-bis(tetradecyldimethyl)-1,6-hexanediammonium dibromide, $[C_{14}Im\text{-}6\text{-}C_{14}Im]Br_2$, 3,3´-(1,6-hexanedyl)bis(1-tetradecylimidazolium) dibromide and $[N_{1,1,1,14}][C_{10}SO_4]$, *N,N,N*-trimethyl-*N*-tetradecylammonium decylsulfate. Their acronym and chemical structure are depicted in Figure 1. Imidazole (99 wt % of purity), 1-bromotetradecane (97 wt % of purity), 1-methylimidazole (99 wt % of purity), 1,6-dibromohexane (96 wt % of purity), 1-chlorotetradecane (98 wt % of purity), trimethylamine (4.2 M in ethanol), 1-iododecane (98 wt % of purity), dimethylsulfate (99.8 wt % of purity), 1-decanol (99 wt % of purity), trimethylphosphine (1.0 M in toluene), sodium sulfate (99.9 wt % of purity),

methanesulfonic acid (99.5 wt % of purity) and potassium carbonate (99 wt % of purity) were acquired from Sigma-Aldrich®. All organic solvents used (HPLC grade), namely methanol, ethyl acetate, hexane, dichloromethane, toluene and diethyl ether were from VWR. *Escherichia coli* (*E. coli*) BL21(DE3) pLysS carrying the pET-28(a) plasmid encoding the GFP gene were kindly provided by the Molecular and Cellular Biology Laboratory of the School of Pharmaceuticals Sciences from the Estadual Paulista "Júlio de Mesquita Filho" University. The components of Luria-Bertani (LB) culture media for the *E. coli* growth, tryptone and yeast extract were purchased from Oxoid, while sodium chloride (99.5 wt % of purity) was acquired from Panreac. The antibiotic used in cell culture, kanamycin and chloramphenicol, the inducer isopropyl β-D-1-thiogalactopyranoside (IPTG), as well as the components of the Tris-HCl buffer, tris(hydroxymethyl) aminomethane (99.8 wt % of purity) and chloridric acid (37 wt % in aqueous solution), were purchased from Sigma-Aldrich®. The water used was double distilled, passed by a reverse osmosis system and further treated with a Milli-Q plus 185 water purification apparatus.

Synthesis of surface active ILs: Generally, these ILs with surfactant nature were synthesized via quaternization reaction. Additionally, a transesterification reaction was performed in order to prepare the $[N_{1,1,1,14}][C_{10}SO_4]$.[38,42,45,104,400] More details about the synthesis of these ILs are reported in the Appendix D, being those divided into four major topics: I) synthesis of 1-tetradecylimidazole; II) synthesis of imidazolium-based ILs; III) synthesis of ammonium-based ILs and IV) synthesis of phosphonium-based ILs. The structure of all compounds synthesized was confirmed by ^{1}H and ^{13}C NMR, showing the high purity level of all ionic structures after their synthesis, as reported in the Appendix D.

Electric conductivity measurements: Conductivity measurements were performed using a SevenMulti™ (Mettler Toledo Instruments) at 25 °C, within an uncertainty of ± 0.01 $\mu S \cdot cm^{-1}$. The conductivity meter was calibrated with a standard solution of KCl with known conductivity (10 $\mu S \cdot cm^{-1}$, 84 $\mu S \cdot cm^{-1}$, 500·µS cm^{-1}, 1413·µS cm^{-1} and 12.88 $mS \cdot cm^{-1}$). The conductivity measurements of the IL-based surfactants studied were carried out by continuous dilution of a IL-based concentrated solution into water. After any addition of the IL solution, the solution obtained was stirred and equilibrated for 10

min, and then three successive measurements of conductivity were performed (Appendix D, Figure D1). Duplicated measurements were carried out.

Surface tension: The surface tension of a range of diluted aqueous solutions of each IL was determined by the analysis of the shape of a pendant drop and measured using a Dataphysics (model OCA-20) contact angle system (Appendix D, Figure D2). For that, a Hamilton DS 500/GT syringe was used, being connected to a Teflon coated needle placed inside an aluminum air chamber able to maintain the temperature of interest within ± 0.1 °C. The surface tension measurements were performed at 25 °C. The temperature inside the aluminum chamber in which the surface tensions were determined was measured with a Pt100 within ± 0.1 °C. After reaching a specific temperature inside the aluminum chamber, the measurements were carried out after 10 min to guarantee the thermal stabilization. Silica gel was kept inside the air chamber aiming at keeping a dry environment. For the surface tensions determination at each sample, at least 3 drops were formed and analyzed. For each drop, an average of 250 images was captured. The analysis of the drop shape was done with the software modules SCA 20 where the gravitational acceleration (g = 9.8018 $m \cdot s^2$) and latitude (lat = 40°) were used according to the location of the assay. Further details on the equipment and its validity to measure surface tensions of ILs were previously addressed.[401]

Thermogravimetric analysis: The decomposition temperature was determined by TGA. TGA was conducted on a Setsys Evolution 1750 (SETARAM) instrument. The sample was heated in an alumina pan, under a nitrogen atmosphere, over a temperature range of 25 - 800 °C, and with a heating rate of 10 $°C \cdot min^{-1}$.

Differential Scanning Calorimetry: Thermal transition temperature and the melting temperature were measured in a DSC, PERKIN ELMER model Pyris Diamond DSC, using hermetically sealed aluminum crucibles with a constant flow of nitrogen (50 $mL \cdot min^{-1}$). Samples of about 15 mg were used in each experiment. The temperature and heat flux scales of the power compensation DSC were calibrated by measuring the temperature and the enthalpy of fusion of reference materials, at the scanning rate of 2 $°C \cdot min^{-1}$ and

flow of nitrogen. Temperatures of the thermal transitions and melting temperature were taken as the onset temperatures.

Microtox Assay: To evaluate the ecotoxicity of the SAILs synthesized towards the marine bacteria *V. fischeri*, the Standard Microtox liquid-phase assay was applied. This test is described in detail in the Experimental Section of Chapter 2.

Cell disruption of Escherichia coli: In order to evaluate one possible application of the ILs here synthetized, their ability to promote cell disruption of *Escherichia coli* (*E. coli*) was investigated. For that, aqueous solutions of these ILs-based surfactants were evaluated in their capacity to release the intracellular GFP by their action in the lipid membranes. This protein is largely used as a promising biomarker in biomedical applications due to its unique spectral and fluorescence features. The GFP extraction from *E. coli* cells by using tensioactive compounds was recently proposed by our group as an alternative method to conventional ultrasonic-assisted extraction. The preparation of the cell culture and the GFP release (cell disruption) was performed according to previous work.[402] Briefly, the *E. coli* strain was grown at 37 °C in LB medium with kanamycin and chloramphenicol (50 $\mu g \cdot mL^{-1}$) with a constant stirring (150 rpm). Six hours later, IPTG was added to induce the GFP expression at a final concentration of 0.25 mM. After 17h of protein induction, the culture medium was centrifuged at 5000 rpm for 30 minutes at 4 °C and the weight of wet cells was calculated. Cell pellets containing GFP were resuspended in 50 mM Tris-HCl buffer at pH 8 in a concentration of approximately 0.025 wet cells wt %. To evaluate the ability of the IL-based surfactants here synthesized to solubilize the cell membrane, a concentration of 100 mM was used. Moreover, it was studied the effect of the IL concentration between 50 and 500 mM. The cell suspensions were centrifuged at 25 rpm during 30 min, and the supernatant was analyzed in terms of GFP content by its fluorescence (emission at 485 nm and excitation at 530 nm).

RESULTS AND DISCUSSION

Twelve tensioactive ILs, based on the imidazolium, ammonium and phosphonium cations and containing one or more long alkyl chains in the cation and/or anion, were synthetized

and characterized. Their chemical structure and acronym are depicted in Figure 5.1. These surface active compounds were obtained with high purity levels and yield – cf. Experimental Section.

The self-organization of these ILs-based surfactants in aqueous solution, as well as their adsorption behavior, was investigated using surface tension and conductivity. The data thus obtained was employed to calculate the CMC, the surface tension at the CMC (γ_{CMC}), the concentration required to reduce the surface tension of the solvent by 20 mN m^{-1} (C_{20}), CMC/C_{20} ratio (a measure of the tendency to form micelles relative to adsorb at the air/water interface), the minimum area *per* surfactant molecule at the air/water interface (A_{min}), the maximum surface excess concentration at the air/aqueous solution interface (Γ_{max}), as well as the degree of ionization of the aggregates (α). These parameters are presented in Table 5.1. CMC is the concentration at which the solution property of a tensioactive compound shows an abrupt change, and constitutes a basic parameter of the surface chemistry and colloid science.[403] This critical concentration reflects the balance between the hydrophobic interaction of the hydrophobic tails of amphiphilic molecules and the hydration and electrostatic repulsive effects of their hydrophilic head groups.[404] The CMC values were obtained from both conductivity and surface tension. The results acquired with both methodologies are consistent with each other, as shown in Table 5.1. Furthermore, the CMC values obtained show the high capacity of these tensioactive ILs to form microaggregates by their self-aggregation. For $[N_{1,1,14,14}]Cl$, $[N_{1,1,10,14}]I$, $[C_{14}C_{14}Im]Br$, $[C_{14}Im\text{-}6\text{-}C_{14}Im]Br_2$ and $[N_{1,1,1,14}][C_{10}SO_4]$, it was not possible to accurately determine the CMC values due to restrictions regarding their solubility limits in water.

The introduction of the second alkyl chain on the ammonium cation plays a dominant role in CMC values of ILs, as observed for $[N_{1,1,1,14}]Br$ (3.91mM) and $[N_{1,1,14,14}]Br$ (0.07 mM) pair. Furthermore, the CMC values of $[N_{1,1,1,14}]Br$ and $[P_{1,1,1,14}]Br$ suggest that changes in the cation's central atom have impact on their aggregation behaviour. According to the results obtained, phosphonium-based ILs present lower CMC than the respective ammonium ILs. Finally, the mono cationic ammonium IL $[N_{1,1,14,14}]Br$ (0.07 mM) presents lower CMC value than the dicationic ammonium IL $[N_{1,1,14}\text{-}6\text{-}N_{1,1,14}]Br_2$ (0.68 mM).

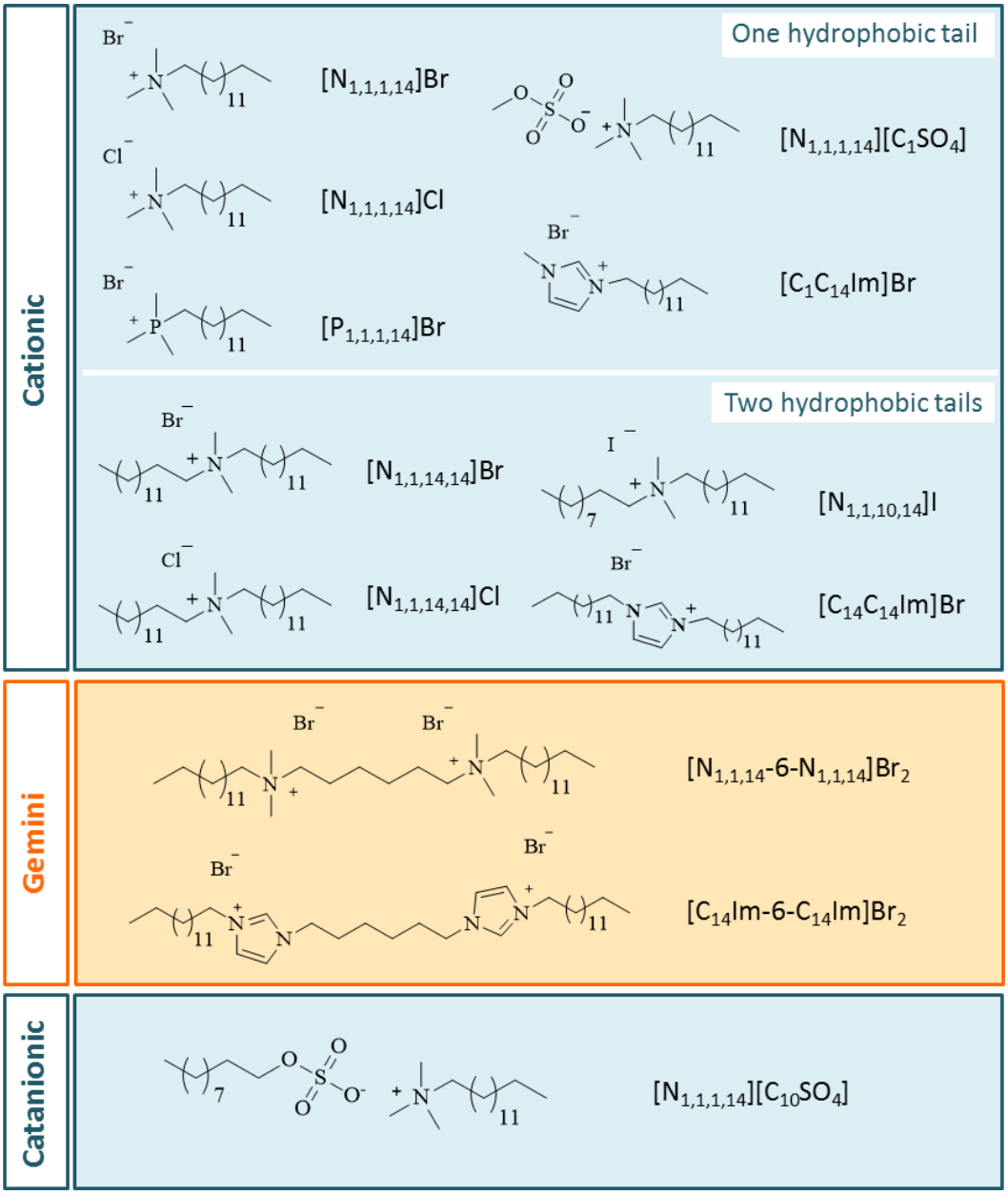

Figure 5.1. Chemical structures and acronyms of the SAILs synthesized in this work.

Table 5.1. Physical properties of the SAILs synthetized in this work.

	Conductivity		**Surface Tension**						
	CMC / mM	α	CMC / mM	γ_{CMC} /mN m^{-1}	C_{20} / mM	CMC/C_{20}	pC20 / mM	Γ_{max} / mol m^{-2}	A_{min} / Å^2
$[N_{1,1,1,14}]Br$	3.91	0.27	3.43	37.46	1.30	2.64	-0.11	6.04E-06	27.48
$[P_{1,1,1,14}]Br$	3.00	0.23	2.48	36.18	0.85	2.91	0.07	5.98E-06	27.78
$[C_1C_{14}Im]Br$	2.43	0.27	2.61	37.16	0.93	2.80	0.03	5.81E-06	28.60
$[N_{1,1,1,14}][C_1SO_4]$	3.47	0.30	3.30	37.44	0.97	3.40	0.01	4.80E-06	34.59
$[N_{1,1,14,14}]Br$	0.07	0.17							
$[N_{1,1,14}\text{-}6\text{-}N_{1,1,14}]Br_2$	0.68	0.76	0.18	39.83	0.03	6.78	1.58	2.56E-06	64.79

Conductivity measurements are commonly used in the study of ionic micellar solutions due to a substantial change of slope at the onset of aggregation. The conductivity below the CMC is due to the sum of the contributions of the free anions and cations. Above the CMC, the rate of conductivity increase is smaller because micelles have a lower mobility than the free ions, and a fraction of the counter ion are ion-paired with the micelles.[208] The ionization degree (α) of micelles of the ILs under study was estimated from the ratio of the slopes above and below CMC. The high ionization degree of $[N_{1,1,14}\text{-}6\text{-}N_{1,1,14}]Br_2$ is related to its low degree of compactness, which implies that less counter ions are attracted to the layer around the ''heads" which will increse the ionisation degree of the micelles.[405] The high A_{min} of $[N_{1,1,14}\text{-}6\text{-}N_{1,1,14}]Br_2$ reflects the low packing of its monomers at the interface.[198]

The thermal properties of the ILs-based surfactants here studied, namely melting point and decomposition temperature, were additionally addressed. The melting temperatures (T_{fus}), and thermal transition temperatures (T_{tr}) were measured by DSC data and are presented in Table 5.2. The onset temperatures of decomposition (T_d) were further evaluated by TGA, and are also reported in Table 5.2. From the TGA profiles of these tensioactive compounds (shown in the Appendix D, Figure D3), as well as from the T_d values reported in Table 5.2, it is possible to conclude that all compounds studied present a high thermal stability – at least up to 180 °C.

Although the presence of at least one long alkyl chain in the IL structure is essential for their capacity to self-aggregate, also this may lead to an increase on their aquatic toxicity. In order to evaluate the ecotoxicity of the SAILs here synthesized, the Microtox® Acute toxicity test[292] was used. Their EC_{50} values ($mg{\cdot}L^{-1}$), the estimated concentration yielding 50% of inhibition of the bacteria luminescence, were determined after 5, 15 and 30 min of exposure to the bacteria *V. fischeri*, and reported in the Appendix D, Table D1. According to the hazard ranking described by Passino's group,[302] and considering the results obtained after 30 min of exposure time, it is possible to categorize these compounds as "toxic" ($[N_{1,1,10,14}]I$, $[N_{1,1,14}\text{-}6\text{-}N_{1,1,14}]Br_2$ and $[C_{14}Im\text{-}6\text{-}C_{14}Im]Br_2$, with 1 $mg{\cdot}L^{-1} < EC_{50} < 10\ mg{\cdot}L^{-1}$) and as "highly toxic" ($[N_{1,1,1,14}][C_1SO_4]$, $[N_{1,1,1,14}]Cl$, $[N_{1,1,1,14}]Br$, $[N_{1,1,1,14}][C_{10}SO_4]$, $[P_{1,1,1,14}]Br$ and $[C_1C_{14}Im]Br$, with 0.1 $mg{\cdot}L^{-1} < EC_{50} < 1\ mg{\cdot}L^{-1}$).

Considering the limits imposed by the European Legislation for the aquatic compartment,[301] these SAILs belong to the category "acute 1" (EC_{50} < 1 mg·L^{-1}) and "acute 2" (1 mg·L^{-1} < EC_{50} < 10 mg·L^{-1}). The obtained results show that the bacteria *V. fischeri* is highly affected by the presence of all ILs tested.

Table 5.2. Thermal properties of the synthetized SAILs, namely the thermal transition (T_{tr}), melting temperature (T_{fus}) and temperature of decomposition (T_d).

	T_{tr}	T_{fus} / °C	T_d / °C
$[N_{1,1,1,14}]Br$		99.7	213.1
$[N_{1,1,1,14}]Cl$		81.7	205.2
$[P_{1,1,1,14}]Br$	71.7	224.4	354.8
$[C_1C_{14}Im]Br$			228.4
$[N_{1,1,1,14}][C_1SO_4]$	93.9	179.1	249.9
$[N_{1,1,14,14}]Br$	66.8	166.7	181.5
$[N_{1,1,14,14}]Cl$		47.0	180.1
$[N_{1,1,10,14}]I$	44.3	131.4	188.6
$[C_{14}C_{14}Im]Br$			227.8
$[N_{1,1,14}\text{-}6\text{-}N_{1,1,14}]Br_2$			203.6
$[C_{14}Im\text{-}6\text{-}C_{14}Im]Br_2$			233.2
$[N_{1,1,1,14}][C_{10}SO_4]$	59.6	179.47	250.3

Figure 5.2 depicts the EC_{50} data in μM after 5, 15 and 30 min of exposure to the marine bacteria. In general, the exposure time seems to be an important condition in what concerns the toxicity effect of these ILs. In this sense, to ensure the complete toxic effect, only the EC_{50} values obtained after 30 min of exposure were considered for further discussion. Thus, the EC_{50} values can be ranked as follows: $[N_{1,1,10,14}]I$ > $[N_{1,1,14}\text{-}6\text{-}N_{1,1,14}]Br_2$ > $[C_{14}Im\text{-}6\text{-}C_{14}Im]Br_2$ > $N_{1,1,1,14}][C_1SO_4]$ ≈ $[N_{1,1,1,14}]Cl$ ≈ $[N_{1,1,1,14}]Br$ ≈ $[N_{1,1,1,14}][C_{10}SO_4]$ > $[P_{1,1,1,14}]Br$ > $[C_1C_{14}Im]Br$, being $[N_{1,1,10,14}]I$ the less toxic and $[C_1C_{14}Im]Br$ the most toxic ILs, respectively. The higher EC_{50} value of $[N_{1,1,10,14}]I$, $[N_{1,1,14}\text{-}6\text{-}N_{1,1,14}]Br_2$ and $[C_{14}Im\text{-}6\text{-}$

$C_{14}Im]Br_2$ can be related to the presence of two long alkyl chains on the cation, which probably hinders their interaction with the bacteria. Moreover, EC_{50} values of $[N_{1,1,1,14}]Br$ and $[P_{1,1,1,14}]Br$ suggest that changes in the cation's central atom have impact on the ecotoxicity. Actually, these results seem to demonstrate that ammonium-based ILs present lower toxicity than the respective phosphonium ILs, which is in accordance with literature.[406] Considering the $[N_{1,1,1,14}]$-based ILs, the anion seems to have an insignificant influence in the EC_{50} results. Considering the cation core, the results obtained for the bromide-based ILs suggest that the aromatic cations ($[C_1C_{14}Im]Br$ and $[C_{14}Im\text{-}6\text{-}C_{14}Im]Br_2$) are, in general, more toxic than the non-aromatic ILs ($[N_{1,1,1,14}]Br$, $[P_{1,1,1,14}]Br$ and $[N_{1,1,14}\text{-}6\text{-}N_{1,1,14}]Br_2$), which is in agreement with previous data reported in literature.[228] Due to the reduced water solubility of $[N_{1,1,14,14}]Br$, $[N_{1,1,14,14}]Cl$ and $[C_{14}C_{14}Im]Br$, it was not possible to determinate their EC_{50} values.

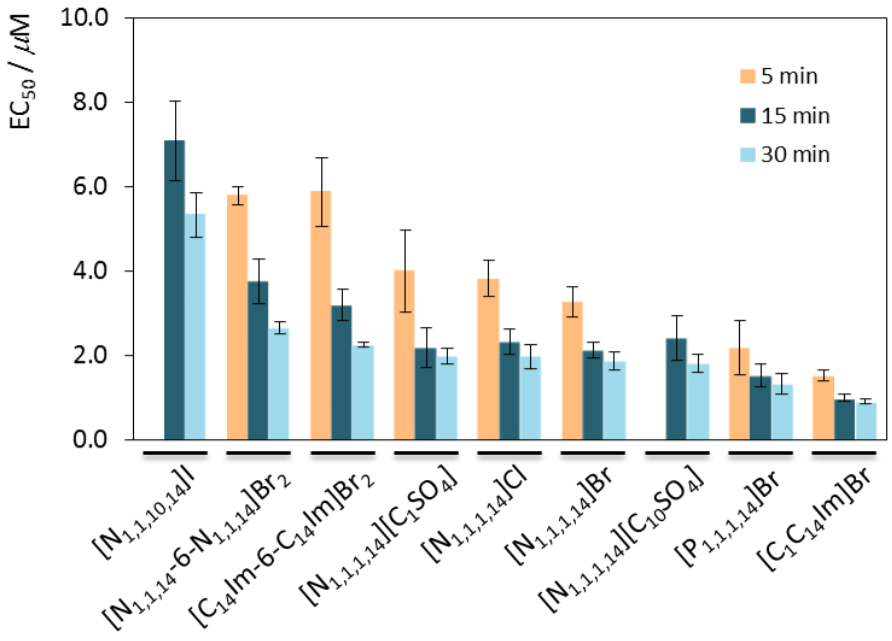

Figure 5.2. EC_{50} values (μM) determined towards *V. fischeri* after 5, 15 and 30 minutes of exposure. The error bars correspond to 95 % confidence level limits.

The ability of the prepared ILs to promote cell disruption of *E. coli* was investigated. For that, aqueous solutions of these SAILs were evaluated in their capacity to release the

intracellular GFP by their action in the lipid membranes. All measurements were performed under the same wet cells concentration and compared with the conventional method (ultrasonication) and with a blank (Tris-HCl buffer), as reported in Figure 5.3. It is possible to conclude that the Tris-HCl buffer, the aqueous medium where the GFP was solubilized, has no influence in the GFP extraction from *E. coli* cells. Due to their capacity to self-aggregate in aqueous medium above the CMC, SAILs can promote the disruption of the bacteria membrane leading to the release of their intracellular material.[407,408] Figure 5.3 shows that, in general, the ILs studied present high ability to induce cell disruption of *E. coli* and, consequently, to release the intracellular GFP. With the exception of $[N_{1,1,14}\text{-6-}N_{1,1,14}]Br_2$, ILs with only one long alkyl chain seem to be more effective in the cell permeation/disruption. The presence of two long alkyl chains in the IL can hinders its interaction with the cell membrane. In order to analyze the impact of the IL concentration on the GFP extraction, the five ILs with the best results were selected and studied using concentrations between 50 and 500 mM, as depicted in Figure 5.4. The results show that for the five compounds evaluated, the maximum extraction was found for 250 mM of IL, remaining almost constant for higher concentrations.

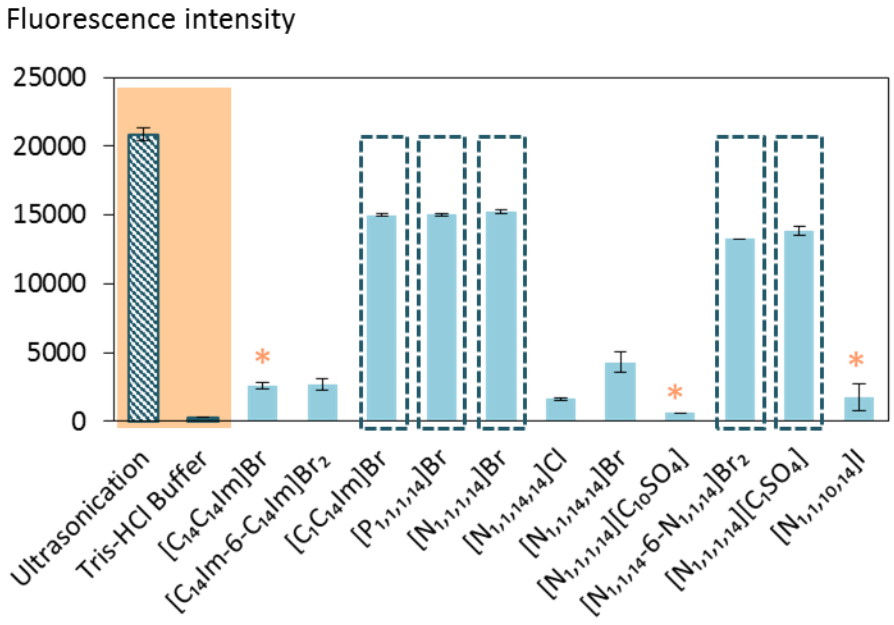

Figure 5.3. Results of fluorescence intensity describing the release of GFP to extracellular medium using aqueous solutions of SAILs, with a concentration of 100 mM (except for *, with 25 mM).

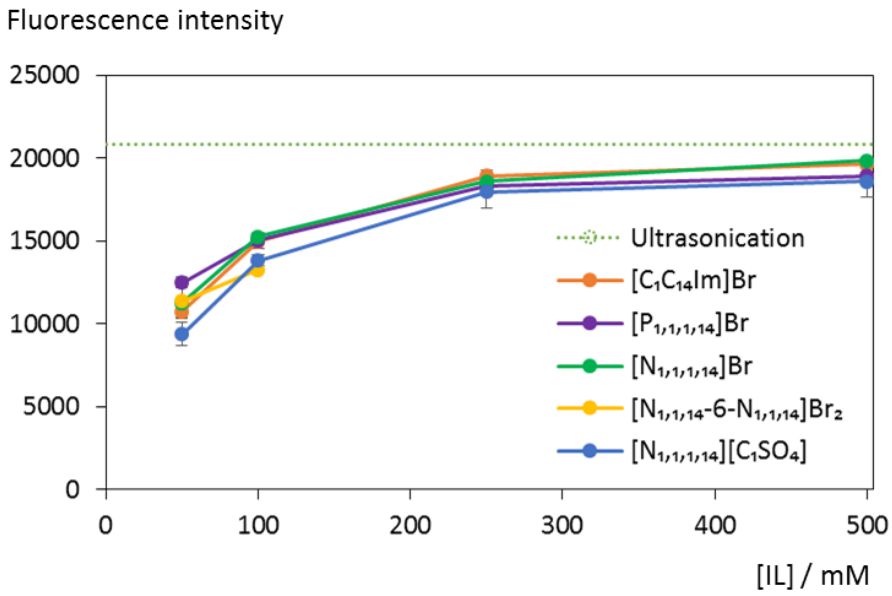

Figure 5.4. Influence of the IL concentration (mM) in GFP release to extracellular medium.

CONCLUSION

In this work, twelve SAILs were synthesized with high purity level. The CMC values obtained show that these tensioactive ILs are easily capable of forming microaggregates by their self-aggregation. In addition, all ILs studied present a high thermal stability – at least up to 180 °C. Albeit the presence of at least a long alkyl chain in the IL is crucial for their surface activity, this may lead to an increase on their aquatic toxicity. In fact, the results obtained show that the bacteria *V. fischeri* is affected by the presence of all ILs tested, being these compounds considered as "toxic" or even "highly toxic". Moreover, the chemical structure of the ILs seems to play a key role in their ecotoxicity against this marine luminescent bacteria. Finally, and as an example of one possible application, it was demonstrated that some of these SAILs studied can induce cell disruption of *E. coli* and, consequently, the intracellular GFP release.

Chapter 6 - Magnetic Ionic Liquids

Ecotoxicological evaluation of magnetic ionic liquids

Tânia E. Sintra, Maryam Nasirpour, Filipa Siopa, Andreia A. Rosatella, Fernando Gonçalves, João A. P. Coutinho, Carlos A. M. Afonso and Sónia P. M. Ventura, Submitted to the *Ecotoxicology and Environmental Safety.*

(In this communication Tânia E. Sintra contributed with ecotoxicological evaluation of prepared MILs and with the manuscript preparation/writing.)

ABSTRACT

Although MILs are not yet industrially used, their continued development and eventual commercial use may lead to their appearance into the aquatic ecosystem through accidental spills or effluents, consequently promoting aquatic contaminations. Furthermore, the deficient information and uncertainty surrounding the environmental impact of MILs could be a major barrier to their widespread industrial application and international registration. Thus, in the present work, a range of cholinium salt derivatives with magnetic properties was synthesized and their ecotoxicity was evaluated towards the luminescent bacteria *V. fischeri*. The results suggest that all MILs structures tested are moderately toxic, or even toxic, to the bacteria. Furthermore, their toxicity is highly dependent on the structural modifications of the cation, namely the alkyl side chain length and the number of hydroxyethyl groups, as well as the atomic number of the metal anion. Finally, from the magnetic anions evaluated, the $[MnCl_4]^{2-}$ is the less toxic. In order to improve the knowledge for the prospective design of environmentally safer MILs, it is important to expand this study to other aquatic organisms at different trophic levels.

INTRODUCTION

MILs appear as an emerging class of ILs that are inherently paramagnetic, being able to respond to an external magnetic field. These magnetic compounds favourably combine the advantageous properties of ILs with magnetic characteristics, which can be interesting for applications in process and product engineering as an expanding field full of opportunities to create devices, processes and products.[265,409–411] In fact, MILs have been studied in fluid-fluid separations,[412–414] in the extraction of nucleic acids like DNA,[415] in chemical reactions, namely as catalysts,[416–418] reaction medium[419,420] and solvents,[421,422] in polymer chemistry,[423,424] in electrochemical devices[425,426] and as magnetic fluids.[427,428] The paramagnetic properties of MILs may be located on the anion, cation or both. Their synthesis is normally based on the use of transition metals or lanthanide complexes in the anion structure.[411] The first MIL, namely the 1-butyl-3-methylimidazolium tetrachloroferrate, $[C_4C_1im][FeCl_4]$ was reported in 2004.[429] Since then, other MILs based on transition-metal coordination complexes such as Fe(III),[430–434] Co(II)[430–432,435,436] and Mn(II)[431,436] have been reported. Furthermore, lanthanide complexes, like gadolinium (Gd), neodymium (Nd) and dysprosium (Dy), have also emerged due to their strong response to an external magnetic field and, in some cases, luminescent properties.[432,437,438] In general, these magnetic anions have been combined with imidazolium-,[434] phosphonium-,[431,432,436] cholinium-[421,439] and ammonium-based cations.[440,441] Recently, the first magnetic chiral ILs, which simultaneously contain chiral and magnetic properties, have been synthesized by the simple combination of a chiral cation with the tetrachloroferrate magnetic anion.[442] Considering not only the variability of structures and properties (including the magnetic ones) and the importance of MILs in different applications using water as the principal media, it seems to be crucial to analyse and evaluate their (eco)toxicity. In this context, Luis et al.[443] have evaluated the ecotoxicity of some MILs towards the *V. fischeri* (*V. fischeri*) bioluminescent marine bacteria. In addition, a QSAR based on group contribution methods was applied to describe the influence of the molecular structure of common ILs and MILs on the (eco)toxicity.[443] The authors have shown that the presence of iron in the molecular structure of imidazolium-based ILs leads to an increase in ecotoxicity.[443] Alvarez-Guerra

and Irabien[255] reported a new approach for estimating the (eco)toxicity of ILs, including MILs, using a Partial Least Squares-Discriminant Analysis (PLS-DA). In this study, the $[FeCl_4]^-$ anion had the most severe influence on the PLS-DA model as positive discriminator, being more toxic than toluene, taken as reference for common volatile solvents. Despite the initial efforts carried to offer a preliminary insight into the environmental behaviour of MILs, data on their ecotoxicity is still scarce, and needs to be expanded to improve the knowledge for the adequate design of safer MILs. Moreover, the (eco)toxicological hazard profile of ILs with industrial potential must address a set of different rules, including those related with the regulatory demands defined by the European Union regulation for REACH.[10] In this context, the present study proposes the ecotoxicological assessment of a series of MILs based on the cholinium derivative cation in combination with $[FeCl_4]^-$, $[MnCl_4]^{2-}$, $[CoCl_4]^{2-}$ and $[GdCl_6]^{3-}$ anions, towards the *V. fischeri* marine bacteria. This work is part of an integrated study being performed by our group in which different cholinium IL structures have been analysed. The purpose is not only to evaluate the effect of different anions conjugated with the cholinium cation but also to infer about the benign toxicological character normally claimed for cholinium-based ILs and derivatives when this structure is conjugated with magnetic anions.

EXPERIMENTAL SECTION

Materials: All solvents were distilled prior to use. All chemicals were purchased from Sigma-Aldrich.

Synthesis of MILs:

I) General method for cholinium chloride derivative based ILs: Synthesis of $[N_{x,x,x,x}]Cl$ (x = alkyl or ethanol) was adapted from e Silva et al.[232] and Rosatella et al.[444] In a closed vessel at room temperature, was added *N*-methyldiethanolamine (143 mmol), or *N*-dimethylethanolamine (143 mmol) to the correspondent alkyl chloride (1-4 mol eq.), and sodium iodide (10-30 mol eq.). In some procedures acetonitrile was used as a solvent. The solution was heated at 60-80 °C for 1-7 days. The solvent was removed on a rotary evaporator. The resulted salt was dissolved in dichloromethane and the sodium halide

removed by filtration. The obtained salt was dried under vacuum and used in the next step without further purification. For more details see the Appendix E.

II) General method for magnetic ILs $[N_{1,1,n,2(OH)}][MCl_y]$ and $[N_{1,n,2(OH),2(OH)}][MCl_y]$: The MILs were prepared using the reported procedures with some modifications.[431,439,444] The metal chloride hydrated salt $MCl_Y \cdot H_2O$ (1 equiv. for $FeCl_3 \cdot 6H_2O$; 0.5 equiv. for $CoCl_2 \cdot 6H_2O$ and $MnCl_2 \cdot 4H_2O$, and 0.3 equiv. for $GdCl_3 \cdot 6H_2O$) was added to a solution of cholinium derivative chloride salt (10 mmol) in methanol (20 mL). The reaction mixture was stirred overnight at room temperature. The solvent was evaporated on a rotary evaporator at 50 °C, and then kept under vacuum for 48 h at 1–4 x 10^{-2} mbar (rotatory pump) and for 48 h at 6 x 10^{-5} mbar with stirring at 50 °C. More detailed information about the synthesis of MILs is reported in the Appendix E, namely in Table E1.

Microtox Assay: In order to evaluate the ecotoxicity of the MILs prepared, the Standard Microtox liquid-phase assay was applied. This test is described in detail in the Experimental Section of Chapter 2.

RESULTS AND DISCUSSION

Cholinium and distinct cholinium derivatives, with different number of hydroxyethyl groups and lengths of the alky side chain, were combined with the magnetic anions $[FeCl_4]^-$, $[MnCl_4]^{2-}$, $[CoCl_4]^{2-}$, $[GdCl_6]^{3-}$ in order to obtain 24 MILs, whose toxicities were tested against the marine bacteria (Figure 6.1). All MILs were soluble in water for the range of concentrations used. The ecotoxicological impact of these MILs was evaluated using the standard Microtox® acute assay. Although this is not a standard toxicity test defined in the European Union legislation and by REACH, it is nevertheless a quick and cost-efficient first-approach to evaluate the toxicity of various compounds. Moreover, this is a methodology well accept in the development of QSAR models for the prediction of ILs toxicity,[445–450] and the QSAR approach for toxicity predictions is encouraged by the REACH legislation of the European Union. This assay has been widely used to evaluate the toxicity of ILs, including cholinium derivatives.[230–232,248,451] This test is based on the bioluminescent bacteria *V. fischeri*, with the luminescence being a natural part of its

metabolism. When exposed to a toxic compound, the respiratory process of the bacteria is disturbed, reducing the light output, causing the bioluminescence inhibition correlated with the toxicity.

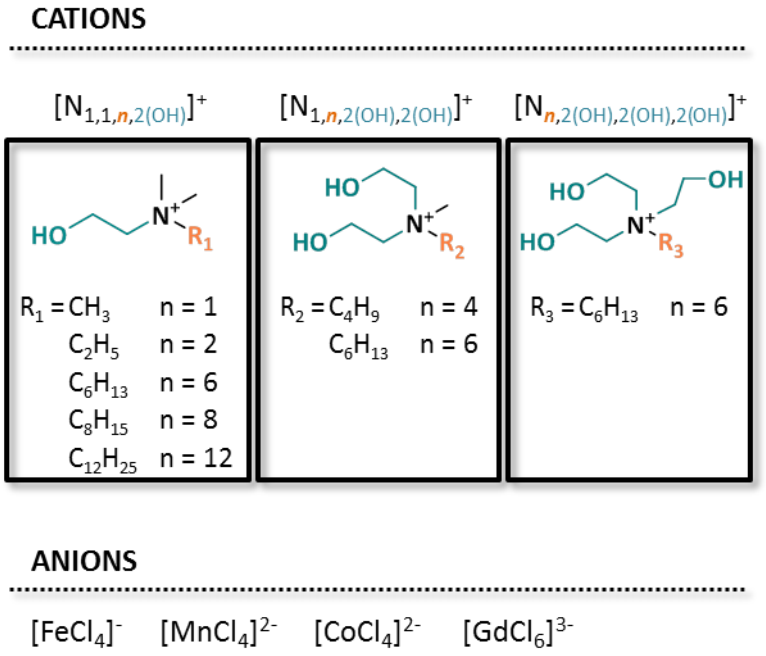

Figure 6.1. Cations and anions used in the design of the MILs studied in this work.

Thus, EC_{50} values ($mg \cdot L^{-1}$), the estimated concentration yielding a 50% reduction in the luminescence, were determined for the synthetized MILs after 5, 15 and 30 minutes of exposure to the marine bacteria, and presented in Table 6.1, Table 6.2 and Table 6.3, respectively. The results obtained for the MILs composed of $[CoCl_4]^{2-}$ and $[GdCl_6]^{3-}$ anions, $[N_{1,1,1,2(OH)}]_2[MnCl_4]$ and $[N_{1,6,2(OH),2(OH)}]_2[MnCl_4]$ show a decreasing order of the EC_{50} values with the increase of the exposure time from 5 to 30 minutes. This behavior can be justified by their toxicokinetics,[248] that means the passage of the MILs troughout the cell wall increased over the time and/or the sorption of the MILs to the bacterial surface increased over the time, both disturbing the physiological process of the organism. This relationship was not observed for the other compounds studied, namely those based in the $[FeCl_4]^-$ and $[MnCl_4]^{2-}$ anions, probably because the permeability ratios of Gram-

negative cell wall channels were rather high in favor of the cations, being the number of charges important in this process. On the other hand, the detoxication phenomenon, described as the momentary physiological adaptation of the microorganism to the toxicant effect, which is identified during the period of exposure,[452,453] can contribute to explain our results. The outer membrane of Gram-negative bacteria (like *V. fischeri*) plays an important role controlling the binding process (or passage) of some substances that can impair the physiology of these organisms. Among the factors that may shape this process, one can identify the charge, the chain length of the substances, the selectivity of cell wall channel, and the presence of the specific binding sites, which can contribute to fully explain our results.

Table 6.1. EC_{50} values ($mg \cdot L^{-1}$) for MILs under study after 5 minutes of exposure to the luminescent marine bacteria *V. fischeri*, with the respective 95% confidence limits (in brackets).

	EC_{50} / $mg \cdot L^{-1}$ at 5 minutes (lower limit; upper limit)			
	$[FeCl_4]^-$	**$[MnCl_4]^{2-}$**	**$[CoCl_4]^{2-}$**	**$[GdCl_6]^{3-}$**
$[N_{1,1,1,2(OH)}]^+$	16.67 (15.09 – 18.25)	*	*	128.56 (56.51 – 200.60)
$[N_{1,1,2,2(OH)}]^+$	17.55 (16.27 – 18.82)	n.d.	n.d.	n.d.
$[N_{1,1,6,2(OH)}]^+$	18.04 (15.81 – 20.26)	56.46 (53.90 – 59.02)	n.d.	n.d.
$[N_{1,1,8,2(OH)}]^+$	19.05 (17.06 – 21.03)	27.89 (20.54 – 35.24)	39.14 (31.64 – 46.64)	n.d.
$[N_{1,1,12,2(OH)}]^+$	0.68 (0.59 – 0.76)	0.46 (0.41 – 0.51)	360.83 (244.08 – 477.59)	n.d.
$[N_{1,4,2(OH),2(OH)}]^+$	n.d.	34.79 (33.37 – 36.20)	598.88 (386.25 – 811.50)	34.40 (26.78 – 42.02)
$[N_{1,6,2(OH),2(OH)}]^+$	20.97 (19.02 – 22.92)	*	178.60 (125.57 – 231.62)	126.59 (93.70 – 159.48)
$[N_{6,2(OH),2(OH),2(OH)}]^+$	9.57 (7.76 – 11.39)	12.61 (9.91 – 15.31)	23.56 (21.25 – 25.88)	27.88 (22.25 – 33.52)

n.d. – not determined; * - The EC_{50} value was not achieved due to the low exposure time.

Table 6.2. EC_{50} values ($mg \cdot L^{-1}$) for MILs under study after 15 minutes of exposure to the luminescent marine bacteria *V. fischeri*, with the respective 95% confidence limits (in brackets).

	EC_{50} / $mg \cdot L^{-1}$ at 15 minutes (lower limit; upper limit)			
	$[FeCl_4]^-$	**$[MnCl_4]^{2-}$**	**$[CoCl_4]^{2-}$**	**$[GdCl_6]^{3-}$**
$[N_{1,1,1,2(OH)}]^+$	14.73 (13.72 – 15.73)	325.96 (202.09 – 449.83)	37.07 (20.34 – 53.81)	92.34 (62.15 – 122.52)
$[N_{1,1,2,2(OH)}]^+$	16.43 (15.11 – 17.71)	n.d.	n.d.	n.d.
$[N_{1,1,6,2(OH)}]^+$	17.67 (15.15 – 20.19)	55.49 (49.70 – 61.28)	n.d.	n.d.
$[N_{1,1,8,2(OH)}]^+$	17.82 (15.58 – 20.06)	30.93 (22.90 – 38.97)	21.59 (17.78 – 25.41)	n.d.
$[N_{1,1,12,2(OH)}]^+$	0.65 (0.55 – 0.75)	0.43 (0.35 – 0.50)	34.35 (21.16 – 47.54)	n.d.
$[N_{1,4,2(OH),2(OH)}]^+$	n.d.	34.68 (33.38 – 35.98)	36.64 (24.75 – 48.53)	29.84 (24.41 – 35.26)
$[N_{1,6,2(OH),2(OH)}]^+$	18.55 (15.97 – 21.12)	502.99 (187.61 – 818.36)	62.24 (31.70 – 92.78)	62.11 (54.62 – 69.60)
$[N_{6,2(OH),2(OH),2(OH)}]^+$	6.50 (5.53 – 7.46)	11.62 (8.41 – 14.84)	18.42 (17.36 – 19.47)	20.76 (17.98 – 23.55)

n.d. – not determined

In order to easily understand the impact of the chemical structure of MILs studied on their ecotoxicity, the EC_{50} values obtained after 30 minutes of exposure were considered for further discussion, since this is the time recommended for the toxicity analysis of chemical compounds using Microtox® assay.[452] Thus, according to these values, it is possible to categorize these compounds as moderately toxic (meaning $10\ mg \cdot L^{-1} < EC_{50} < 100\ mg \cdot L^{-1}$), except for $[N_{1,1,1,2(OH)}]_2[CoCl_4]$, $[N_{1,1,12,2(OH)}][FeCl_4]$, $[N_{1,1,12,2(OH)}]_2[MnCl_4]$, $[N_{1,1,12,2(OH)}]_2[CoCl_4]$ and $[N_{6,2(OH),2(OH),2(OH)}][FeCl_4]$, that are considered as toxic substances, with $1\ mg \cdot L^{-1} < EC_{50} < 10\ mg \cdot L^{-1}$.[301,302] Curiously, among the MILs studied, the compounds presenting the lowest and highest toxicity against *V. fischeri* are MILs based on the $[MnCl_4]^{2-}$ anion, the $[N_{1,6,2(OH),2(OH)}]_2[MnCl_4]$ and $[N_{1,1,12,2(OH)}]_2[MnCl_4]$. This suggests that part of the toxicity observed is derived from the cation and not the anion (see above), further supporting previous results suggesting that the cholinium derivatives are not innocuous,[236,248] contrary to several studies.[95,221,281,282]

Table 6.3. EC_{50} values ($mg \cdot L^{-1}$) for MILs under study after 30 minutes of exposure to the luminescent marine bacteria *V. fischeri*, with the respective 95% confidence limits (in brackets).

	EC_{50} / $mg.L^{-1}$ at 30 minutes (lower limit; upper limit)				
	$[FeCl_4]^-$	**$[MnCl_4]^{2-}$**	**$[CoCl_4]^{2-}$**	**$[GdCl_6]^{3-}$**	**Br**
$[N_{1,1,1,2(OH)}]^+$	14.17 (12.95 – 15.39)	48.38 (29.06 – 67.71)	8.90 (7.04 – 10.76)	26.12 (21.12 – 31.12)	---
$[N_{1,1,2,2(OH)}]^+$	15.49 (13.72 – 17.25)	n.d.	n.d.	n.d.	25619.07[a] (17592.81 – 33645.32)
$[N_{1,1,6,2(OH)}]^+$	17.19 (13.54 – 20.85)	37.51 (23.88 – 51.14)	n.d.	n.d.	746.30[a] (699.73 – 792.86)
$[N_{1,1,8,2(OH)}]^+$	17.49 (15.10 – 19.88)	27.96 (21.10 – 34.82)	10.75 (8.81 – 12.69)	n.d.	162.96[a] (158.59 – 167.32)
$[N_{1,1,12,2(OH)}]^+$	1.04 (0.89 – 1.18)	0.76 (0.53 – 0.98)	7.84 (5.84 – 9.84)	n.d.	0.8[a] (0.79 – 0.82)
$[N_{1,4,2(OH),2(OH)}]^+$	n.d.	32.26 (26.56 – 37.96)	10.41 (8.60 – 12.22)	24.10 (19.62 -28.58)	---
$[N_{1,6,2(OH),2(OH)}]^+$	16.81 (14.57 – 19.05)	69.54 (35.95 – 103.13)	18.08 (10.75 – 25.42)	34.17 (26.16 – 42.19)	276.96[a] (220.22 – 333.70)
$[N_{6,2(OH),2(OH),2(OH)}]^+$	5.99 (5.05 – 6.92)	10.19 (7.28 – 13.10)	13.11 (11.81 – 14.40)	17.52 (15.59 – 19.44)	19.74[a] (18.20 – 21.27)

n.d. – not determined; [a] – values from e Silva et al.[232]

The range of MILs studied allows the assessment of the impact of several structural features on their ecotoxicity, such as the increase in the alkyl chain length and the addition of hydroxyethyl groups to the cation, and the impact of various magnetic anions. For this analysis, the EC_{50} values (in μM units) after 30 minutes of exposure to the bacteria were calculated, these values are reported in the Appendix E, Table E2. Figure 6.2 depicts the results of toxicity towards the marine bacteria considering the series with one hydroxyethyl group and the various metal anions, with the exception of ILs based in the $[GdCl_6]^{3-}$, due to the absence of experimental data (for more details see Table 6.3).

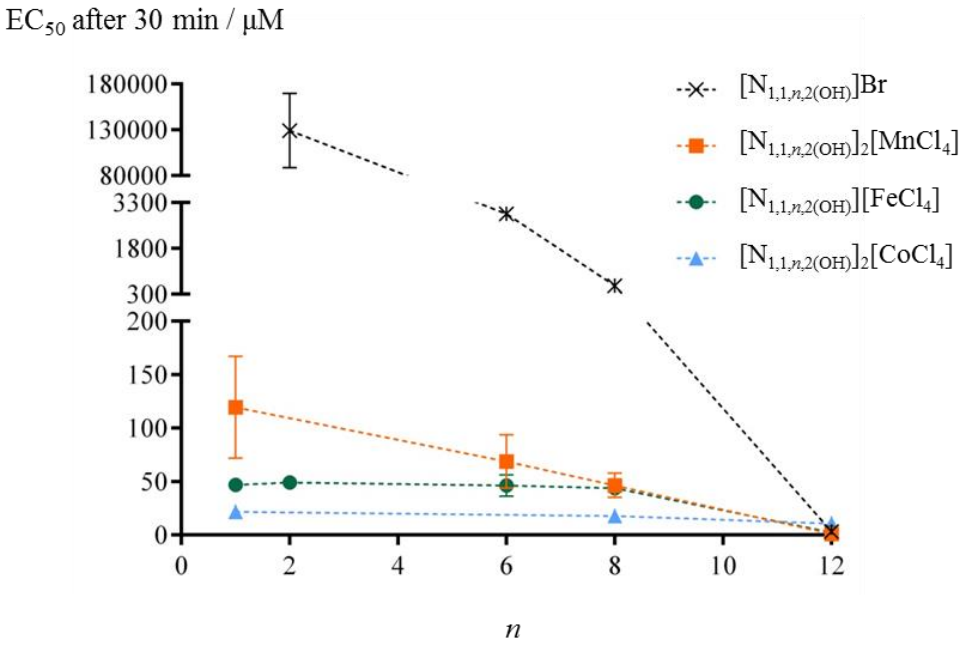

Figure 6.2. The effect of the alkyl chain length on the ecotoxicity of the series $[N_{1,1,n,2(OH)}][M]$, where *n* is the number of carbons and M represents the metal anion. The experimental data presented for the bromide anion (Br) can be checked elsewhere.[232]

The results reported in Figure 6.2 display a trend of increasing toxicity with the cation alkyl chain's length for the series $[N_{1,1,n,2(OH)}]_2[MnCl_4]$ (n = 1, 6, 8, 12), as well-reported in literature for a variety of ILs.[232] This phenomenon has been justified by the enhancement of the ILs hydrophobic/lipophilic character, defined in several woks by the octanol-water partition coefficients.[454,455] Thus, the increase in the length of the alkyl chain makes

possible their interaction with the membrane phospholipids and/or the hydrophobic domains of the membrane proteins, leading to the disruption of the membrane physiological functions and, consequently, to cell death.[226,240] However, this dependency is less significant for the series $[N_{1,1,n,2(OH)}][FeCl_4]$ (n = 1, 2, 6, 8, 12) and $[N_{1,1,n,2(OH)}]_2[CoCl_4]$ (n=1, 8, 12), except in the transition from $[N_{1,1,8,2(OH)}]_2[CoCl_4]$ to $[N_{1,1,12,2(OH)}]_2[CoCl_4]$. Furthermore, when the alkyl chain increases from 4 to 6 carbons in the series $[N_{1,n,2(OH),2(OH)}][M]$ (M = metal anion), the EC_{50} (μM) is practically constant, if considering the confidence limits, as present in Figure 6.3. In a previous work, the toxicity of similar series based on the bromide anion, $[N_{1,1,n,2(OH)}]Br$ (n = 2, 3, 4, 5, 6, 8, 12) and $[N_{1,n,2(OH),2(OH)}]Br$ (n = 3, 6, 12), were also assessed using the luminescent bacteria *V. fischeri*.[232] For these series based on the bromide anion, the effect of the alkyl chain length was pronounced. The EC_{50} values for the $[N_{1,1,n,2(OH)}]Br$ are also presented in Figure 6.2. These results highlight the impact of the replacement of a halide (bromide) by a metal anion, leading to a very significant increase in the toxicity against *V. fischeri*.[232] The results shown in Figure 6.2 indicate that although the toxicity of the MILs is highly dependent on the magnetic anion, for long alkyl chains (n=12) the cation toxicity becomes dominant.

The impact of the number of hydroxyethyl groups was also evaluated using the series of $[N_{1,1,6,2(OH)}]^+$, $[N_{1,6,2(OH),2(OH)}]^+$ and $[N_{6,2(OH),2(OH),2(OH)}]^+$ cations conjugated with the four magnetic anions under study. The results presented in Figure 6.4 suggest that the insertion of hydroxyethyl groups in the cation alkyl chains increases the toxicity towards the bacteria. This trend is in accordance with what was previously observed in literature.[232,444] Actually, the incorporation of hydroxyl groups of oxygenated alkyl chains is being subject of distinct analysis, not only from the point of view of potential applications but also due to their increased biodegradable nature.[220] The only exception is the transition from $[N_{1,1,6,2(OH)}]_2[MnCl_4]$ to $[N_{1,6,2(OH),2(OH)}]_2[MnCl_4]$. For these cations, unlike those discussed above for the long alkyl chain, the EC_{50} values show a significant increase in the toxicity of the MIL with metal containing anions, when compared with the corresponding bromide containing ILs.[232] Moreover, and contrary to what is observed in the imidazolium family functionalized with polar groups, the incorporation of oxygenated

alkyl chains increases the toxicity of the cholinium derivatives.[240] This reinforces the idea that the cholinium derivatives have different mechanisms of toxicity from those of imidazolium-based ILs.[248]

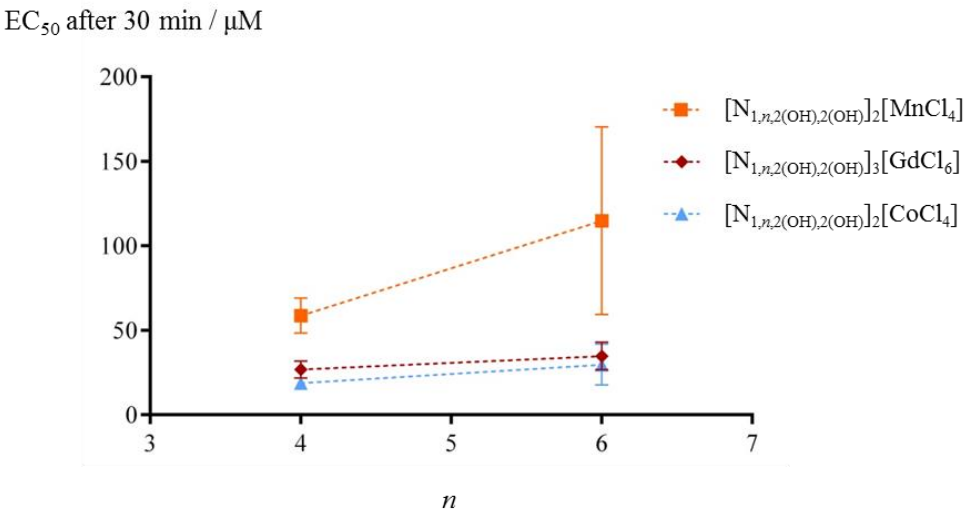

Figure 6.3. The effect of the alkyl chain length on the ecotoxicity of the series $[N_{1,n,2(OH),2(OH)}][M]$, where *n* is the number of carbons and M represents the metal anion.

In order to compare the effect of the magnetic anions, the increasing order of ecotoxicity, decreasing order of EC_{50}, was determined for each cation, as shown in Table 6.4. From the seven sequences analysed, the $[MnCl_4]^{2-}$ anion appears consistently as the least toxic (in five of this seven sequences) to *V. fischeri*. However, this same anion, $[MnCl_4]^{2-}$ is the most toxic when conjugated with the $[N_{1,1,12,2(OH)}]^+$ cation, which has itself a pronounced influence on the bacterial toxicity. On the other hand, the $[CoCl_4]^{2-}$ anion seems to present a contradictory behaviour. Although the $[CoCl_4]^{2-}$ anion appears as the least toxic when conjugated with $[N_{1,1,12,2(OH)}]^+$ and $[N_{6,2(OH),2(OH),2(OH)}]^+$ cations, it is the anion most frequently reported as the most toxic to the bacteria.

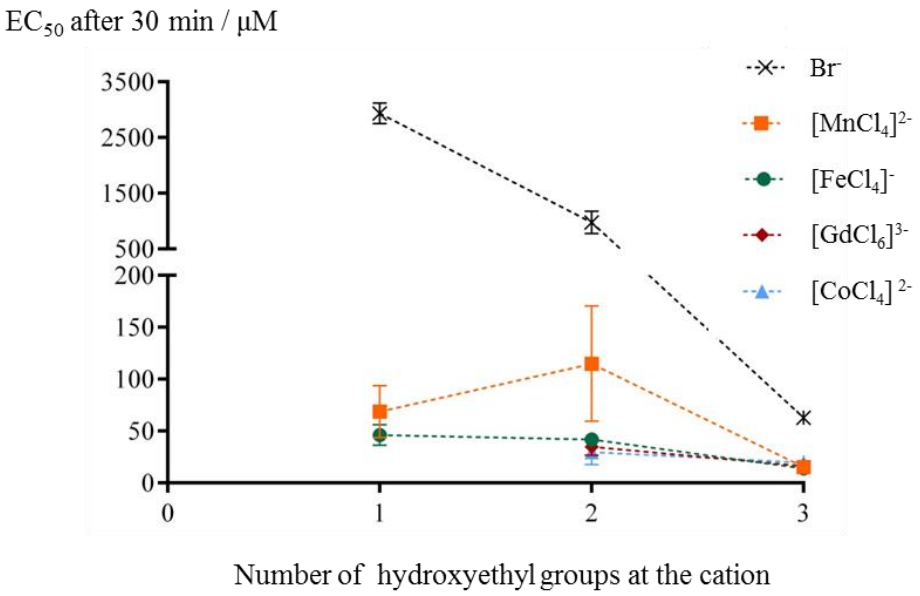

Figure 6.4. The effect of the number of hydroxyethyl groups in the cations on the ecotoxicity of the MILs. The number 1, 2 and 3 represent $[N_{1,1,6,2(OH)}]$, $[N_{1,6,2(OH),2(OH)}]$ and $[N_{6,2(OH),2(OH),2(OH)}]$ cations, respectively. The experimental data presented for the bromide anion (Br) can be checked elsewhere.[232]

Table 6.4. The impact of the magnetic anion on the ecotoxicity of the MILs, according to EC_{50} values (μM) after 30 minutes of exposure towards *V. fischeri*.

	Order of ecotoxicity
$\mathbf{[N_{1,1,1,2(OH)}]^+}$	$[MnCl_4]^{2-} < [FeCl_4]^- < [GdCl_6]^{3-} < [CoCl_4]^{2-}$
$\mathbf{[N_{1,1,6,2(OH)}]^+}$	$[MnCl_4]^{2-} < [FeCl_4]^-$
$\mathbf{[N_{1,1,8,2(OH)}]^+}$	$[MnCl_4]^{2-} \approx [FeCl_4]^- < [CoCl_4]^{2-}$
$\mathbf{[N_{1,1,12,2(OH)}]^+}$	$[CoCl_4]^{2-} < [FeCl_4]^- < [MnCl_4]^{2-}$
$\mathbf{[N_{1,4,2(OH),2(OH)}]^+}$	$[MnCl_4]^{2-} < [GdCl_6]^{3-} < [CoCl_4]^{2-}$
$\mathbf{[N_{1,6,2(OH),2(OH)}]^+}$	$[MnCl_4]^{2-} < [FeCl_4]^- \approx [GdCl_6]^{3-} \approx [CoCl_4]^{2-}$
$\mathbf{[N_{6,2(OH),2(OH),2(OH)}]^+}$	$[CoCl_4]^{2-} < [GdCl_6]^{3-} \approx [MnCl_4]^{2-} \approx [FeCl_4]^-$

Many authors have tried to prove correlations between the physico-chemical properties of different metal ions and their toxicity.[456] In the present work, and not considering the $[GdCl_6]^{3-}$ anion, it seems that an increased toxicity is observed by increasing the atomic number of the metal atoms: Mn (25) < Fe (26) < Co (27). This behaviour is in agreement with the results obtained by Li et al.,[457] where a positive correlation between the atomic number of the metal ion and their toxicity against *V. fischeri* was observed. However, this trend was not observed when these magnetic anions were combined with the $[N_{1,1,12,2(OH)}]^+$ and $[N_{6,2(OH),2(OH),2(OH)}]^+$ cations, which can be justified again by the high toxicity associated to these cations, which seems to dominate their toxicity.

The toxicological impact of MILs based in the $[C_8mim]^+$, $[N_{1,1,n,2(OH)}]^+$, $[N_{1,6,2(OH),2(OH)}]^+$ and $[N_{6,2(OH),2(OH),2(OH)}]^+$ cations (n = 1, 2, 3, 4, 6, 8, 12) with the metal anions studied in this work, was evaluated towards the human skin fibroblasts (CRL-1502) and/or human colorectal adenocarcinoma (CaCo-2) cell lines.[439,444] Considering the $[C_8mim]^+$ and $[N_{1,1,n,2(OH)}]^+$-based MILs, and contrary to what was observed with the Microtox® assay, these results suggest that $[FeCl_4]^-$ and $[GdCl_6]^{3-}$ were the anions with lower cytotoxicity whereas $[CoCl_4]^{2-}$ and $[MnCl_4]^{2-}$ were likely the most toxic.[439] Nevertheless, with regard to $[N_{1,6,2(OH),2(OH)}]^+$ cation, $[MnCl_4]^{2-}$ seems to be the less toxic cytotoxic.[444] This comparison supports the idea that the toxicological effect of the ILs depends not only of their structure but also on the biological system under study. Thus, in order to evaluate the aquatic toxicity more comprehensively, it is crucial to extend this study to other aquatic organisms of different trophic levels.

CONCLUSION

This work presents the ecotoxicological impact of a series of MILs based on cholinium derivative cations combined with $[FeCl_4]^-$, $[MnCl_4]^{2-}$, $[CoCl_4]^{2-}$ and $[GdCl_6]^{3-}$ anions, towards the marine bacteria *V. fischeri*. Although their interesting broad of applications, all MILs tested are considered moderately toxic or even toxic to the bacteria. The results indicate that their toxicity is highly dependent on the structural modifications of the cation, namely the alkyl side chain length and the number of hydroxyethyl groups, as well as the

metal atom of the anion. Long alkyl chains, the increase in the number of hydroxyethyl groups and the increase in the atomic number of the metal atom are structural features capable of significantly increasing the toxicity of the MILs based on cholinium or cholinium derivatives. Moreover, and contrary to what was reported in previous studies with cell lines, the $[MnCl_4]^{2-}$ is the anion presenting low toxicity towards the bacteria, clearly showing that the toxicological effect of the MILs depends not only of their structure but also of the biological system under study. In this sense, it is crucial to expand this study to other aquatic organisms and different trophic levels to improve the knowledge for the prospective design of safer materials.

Chapter 7 - Hydrophobic Ionic Liquids

A Simple Method for Preparation of a Novel Hydrophobic Ionic Liquid with a Per-fluoro-tert-butoxide Anion

Kiki A. Kurnia, Tânia E. Sintra, Yann Danten, Maria Isabel Cabaço, Marcel Besnard and João A. P. Coutinho, *New Journal of Chemistry*, **2017**, 41, 47-50, DOI: 10.1039/C6NJ02575G.

(In this communication Tânia E. Sintra contributed with synthesis and characterization of the new hydrophobic IL, measurement of its ecotoxicity, and with the manuscript preparation.)

ABSTRACT

In this work, we demonstrate a simple and atom-economic method for preparation of a novel hydrophobic IL from hydrophilic ILs and its characterization data are disclosed. The simple preparation route also provides opportunities for removal/recovery of the IL during cellulose dissolution.

INTRODUCTION

ILs are organic salts with a melting point below 100 °C that have widespread application in organic synthesis, catalysis, biomass dissolution, and liquid–liquid extraction, among many others.[1,458] Their unique feature is essentially determined by their structural characteristics, which originated from, at least, cations, anions, alkyl chain length, and functional groups. It is evaluated that there are about one million possible pure ILs and 10^{18} ternary liquid mixtures.[459] It should, however, be highlighted that hydrophobic ILs are far outnumbered by hydrophilic ILs, even if that class of ILs has been shown to be promising media for the extraction of (bio)molecules and (bio)fuels from aqueous solutions.[266–268] With the ever-growing demands for novel ILs with desired structures and

functions, the designed synthesis of such compounds has aroused considerable interest. In the absence of predictive computational methods to direct their design, the discovery-based development of novel ILs will remain vital to the field. This is especially the case *vis-a´-vis* heretofore unknown and unused classes of ions when such entities are easily prepared and provide access to potentially unique structural or electronic attributes. In light of these considerations, we report here, for the first time, the synthesis and characterization of the novel IL 1-butyl-3-methylimidazolium per-fluoro-*tert*-butoxide, $[C_4C_1im][Pftb]$, made from 1-butyl-3-methylimidazolium acetate, $[C_4C_1im][OAc]$, or from an ever simpler and cheaper starting material, 1-butyl-3-methylimidazolium chloride, $[C_4C_1im]Cl$, both commercially available and simple to synthesize. This new anion offers the potential to further tailor the physical properties, such as density, viscosity, and surface tension, and, most importantly, to create a new family of hydrophobic and water immiscible ILs.

EXPERIMENTAL SECTION

Materials: 1-butyl-3-methylimidazolium acetate, $[C_4C_1im][OAc]$ (98 wt % of purity) and 1-butyl-3-methylimidazolium chloride, $[C_4C_1im]Cl$ (98 wt % of purity) were obtained from Iolitec. Prior to the synthesis, these chemicals were further purified (to reduce the content of water and impurities) by drying under vacuum at 313.15 K and 0.1 Pa under constant stirring for at least 48h. After this procedure, ^{1}H and ^{13}C NMR analyses confirmed the purity of the $[C_4C_1im][OAc]$ and $[C_4C_1im]Cl$ samples as stated by the supplier. Per-fluoro-*tert*-butanol, C_4HF_9O (97 wt % of purity) was purchased from fluorochem, United Kingdom, and was used without further purification.

Synthesis of novel hydrophobic ionic liquid: To a round-bottom flask containing 1 equimolar of aqueous solution of $[C_4C_1im][OAc]$ was added 1.05 equimolar of per-fluoro-*tert*-butanol. The flask was fitted with condenser, thus allowing refluxing the mixture at 313.15 K. The reaction was monitored by Thin Layer Chromatography method, using silica sheet and methanol : ethylacetate (1:1) as eluent. After 24 hours, the reaction was assumed to be completed. The mixture was then transferred to another round-bottom

flask specially designed to dry the IL under vacuum and was let under vacuum at 0.1 P and at 313.15 K under constant stirring for at least 48 h to ensure complete removal of water, acetic acid and possible unreacted materials. This procedure was adapted for the others synthetic routes, as shown in Figure 7.1. The synthesized IL was kept in sealed bottle with PTFE septum. For the characterization and thermophysical properties measurement, required amount of IL sample was taken using syringe equipped with needle, through the PTFE septum. The structure of the new hydrophobic IL was confirmed by ^{1}H, ^{13}C and ^{19}F NMR and IR spectroscopy, showing a high purity level after its synthesis.

Density and viscosity: The density, ρ, and viscosity, η, of the synthesized IL were determined using an automated SVM 3000 Anton-Paar rotational Stabinger viscometer-densimeter at temperature 298.15 K and at atmospheric pressure. Prior to the measurement, the equipment was calibrated using the standard solution given by the supplier and was further validated by measuring the density and viscosity of several ILs for which the data have been established by our research group. The accuracy of the density measurements was found to be better than 0.5 $kg \cdot m^{-3}$, whereas the relative uncertainty in dynamic viscosity was found to be ± 1%. The relative uncertainty in temperature is within ± 0.02 K.

Refractive index: The refractive index, n_D, of the studied IL was measured at 589.3 nm using an automated Abbemat 500 Anton Paar refractometer, enabling to measure either liquid or solid samples. The refractive index measurements were carried at temperature 298.15 K and at atmospheric pressure.

Water solubility: Double-distilled water, used for the water solubility measurement, was passed by a reverse osmosis system and further treated with a MilliQ plus 185 water purification apparatus. The purity analyses revealed resistivity values of 18.2 MΩ·cm and a Total Organic Carbon content smaller than 5 $\mu g \cdot dm^{-3}$. The analyte used for the coulometric KF titration was Hydranal® - Coulomat AG from Riedel-de Haen.

Surface tension: The surface tension was determined through the analysis of the shape of a pendant drop and measured using a Dataphysics contact angle system OCA-20. Drop volumes of (10 ± 1) µL were obtained using a Hamilton DS 500/GT syringe connected to a

Teflon coated needle placed inside an aluminium air chamber. The temperature was attained by circulating water in a double jacketed aluminium cell by means of a Julabo F-25 water bath. The temperature inside the aluminium chamber was measured with a Pt100 within ± 0.1 K, placed at a distance of approximately 2 cm to the liquid drop. Silica gel was kept inside the air oven to assure a dry environment and to avoid moisture absorption during the equilibration period. For the surface tensions determination, at each temperature and for each IL, at least 5 drops were formed and measured. For each drop, an average of 200 images was captured. The analysis of the drop shape was performed with the software module SCA 20 where the gravitational acceleration (g = 9.8018 $m \cdot s^2$) and latitude (lat = 40°) were used according to the location of the assay.

Thermogravimetric analysis: The thermogravimetric analysis was determined using a thermal analysis on a thermogravimetric analyser with DSC capacity (Mettler Toledo, model TGA/DSC 1 LF) using the STAR analysis software. The samples were prepared in the aluminum pans and heated from (303.15 to 873.15) K, with a heating rate of 5 $K \cdot min^{-1}$ and under nitrogen gas flow of 40 $mL \cdot min^{-1}$. The standard uncertainty of temperature is 0.2 K. The decomposition temperatures presented are the onset temperatures, which are the intersection of the baseline below the decomposition temperature with the tangent to the mass loss versus the temperature plots in the TGA profiles. The results are expressed as the average of duplicate measurements.

Microtox Assay: To evaluate the ecotoxicity of the novel hydrophobic IL prepared, the Standard Microtox liquid-phase assay was applied. This test is described in detail in the Experimental Section of Chapter 2.

RESULTS AND DISCUSSION

We have explored six different routes for the preparation of $[C_4C_1im][Pftb]$ as shown in Figure 7.1. The first approach involved the direct mixing of $[C_4C_1im][OAc]$ and a slightly excess molar ratio of per-fluoro-*tert*-butanol under solvent free conditions, followed by the removal of the unreacted material and by-product (acetic acid) under vacuum, to give

a transparent liquid in 98% yield. This one-step procedure is a typical atom-economic reaction without poisonous by-product.

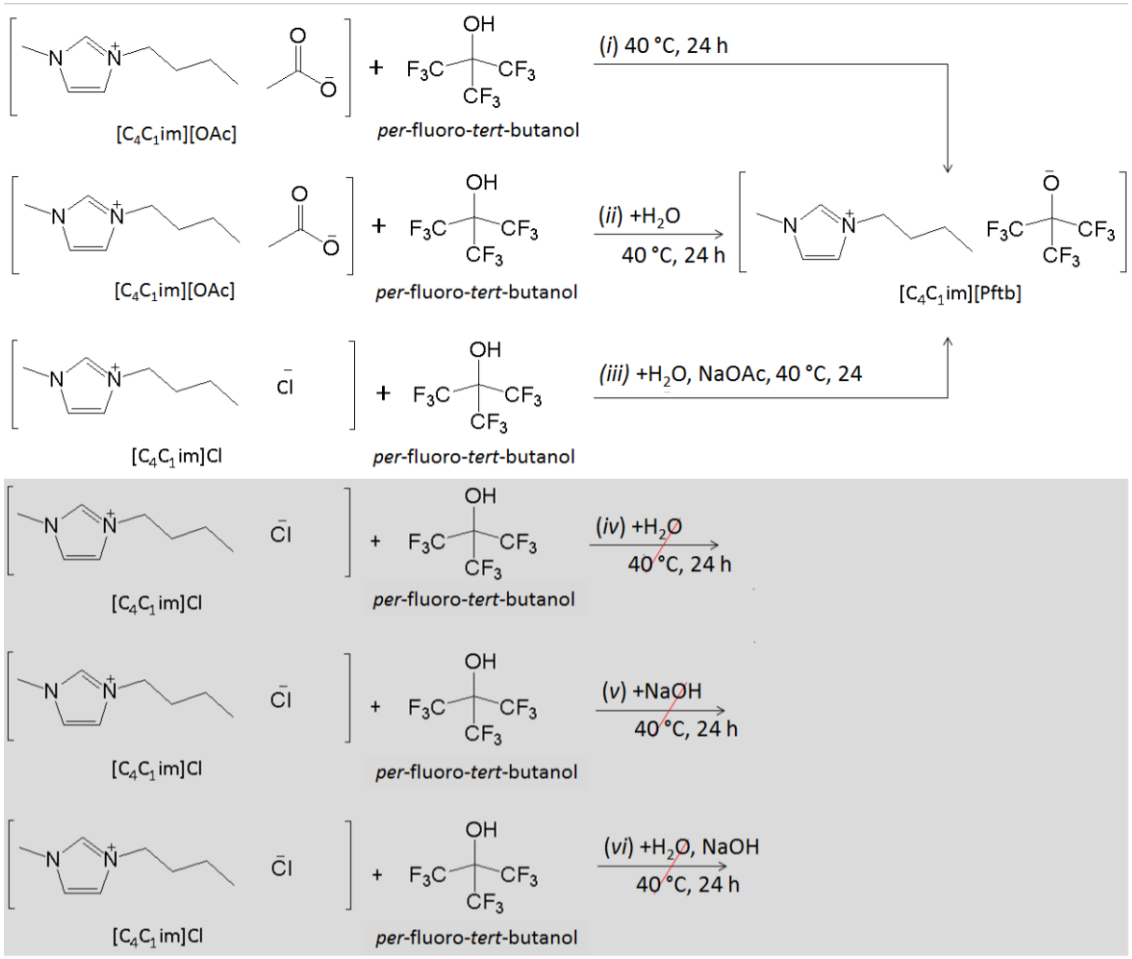

Figure 7.1. Schematic preparation of IL [C_4C_1im][Pftb].

The novel IL was characterized by Fourier transform infrared (FTIR) spectroscopy; ^{1}H, ^{13}C, and ^{19}F NMR spectroscopies; and TGA. Four changes in the FTIR spectra (Figure 7.2) reveal the structural information about the product. (1) The FTIR spectrum of [C_4C_1im][OAc] displays four bands detected at 630, 1174, 1382, and 1582 cm^{-1}. It is clear that the last two bands (the symmetric and asymmetric stretches of COO^-, respectively) disappear for the synthesized novel hydrophobic IL, whereas the first two are observed (bending and vibrations of the imidazolium ring cation), although the second one is found in the large and composed region at around 1205 cm^{-1}. (2) A decrease in CH vibrations is observed at

around 2917 cm^{-1} (symmetry vibration of the methyl acetate) for the synthesized IL. (3) The characteristic bands of the CF stretching of the per-fluoro-*tert*-butanol spectrum are observed at about 1135 and 1243 cm^{-1}, which overlap with the $[C_4C_1im][Pftb]$. Two other bands at 727 (CF_3 asymmetry deformation) and 955–972 cm^{-1} (skeletal stretching) are yet to be detected for the novel IL. (4) The OH stretching and bending at around 3610 and 1380 cm^{-1}, respectively, observed in the per-fluoro-*tert*-butanol spectrum were not observed in the spectrum of $[C_4C_1im][Pftb]$. Thus, it is clear from (1) and (2) behavioural changes that the acetate anion is not present in the final product, and from the third and fourth that the anion $[Pftb]^-$ (produced from the per-fluoro-*tert*-butanol that lost its acidic proton) is detected. Moreover, the formed acetic acid (by-product) is not detected in the NMR spectra of the final product, indicating the high purity of the synthesized novel hydrophobic IL.

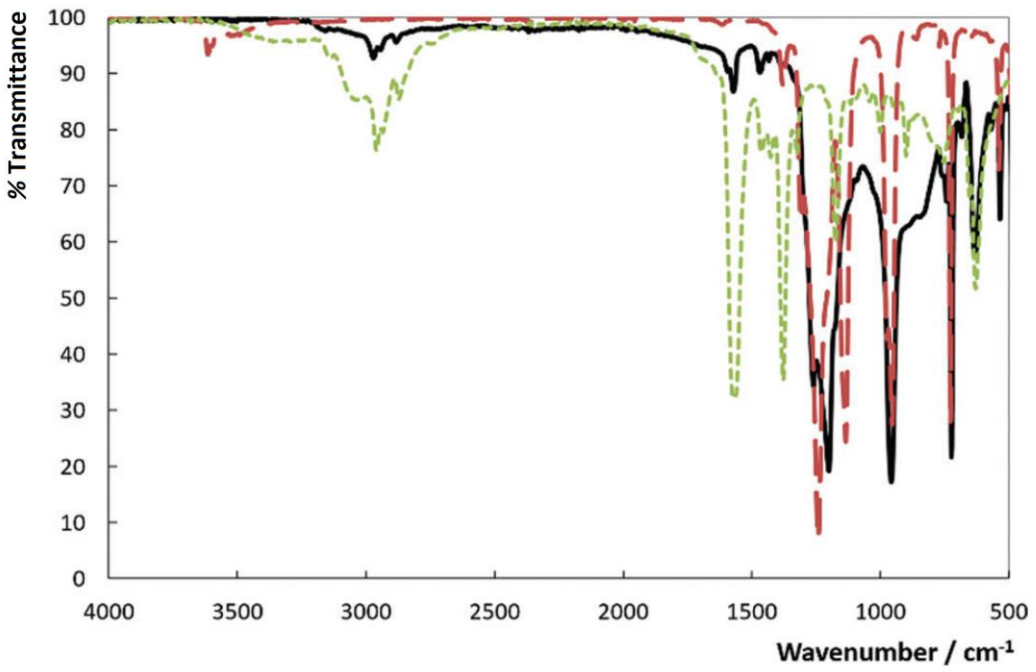

Figure 7.2. FTIR spectra of the novel synthesized IL and the starting material. $[C_4C_1im][Pftb]$, solid line; per-fluoro-*tert*-butanol, dashed-line; $[C_4C_1im][OAc]$, dotted-line.

The absence of both acetate anion (starting material) and acetic acid (by-product) in the final product is also confirmed by NMR spectra (Figure 7.3). The proton NMR spectrum of the synthesized IL recorded in DMSO-d_6 showed eight resonances, as shown in Figure 7.3a, which are assigned to the hydrogen atoms of the cationic part of the IL. The absence of extra peaks, particularly for acetate (from the starting material) and acetic acid (produced as the by-product), indicates the high purity of the synthesized IL. The ^{13}C NMR spectrum showed 10 resonances corresponding to the 8 carbons of the cationic part of the IL, while 2 resonances originated from the anionic part. The ^{13}C NMR spectrum of [C_4C_1im][Pftb] without proton decoupling is presented in the Appendix F, Figure F1. One single resonance is observed at -97.61 ppm in the ^{19}F spectrum of the synthesized IL, assigned to the fluorine atom on the anionic counterpart. No additional peak in both ^{13}C and ^{19}F spectra was observed, further confirming the high purity of the synthesized novel IL, [C_4C_1im][Pftb]. The assignment of the observed resonances is presented in the Appendix F, Table F1.

The thermogravimetric curve of the IL showed decomposition onset temperature at 494 K and the thermogravimetric curves of the derivatives showed only one peak at 533 K (Figure 7.4). This novel IL appears to have a similar thermal stability to the corresponding starting material, [C_4C_1im][OAc], whose decomposition temperature is 493 K (Appendix F, Figure F2).

The second preparation method attempted (cf. Figure 7.1) involved addition of water to a mixture of [C_4C_1im][OAc] and per-fluoro-*tert*-butanol. The obtained IL was also characterized by the same techniques used in the first preparation, and showed spectroscopic and thermogravimetric data identical to those of the IL sample prepared using the first method. It is worth mentioning that we also attempted the reaction between [C_4C_1im][OAc] and *tert*-butanol, yet no reaction occurred. The reaction between [C_4C_1im][OAc] and per-fluoro-*tert*-butanol is an acid–base reaction, in which the latter compound act as the acid (p*K*a = 5.6),[460] providing a hydrogen atom to combine with the acetate anion of the IL, and thus producing acetic acid as the by-product and [C_4C_1im][Pftb] as the main product. The much higher value of the p*K*a of tert-butanol (p*K*a = 16.58)[7] accounts for its inability to provide a hydrogen atom in this reaction as it is too

weak acid to react with. The replacement of the hydrogen atom by fluorine in *tert*-butanol to give per-fluoro-*tert*-butanol significantly increases the acidity. This is due to the fact that the electron-withdrawing character of the fluorine atom causes the hydrogen atom of the hydroxyl group in per-fluoro-*tert*-butanol (δ^+ of H = 0.417) to have a higher partial positive charge (Appendix F) when compared to *tert*-butanol (δ^+ of H = 0.383); thus the former has higher acidity that allows the reaction with $[C_4C_1im][OAc]$.

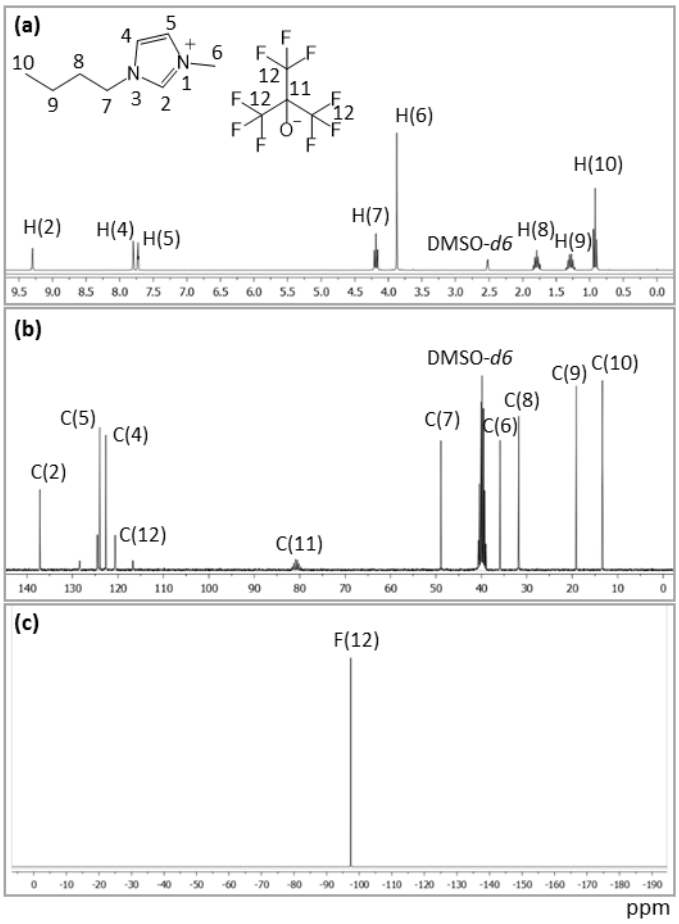

Figure 7.3. ^{1}H (a), ^{13}C (b), and ^{19}F (c) spectra of $[C_4C_1im][Pftb]$ in DMSO-d_6 produced from route 1.

$[C_4C_1im][Pftb]$ can also be prepared from other hydrophilic ILs, namely $[C_4C_1im]Cl$, and per-fluoro-*tert*-butanol in the presence of an aqueous solution of sodium acetate, NaOAc (method (iii) in Figure 7.1). The synthesized IL, which appears as a new phase, also presents identical spectra and thermogravimetric curves to the IL prepared using method

(i). However, method (iii) gives a somewhat lower yield, 85%, that can be due to the loss of the IL into the NaCl/NaOAc aqueous phase. Direct mixing of $[C_4C_1im]Cl$ and per-fluoro-*tert*-butanol, however, did not lead to any chemical reaction. As previously mentioned, the formation of $[C_4C_1im][Pftb]$ can be simply considered as an acid–base reaction, in which the per-fluoro-*tert*-butanol serves as the acid source, while the IL anion acts as the base. Thus, the inability of $[C_4C_1im]Cl$ to directly react with per-fluoro-*tert*-butanol can be addressed due to the weak basicity of Cl^- (solvatochromic β parameter = 0.87) when compared with $[OAc]^-$ (β = 1.09).[461] In addition, we also made an effort to prepare $[C_4C_1im][Pftb]$ by mixing $[C_4C_1im]Cl$ with NaOH in the presence and absence of H_2O. Nevertheless, these two methods did not produce the desired product.

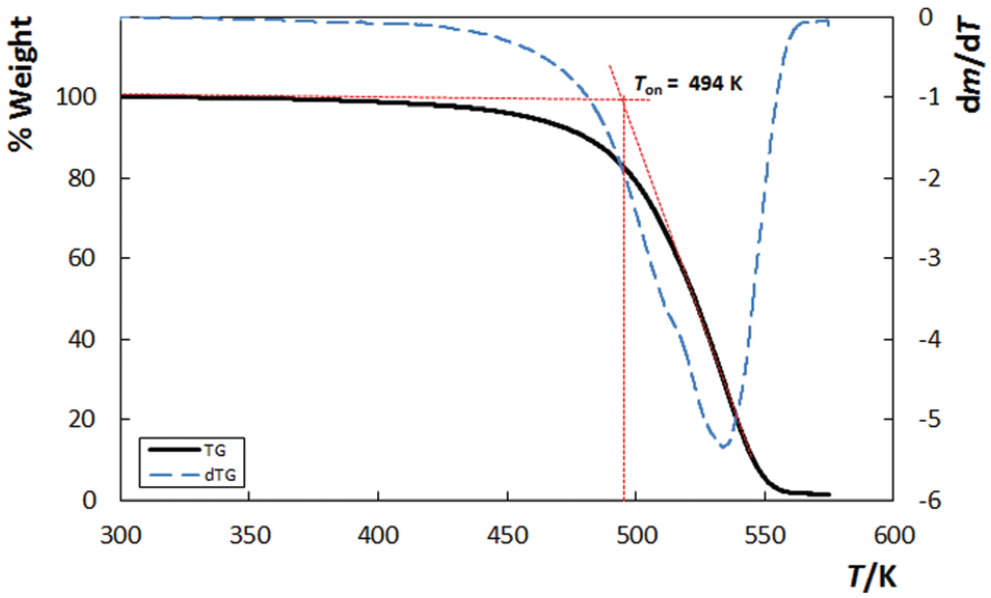

Figure 7.4. Thermogravimetric analysis of $[C_4C_1im][Pftb]$. Heating rate 5 $K \cdot s^{-1}$.

The physical properties and toxicity of the novel IL at 298 K were also characterized and the results are presented in Table 7.1. From these data, it can be concluded that this novel hydrophobic IL displays physical properties and toxicity similar to the well-known fluorine-containing IL $[C_4C_1im][NTf_2]$.[147,190] As expected this synthesis can be straightforwardly applied to produce hydrophobic ILs.

Table 7.1. Physical properties and toxicity of the novel IL [C_4C_1im][Pftb] at 298 K.

Properties	**Value**
Density (ρ/kg·m^{-3})	1513.90
Viscosity (η /mPa·s)	215.95
Refractive index (n_D)	1.372878
Surface tension (γ/mN·m^{-1})	26.82
Water solubility (xH_2O)	0.3632
Solubility in water (xIL)	6.02 x 10^{-4}
Toxicity (EC_{50}/mg·L^{-1})	84.41 (5 min); 84.92 (15 min); 85.62 (30 min)

In addition, it is interesting to observe that this novel IL is immiscible with water, while the starting material, [C_4C_1im][OAc], is extremely soluble. Here we show that the miscibility of the IL can be easily tuned by changing its counter anion. This unique feature, water miscibility changes – which can be straightforwardly achieved by simply adding the per-fluoro-*tert*-butanol to the hydrophilic IL, [C_4C_1im][OAc], to make the hydrophobic IL, [C_4C_1im][Pftb], has a number of practical implications for designing processes with ILs. For example, both [C_4C_1im]Cl and [C_4C_1im][OAc] are reported to be highly efficient solvents for the dissolution and regeneration of cellulose.[462–464] The regenerated cellulose could be precipitated from the IL solutions by adding water.[462–464] In this separation process, large volumes of dilute aqueous solutions of ILs are produced. The high values of ILs also call for efficient recycling of them from these aqueous solutions. In light of this consideration, we then turned our attention to apply this simple synthesis method to recover the IL from aqueous solution after it was used for the dissolution and regeneration of cellulose. Using this method, we could recover 82% of the IL. Furthermore, the spectroscopic and thermogravimetric data of the recovered IL also are identical to those of the IL prepared using method (i), indicating there is no cellulose in the IL phase. A detailed discussion on this matter will be presented elsewhere.

CONCLUSION

To summarize, we have shown that a novel hydrophobic IL can be prepared by three simple alternative routes in excellent yields, and as far as we know this is the first report on this type of IL. The simple preparation involved encourages the commercialization of processes based on this type of IL. We anticipate that this novel hydrophobic IL will find application in many areas of interest, not the least in liquid–liquid extraction from aqueous solution.

Chapter 8 - More Biocompatible Ionic Liquids - Predictive QSAR Models

Development of Predictive QSAR Models for Vibrio fischeri Toxicity of Ionic Liquids and Their True External and Experimental Validation Tests

Rudra Narayan Das, Tânia E. Sintra, João A. P. Coutinho, Sónia P. M. Ventura, Kunal Roy and Paul L. A. Popelier, *Toxicology Research*, **2016**, 5, 1388-1399, DOI: 10.1039/C6TX00180G.

(In this communication Tânia E. Sintra contributed with synthesis and characterization of the morpholinium-based ILs, measurement of their ecotoxicity, and with the manuscript preparation.)

ABSTRACT

Despite possessing an interesting chemical nature and tuneable physicochemical properties, ILs must have their ecotoxicity tested in order to be commercialized. The water solubility of ILs allows their easy access to the aquatic compartment of the ecosystem creating a potential hazard to aquatic organisms. Hence, it is relevant to design ILs with lower toxicity while keeping the desired properties of interest. Considering the possibility of an enormous number of combinations of different cations and anions, a rational guidance for the structural design of ILs is essential in order to prioritize the synthesis as well as testing of selected molecules only. Predictive in silico models, such as QSAR models, can play a pivotal role in exploring the important chemical attributes contributing to the response activity. These models may then lead to the design of novel ILs. The present study aims at developing predictive QSAR models for the ecotoxicity of ILs using the bacteria *V. fischeri* as an indicator response species. Instead of a single model, here we have used multiple models to capture more complete structural information of ILs for toxicity towards *V. fischeri*. The derived chemical attributes have

been implemented in designing new analogues, some of which have been synthesized and had their ecotoxicity tested for the same model organism. The predictive QSAR models reported here can be used for ecotoxicity prediction of new IL chemicals and for data-gap filling. Moreover, the synthesized low-toxic ILs could be considered for evaluation as well as for application in suitable processes serving the purpose of industry and academia.

INTRODUCTION

ILs can be used for multi-tasking because of their easily tuneable nature arising from their intrinsic properties. It may be noted that approximately one billion (10^{12}) binary and one trillion (10^{18}) ternary combination systems of ILs would be possible only by using 1 million simple systems (cations and anions).[465] It would be time consuming, expensive and even impossible to obtain different physical, chemical and biological (toxicological) properties data by measuring all possible ILs in order to screen for an optimum IL given a special purpose. Due to the huge number of potential ILs, experimental data for different properties are currently available only for a small fraction of these ILs. This lack of data can be a major drawback, especially in systematic screening to find the best-suited solvent for a particular task. In order to design any new process involving ILs on an industrial scale, it is necessary to have knowledge of various properties as well as an understanding of the molecular structure of the compounds. Therefore, it is necessary to develop mathematical models to predict the various property endpoints of ILs. Quantitative structure–property/activity relationship (QSPR/QSAR) methods[269,466,467] would help to develop quantitative models capable of predicting the properties directly from molecular structure information.

ILs could theoretically be designed to have a desired property by combining different pairs of ions. To explore the “tuneability” and “designability” features of ILs, predictive QSPR models have to be developed to relate the properties to the chemical structure or other physicochemical properties.[467,468] Such models should also be rigorously validated in order to prove their predictive capacity and applicability to a new set of ILs.

Although ILs were originally promoted as green solvents, studies have also shown that ILs, as any organic solvent, may have some degree of toxicity to the various organisms of the ecosystem.[222,261] Predictive QSAR models can explore the structural attributes of ILs towards various physicochemical and toxicological endpoints, thereby leading to the design of "greener" analogues with higher process selectivity. This approach can lead to filling large data gaps, since the toxicity data are only available for a limited number of ILs against different indicator organisms of the ecosystem. The QSAR approach for toxicity predictions is also encouraged in the REACH legislation of the European Union.[469] However, the *in silico* models should be developed in accordance with the guidelines of the Organization for Economic Cooperation and Development (OECD).[470]

V. fischeri is a Gram-negative, rod-shaped bacterium, and considered as an important member in a marine ecosystem.[471] It can be easily cultured and bred in the laboratory. Thus, *V. fischeri* can be easily applied as a test organism for assessment of toxicity of chemicals in the aquatic systems. Bioassays based on *V. fischeri* (such as Microtox®) involve a simple procedure, short testing times and are cost-effective. Such assays are recommended by international standards to monitor the toxicity of environmental contaminants.[472] There have been a few reports in the literature on modelling the toxicity of ILs towards *V. fischeri*.[256,258,260,447,448,473,474] In the present work, we have developed QSAR models for *V. fischeri* toxicity using the largest available set of ILs with the experimental toxicity data using Microtox®. We have also applied these models for prediction of toxicity of a recently available set of ILs for a true external validation of the developed models. In order to experimentally validate the models, a set of IL compounds with low predicted toxicity values was designed, subsequently synthesized and experimentally tested for their toxicity towards *V. fischeri*. Note that this is the first attempt to perform both true external validation and experimental validation of QSPR models for toxicity of ILs to *V. fischeri*. We have also given serious attention to the applicability domain of the developed models during the prediction of external compounds as recommended by the OECD guidelines.[470]

EXPERIMENTAL SECTION

The dataset and descriptors: We have assembled from the literature a large dataset of 305 ILs with their ecotoxicity values on Microtox® based on the luminescence inhibition of *V. fischeri*.[100,120,190,228,229,232,248,255,256,258–260,448,450,475–478] It should be mentioned that we have considered the median effective concentration (EC_{50}) data determined at 15 min or 30 min exposure. When both data are available, their average values were used considering the insignificant impact of the exposure time[255] on *V. fischeri* toxicity for ILs. For maintaining uniformity, the EC_{50} data obtained from different literature sources were converted to the molar unit ($mol \cdot L^{-1}$) followed by their transformation into a negative logarithmic scale i.e., pEC_{50} (EC_{50} in $mol \cdot L^{-1}$). The cationic composition of the dataset varies within ammonium, cholinium, imidazolium, morpholinium, melanimium, phosphonium, tropinium, piperidinium, pyridinium, pyrrolidinium, quinuclidinium, and sulphonium in suitable combination of various inorganic as well as organic anions. The predictor variables employed in this study were computed for both the cations and anions, and include various one- and two-dimensional descriptors involving constitutional features, connectivity parameters, information indices, extended topochemical atom (ETA) indices,[479] functional group counts, atom-centred fragments, molecular profiles, 2D-atom pair based parameters, *etc.*,[480] in addition to quantum chemical attributes namely Quantum Topological Molecular Similarity (QTMS) parameters,[481,482] and computed lipophilicity measures. The detailed categorical list of the descriptors can be found in Table G1 of Appendix G. While the other descriptors were obtained without the need of any geometry optimization process, the QTMS parameters were derived from the *ab initio* based optimized geometry at the HF/6-31G(d) level of theory, and were limited to only cations. The log k_0 values were computed using QTMS and ETA indices as proposed by Roy and Popelier.[483] Finally, we have employed an additional external dataset of eight compounds (not used for developing the models), but for judging the true external predictivity of the models.[449]

Development of predictive QSTR models:

I) *Dataset division and descriptor pre-treatment*. Variance and correlation based criteria were implemented for the thinning of the descriptor pool giving predictor

variables with a variance > 0.0001 and an inter-correlation (*r*) among descriptors < 0.95. The dataset was divided into a training set and a test set of compounds using the *k*-means clustering algorithm.[484] A total of six clusters were derived for the whole data followed by random selection of approximately 70% of compounds in the training set ($n_{training}$ = 213) and the remaining 30% compounds in the test set (n_{test} = 92) from each cluster. We preferred to choose the *k*-means clustering technique over a mere random method in order to achieve a rational and uniform division of the dataset so that the training set can encompass the entire structural domain with the test set chemicals lying in the vicinity of one or more training set molecules. Note that QSAR models make predictions that are based on the similarity principle and will thus perform better when the test set molecules are structurally similar to the training set compounds and are thus within the applicability domain of the models. The information on the *k*-clusters can be found in Table G2 of the Appendix G.

II) Employed statistical analyses, chemometric tools and validation parameters for in silico modeling. Multiple linear regression (MLR)[485] and partial least squares (PLS)[486] techniques have been used as the statistical methods for the derivation of the QSAR models while the selection of features has been performed by employing chemometric tools, namely, genetic function approximation (GFA)[487] and a stepwise based method[488] coupled with Fischer value (*F*-value) based criteria. In the present study, we have used the GFA technique for the identification of most occurring descriptors, which were subsequently used for stepwise based MLR analysis using the stepping criteria of *F* to enter = 4.0 and *F* to remove = 3.9.[485] The best equation obtained from the latter was then subjected to a PLS run considering PLS to be a more robust method for avoiding the problems of multicollinearity.[486] The PLS model was also optimized considering a 5% rise in the Q^2 value as the indicator. Thus, a three layered treatment, that is, GFA followed by a stepwise-based MLR followed by PLS regression was applied for the development of QSAR models.

The developed models were subjected to sufficient statistical validation tests using various metrics to denote model fitness as well as predictivity. Multiple validation strategies involving quality parameters (R^2, R_a^2, *F*-value),[485] internal (Q^2_{LOO}) and external

($Q^2_{ext(F1)}$, $Q^2_{ext(F2)}$, $Q^2_{ext(F3)}$) validation metrics have been adopted. The chemical domain of applicability[489] of the developed models was determined using the distance to model X (DModX) based approach.[486]

III) *Used software tools for QSTR analysis*. The chemical structures of the cations and anions were drawn using MarvinSketch (version 15.12.7) software,[490] while Dragon (version 6)[491] and PaDEL-Descriptor (version 2.11) software[492] were employed for the computation of various two-dimensional variables. The determination of an estimated geometry and *ab initio* optimization of the cations were respectively carried out using the GUI GaussView[493] and the program GAUSSIAN03[494] followed by derivation of the QTMS indices using the in-house computer program MORPHY.[495] The *k*-means cluster based division was performed using SPSS (version 9.0.0) software.[496] The GFA analysis was performed using Cerius^2 (version 4.10) software,[497] while the stepwise based MLR and PLS operations were respectively carried out by employing MINITAB (version 14.13)[498] and SIMCA-P (version 10.0)[499] software, which was also used for the determination of DModX values.

Synthesis of morpholinium-based ILs:

I) *Materials*. Bromoethane (98.0 wt% of purity), 1-bromopropane (99.0 wt% of purity), dimethylsulfate (99.8 wt% ofpurity), iodomethane (99.0 wt% of purity), morpholine (99.0 wt% of purity), 4-methylmorpholine (99.0 wt% of purity), 4-(2-hydroxyethyl)morpholine (99.0 wt% of purity), potassium acetate (99.0 wt% of purity), acetic acid glacial (99.9 wt% of purity) and toluene (99.8 wt% of purity) were acquired from Sigma-Aldrich. Ethyl acetate (99.0 wt% of purity) and ethanol (99.9 wt% of purity) were purchased from Carlo Herba. Silver nitrate (99.8 wt% of purity) and formic acid (91.0 wt% of purity) were bought from Panreac. 4-Ethylmorpholine (97 wt% of purity), potassium hydroxide (pure) and acetone (HPLC grade) were acquired from Fluka, Pronalab and VWR, respectively. The water used was double distilled, passed by using a reverse osmosis system and further treated with a Milli-Q plus 185 water purification apparatus. Seven morpholinium-based ILs were synthesized, namely *N*-ethyl-*N*-methylmorpholinium bromide, [C_2C_1mor]Br; *N*-ethyl-*N*-methylmorpholinium acetate, [C_2C_1mor][OAc]; *N*-ethyl-*N*-methylmorpholinium formate, [C_2C_1mor][For]; *N*-ethyl-*N*-

methylmorpholinium methylsulfate, [C_2C_1mor][C_1SO_4]; *N*-methyl-*N*-propylmorpholinium bromide, [C_3C_1mor]Br, *N*-hydroxyethyl-*N*-methylmorpholinium iodide, [$C_{2(OH)}C_1$mor]I; and morpholinium acetate, [Mor][OAc]. Their respective acronyms and chemical structures are depicted in Figure 8.1. The structure of all compounds synthesized was confirmed by ^{1}H and ^{13}C NMR spectroscopy, showing the high purity level of all the ionic structures after their synthesis. Due to the quadrupole moment of the ^{14}N nucleus, ^{1}H-^{14}N and ^{13}C-^{14}N couplings were observed in the NMR spectra of the [C_2C_1mor] cation, which are in accordance with the literature.[500]

II) *Synthesis and characterization of morpholinium-based ILs*.

- *N*-Ethyl-*N*-methylmorpholinium bromide, [C_2C_1mor]Br, was prepared by dropwise addition of 6 mL of bromoethane (80.4 mmol) to a solution of 4-methylmorpholine (72.3 mmol, 7.32 g) in ethyl acetate, at room temperature. The reaction mixture was refluxed, stirred at 55 °C, and protected from light overnight. A solid was formed, which was filtered off and washed with ethyl acetate (3 × 15 mL). Finally, the residual solvent was removed under reduced pressure and the obtained compound was dried under high vacuum for at least 48 h.[500] [C_2C_1mor]Br was obtained as a white solid (44% yield, 6.67 g). ^{1}H NMR (D_2O, 300 MHz, [ppm]): δ 1.39 (tt, 3H, J_{HH} = 7.3 Hz and J_{NH} = 1.9 Hz, $NCH_2C\underline{H}_3$), 3.18 (s, 3H, $NC\underline{H}_3$), 3.39–3.65 (m, 6H, $N(C\underline{H}_2)_3$), 3.98–4.12 (m, 4H, $O(C\underline{H}_2)_2$). ^{13}C NMR (D_2O, 75.47 MHz, [ppm]): δ 6.57, 46.01 (t, J_{CN}, NCH_3), 59.06 (t, J_{CN}, NCH_2CH_3), 60.40, 60.81.

- *N*-Ethyl-*N*-methylmorpholinium acetate, [C_2C_1mor][OAc]. As a first step, potassium acetate in a water solution (5.2 mmol, 0.51 g) was added to an aqueous solution of silver nitrate (4.7 mmol, 0.80 g). The solution was stirred at room temperature for 3 h, leading to the formation and precipitation of silver acetate. After filtration, the solid was washed with water (3 × 10 mL). The residual water was removed under reduced pressure. Silver acetate was obtained with 90% yield (0.71 g). In the second stage, a stoichiometric amount of silver acetate (1.2 mmol, 0.20 g) was added to an aqueous solution of *N*-ethyl-*N*-methylmorpholinium bromide (1.2 mmol, 0.25 g). The reaction mixture was stirred at room temperature, and protected from light for 1.5 h. The reaction flask was then placed into a water-ice bath in order to ensure the complete precipitation of silver bromide, which was later removed by filtration. Finally, the water was removed under reduced

pressure and the obtained compound was dried under high vacuum for at least 48 h.[62] $[C_2C_1mor][OAc]$ was obtained as a white solid (92% of yield, 0.21 g). ^1H NMR (D_2O, 300 MHz, [ppm]): δ 1.39 (tt, 3H, J_{HH} = 7.3 Hz and J_{NH} = 1.9 Hz, $NCH_2C\underline{H}_3$), 1.91 (s, 3H, $COOC\underline{H}_3$), 3.17 (s, 3H, $NC\underline{H}_3$), 3.42–3.61 (m, 6H, $N(C\underline{H}_2)_3$), 3.97–4.10 (m, 4H, $O(C\underline{H}_2)_2$). ^{13}C NMR (D_2O, 75.47 MHz, [ppm]): δ 6.45, 23.23, 45.94 (t, J_{CN}, NCH_3), 59.00 (t, J_{CN}, NCH_2CH_3), 60.33, 60.75, 181.26.

- *N*-Ethyl-*N*-methylmorpholinium formate, $[C_2C_1mor][For]$. Firstly, a stoichiometric amount of potassium hydroxide was added to a solution of *N*-ethyl-*N*-methylmorpholinium bromide (2.4 mmol) prepared in ethanol. The solutions were stirred at room temperature for 0.5 h, after which the precipitated potassium bromide was removed by filtration. Then, a stoichiometric amount of formic acid was added to the filtrate. Again, the solutions were stirred overnight at room temperature, then the reaction flask was placed in a water-ice bath and the remaining inorganic salt was removed. Finally, the ethanol was removed under reduced pressure and the obtained compound was dried under high vacuum for at least 48 h.[501] $[C_2C_1mor][For]$ was obtained as a white solid (95% of yield, 0.40 g). ^1H NMR (D_2O, 300 MHz, [ppm]): δ 1.37 (tt, 3H, J_{HH} = 7.3 Hz and J_{NH} = 1.8 Hz, $NCH_2C\underline{H}_3$), 3.16 (s, 3H, $NC\underline{H}_3$), 3.35–3.64 (m, 6H, $N(C\underline{H}_2)_3$), 3.94–4.15 (m, 4H, $O(C\underline{H}_2)_2$), 8.41 (s, 1H, $\underline{H}CO_2$). ^{13}C NMR (D_2O, 75.47 MHz, [ppm]): δ 6.45, 45.96 (t, J_{CN}, NCH_3), 59.01 (t, J_{CN}, NCH_2CH_3), 60.34, 60.77, 170.18.

- *N*-Ethyl-*N*-methylmorpholinium methylsulfate, $[C_2C_1mor][C_1SO_4]$, was prepared by slow dropwise addition of 2.0 mL of dimethylsulfate (21.1 mmol) to a solution of 4-ethylmorpholine (19.0 mmol, 2.19 g) in toluene, at 0 °C, under a nitrogen atmosphere. The reaction mixture was stirred at room temperature under a nitrogen atmosphere and protected from light for 4 h. The obtained white solid was isolated by filtration and washed with ethyl acetate (2 × 15 mL). Finally, the residual solvent was removed under reduced pressure and the obtained compound was dried under high vacuum for at least 48 h.[45] $[C_2C_1mor][C_1SO_4]$ was obtained as a white solid (68% of yield, 3.10 g). ^1H NMR (D_2O, 300 MHz, [ppm]): δ 1.37 (tt, 3H, J_{HH} = 7.3 Hz and J_{NH} = 1.8 Hz, $NCH_2C\underline{H}_3$), 3.15 (s, 3H, $NC\underline{H}_3$), 3.37–3.61 (m, 6H, $N(C\underline{H}_2)_3$), 3.73 (s, 3H, $OC\underline{H}_3$), 3.97–4.11 (m, 4H, $O(C\underline{H}_2)_2$). ^{13}C

NMR (D_2O, 75.47 MHz, [ppm]): δ 6.43, 45.93 (t, J_{CN}, NCH_3), 55.38, 59.01 (t, J_{CN}, NCH_2CH_3), 60.34, 60.76.

- *N*-Methyl-*N*-propylmorpholinium bromide, $[C_3C_1mor]Br$, was prepared by dropwise addition of 4.5 mL of 1-bromopropane (49.5 mmol) to a solution of 4-methylmorpholine (44.6 mmol, 4.51 g) in ethyl acetate, at room temperature. The reaction mixture was refluxed and stirred at 55 °C, and protected from light overnight. After cooling, a solid was formed, then filtered off and washed with ethyl acetate (3 × 15 mL). Finally, the residual solvent was removed under reduced pressure and the obtained compound was dried under high vacuum for at least 48 h.[500] $[C_3C_1mor]Br$ was obtained as a white solid (43% of yield, 4.30 g). ^{1}H NMR (D_2O, 300 MHz, [ppm]): δ 1.00 (t, 3H, J_{HH} = 7.3 Hz, $NCH_2CH_2C\underline{H}_3$), 1.74–1.92 (m, 2H, $NCH_2C\underline{H}_2CH_3$), 3.19 (s, 3H, $NC\underline{H}_3$), 3.35–3.64 (m, 6H, $N(C\underline{H}_2)_3$), 3.98–4.13 (m, 4H, $O(C\underline{H}_2)_2$). ^{13}C NMR (D_2O, 75.47 MHz, [ppm]): δ 9.73, 14.63, 46.74, 59.51, 60.34, 66.43.

- *N*-Hydroxyethyl-*N*-methylmorpholinium iodide, $[C_{2(OH)}C_1mor]I$, was prepared by dropwise addition of 2.0 mL of iodomethane (32.1 mmol) to a solution of 4-(2-hydroxyethyl)morpholine (21.6 mmol, 2.83 g) in ethyl acetate, at room temperature, under a nitrogen atmosphere. The reaction mixture was refluxed and stirred at 45 °C, under a nitrogen atmosphere and protected from light overnight. A solid was formed, which was filtered off and washed with ethyl acetate (3 × 25 mL). Finally, the residual solvent was removed under reduced pressure and the obtained compound was dried under high vacuum for at least 48 h.[500] $[C_{2(OH)}C_1mor]I$ was obtained as a white solid (88% of yield, 5.18 g). ^{1}H NMR (DMSO-d_6, 300 MHz, [ppm]): δ 3.24 (s, 3H, $NC\underline{H}_3$), 3.40–3.69 (m, 6H, $N(C\underline{H}_2)_3$), 3.80–4.03 (m, 6H, $O(C\underline{H}_2)_2$ and $C\underline{H}_2OH$), 5.21 (t, 1H, J_{HH} = 4.6 Hz, $O\underline{H}$). ^{13}C NMR (DMSO-d_6, 75.47 MHz, [ppm]): δ 48.30, 54.94, 60.21, 60.31, 65.08.

- Morpholinium acetate, [Mor][OAc], was prepared by dropwise addition of 2 mL of acetic acid (35.0 mmol) to a solution of morpholine (35.0 mmol, 3.05 g) in ethyl acetate, at 0 °C. The reaction mixture was stirred at room temperature overnight. A solid was formed, which was filtered off and washed with ethyl acetate (2 × 20 mL). Finally, the residual solvent was removed under reduced pressure and the obtained compound was

dried under high vacuum for at least 48 h.[36] [Mor][OAc] was obtained as a white solid (97% of yield, 4.99 g). ^{1}H NMR (D_2O, 300 MHz, [ppm]): δ 1.92 (s, 3H, $C\underline{H}_3$), 3.23–3.35 (m, 4H, $N(C\underline{H}_2)_2$), 3.90–4.01 (m, 4H, $O(C\underline{H}_2)_2$). ^{13}C NMR (D_2O, 75.47 MHz, [ppm]): δ 23.18, 42.95, 63.49, 181.17.

Microtox Assay: In order to validate the predictive QSAR models herein reported, the ecotoxicity of the morpholinium-based ILs synthesized was evaluated using Standard Microtox liquid-phase assay. This test is described in detail in the Experimental Section of Chapter 2.

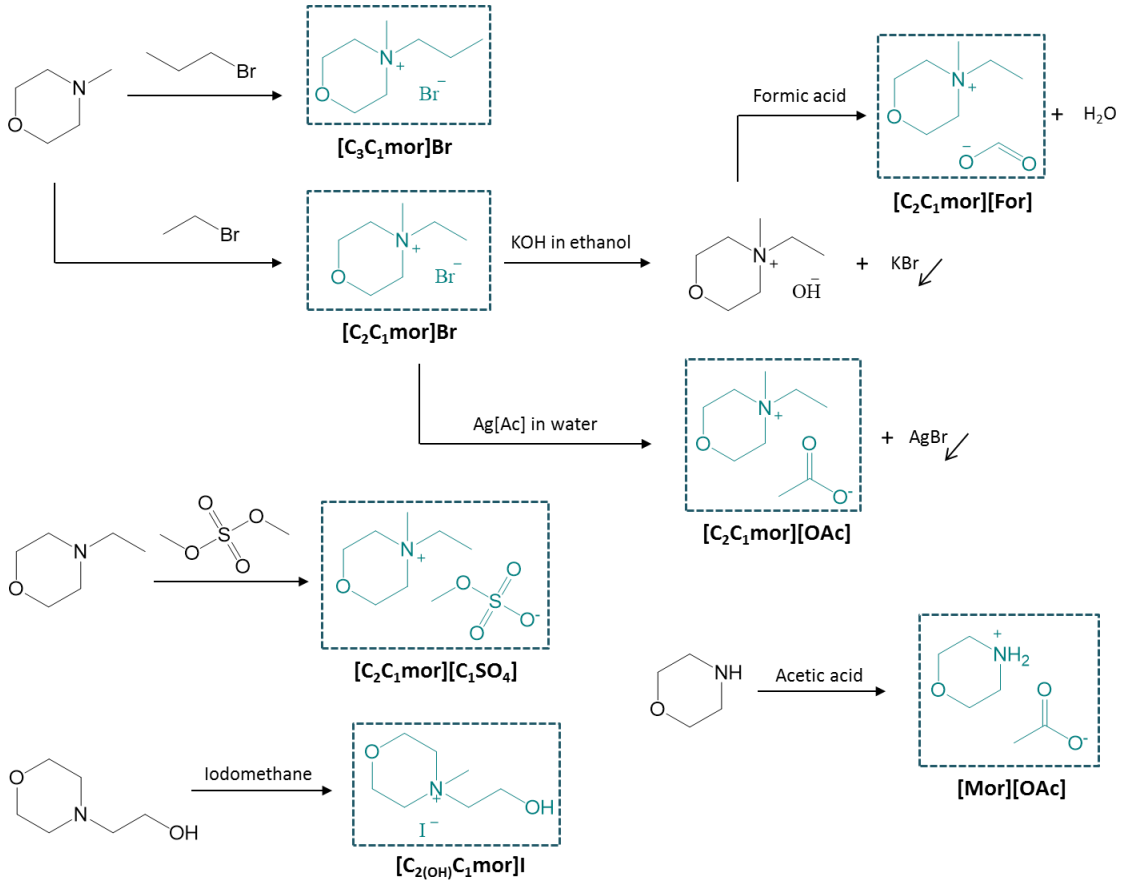

Figure 8.1. Synthesis scheme and chemical structure of the morpholinium-based ILs synthesized specifically for this study.

RESULTS AND DISCUSSION

Developed QSAR models. The QSAR models developed in the present study follow the OECD guidelines as characterized by a uniformly defined response data (principle 1), explicitly described methodology (principle 2), suitable chemical domain of applicability (principle 3), statistical measures defining fitness, predictivity and robustness (principle 4), as well as interpretation of the captured chemical information (principle 5).[470] A total of six PLS models have been developed. Here, we have used the spline option of the GFA algorithm in order to account for the presence of any non-linear relationship along with the linear variables. Table 8.1 presents the statistical quality of the developed equations and their external predictivity on the same test set, which were not used during model development. All models show acceptable quality in terms of fitness, stability and classical predictivity measures. Recently, it has been shown by Roy et al.[496] that the R^2 based criteria for model validation might be insufficient and misleading in some cases. Instead, mean absolute error (MAE) based criteria[502] have been proposed for a better understanding of the quality of predictions. Here, using the MAE-based judgement of model external predictivity, the external predictive quality of the first three models was characterized as 'moderate' while the remaining three as 'bad'. Interestingly, classical validation metrics such as $Q^2_{ext(F1)}$ and $Q^2_{ext(F2)}$ show acceptable quality of external predictions for all the models on the same test set data, but the MAE-based criteria penalize the last three models employing an error threshold using a range of training set responses.[502] Here, both $Q^2_{ext(F1)}$ and $Q^2_{ext(F2)}$ show overpredictivity for models 4, 5, and 6, since the response values of the test set observations lie away from the mean value of the training and test set responses. The summed predicted residual values obtained from these models were found to be higher than those obtained using models 1, 2 and 3 portraying relatively poor model performances by the models 4, 5, and 6. We have omitted the latter models from consensus predictions in order to obtain more precise prediction values based on models 1, 2 and 3 (Table G3 in Appendix G).

Table 8.1. Predictive QSAR models developed using the ecotoxicity values of ILs to *V. fischeri*. Here, $n_{training}$=213, n_{test}=92.

Sl. No.	Predictive models	LVs	R^2	R_a^2	Q^2_{LOO}	$Q^2_{ext(F1)}$	$Q^2_{ext(F2)}$	MAE based criteria	Consensus prediction		
									$Q^2_{ext(F1)}$	$Q^2_{ext(F2)}$	MAE based
1	$pEC_{50}(M) = 5.390 - 0.354\times < 6 - CATS2D\_03\_LL >_{(cation)} - 1.083\times B05[C-O]_{(cation)}$ $+0.007\times ZM1V_{(cation)} - 0.003\times < 435.42 - MW >_{(total)} - 0.304\times CATS2D\_05\_PL_{(cation)}$ $-0.827\times B02[C-S]_{(anion)} - 17.292\times < 0.328 - {}^2\chi_{avg} >_{(cation)} + 0.000\times GMTIV_{(cation)}$ $+0.164\times nCs_{(anion)} - 1.631\times nRCN_{(cation)} + 0.474\times Cl-102_{(anion)} - 0.534\times MCD_{(cation)}$	5	0.746	0.740	0.711	0.696	0.696	Moderate			
2	$pEC_{50}(M) = 5.665 - 0.315\times < 6 - CATS2D\_03\_LL >_{(cation)} - 2.305\times \Sigma\beta'_{(cation)}$ $+0.903\times Iarom_{(cation)} + 0.875\times < 1 - nO >_{(cation)} + 0.136\times naAromAtom_{(cation)}$ $-8.839\times \Delta\varepsilon_{C(cation)} - 0.003\times < 435.42 - MW >_{total} + 0.445\times < C-005-2 >_{(cation)}$ $-16.397\times < 0.328 - {}^2\chi_{avg} >_{(cation)} - 1.166\times \lambda_{3(cation)}$	7	0.703	0.693	0.664	0.645	0.645	Moderate	0.704	0.704	Moderate
3	$pEC_{50}(M) = 4.796 - 0.326\times < 6 - CATS2D\_03\_LL >_{(cation)} - 0.008\times ZM1V_{(cation)}$ $-0.899\times B05[C-O]_{(cation)} - 0.0001\times GMTIV_{(cation)} - 0.003\times < 435.42 - MW >_{total}$ $+0.688\times Cl-102_{(anion)} + 0.206\times nCs_{(anion)} - 0.683\times B02[C-S]_{(anion)}$ $-13.595\times < 0.328 - {}^2\chi_{avg} >_{(cation)} - 0.557\times MCD_{(cation)} + 0.234\times V_{index\ (anion)} - 1.468\times nRCN_{(cation)}$	5	0.748	0.742	0.710	0.656	0.656	Moderate			
4 [a]	$pEC_{50}(M) = 0.563 + 0.118\times H-046_{(cation)} - 0.122\times (\log k_0)^2_{(cation)} + 0.419\times MSD_{(cation)}$ $+1.601\times \eta'_{F(cation)} - 0.573\times nBR_{(anion)} + 0.267\times nHM_{(anion)} + 0.225\times nCs_{(anion)} - 0.325\times SdssC_{(anion)}$ $-0.598\times {}^4\chi^v_{avg(cation)} - 4.054\times {}^5\chi_{avg(cation)} - 1.340\times nRCN - 0.101\times C-006_{(anion)}$	7	0.697	0.687	0.655	0.635	0.635	Bad			
5 [a]	$pEC_{50}(M) = 5.317 - 0.270\times < 6 - CATS2D\_03\_LL >_{(cation)}$ $-0.060\times < 19.549 - (ALOGP)^2 >_{(cation)} + 0.572\times < C-005-2 >_{(cation)}$ $+0.409\times N-075_{(cation)} - 0.002\times < 435.42 - MW > - 0.626\times nCq_{(cation)}$ $-1.037\times nI_{(anion)} - 0.319\times nBR_{(anion)} - 1.446\times nROR_{(anion)}$	3	0.705	0.701	0.677	0.609	0.609	Bad	–	–	–
6 [a]	$pEC_{50}(M) = 5.172 - 0.361\times < 6 - CATS2D\_03\_LL >_{(cation)}$ $-0.067\times (\log k_0)^2_{(cation)} - 0.004\times < 435.42 - MW_{(total)} > + 0.034\times H-046_{(cation)}$ $+0.975\times Cl-102_{(anion)} + 1.339\times lap_{(cation)} - 0.349\times H-053_{(cation)}$ $-0.289\times SdssC_{(anion)} + 0.260\times Vindex_{(anion)} + 0.135\times nCS_{(anion)} + 0.001\times MW_{(cation)}$	5	0.718	0.711	0.689	0.609	0.609	Bad			

[a] Models showing 'bad' external predictivity as identified by the MAE based criteria.

However, we have retained models 4, 5, 6 in Table 8.1 as these models might still provide useful information about the structure–toxicity relationships in the form of uncommon descriptors not present in models 1, 2 and 3, and may hence be useful for designing new chemicals. The number of latent variables (LVs) reported in Table 8.1 varies from three to seven, which is encouraging, considering the training set size comprising 213 chemicals.[503] Here, we explain the chemical information captured by models 1, 2, and 3, which are characterized as 'moderate' by the MAE based criteria. The reported models have captured information of both the cations and anions for the toxicity of ILs towards *V. fischeri*. The repeated occurrence of the descriptor CATS2D_03_$LL_{(cation)}$ in models 1, 2, and 3 emphasizes its greater importance in encoding the toxicity of ILs. This parameter is characterized by a spline function with a knot value of 6 signifying that the spline term will vanish if the value of the descriptor CATS2D_03_$LL_{(cation)}$ is more than or equal to 6. The descriptor belongs to the pharmacophoric point pair based CATS2D group and designated as the 'lipophilic–lipophilic at lag 03' portraying the presence of two lipophilic atoms at topological distance 3 in cations. Considering the nature of the present dataset, the value of the descriptor was found to increase with the alkyl chain length of the cationic substituent. Now, the cationic substituents consist of carbon atoms that are considered as lipophilic in the CATS2D formalism. Hence, the parameter portrays information on cationic lipophilicity. An additional descriptor of the pharmacophore point pair type, namely CATS2D_05_$PL_{(cation)}$ in model 1, signifying the presence of a positively charged atom and a lipophilic atom at a distance of 5, also gives information on cationic lipophilicity.

In Table 8.1, a spline form of the descriptor MW_{total} coding for the total molecular weight of an ionic liquid (considering both cations and anions) is present in the three models (*i.e.*, models 1, 2 and 3). The spline function $<435.42 - MW>_{total}$ determines that ILs with a molecular weight value less than 435.42 will influence the toxicity response. The molecular weight gives a measure of the bulk of analysed chemicals, which can be correlated with the hydrophobic behaviour. The spline function is appended with a negative coefficient in the equations signifying that compounds with a lower molecular weight value will have a higher value of the spline term and a lower value of toxicity

thereof compared to those having a higher MW_{total} value. Hence, considering a knot value of 435.42, ILs with a lower molecular weight will be less toxic than the ones with a higher molecular weight value. The compound $[C_2C_1im]Cl$ (Sl. no. 137, pEC_{50} = 1.450) with a $<435.42 - MW_{total}>$ value of 288.78 is less toxic than $[C_{16}C_1im]Cl$ (Sl. no. 211, pEC_{50} = 5.770) having a value of 92.36 for the same parameter. The descriptor $nCs_{(anion)}$ encoding the total number of secondary sp^3 hybridized carbon atoms, *i.e.*, a $–CH_2$ group in anions is present in models 1 and 3 and highlights the contribution of non-halogenated organic anions towards toxicity.

The higher toxicity value of the compound [2-HDEA][Pe] (Sl. no. 120, pEC_{50} = 2.772) compared to that of [2-HDEA][Pr] (Sl. no. 113, pEC_{50} = 2.440) is due to the possession of a higher number of $–CH_2$ groups in the pentanoate anion ([Pe]) of the former compound than propionate ([Pr]) in the latter. Another anionic descriptor $Cl\text{-}102_{(anion)}$ present in models 1 and 3 emphasizes the contribution of the chloride anion towards toxicity. The occurrence of the cationic descriptor $nRCN_{(cation)}$ with a negative coefficient in models 1 and 3 suggests a negative impact of the count of aliphatic nitrile groups in cations on the toxicity. The presence of a nitrile group in cations incorporates H-bonding behaviour to the molecule and hence reduced toxicity due to a decreased lipophilic nature. The compound $[C_4C_{3(CN)}pyrr]Br$ (Sl. no. 280, pEC_{50} = 0.670) is less toxic than $[C_4pyrr]Cl$ (Sl. no. 282, pEC_{50} = 1.700) since the former contains a nitrile functionality in its cationic moiety. Another cationic descriptor with repeated occurrence is $<0.328 - {}^2\chi_{avg}>_{(cation)}$ (see models 1, 2, and 3), which encodes information on branching. The descriptor ${}^2\chi_{avg}$ is the average second-order connectivity index defining the importance of the cationic branchedness in a non-linear *i.e.*, spline fashion. A few other descriptors describing the cationic features *viz.* $MCD_{(cation)}$, $B05[C–O]_{(cation)}$, $ZM1V_{(cation)}$, $GMTIV_{(cation)}$, $<C\text{-}005 - 2>_{(cation)}$, $<1 - nO>_{(cation)}$, $\lambda_{3(cation)}$, $\Delta\varepsilon_{C(cation)}$, $\Sigma\beta'_{(cation)}$ as well as anionic attributes *viz.* $B02[C–S]_{(anion)}$ and $V_{index(anion)}$ are observed to be present in models 1, 2, and 3.

The descriptor ZM1V is the valence-vertex-degree-based first Zagreb index while GMTIV is the valence vertex degree based Gutman Molecular Topological Index, both of which define the molecular branchedness. MCD is the molecular cyclized degree denoting the importance of acyclic groups and substituents along with cyclic moieties. The descriptor

C-005 codes for the atom type fragment of CH_3X type (X is any heteroatom), *i.e.*, for the given dataset it provides information on the role of methyl groups attached to heteroatoms, *e.g.*, *N* of imidazolium, ammonium, pyrrolidinium and other systems. Another cationic descriptor B05[C–O] shows the presence or absence of C–O at the topological distance of 5 bonds and thereby it provides information on the H-bonding nature of the oxygenated substituents on cations leading to reduced toxicity of ILs principally by modifying the system lipophilicity. The impact of cationic oxygen atoms towards the toxicity of ILs is further emphasized by the spline parameter $<1 - nO>_{(cation)}$ where *n*O represents the number of oxygen atoms. Model 2 additionally captures information on cationic aromaticity (I_{arom}, $na_{AromAtom}$), and electronic distribution for the ecotoxicity of ILs to *V. fischeri*. The information on the electronic distribution of cations is also shown by the ETA indices $\Delta\varepsilon_{C(cation)}$, $\Sigma\beta'_{(cation)}$ and the QTMS variable λ_3 (model 2). Among the anionic descriptors, V_{index} is the Balaban *V* index, which defines the role of anionic branchedness and B02[C–S] depicts the role of sulfated and sulfonated anions for the ecotoxicity of ILs towards *V. fischeri*.

Hence, a chemical interpretation of the descriptors portrays that the toxicity of ILs towards *V. fischeri* is monitored by features such as lipophilicity, hydrogen bonding propensity, branching, aromaticity, and electronegativity. While a parameter such as MW_{total} shows the impact of lipophilicity as a whole, the descriptors *viz.* CATS2D_03_LL, CATS2D_05_PL, MCD, ZM1V, GMTIV, *etc.* provide further insight into the pattern of side chain substituents as well as branching of cations. The lipophilicity attribute of anions was also observed to play a major role in the descriptors *n*Cs and Cl-102. The presence of hydrogen bonding groups on cationic side chains, *e.g.*, groups containing O, N, *etc.* were also observed to influence ionic liquid toxicity towards *V. fischeri* as encoded by the descriptors B05[C–O], *n*RCN, *n*O, C-005, *etc.*

True external validation. The true external prediction was performed on a separate dataset of new eight ILs (which are not common to the 305 ILs used for the development of the QSAR models) using models 1, 2 and 3, which showed encouraging values of the classical external validation metrics as well as the MAE based judgment criteria as portrayed in Table 8.2. The reliability of predictions for these eight molecules was also

verified using the chemical domain of the models (models 1, 2, and 3) by employing the DModX approach.

Table 8.2. Predictive quality of the models for the true external validation set (*n*=8) employing classic metrics and MAE based criteria.

	$Q^2_{ext(F1)}$	$Q^2_{ext(F2)}$	MAE based criteria
Model 1	0.605	-1.738	Moderate
Model 2	0.883	0.190	Good
Model 3	0.652	-1.408	Moderate
Predictions from the best model*	0.736	-0.826	Good
Consensus predictions	0.743	-0.783	Good

* The best model corresponds to the one showing the lowest value of DModX with respect to a particular query compound.

Table 8.3 gives the predicted toxicity values (and the experimental values) of the true external set based on the lowest DModX value out of the three models. We have also determined the consensus prediction values for the compounds, which are reported in Table 8.3. It may be noted that predicted toxicity values obtained using the best model (model with the lowest DModX value with respect to a specific observation) as well as the consensus approach are characterized as 'good' by the MAE based criteria (Table 8.2) although the classical external validation metric $Q^2_{ext(F2)}$ fails to portray the acceptable predictivity. Here, we have found that the absolute values of the predicted residuals for all the eight observations obtained from models 1, 2 and 3 are less than 0.2 times the training set range (where 0.2 × training range = 1.206) signifying good predictions. Only one observation showed a predicted residual (absolute) value more than 0.15 times the training set range (where 0.15 × training range = 0.905) with respect to models 1 and 3. Accordingly, the predictive quality was judged 'moderate' by the MAE based criteria for these two models. However, the $Q^2_{ext(F2)}$ metric renders the models underpredictive because of the low range of the response of the true external set (1.07 log unit) where most of the compounds are close to the mean response of the set, which means that the

mean can perform better than the model. A scatter plot of the observed *versus* computed (consensus from models 1, 2, and 3) toxicity values of ILs is shown in Figure 8.2.

Table 8.3. The experimental and predicted ecotoxicity values for the true external set obtained from best model (with the lowest DModX value) and consensus approach.

Sl. No.	Ionic Liquids	Expt. pEC_{50}	Predicted pEC_{50}		
			Consensus approach [a]	Using the best model	Best model no.
1	2-HEAA	1.8100	2.4376	2.5593	1
2	2-HEAPr	1.8900	2.5651	2.7654	1
3	2-HEAiB	1.9700	2.4824	2.6435	1
4	2-HEAPe	2.0400	2.8688	2.3434	2
5	2-HTEAF	1.7400	2.3491	2.1686	1
6	2-HTEAA	2.6500	2.3561	2.2107	1
7	2-HTEAPr	2.7300	2.4836	2.4910	3
8	2-HTEAiB	2.8100	2.4010	2.3229	3

[a] Based on models 1, 2 and 3.

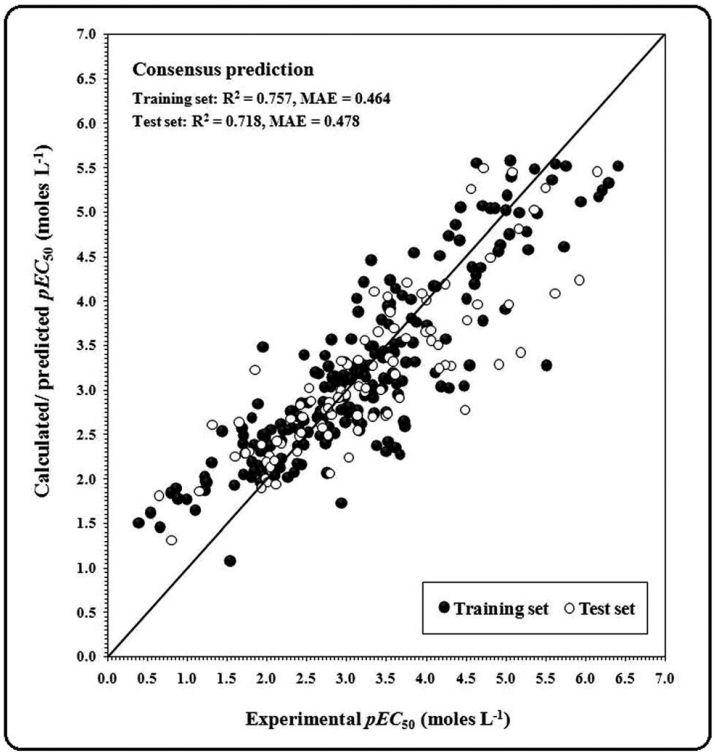

Figure 8.2. Scatter plot of the observed *versus* computed (consensus from models 1, 2, 3) toxicity values of ILs.

In a recent study, some of us[504] have shown that in any predictive modeling analysis, the observations lying close to the mean are more reliably predicted than those lying towards extremities, which may suffer from the trouble of over- or under-predictive attributes. Here, the average pEC_{50} for the training set compounds is 3.221 and the observed pEC_{50} values of the designed compounds lie towards the lower range. The experimental toxicity values of the designed compounds being low, the corresponding predicted values appear to be somewhat higher because of the relatively high value of the mean response (3.221) of the training set, on the basis of which the models have been developed. However, the predicted response values are reliable considering the wide response domain of the training set, which has been used for the development of models and this reliability is also evident from the fact that the MAE-based criteria are satisfactorily met.

Design, synthesis, and evaluation of new ionic liquids. Based on the derived chemical information from the predictive *in silico* modeling analysis, we have designed a series of twenty new "low toxic" or harmless ILs within the chemical domain of the developed models (models 1, 2 and 3) which is reported in Table 8.4. Table 8.4 also shows the predicted toxicity values of all the designed ILs obtained using DModX based best model predictions and consensus predictions.

Out of these twenty ILs, seven were synthesized and experimentally tested for their toxicity potential to *V. fischeri*. The toxicities for these seven new compounds are reported in Table 8.5. According to the obtained results (Table 8.5), it is possible to categorize these compounds as belonging to the Category "Acute III" according to the European Classification,[302] as (1) "practically harmless" ($[C_2C_1mor][C_1SO_4]$ and $[C_2C_1mor][For]$ with 100 $mg{\cdot}L^{-1} < EC_{50} < 1000\ mg{\cdot}L^{-1}$) and as (2) "harmless" ($[C_{2(OH)}C_1mor]I$, $[C_2C_1mor][OAc]$, $[C_2C_1mor]Br$, $[C_3C_1mor]Br$ and [Mor][OAc] with $EC_{50} > 1000\ mg{\cdot}L^{-1}$). Thus, all the seven designed and subsequently synthesized compounds portrayed an ecotoxicity potential categorizable as "harmless" or "practically harmless" as expected from the developed QSAR models. It is sometimes more relevant for a good model to appropriately categorize the test chemicals as toxic or non-toxic, and to maintain a correct rank order prediction, rather than to deliver quantitatively precise predictions.[505]

Table 8.4. Predicted ecotoxicity values of the designed ILs towards *V. fischeri* determined using the best model (model with the lowest DModX value) and the consensus approach.

Sl. No.	Designed ionic liquids		Predicted pEC_{50}		
	Cation	Anion	Consensus approach	Using best model	Best model no.
1	[Mor]	[OAc]	2.0733	1.7458	2
2	[C_2C_1mor]	[For]	1.3866	1.3544	2
3	[C_2C_1mor]	[OAc]	1.3935	1.3965	2
4	[C_2C_1mor]	[C_1SO_4]	1.0161	1.5527	2
5	[C_2C_1mor]	Br	1.3319	1.4591	2
6	[$C_{2(OH)}C_1$mor]	I	1.8729	1.8645	1
7	[C_3C_1mor]	Br	1.5160	1.6001	2
8	[C_2C_1mor]	[SCN]	1.4258	1.3936	2
9	[C_3C_1mor]	[For]	1.5706	1.4954	2
10	[C_3C_1mor]	[Pr]	1.7051	1.5796	2
11	[C_3C_1mor]	[C_1SO_4]	1.2001	1.6937	2
12	[$C_{1(OH)}C_1$im]	[OAc]	1.7109	1.7907	2
13	[$C_{1(OH)}C_1$im]	[*i*But]	1.7558	1.8749	2
14	[$C_{1(OH)}C_1$im]	[C_1SO_4]	1.3334	1.9469	2
15	[$N_{1,1,2OH}$]	[But]	2.6916	1.9335	2
16	[$C_{2(OH)}$py]	[For]	1.7451	1.6763	2
17	[$C_{2(OH)}$py]	[OAc]	1.7521	1.7183	2
18	[$C_{2(OH)}$py]	[Pr]	1.8796	1.7604	2
19	[$C_{2(OH)}$py]	[SCN]	1.7843	1.7155	2
20	[$C_{2(OH)}$py]	[C_1SO_4]	1.3746	1.8745	2

Table 8.5. Experimental ecotoxicity values of the selected synthesized ILs.

Sl. No.	Designed ionic liquids		Expt. EC_{50} ($mg \cdot L^{-1}$)	
	Cation	Anion	15 min	30 min
1	[Mor]	[OAc]	3221.950	2599.860
2	[C_2C_1mor]	[For]	231.180	236.410
3	[C_2C_1mor]	[OAc]	5322.990	4459.700
4	[C_2C_1mor]	[C_1SO_4]	659.300	653.130
5 [a]	[C_2C_1mor]	Br	-	-
6	[$C_{2(OH)}C_1$mor]	I	17502.090	16631.660
7	[C_3C_1mor]	Br	34633.570	23985.450

[a] The EC_{50} value was not measurable using a stock solution of 61760 $mg \cdot L^{-1}$, showing the very low toxicity of [C_2C_1mor]Br to the bacterium *V. fischeri*.

In our present study, the developed models could successfully predict the designed chemicals as “harmless” or “practically harmless”. Summing up, this work allowed the development of predictive models with good predictability performance considering the ILs’ chemical structure and their associated toxicity. In the near future this work will benefit the industrial dissemination of safer ILs.

CONCLUSION

ILs are neoteric solvents with wide industrial applicability. However, comprehensive assessment of their hazardous outcome is necessary to assure their safe use. Considering the ethical issues associated with biological experimentation on living beings, predictive *in silico* modelling provides a rational alternative strategy for prioritizing the chemicals. The present study involves *in silico* modelling of the largest toxicity dataset of ILs to *V. fischeri* currently available. Here, we have developed predictive PLS models using topological and quantum chemical descriptors. The chief aim of this study has been to develop multiple models capturing chemical information, enabling us to design and prepare new ILs with reduced toxicity profile. The whole study has been performed in consonance with the OECD guidelines in terms of dataset selection, model development, applicability domain determination, model validation, and mechanistic interpretation of the diagnosed chemical attributes.

It was very interesting to observe that the classical external validation metrics were unable to portray poor model performance in three cases. By using our newly developed MAE based judgment criteria, we have selected three suitable models, which have been explored further for true external validation as well as the design of new analogues. The synthesis and experimental determination of toxicity of the newly designed ILs were carried out following standard protocols. Note that this is the first attempt to perform both true external validation and experimental validation of QSPR models for toxicity of ILs to *V. fischeri*. The designed ILs were experimentally confirmed to be “harmless” or “practically harmless” as defined in the acute toxicity determination criteria by the

European Commission.[301] Hence, these newly designed and synthesized ILs can be considered as 'greener' analogues, beneficial for industrial use.

Final Remarks and Future Work

The outstanding properties of ILs and the possibility of tailoring their properties for a specific task by the adequate combination of their ions, makes these ionic compounds good candidates for a wide range of applications. Indeed, some authors have highlighted their industrial applications as an innovative approach to "Green Chemistry" and sustainability. Nevertheless, the fact that they have a negligible vapour pressure is not enough to assure that they can be considered as environmentally harmless, namely from the point of view of aquatic ecotoxicity. In this work, ILs from distinct families were prepared for specific applications, taking into consideration their ecotoxicity.

In Chapter 2, it was demonstrated the synthesis and characterization of new antioxidant cholinium-based ILs with outstanding solubility in water, a good thermal stability, and with comparable cytotoxicity and lower ecotoxicity profiles than the respective phenolic acids currently used in the therapeutic. Thus, these compounds have shown to be valuable candidates in the formulation of pharmaceutical/cosmetic products. In order to complement this work, the new antioxidant ILs could be incorporated into a moisturizer and investigated in terms of their permeation in human skin.

Aiming at developing enantioselective CIL-ABS for chiral resolution, two different groups of CILs were prepared and characterized in Chapter 3: CILs with chiral anion and chiral cation. In the first group, twelve CILs composed of tetrabutylammonium and cholinium cations and several anions naturally derived from different chiral amino acids and tartaric acid were synthesized and characterized. These compounds exhibited high thermal stability and low ecotoxicity, being in general considered as "practically harmless". Considering the CILs with chiral cation, three different groups were prepared, namely based on quinine, L-proline and L-valine. The remarkable chemical shift dispersion of the CF_3 signals of racemic Mosher's acid sodium salt induced by some of these CILs demonstrates their potential applications in chiral resolution. In this sence, future characterization of these CILs in terms of their physicochemical and toxicological properties is of extreme importance. Some preliminary tests were already carried out in order to develop an enantioselective CIL-ABS for separation of mandelic acid enantiomers. So far, diferent inorganic/organic salts were combined to CILs to form CIL-ABS, but the enantioselectivities obtained are still limited. Other optically active salts and

other chiral compounds such as amino acids and sugars could be tested in order to enhance the enantioselectivity of the CIL-ABS. Finally, the interaction mechanism of chiral separation behind the CIL-ABS should be better understood to achieve more efficient chiral discrimination.

The impact of the IL chemical structures and their concentration on the solubility of ibuprofen, naproxen and caffeine were evaluated in Chapter 4. The results obtained clearly evidence the exceptional capacity of the ILs to act as a powerful class of catanionic hydrotropes. Cholinium vanillate and cholinium gallate, two antioxidant cholinium-based ILs reported in Chapter 2, seem to be the most promising ILs for the ibuprofen and naproxen solubilisation. In order to better understand the main mechanism behind the enhanced solubilisation observed, this work should be complemented with dynamic light scattering and NMR measurements, as well as molecular dynamics simulations.

Twelve tensioactive ILs, based on imidazolium, ammonium and phosphonium cation and containing one, or more, long alkyl chains in the cation and/or anion, were synthetized and characterized in Chapter 5. Albeit the presence of at least a long alkyl chain in their structure leads to a high capacity to form microaggregates by their self-aggregation, this also makes them "toxic", or even "highly toxic", for *V. fischeri*. As an example of one possible application, it was demonstrated that the ILs studied can induce cell disruption of *E. coli* and, consequently, the intracellular GFP release. In order to complement this work, the aggregation behaviour of these tensionactive compounds should be studied in more detail, namely evaluating the liquid crystal phase progression of each tensionactive IL using a light-polarized optical microscopy.

In Chapter 6, a range of cholinium salt derivatives with magnetic properties was synthesized and their ecotoxicity was evaluated. The results obtained suggest that all compounds tested are moderately toxic, or even toxic, for *V. fischeri*. Furthermore, their toxicity is highly dependent on the structural modifications of the cation, namely the alkyl side chain length and the number of hydroxyethyl groups, as well as the atomic number of the metal anion. In order to improve the knowledge for the prospective design of environmentally safer MILs, it is important to expand the ecotoxicity evaluation to other aquatic organisms at different trophic levels.

A simple method to prepare a novel hydrophobic IL with a per-fluoro-*tert*-butoxide anion from hydrophilic ILs, and its characterization data, was reported in Chapter 7. This new hydrophobic IL was obtained in excellent yields and its new anion offers the potential to further tailor the physical properties and, most importantly, to create a new family of hydrophobic and water immiscible ILs. This simple synthetic route could be expanded to prepare new per-fluoro-*tert*-butoxide-based ILs with more biocompatible cations like quaternary ammonium and cholinium.

Finally, a predictive QSAR models for the ecotoxicity of ILs using the bacteria *V. fischeri* as an indicator response species were developed, in collaboration with another research group, and reported in Chapter 8. The synthesis and experimental determination of toxicity of the newly designed morpholinium-based ILs were carried. These compounds were experimentally confirmed to be “harmless” or “practically harmless”, and can be considered as ‘greener’ analogues, beneficial for industrial use.

List of Publications

1. K.A. Kurnia, T.E. Sintra, Y. Danten, M.I. Cabaço, M. Besnard, J.A.P. Coutinho, Simple method of preparation of novel hydrophobic ionic liquid with a per-fluoro-*tert*-butoxide anion, *New J. Chem.*, **2017**, 41, 47-50.

2. R.N. Das, T.E. Sintra, J.A.P. Coutinho, S.P.M. Ventura, K. Roy, P.L.A. Popelier, Development of predictive QSAR models for *Vibrio fischeri* toxicity of ionic liquids and their true external and experimental validation tests. *Toxicol. Res.*, **2016**, 5, 1388-1399.

3. S.P.M. Ventura, P. de Morais, J.A.S. Coelho, T.E. Sintra, J.A.P. Coutinho, C. Afonso, Evaluating the toxicity of biomass derived platform chemicals. *Green Chem.*, **2016**, 18, 4733-4742.

4. S.Y. Lee, F.A. Vicente, F.A. e Silva, T.E. Sintra, M. Taha, I. Khoiroh, J.A.P. Coutinho, P.L. Show, S.P.M. Ventura, Evaluating self-buffering ionic liquids for biotechnological applications. *ACS Sustain. Chem. Eng.*, **2016**, 3, 3420-3428.

5. T.E. Sintra, A. Luís, S.N. Rocha, A.I.M.C. Lobo Ferreira, F. Gonçalves, L.M.N.B.F. Santos, B.M. Neves, M.G. Freire, S.P.M. Ventura, J.A.P. Coutinho, Enhancing the antioxidant characteristics of phenolic acids by their conversion into cholinium salts. *ACS Sustain. Chem. Eng.*, **2015**, 3, 2558-2565.

6. K.A. Kurnia, T.E. Sintra, C.M.S.S. Neves, K. Shimizu, J.N. Canongia Lopes, F. Gonçalves, S.P.M. Ventura, M.G. Freire, L.M.N.B.F. Santos, J.A.P. Coutinho, The effect of the cation alkyl chain branching on mutual solubilities with water and toxicities. *Phys. Chem. Chem. Phys.*, **2014**, 16, 19952-19963.

7. T.E. Sintra, S.P.M. Ventura, J.A.P. Coutinho, Superactivity induced by micellar systems as the key for boosting the yield of enzymatic reactions. *J. Mol. Catal. B: Enzym.*, **2014**, 107, 140-151.

8. T.E. Sintra, R. Cruz, S.P.M. Ventura, J.A.P. Coutinho, Phase diagrams of ionic liquids-based aqueous biphasic systems as a platform for extraction processes. *J. Chem. Thermodyn.*, **2014**, 77, 206-213.

9. F.A. e Silva, T.E. Sintra, S.P.M. Ventura, J.A.P. Coutinho, Recovery of paracetamol from pharmaceutical wastes. *Sep. Purif. Technol.*, **2014**, 122, 315-322.

10. Khan, K.A. Kurnia, T.E. Sintra, J.A. Saraiva, S.P. Pinho, J.A.P. Coutinho, Assessing the activity coefficients of water in cholinium-based ionic liquids: experimental measurements and COSMO-RS modeling. *Fluid Phase Equilibr.*, **2014**, 361, 16-22.

11. S.P.M. Ventura, A.M.M. Gonçalves, T.E. Sintra, J.L. Pereira, F. Gonçalves, J.A.P. Coutinho, Designing ionic liquids: the chemical structure role in the toxicity. *Ecotoxicology*, **2013**, 22, 1-12.

12. S.P.M. Ventura, R.L.F. de Barros, T.E. Sintra, C.M.F. Soares, A.S. Lima, J.A.P. Coutinho, Simple screening method to identify toxic/non-toxic ionic liquids: agar diffusion test adaptation. *Ecotoxicol. Environ. Saf.*, **2012**, 83, 55-62.

References

(1) Plechkova, N. V; Seddon, K. R. *Chem. Soc. Rev.* **2008**, *37* (1), 123–150.
(2) Rogers, R. D. *Science* **2003**, *302* (5646), 792–793.
(3) Seddon, K. *Tce* **2002**, No. 730, 33–35.
(4) Rogers, R. D.; Seddon, K. R.; Industrial, A. C. S. D. of; Chemistry, E.; Meeting, A. C. S. *Ionic liquids: industrial applications for green chemistry*; American Chemical Society, 2002.
(5) Earle Martyn, J. In *Ionic Liquids*; American Chemical Society, 2002; Vol. 818, pp 90–105.
(6) Freire, M. G.; Carvalho, P. J.; Gardas, R. L.; Marrucho, I. M.; Santos, L. M. N. B. F.; Coutinho, J. A. P. *J. Phys. Chem. B* **2008**, *112* (6), 1604–1610.
(7) Freire, M. G.; Neves, C. M. S. S.; Carvalho, P. J.; Gardas, R. L.; Fernandes, A. M.; Marrucho, I. M.; Santos, L. M. N. B. F.; Coutinho, J. A. P. *J. Phys. Chem. B* **2007**, *111* (45), 13082–13089.
(8) Freire, M. G.; Neves, C. M. S. S.; Shimizu, K.; Bernardes, C. E. S.; Marrucho, I. M.; Coutinho, J. A. P.; Lopes, J. N. C.; Rebelo, L. P. N. *J. Phys. Chem. B* **2010**, *114* (48), 15925–15934.
(9) Freire, M. G.; Neves, C. M. S. S.; Ventura, S. P. M.; Pratas, M. J.; Marrucho, I. M.; Oliveira, J.; Coutinho, J. A. P.; Fernandes, A. M. *Fluid Phase Equilib.* **2010**, *294* (1–2), 234–240.
(10) EC 2007. http://ec.europa.eu/environment/chemicals/reach.
(11) Jain, N.; Kumar, A.; Chauhan, S.; Chauhan, S. M. S. *Tetrahedron* **2005**, *61* (5), 1015–1060.
(12) Sheldon, R. *Chem. Commun.* **2001**, No. 23, 2399–2407.
(13) Zhao, H.; Xia, S.; Ma, P. *J. Chem. Technol. Biotechnol.* **2005**, *80* (10), 1089–1096.
(14) Wong, H.; Han, S.; Livingston, A. G. *Chem. Eng. Sci.* **2006**, *61* (4), 1338–1341.
(15) Welton, T.; Endres, F.; Abedin, S. Z. El; Antonietti, M.; Smarsly, B.; Zhou, Y. In *Ionic Liquids in Synthesis*; Wiley-VCH Verlag GmbH & Co. KGaA, 2008; pp 569–617.
(16) Sheldon, R. A. *Chem. - A Eur. J.* **2016**, *22* (37), 12984–12999.
(17) Potdar, M.; Kelso, G.; Schwarz, L.; Zhang, C.; Hearn, M. *Molecules* **2015**, *20* (9), 16788–16816.
(18) Haddleton, D. M.; Welton, T.; Carmichael, A. J. In *Ionic Liquids in Synthesis*; Wiley-VCH Verlag GmbH & Co. KGaA, 2008; pp 619–640.
(19) Holbrey, J. D.; Rogers, R. D.; Mantz, R. A.; Trulove, P. C.; Cocalia, V. A.; Visser, A. E.; Anderson, J. L.; Anthony, J. L.; Brennecke, J. F.; Maginn, E. J.; Welton, T.; Mantz, R. A. In *Ionic Liquids in Synthesis*; Wiley-VCH Verlag GmbH & Co. KGaA, 2008; pp 57–174.
(20) Joglekar, H. G.; Rahman, I.; Kulkarni, B. D. *Chem. Eng. Technol.* **2007**, *30* (7), 819–828.
(21) Zhao, H. *Chem. Eng. Commun.* **2006**, *193* (12), 1660–1677.
(22) Vijayaraghavan, R.; Izgorodin, A.; Ganesh, V.; Surianarayanan, M.; MacFarlane, D. R. *Angew. Chemie Int. Ed.* **2010**, *49* (9), 1631–1633.
(23) Fujita, K.; Forsyth, M.; MacFarlane, D. R.; Reid, R. W.; Elliott, G. D. *Biotechnol. Bioeng.* **2006**, *94* (6), 1209–1213.
(24) Freire, M. G.; Cláudio, A. F. M.; Araújo, J. M. M.; Coutinho, J. A. P.; Marrucho, I. M.; Lopes, J. N. C.; Rebelo, L. P. N. *Chem. Soc. Rev.* **2012**, *41* (14), 4966–4995.

(25) Mondal, D.; Sharma, M.; Quental, M. V.; Tavares, A. P. M.; Prasad, K.; Freire, M. G. *Green Chem.* **2016**, *18* (22), 6071–6081.
(26) Moniruzzaman, M.; Tahara, Y.; Tamura, M.; Kamiya, N.; Goto, M. *Chem. Commun.* **2010**, *46* (9), 1452–1454.
(27) Adawiyah, N.; Moniruzzaman, M.; Hawatulaila, S.; Goto, M. *Med. Chem. Commun.* **2016**, *7* (10), 1881–1897.
(28) Moniruzzaman, M.; Kamiya, N.; Goto, M. *J. Colloid Interface Sci.* **2010**, *352* (1), 136–142.
(29) Hough, W. L.; Smiglak, M.; Rodriguez, H.; Swatloski, R. P.; Spear, S. K.; Daly, D. T.; Pernak, J.; Grisel, J. E.; Carliss, R. D.; Soutullo, M. D.; Davis, J. J. H.; Rogers, R. D. *New J. Chem.* **2007**, *31* (8), 1429–1436.
(30) Wu, D.; Zhou, Y.; Cai, P.; Shen, S.; Pan, Y. *J. Chromatogr. A* **2015**, *1395*, 65–72.
(31) Seddon Kenneth, R.; Stark, A.; Torres, M.-J. In *Clean Solvents*; American Chemical Society, 2002; Vol. 819, pp 34–49.
(32) Walden, P. *Bull. l'Académie Impériale des Sci. St.-pétersbg.* **1914**, *8*, 405–422.
(33) Graenacher, C. Pat. US 1,943,176, 1931.
(34) Hurley, F. H. Pat. US 4,446,331, 1948.
(35) Wier Jr, T. P.; Hurley, F. H. Pat. US 4,446,349, 1948.
(36) Lee, C. K.; Huang, H. W.; Lin, I. J. B. *Chem. Commun.* **2000**, No. 19, 1911–1912.
(37) Smiglak, M.; Hines, C. C.; Reichert, W. M.; Vincek, A. S.; Katritzky, A. R.; Thrasher, J. S.; Sun, L.; McCrary, P. D.; Beasley, P. A.; Kelley, S. P.; Rogers, R. D. *New J. Chem.* **2012**, *36* (3), 702–722.
(38) Gordon, C. M.; Holbrey, J. D.; Kennedy, A. R.; Seddon, K. R. *J. Mater. Chem.* **1998**, *8* (12), 2627–2636.
(39) Verdia, P.; Gonzalez, E. J.; Rodriguez-Cabo, B.; Tojo, E. *Green Chem.* **2011**, *13* (10), 2768–2776.
(40) Visser, A. E.; Holbrey, J. D.; Rogers, R. D. *Chem. Commun.* **2001**, No. 23, 2484–2485.
(41) MacFarlane, D. R.; Meakin, P.; Sun, J.; Amini, N.; Forsyth, M. *J. Phys. Chem. B* **1999**, *103* (20), 4164–4170.
(42) Sun, J.; Forsyth, M.; MacFarlane, D. R. *J. Phys. Chem. B* **1998**, *102* (44), 8858–8864.
(43) Bonhôte, P.; Dias, A.-P.; Papageorgiou, N.; Kalyanasundaram, K.; Grätzel, M. *Inorg. Chem.* **1996**, *35* (5), 1168–1178.
(44) Karodia, N.; Guise, S.; Newlands, C.; Andersen, J.-A. *Chem. Commun.* **1998**, No. 21, 2341–2342.
(45) Holbrey, J. D.; Reichert, W. M.; Swatloski, R. P.; Broker, G. A.; Pitner, W. R.; Seddon, K. R.; Rogers, R. D. *Green Chem.* **2002**, *4* (5), 407–413.
(46) Gordon, C. M.; Muldoon, M. J.; Wagner, M.; Hilgers, C.; Davis, J. H.; Wasserscheid, P. In *Ionic Liquids in Synthesis*; Wiley-VCH Verlag GmbH & Co. KGaA, 2008; pp 7–55.
(47) Waterkamp, D. A.; Heiland, M.; Schluter, M.; Sauvageau, J. C.; Beyersdorff, T.; Thoming, J. *Green Chem.* **2007**, *9* (10), 1084–1090.
(48) Burrell, A. K.; Sesto, R. E. Del; Baker, S. N.; McCleskey, T. M.; Baker, G. A. *Green Chem.* **2007**, *9* (5), 449–454.
(49) Varma, R. S.; Namboodiri, V. V. *Chem. Commun.* **2001**, No. 7, 643–644.
(50) Lévêque, J.-M.; Estager, J.; Draye, M.; Cravotto, G.; Boffa, L.; Bonrath, W. *Monatshefte für Chemie - Chem. Mon.* **2007**, *138* (11), 1103–1113.

(51) Namboodiri, V. V.; Varma, R. S. *Org. Lett.* **2002**, *4* (18), 3161–3163.
(52) Payagala, T.; Armstrong, D. W. *Chirality* **2012**, *24* (1), 17–53.
(53) Miao, J.; Wan, H.; Guan, G. *Catal. Commun.* **2011**, *12* (5), 353–356.
(54) Li, L.; Yu, S.-T.; Xie, C.-X.; Liu, F.-S.; Li, H.-J. *J. Chem. Technol. Biotechnol.* **2009**, *84* (11), 1649–1652.
(55) Hurley, F. H.; WIer, T. P. *J. Electrochem. Soc.* **1951**, *98* (5), 207–212.
(56) Jiang, T.; Chollier Brym, M. J.; Dubé, G.; Lasia, A.; Brisard, G. M. *Surf. Coatings Technol.* **2006**, *201* (1), 1–9.
(57) Lai, P. K.; Skyllas-Kazacos, M. *J. Electroanal. Chem. Interfacial Electrochem.* **1988**, *248* (2), 431–440.
(58) Gilbert, B.; Chauvin, Y.; Olivier, H.; Di Marco-Van Tiggelen, F. *J. Chem. Soc. Dalt. Trans.* **1995**, No. 23, 3867–3871.
(59) Williams, S. D.; Schoebrechts, J. P.; Selkirk, J. C.; Mamantov, G. *J. Am. Chem. Soc.* **1987**, *109* (7), 2218–2219.
(60) Parshall, G. W. *J. Am. Chem. Soc.* **1972**, *94* (25), 8716–8719.
(61) Sitze, M. S.; Schreiter, E. R.; Patterson, E. V; Freeman, R. G. *Inorg. Chem.* **2001**, *40* (10), 2298–2304.
(62) Wilkes, J. S.; Zaworotko, M. J. *J. Chem. Soc. Chem. Commun.* **1992**, No. 13, 965–967.
(63) Cammarata, L.; Kazarian, S. G.; Salter, P. A.; Welton, T. *Phys. Chem. Chem. Phys.* **2001**, *3* (23), 5192–5200.
(64) D. Holbrey, J.; R. Seddon, K. *J. Chem. Soc. Dalt. Trans.* **1999**, No. 13, 2133–2140.
(65) Fuller, J.; Carlin, R. T.; De Long, H. C.; Haworth, D. *J. Chem. Soc. Chem. Commun.* **1994**, No. 3, 299–300.
(66) Lévêque, J.-M.; Luche, J.-L.; Petrier, C.; Roux, R.; Bonrath, W. *Green Chem.* **2002**, *4* (4), 357–360.
(67) Keil, P.; Schwiertz, M.; König, A. *Chem. Eng. Technol.* **2014**, *37* (6), 919–926.
(68) Lancaster, N. L.; Welton, T.; Young, G. B. *J. Chem. Soc. Perkin Trans. 2* **2001**, No. 12, 2267–2270.
(69) Pernak, J.; Syguda, A.; Mirska, I.; Pernak, A.; Nawrot, J.; Prądzyńska, A.; Griffin, S. T.; Rogers, R. D. *Chem. – A Eur. J.* **2007**, *13* (24), 6817–6827.
(70) Costa, A. J. L.; Soromenho, M. R. C.; Shimizu, K.; Marrucho, I. M.; Esperança, J. M. S. S.; Lopes, J. N. C.; Rebelo, L. P. N. *ChemPhysChem* **2012**, *13* (7), 1902–1909.
(71) Couling, D. J.; Bernot, R. J.; Docherty, K. M.; Dixon, J. K.; Maginn, E. J. *Green Chem.* **2006**, *8* (1), 82–90.
(72) Fuller, J.; Carlin, R. T. *Proc. Electrochem. Soc.* **1999**, *98*, 227.
(73) Seddon, K. R.; Stark, A.; Torres, M. J. *Pure Appl. Chem.* **2000**, *72*, 2275–2287.
(74) MacFarlane, D. R.; Golding, J.; Forsyth, S.; Forsyth, M.; Deacon, G. B. *Chem. Commun.* **2001**, No. 16, 1430–1431.
(75) Larsen, A. S.; Holbrey, J. D.; Tham, F. S.; Reed, C. A. *J. Am. Chem. Soc.* **2000**, *122* (30), 7264–7272.
(76) Nockemann, P.; Thijs, B.; Driesen, K.; Janssen, C. R.; Van Hecke, K.; Van Meervelt, L.; Kossmann, S.; Kirchner, B.; Binnemans, K. *J. Phys. Chem. B* **2007**, *111* (19), 5254–5263.
(77) Carter, E. B.; Culver, S. L.; Fox, P. A.; Goode, R. D.; Ntai, I.; Tickell, M. D.; Traylor, R.

K.; Hoffman, N. W.; Davis, J. J. H. *Chem. Commun.* **2004**, No. 6, 630–631.
(78) Hasan, M.; Kozhevnikov, I. V; Siddiqui, M. R. H.; Steiner, A.; Winterton, N. *Inorg. Chem.* **1999**, *38* (25), 5637–5641.
(79) Clare, B.; Sirwardana, A.; MacFarlane, D. In *Ionic Liquids*; Kirchner, B., Ed.; Springer Berlin Heidelberg, 2010; Vol. 290, pp 1–40.
(80) Lall, S. I.; Mancheno, D.; Castro, S.; Behaj, V.; Cohen, J. I.; Engel, R. *Chem. Commun.* **2000**, No. 24, 2413–2414.
(81) Wasserscheid, P.; Keim, W. *Angew. Chemie Int. Ed.* **2000**, *39* (21), 3772–3789.
(82) Mizuta, K.; Kasahara, T.; Arimoto, Y.; Hashimoto, H.; Takei, K.; Katsuyama, H. PCT/JP2006/322693 2007.
(83) Himmler, S.; König, A.; Wasserscheid, P. *Green Chem.* **2007**, *9* (9), 935–942.
(84) Kuhn, N.; Steimann, M.; Weyers, G. *Zeitschrift Fur Naturforsch. Sect B J. Chem. Sci.* **1999**, *54*, 427–433.
(85) Gao, J.; Liu, J.; Li, B.; Liu, W.; Xie, Y.; Xin, Y.; Yin, Y.; Jie, X.; Gu, J.; Zou, Z. *New J. Chem.* **2011**, *35* (8), 1661–1666.
(86) Ohno, H.; Fukumoto, K. *Acc. Chem. Res.* **2007**, *40* (11), 1122–1129.
(87) Zeisel, S. H.; Da Costa, K.-A. *Nutr. Rev.* **2009**, *67* (11), 615–623.
(88) Hu, S.; Jiang, T.; Zhang, Z.; Zhu, A.; Han, B.; Song, J.; Xie, Y.; Li, W. *Tetrahedron Lett.* **2007**, *48* (32), 5613–5617.
(89) García-Suárez, E. J.; Menéndez-Vázquez, C.; García, A. B. *J. Mol. Liq.* **2012**, *169* (0), 37–42.
(90) Moriel, P.; García-Suárez, E. J.; Martínez, M.; García, A. B.; Montes-Morán, M. A.; Calvino-Casilda, V.; Bañares, M. A. *Tetrahedron Lett.* **2010**, *51* (37), 4877–4881.
(91) Gouveia, W.; Jorge, T. F.; Martins, S.; Meireles, M.; Carolino, M.; Cruz, C.; Almeida, T. V; Araújo, M. E. M. *Chemosphere* **2014**, *104* (0), 51–56.
(92) Fukaya, Y.; Iizuka, Y.; Sekikawa, K.; Ohno, H. *Green Chem.* **2007**, *9* (11), 1155–1157.
(93) Muhammad, N.; Hossain, M. I.; Man, Z.; El-Harbawi, M.; Bustam, M. A.; Noaman, Y. A.; Mohamed Alitheen, N. B.; Ng, M. K.; Hefter, G.; Yin, C.-Y. *J. Chem. Eng. Data* **2012**, *57* (8), 2191–2196.
(94) Vijayaraghavan, R.; Thompson, B. C.; MacFarlane, D. R.; Kumar, R.; Surianarayanan, M.; Aishwarya, S.; Sehgal, P. K. *Chem. Commun.* **2010**, *46* (2), 294–296.
(95) Sekar, S.; Surianarayanan, M.; Ranganathan, V.; MacFarlane, D. R.; Mandal, A. B. *Environ. Sci. Technol.* **2012**, *46* (9), 4902–4908.
(96) Winther-Jensen, O.; Vijayaraghavan, R.; Sun, J.; Winther-Jensen, B.; MacFarlane, D. R. *Chem. Commun.* **2009**, No. 21, 3041–3043.
(97) Ninomiya, K.; Yamauchi, T.; Kobayashi, M.; Ogino, C.; Shimizu, N.; Takahashi, K. *Biochem. Eng. J.* **2013**, *71* (0), 25–29.
(98) Yu, Y.; Lu, X.; Zhou, Q.; Dong, K.; Yao, H.; Zhang, S. *Chem. – A Eur. J.* **2008**, *14* (35), 11174–11182.
(99) Demberelnyamba, D.; Ariunaa, M.; Shim, Y. *Int. J. Mol. Sci.* **2008**, *9* (5), 864–871.
(100) Taha, M.; e Silva, F. A.; Quental, M. V.; Ventura, S. P. M.; Freire, M. G.; Coutinho, J. A. P. *Green Chem.* **2014**, *16* (6), 3149–3159.
(101) Lee, S. Y.; Vicente, F. A.; e Silva, F. A.; Sintra, T. E.; Taha, M.; Khoiroh, I.; Coutinho, J. A. P.; Show, P. L.; Ventura, S. P. M. *ACS Sustain. Chem. Eng.* **2015**, *3* (12), 3420–3428.

(102) Taha, M.; Almeida, M. R.; Silva, F. A. e; Domingues, P.; Ventura, S. P. M.; Coutinho, J. A. P.; Freire, M. G. *Chem. – A Eur. J.* **2015**, *21* (12), 4781–4788.
(103) Zgonnik, V.; Zedde, C.; Genisson, Y.; Mazieres, M.-R.; Plaquevent, J.-C. *Chem. Commun.* **2012**, *48* (26), 3185–3187.
(104) Himmler, S.; Hormann, S.; van Hal, R.; Schulz, P. S.; Wasserscheid, P. *Green Chem.* **2006**, *8* (10), 887–894.
(105) Blesic, M.; Swadzba-Kwasny, M.; Belhocine, T.; Gunaratne, H. Q. N.; Lopes, J. N. C.; Gomes, M. F. C.; Padua, A. A. H.; Seddon, K. R.; Rebelo, L. P. N. *Phys. Chem. Chem. Phys.* **2009**, *11* (39), 8939–8948.
(106) Mahrova, M.; Vilas, M.; Domínguez, Á.; Gómez, E.; Calvar, N.; Tojo, E. *J. Chem. Eng. Data* **2012**, *57* (2), 241–248.
(107) Aparicio, S.; Atilhan, M.; Karadas, F. *Ind. Eng. Chem. Res.* **2010**, *49* (20), 9580–9595.
(108) Dean, P. M.; Pringle, J. M.; MacFarlane, D. R. *Phys. Chem. Chem. Phys.* **2010**, *12* (32), 9144–9153.
(109) Huddleston, J. G.; Visser, A. E.; Reichert, W. M.; Willauer, H. D.; Broker, G. A.; Rogers, R. D. *Green Chem.* **2001**, *3* (4), 156–164.
(110) López-Martin, I.; Burello, E.; Davey, P. N.; Seddon, K. R.; Rothenberg, G. *ChemPhysChem* **2007**, *8* (5), 690–695.
(111) Rodrigues, A. S. M. C.; Santos, L. M. N. B. F. *ChemPhysChem* **2016**, *17* (10), 1512–1517.
(112) Forsyth, S. A.; Batten, S. R.; Dai, Q.; MacFarlane, D. R. *Aust. J. Chem.* **2004**, *57* (2), 121–124.
(113) Rodrigues, A. S. M. C.; Almeida, H. F. D.; Freire, M. G.; Lopes-da-Silva, J. A.; Coutinho, J. A. P.; Santos, L. M. N. B. F. *Fluid Phase Equilib.* **2016**, *423*, 190–202.
(114) Berg, R. W.; Riisager, A.; Van Buu, O. N.; Fehrmann, R.; Harris, P.; Tomaszowska, A. A.; Seddon, K. R. *J. Phys. Chem. B* **2009**, *113* (26), 8878–8886.
(115) Holbrey, J. D.; Reichert, W. M.; Rogers, R. D. *Dalt. Trans.* **2004**, No. 15, 2267–2271.
(116) Henderson, W. A.; Jr, V. G. Y.; Pearson, W.; Passerini, S.; Long, H. C. De; Trulove, P. C. *J. Phys. Condens. Matter* **2006**, *18*, 10377–10390.
(117) Holbrey, J. D.; Reichert, W. M.; Nieuwenhuyzen, M.; Johnson, S.; Seddon, K. R.; Rogers, R. D. *Chem. Commun.* **2003**, No. 14, 1636–1637.
(118) Ohno, H. *Bull. Chem. Soc. Jpn.* **2006**, *79*, 1665–1680.
(119) J. Golding, J.; R. MacFarlane, D.; Spiccia, L.; Forsyth, M.; W. Skelton, B.; H. White, A. *Chem. Commun.* **1998**, No. 15, 1593–1594.
(120) Carvalho, P. J.; Ventura, S. P. M.; Batista, M. L. S.; Schröder, B.; Gonçalves, F.; Esperança, J.; Mutelet, F.; Coutinho, J. A. P. *J. Chem. Phys.* **2014**, *140* (6), 064505.
(121) Valkenburg, M. E. V.; Vaughn, R. L.; Williams, M.; Wilkes, J. S. *Thermochim. Acta* **2005**, *425* (1), 181–188.
(122) Awad, W. H.; Gilman, J. W.; Nyden, M.; Harris, R. H.; Sutto, T. E.; Callahan, J.; Trulove, P. C.; DeLong, H. C.; Fox, D. M. *Thermochim. Acta* **2004**, *409* (1), 3–11.
(123) Chan, B.; Chang, N.; Grimmett, M.; Chan, B.; Chang, N.; Grimmett, M. *Aust. J. Chem.* **1977**, *30* (9), 2005–2013.
(124) Zhang, S.; Sun, N.; He, X.; Lu, X.; Zhang, X. *J. Phys. Chem. Ref. Data* **2006**, *35* (4), 1475–1517.
(125) Pensado, A. S.; Comuñas, M. J. P.; Fernández, J. *Tribol. Lett.* **2008**, *31* (2), 107–118.

(126) Maton, C.; De Vos, N.; Stevens, C. V. *Chem. Soc. Rev.* **2013**, *42* (13), 5963–5977.
(127) Ngo, H. L.; LeCompte, K.; Hargens, L.; McEwen, A. B. *Thermochim. Acta* **2000**, *357*, 97–102.
(128) MacFarlane, D. R.; Forsyth, S. A.; Golding, J.; Deacon, G. B. *Green Chem.* **2002**, *4* (5), 444–448.
(129) Crosthwaite, J. M.; Muldoon, M. J.; Dixon, J. K.; Anderson, J. L.; Brennecke, J. F. *J. Chem. Thermodyn.* **2005**, *37* (6), 559–568.
(130) Tokuda, H.; Ishii, K.; Susan Md., A. B. H.; Tsuzuki, S.; Hayamizu, K.; Watanabe, M. *J. Phys. Chem. B* **2006**, *110* (6), 2833–2839.
(131) Kosmulski, M.; Gustafsson, J.; Rosenholm, J. B. *Thermochim. Acta* **2004**, *412* (1), 47–53.
(132) Prasad, M. R. R.; Krishnamurthy, V. N. *Thermochim. Acta* **1991**, *185* (1), 1–10.
(133) Tokuda, H.; Hayamizu, K.; Ishii, K.; Susan Md., A. B. H.; Watanabe, M. *J. Phys. Chem. B* **2005**, *109* (13), 6103–6110.
(134) Gardas, R. L.; Coutinho, J. A. P. *Fluid Phase Equilib.* **2008**, *266* (1–2), 195–201.
(135) Diogo, J. C. F.; Caetano, F. J. P.; Fareleira, J. M. N. A.; Wakeham, W. A.; Afonso, C. A. M.; Marques, C. S. *J. Chem. Eng. Data* **2012**, *57* (4), 1015–1025.
(136) Jacquemin, J.; Husson, P.; Padua, A. A. H.; Majer, V. *Green Chem.* **2006**, *8* (2), 172–180.
(137) Tariq, M.; Carvalho, P. J.; Coutinho, J. A. P.; Marrucho, I. M.; Lopes, J. N. C.; Rebelo, L. P. N. *Fluid Phase Equilib.* **2011**, *301* (1), 22–32.
(138) Rilo, E.; Varela, L. M.; Cabeza, O. *J. Chem. Eng. Data* **2012**, *57* (8), 2136–2142.
(139) Gardas, R. L.; Costa, H. F.; Freire, M. G.; Carvalho, P. J.; Marrucho, I. M.; Fonseca, I. M. A.; Ferreira, A. G. M.; Coutinho, J. A. P. *J. Chem. Eng. Data* **2008**, *53* (3), 805–811.
(140) Baker, S. N.; Baker, G. A.; Kane, M. A.; Bright, F. V. *J. Phys. Chem. B* **2001**, *105* (39), 9663–9668.
(141) Cabeza, O. In *Ionic Liquids in Separation Technology*; 2014; pp 1–93.
(142) Izgorodina, E. I. *Phys. Chem. Chem. Phys.* **2011**, *13* (10), 4189–4207.
(143) Greaves, T. L.; Drummond, C. J. *Chem. Rev.* **2007**, *108* (1), 206–237.
(144) Yu, G.; Zhao, D.; Wen, L.; Yang, S.; Chen, X. *AIChE J.* **2012**, *58* (9), 2885–2899.
(145) Sánchez, L. G.; Espel, J. R.; Onink, F.; Meindersma, G. W.; Haan, A. B. de. *J. Chem. Eng. Data* **2009**, *54* (10), 2803–2812.
(146) Yoshida, Y.; Baba, O.; Saito, G. *J. Phys. Chem. B* **2007**, *111* (18), 4742–4749.
(147) Rocha, M. A. A.; Neves, C. M. S. S.; Freire, M. G.; Russina, O.; Triolo, A.; Coutinho, J. A. P.; Santos, L. M. N. B. F. *J. Phys. Chem. B* **2013**, *117* (37), 10889–10897.
(148) Gaciño, F. M.; Paredes, X.; Comuñas, M. J. P.; Fernández, J. *J. Chem. Thermodyn.* **2013**, *62*, 162–169.
(149) Zheng, W.; Mohammed, A.; Hines, L. G.; Xiao, D.; Martinez, O. J.; Bartsch, R. A.; Simon, S. L.; Russina, O.; Triolo, A.; Quitevis, E. L. *J. Phys. Chem. B* **2011**, *115* (20), 6572–6584.
(150) Seki, S.; Kobayashi, T.; Kobayashi, Y.; Takei, K.; Miyashiro, H.; Hayamizu, K.; Tsuzuki, S.; Mitsugi, T.; Umebayashi, Y. *J. Mol. Liq.* **2010**, *152* (1), 9–13.
(151) Chiappe, C.; Sanzone, A.; Mendola, D.; Castiglione, F.; Famulari, A.; Raos, G.; Mele, A. *J. Phys. Chem. B* **2013**, *117* (2), 668–676.

(152) Regueira, T.; Lugo, L.; Fernández, J. *J. Chem. Thermodyn.* **2013**, *58*, 440–448.
(153) Pernak, J.; Czepukowicz, A.; Poźniak, R. *Ind. Eng. Chem. Res.* **2001**, *40* (11), 2379–2383.
(154) Zhang, S.; Sun, N.; He, X.; Lu, X.; Zhang, X. *J. Phys. Chem. Ref. Data* **2006**, *35* (4), 1475–1517.
(155) Andresova, A.; Storch, J.; Traïkia, M.; Wagner, Z.; Bendova, M.; Husson, P. *Fluid Phase Equilib.* **2014**, *371*, 41–49.
(156) Regueira, T.; Lugo, L.; Fernández, J. *J. Chem. Thermodyn.* **2012**, *48*, 213–220.
(157) Gaciño, F. M.; Regueira, T.; Lugo, L.; Comuñas, M. J. P.; Fernández, J. *J. Chem. Eng. Data* **2011**, *56* (12), 4984–4999.
(158) Zhao, H. *Phys. Chem. Liq.* **2003**, *41* (6), 545–557.
(159) Rebelo, L. P. N.; Canongia Lopes, J. N.; Esperança, J. M. S. S.; Filipe, E. *J. Phys. Chem. B* **2005**, *109* (13), 6040–6043.
(160) Paulechka, Y. U.; Zaitsau, D. H.; Kabo, G. J.; Strechan, A. A. *Thermochim. Acta* **2005**, *439* (1–2), 158–160.
(161) Earle, M. J.; Esperança, J. M. S. S.; Gilea, M. A.; Lopes, J. N. C.; Rebelo, L. P. N.; Magee, J. W.; Seddon, K. R.; Widegren, J. A. *Nature* **2006**, *439*, 831–834.
(162) Esperança, J. M. S. S.; Canongia Lopes, J. N.; Tariq, M.; Santos, L. M. N. B. F.; Magee, J. W.; Rebelo, L. P. N. *J. Chem. Eng. Data* **2009**, *55* (1), 3–12.
(163) MacFarlane, D. R.; Pringle, J. M.; Johansson, K. M.; Forsyth, S. A.; Forsyth, M. *Chem. Commun.* **2006**, No. 18, 1905–1917.
(164) Rocha, M. A. A.; Lima, C. F. R. A. C.; Gomes, L. R.; Schröder, B.; Coutinho, J. A. P.; Marrucho, I. M.; Esperança, J. M. S. S.; Rebelo, L. P. N.; Shimizu, K.; Lopes, J. N. C.; Santos, L. M. N. B. F. *J. Phys. Chem. B* **2011**, *115* (37), 10919–10926.
(165) Rocha, M. A. A.; Bastos, M.; Coutinho, J. A. P.; Santos, L. M. N. B. F. *J. Chem. Thermodyn.* **2012**, *53*, 140–143.
(166) Rocha, M. A. A.; Coutinho, J. A. P.; Santos, L. M. N. B. F. *J. Phys. Chem. B* **2012**, *116* (35), 10922–10927.
(167) Tariq, M.; Freire, M. G.; Saramago, B.; Coutinho, J. A. P.; Lopes, J. N. C.; Rebelo, L. P. N. *Chem. Soc. Rev.* **2012**, *41* (2), 829–868.
(168) Fernandes, A. M.; Rocha, M. A. A.; Freire, M. G.; Marrucho, I. M.; Coutinho, J. A. P.; Santos, L. M. N. B. F. *J. Phys. Chem. B* **2011**, *115* (14), 4033–4041.
(169) Carvalho, P. J.; Freire, M. G.; Marrucho, I. M.; Queimada, A. J.; Coutinho, J. A. P. *J. Chem. Eng. Data* **2008**, *53* (6), 1346–1350.
(170) Freire, M. G.; Carvalho, P. J.; Fernandes, A. M.; Marrucho, I. M.; Queimada, A. J.; Coutinho, J. A. P. *J. Colloid Interface Sci.* **2007**, *314* (2), 621–630.
(171) Fang, D.-W.; Guan, W.; Tong, J.; Wang, Z.-W.; Yang, J.-Z. *J. Phys. Chem. B* **2008**, *112* (25), 7499–7505.
(172) Ghatee, M. H.; Zolghadr, A. R. *Fluid Phase Equilib.* **2008**, *263* (2), 168–175.
(173) Torrecilla, J. S.; Palomar, J.; García, J.; Rodríguez, F. *J. Chem. Eng. Data* **2009**, *54* (4), 1297–1301.
(174) Santos, C. S.; Baldelli, S. *J. Phys. Chem. B* **2009**, *113* (4), 923–933.
(175) Kolbeck, C.; Lehmann, J.; Lovelock, K. R. J.; Cremer, T.; Paape, N.; Wasserscheid, P.; Fröba, A. P.; Maier, F.; Steinrück, H.-P. *J. Phys. Chem. B* **2010**, *114* (51), 17025–17036.

(176) Sedev, R. *Curr. Opin. Colloid Interface Sci.* **2011**, *16* (4), 310–316.
(177) Martino, W.; de la Mora, J. F.; Yoshida, Y.; Saito, G.; Wilkes, J. *Green Chem.* **2006**, *8* (4), 390–397.
(178) Galiński, M.; Lewandowski, A.; Stępniak, I. *Electrochim. Acta* **2006**, *51* (26), 5567–5580.
(179) Pinkert, A.; Ang, K. L.; Marsh, K. N.; Pang, S. *Phys. Chem. Chem. Phys.* **2011**, *13* (11), 5136–5143.
(180) Liu, H.; Liu, Y.; Li, J. *Phys. Chem. Chem. Phys.* **2010**, *12* (8), 1685–1697.
(181) Makino, T.; Kanakubo, M.; Umecky, T.; Suzuki, A.; Nishida, T.; Takano, J. *J. Chem. Eng. Data* **2012**, *57* (3), 751–755.
(182) Vila, J.; Varela, L. M.; Cabeza, O. *Electrochim. Acta* **2007**, *52* (26), 7413–7417.
(183) Ignat'ev, N. V.; Welz-Biermann, U.; Kucheryna, A.; Bissky, G.; Willner, H. *J. Fluor. Chem.* **2005**, *126* (8), 1150–1159.
(184) Leys, J.; Rajesh, R. N.; Menon, P. C.; Glorieux, C.; Longuemart, S.; Nockemann, P.; Pellens, M.; Binnemans, K. *J. Chem. Phys.* **2010**, *133* (3), 034503.
(185) Zhao, D.; Liao, Y.; Zhang, Z. *CLEAN – Soil, Air, Water* **2007**, *35* (1), 42–48.
(186) Martins, M. A. R.; Neves, C. M. S. S.; Kurnia, K. A.; Luís, A.; Santos, L. M. N. B. F.; Freire, M. G.; Pinho, S. P.; Coutinho, J. A. P. *Fluid Phase Equilib.* **2014**, *375*, 161–167.
(187) Neves, C. M. S. S.; Rodrigues, A. R.; Kurnia, K. A.; Esperança, J. M. S. S.; Freire, M. G.; Coutinho, J. A. P. *Fluid Phase Equilib.* **2013**, *358*, 50–55.
(188) Kurnia, K. A.; Quental, M. V.; Santos, L. M. N. B. F.; Freire, M. G.; Coutinho, J. A. P. *Phys. Chem. Chem. Phys.* **2015**, *17* (6), 4569–4577.
(189) Freire, M. G.; Santos, L. M. N. B. F.; Fernandes, A. M.; Coutinho, J. A. P.; Marrucho, I. M. *Fluid Phase Equilib.* **2007**, *261* (1–2), 449–454.
(190) Kurnia, K. A.; Sintra, T. E.; Neves, C. M. S. S.; Shimizu, K.; Canongia Lopes, J. N.; Gonçalves, F.; Ventura, S. P. M.; Freire, M. G.; Santos, L. M. N. B. F.; Coutinho, J. A. P. *Phys. Chem. Chem. Phys.* **2014**, *16* (37), 19952–19963.
(191) Ranke, J.; Müller, A.; Bottin-Weber, U.; Stock, F.; Stolte, S.; Arning, J.; Störmann, R.; Jastorff, B. *Ecotoxicol. Environ. Saf.* **2007**, *67* (3), 430–438.
(192) Ranke, J.; Othman, A.; Fan, P.; Müller, A. *Int. J. Mol. Sci.* **2009**, *10* (3), 1271–1289.
(193) Kohno, Y.; Ohno, H. *Chem. Commun.* **2012**, *48* (57), 7119–7130.
(194) Chen, S.; Zhang, S.; Liu, X.; Wang, J.; Wang, J.; Dong, K.; Sun, J.; Xu, B. *Phys. Chem. Chem. Phys.* **2014**, *16* (13), 5893–5906.
(195) Wang, J.; Wang, H. Springer Berlin Heidelberg, 2014; pp 39–77.
(196) Blesic, M.; Marques, M. H.; Plechkova, N. V.; Seddon, K. R.; Rebelo, L. P. N.; Lopes, A. *Green Chem.* **2007**, *9* (5), 481–490.
(197) Cornellas, A.; Perez, L.; Comelles, F.; Ribosa, I.; Manresa, A.; Garcia, M. T. *J. Colloid Interface Sci.* **2011**, *355* (1), 164–171.
(198) El Seoud, O. A.; Pires, P. A. R.; Abdel-Moghny, T.; Bastos, E. L. *J. Colloid Interface Sci.* **2007**, *313* (1), 296–304.
(199) Sirieix-Plénet, J.; Gaillon, L.; Letellier, P. *Talanta* **2004**, *63* (4), 979–986.
(200) Bowers, J.; Butts, C. P.; Martin, P. J.; Vergara-Gutierrez, M. C. **2004**, *20* (6), 2191–2198.
(201) Goodchild, I.; Collier, L.; Millar, S. L.; Prokeš, I.; Lord, J. C. D.; Butts, C. P.; Bowers, J.; Webster, J. R. P.; Heenan, R. K. *J. Colloid Interface Sci.* **2007**, *307* (2), 455–468.

(202) Miskolczy, Z.; Sebők-Nagy, K.; Biczók, L.; Göktürk, S. *Chem. Phys. Lett.* **2004**, *400* (4), 296–300.
(203) Tariq, M.; Freire, M. G.; Saramago, B.; Coutinho, J. A. P.; Lopes, J. N. C.; Rebelo, L. P. N. *Chem. Soc. Rev.* **2012**, *41* (2), 829–868.
(204) Łuczak, J.; Hupka, J.; Thöming, J.; Jungnickel, C. *Colloids Surfaces A Physicochem. Eng. Asp.* **2008**, *329* (3), 125–133.
(205) Inoue, T.; Ebina, H.; Dong, B.; Zheng, L. *J. Colloid Interface Sci.* **2007**, *314* (1), 236–241.
(206) Łuczak, J.; Jungnickel, C.; Joskowska, M.; Thöming, J.; Hupka, J. *J. Colloid Interface Sci.* **2009**, *336* (1), 111–116.
(207) Jungnickel, C.; Łuczak, J.; Ranke, J.; Fernández, J. F.; Müller, A.; Thöming, J. *Colloids Surfaces A Physicochem. Eng. Asp.* **2008**, *316* (1), 278–284.
(208) Bai, G.; Lopes, A.; Bastos, M. *J. Chem. Thermodyn.* **2008**, *40* (10), 1509–1516.
(209) Vanyúr, R.; Biczók, L.; Miskolczy, Z. *Colloids Surfaces A Physicochem. Eng. Asp.* **2007**, *299* (1), 256–261.
(210) Huibers, P. D. T.; Lobanov, V. S.; Katritzky, A. R.; Shah, D. O.; Karelson, M. *J. Colloid Interface Sci.* **1997**, *187* (1), 113–120.
(211) Baltazar, Q. Q.; Chandawalla, J.; Sawyer, K.; Anderson, J. L. *Colloids Surfaces A Physicochem. Eng. Asp.* **2007**, *302* (1), 150–156.
(212) Wang, H.; Wang, J.; Zhang, S.; Xuan, X. *J. Phys. Chem. B* **2008**, *112* (51), 16682–16689.
(213) Sepulveda, L.; Cortes, J. *J. Phys. Chem.* **1985**, *89* (24), 5322–5324.
(214) Trivedi, T. J.; Rao, K. S.; Singh, T.; Mandal, S. K.; Sutradhar, N.; Panda, A. B.; Kumar, A. *ChemSusChem* **2011**, *4* (5), 604–608.
(215) Cheng, N.; Yu, P.; Wang, T.; Sheng, X.; Bi, Y.; Gong, Y.; Yu, L. *J. Phys. Chem. B* **2014**, *118* (10), 2758–2768.
(216) Jiao, J.; Dong, B.; Zhang, H.; Zhao, Y.; Wang, X.; Wang, R.; Yu, L. *J. Phys. Chem. B* **2012**, *116* (3), 958–965.
(217) Blesic, M.; Swadźba-Kwaśny, M.; Holbrey, J. D.; Canongia Lopes, J. N.; Seddon, K. R.; Rebelo, L. P. N. *Phys. Chem. Chem. Phys.* **2009**, *11* (21), 4260–4268.
(218) Barycki, M.; Sosnowska, A.; Puzyn, T. *J. Colloid Interface Sci.* **2017**, *487*, 475–483.
(219) Vieira, O. V.; Hartmann, D. O.; Cardoso, C. M. P.; Oberdoerfer, D.; Baptista, M.; Santos, M. A. S.; Almeida, L.; Ramalho-Santos, J.; Vaz, W. L. C. *PLoS One* **2008**, *3* (8), e2913.
(220) Coleman, D.; Gathergood, N. *Chem. Soc. Rev.* **2010**, *39* (2), 600–637.
(221) Petkovic, M.; Seddon, K. R.; Rebelo, L. P. N.; Silva Pereira, C. *Chem. Soc. Rev.* **2011**, *40* (3), 1383–1403.
(222) Thuy Pham, T. P.; Cho, C.-W.; Yun, Y.-S. *Water Res.* **2010**, *44* (2), 352–372.
(223) Matzke, M.; Arning, J.; Ranke, J.; Jastorff, B.; Stolte, S. In *Handbook of Green Chemistry*; Wiley-VCH Verlag GmbH & Co. KGaA, 2010.
(224) Heckenbach, M. E.; Romero, F. N.; Green, M. D.; Halden, R. U. *Chemosphere* **2016**, *150*, 266–274.
(225) Egorova, K. S.; Ananikov, V. P. *ChemSusChem* **2014**, *7* (2), 336–360.
(226) Cvjetko Bubalo, M.; Radošević, K.; Radojčić Redovniković, I.; Halambek, J.; Gaurina Srček, V. *Ecotoxicol. Environ. Saf.* **2014**, *99*, 1–12.

(227) Hseu, Y.-C.; Chou, C.-W.; Senthil Kumar, K. J.; Fu, K.-T.; Wang, H.-M.; Hsu, L.-S.; Kuo, Y.-H.; Wu, C.-R.; Chen, S.-C.; Yang, H.-L. *Food Chem. Toxicol.* **2012**, *50* (5), 1245–1255.
(228) Ventura, S. P. M.; Gonçalves, A. M. M.; Sintra, T. E.; Pereira, J. L.; Gonçalves, F.; Coutinho, J. A. P. *Ecotoxicology* **2013**, *22* (1), 1–12.
(229) Ventura, S. P. M.; Marques, C. S.; Rosatella, A. A.; Afonso, C. A. M.; Gonçalves, F.; Coutinho, J. A. P. *Ecotoxicol. Environ. Saf.* **2012**, *76* (0), 162–168.
(230) Ranke, J.; Mölter, K.; Stock, F.; Bottin-Weber, U.; Poczobutt, J.; Hoffmann, J.; Ondruschka, B.; Filser, J.; Jastorff, B. *Ecotoxicol. Environ. Saf.* **2004**, *58* (3), 396–404.
(231) Samorì, C.; Pasteris, A.; Galletti, P.; Tagliavini, E. *Environ. Toxicol. Chem.* **2007**, *26* (11), 2379–2382.
(232) e Silva, F. A.; Siopa, F.; Figueiredo, B. F. H. T.; Gonçalves, A. M. M.; Pereira, J. L.; Gonçalves, F.; Coutinho, J. A. P.; Afonso, C. A. M.; Ventura, S. P. M. *Ecotoxicol. Environ. Saf.* **2014**, *108*, 302–310.
(233) Cho, C.-W.; Jeon, Y.-C.; Pham, T. P. T.; Vijayaraghavan, K.; Yun, Y.-S. *Ecotoxicol. Environ. Saf.* **2008**, *71* (1), 166–171.
(234) Cho, C.-W.; Phuong Thuy Pham, T.; Jeon, Y.-C.; Yun, Y.-S. *Green Chem.* **2008**, *10* (1), 67–72.
(235) Kulacki, K. J.; Lamberti, G. A. *Green Chem.* **2008**, *10* (1), 104–110.
(236) Santos, J. I.; Goncalves, A. M. M.; Pereira, J. L.; Figueiredo, B. F. H. T.; e Silva, F. A.; Coutinho, J. A. P.; Ventura, S. P. M.; Goncalves, F. *Green Chem.* **2015**, *17* (9), 4657–4668.
(237) Pretti, C.; Chiappe, C.; Baldetti, I.; Brunini, S.; Monni, G.; Intorre, L. *Ecotoxicol. Environ. Saf.* **2009**, *72* (4), 1170–1176.
(238) Luo, Y.-R.; Li, X.-Y.; Chen, X.-X.; Zhang, B.-J.; Sun, Z.-J.; Wang, J.-J. *Environ. Toxicol.* **2008**, *23* (6), 736–744.
(239) *EC 2002 - Eur. Comm. Guid. Doc. Aquat. ecotoxicology. Under Counc. Dir. 91/414/EEC. SANCO / 3268/2001 Rev 4*.
(240) Stolte, S.; Matzke, M.; Arning, J.; Boschen, A.; Pitner, W.-R.; Welz-Biermann, U.; Jastorff, B.; Ranke, J. *Green Chem.* **2007**, *9* (11), 1170–1179.
(241) Morrissey, S.; Pegot, B.; Coleman, D.; Garcia, M. T.; Ferguson, D.; Quilty, B.; Gathergood, N. *Green Chem.* **2009**, *11* (4), 475–483.
(242) Arning, J.; Stolte, S.; Böschen, A.; Stock, F.; Pitner, W.-R.; Welz-Biermann, U.; Jastorff, B.; Ranke, J. *Green Chem.* **2008**, *10* (1), 47–58.
(243) Bernot, R. J.; Brueseke, M. A.; Evans-White, M. A.; Lamberti, G. A. *Env. Toxicol Chem.* **2005**, *24*, 87–92.
(244) Matzke, M.; Stolte, S.; Thiele, K.; Juffernholz, T.; Arning, J.; Ranke, J.; Welz-Biermann, U.; Jastorff, B. *Green Chem.* **2007**, *9* (11), 1198–1207.
(245) Garcia, M. T.; Gathergood, N.; Scammells, P. J. *Green Chem.* **2005**, *7* (1), 9–14.
(246) Salminen, J.; Papaiconomou, N.; Kumar, R. A.; Lee, J.-M.; Kerr, J.; Newman, J.; Prausnitz, J. M. *Fluid Phase Equilib.* **2007**, *261* (1–2), 421–426.
(247) Stolte, S.; Arning, J.; Bottin-Weber, U.; Muller, A.; Pitner, W.-R.; Welz-Biermann, U.; Jastorff, B.; Ranke, J. *Green Chem.* **2007**, *9* (7), 760–767.
(248) Ventura, S. P. M.; e Silva, F. A.; Gonçalves, A. M. M.; Pereira, J. L.; Gonçalves, F.; Coutinho, J. A. P. *Ecotoxicol. Environ. Saf.* **2014**, *102* (0), 48–54.

(249) Docherty, K. M.; Dixon, J. K.; Kulpa Jr, C. F. *Biodegradation* **2007**, *18* (4), 481–493.
(250) Gathergood, N.; Garcia, M. T.; Scammells, P. J. *Green Chem.* **2004**, *6* (3), 166–175.
(251) Stolte, S.; Abdulkarim, S.; Arning, J.; Blomeyer-Nienstedt, A.-K.; Bottin-Weber, U.; Matzke, M.; Ranke, J.; Jastorff, B.; Thöming, J. *Green Chem.* **2008**, *10* (2), 214–224.
(252) Stolte, S.; Steudte, S.; Igartua, A.; Stepnowski, P. *Curr. Org. Chem.* **2011**, *15* (12), 1946–1973.
(253) Harjani, J. R.; Singer, R. D.; Garcia, M. T.; Scammells, P. J. *Green Chem.* **2008**, *10* (4), 436–438.
(254) Gathergood, N.; Scammells, P. J.; Garcia, M. T. *Green Chem.* **2006**, *8* (2), 156–160.
(255) Alvarez-Guerra, M.; Irabien, A. *Green Chem.* **2011**, *13* (6), 1507–1516.
(256) Bruzzone, S.; Chiappe, C.; Focardi, S. E.; Pretti, C.; Renzi, M. *Chem. Eng. J.* **2011**, *175*, 17–23.
(257) Ismail Hossain, M.; Samir, B. B.; El-Harbawi, M.; Masri, A. N.; Abdul Mutalib, M. I.; Hefter, G.; Yin, C.-Y. *Chemosphere* **2011**, *85* (6), 990–994.
(258) Ma, S.; Lv, M.; Deng, F.; Zhang, X.; Zhai, H.; Lv, W. *J. Hazard. Mater.* **2015**, *283*, 591–598.
(259) Viboud, S.; Papaiconomou, N.; Cortesi, A.; Chatel, G.; Draye, M.; Fontvieille, D. *J. Hazard. Mater.* **2012**, *215*, 40–48.
(260) Yan, F.; Shang, Q.; Xia, S.; Wang, Q.; Ma, P. *J. Hazard. Mater.* **2015**, *286*, 410–415.
(261) Das, R. N.; Roy, K. *Mol. Divers.* **2013**, *17* (1), 151–196.
(262) Briganti, S.; Picardo, M. *J. Eur. Acad. Dermatology Venereol.* **2003**, *17* (6), 663–669.
(263) Lorenz, H.; Seidel-Morgenstern, A. *Angew. Chemie Int. Ed.* **2014**, *53* (5), 1218–1250.
(264) Jain, P.; Goel, A.; Sharma, S.; Parmar, M. *Int. J. Pharma Prof. Res.* **2010**, *1* (1), 34–45.
(265) Clark, K. D.; Nacham, O.; Purslow, J. A.; Pierson, S. A.; Anderson, J. L. *Anal. Chim. Acta* **2016**, *934*, 9–21.
(266) Chapeaux, A.; Simoni, L. D.; Ronan, T. S.; Stadtherr, M. A.; Brennecke, J. F. *Green Chem.* **2008**, *10* (12), 1301–1306.
(267) Rabari, D.; Banerjee, T. *Fluid Phase Equilib.* **2013**, *355*, 26–33.
(268) Wang, J.; Pei, Y.; Zhao, Y.; Hu, Z. *Green Chem.* **2005**, *7* (4), 196–202.
(269) Dearden, J. C. *Int. J. Quant. Struct. Relationships* **2016**, *1* (1), 1–44.
(270) Kovacic, P.; Somanathan, R. In *Reviews of Environmental Contamination and Toxicology*; Whitacre, D. M., Ed.; Springer New York, 2010; Vol. 203, pp 119–138.
(271) Lin, C. B.; Southall, M. D. In *Skin Aging: New Research*; 2013; pp 23–41.
(272) Podda, M.; Grundmann-Kollmann, M. *Clin. Exp. Dermatol.* **2001**, *26* (7), 578–582.
(273) Fuchs, J. *Free Radic. Biol. Med.* **1998**, *25* (7), 848–873.
(274) Qi, H.; Zhang, Q.; Zhao, T.; Chen, R.; Zhang, H.; Niu, X.; Li, Z. *Int. J. Biol. Macromol.* **2005**, *37* (4), 195–199.
(275) Dai, J.; Mumper, R. J. *Molecules* **2010**, *15* (10), 7313–7352.
(276) Škrovánková, S.; Mišurcová, L.; Machů, L. In *Advances in Food and Nutrition Research*; Jeyakumar, H., Ed.; Academic Press, 2012; Vol. Volume 67, pp 75–139.
(277) Bagby, R. S.; Emil, L. Pat. US 3,141,035, 1964.
(278) Broh-Kahn, R. H.; Sasmor, E. J. Pat. US 3,069,321, 1962.
(279) *Lamp* **1972**, *29* (1), 24.
(280) Petkovic, M.; Ferguson, J. L.; Gunaratne, H. Q. N.; Ferreira, R.; Leitao, M. C.;

Seddon, K. R.; Rebelo, L. P. N.; Pereira, C. S. *Green Chem.* **2010**, *12* (4), 643–649.
(281) Li, Z.; Liu, X.; Pei, Y.; Wang, J.; He, M. *Green Chem.* **2012**, *14* (10), 2941–2950.
(282) Gorke, J.; Srienc, F.; Kazlauskas, R. *Biotechnol. Bioprocess Eng.* **2010**, *15* (1), 40–53.
(283) Hou, X.-D.; Li, N.; Zong, M.-H. *ACS Sustain. Chem. Eng.* **2013**, *1* (5), 519–526.
(284) Mourão, T.; Tomé, L. C.; Florindo, C.; Rebelo, L. P. N.; Marrucho, I. M. *ACS Sustain. Chem. Eng.* **2014**, *2* (10), 2426–2434.
(285) Dias, A. M. A.; Cortez, A. R.; Barsan, M. M.; Santos, J. B.; Brett, C. M. A.; de Sousa, H. C. *ACS Sustain. Chem. Eng.* **2013**, *1* (11), 1480–1492.
(286) Garcia, H.; Ferreira, R.; Petkovic, M.; Ferguson, J. L.; Leitao, M. C.; Gunaratne, H. Q. N.; Seddon, K. R.; Rebelo, L. P. N.; Silva Pereira, C. *Green Chem.* **2010**, *12* (3), 367–369.
(287) Molyneux, P. *Songklanakarin J. Sci. Technol.* **2004**, *26*, 211–219.
(288) Blois, M. S. *Nature* **1985**, *181*, 1199–1200.
(289) Alam, M. N.; Bristi, N. J.; Rafiquzzaman, M. *Saudi Pharm. J.* **2013**, *21* (2), 143–152.
(290) Hochstein, F. A. Pat. US 3,576,007, 1971.
(291) Korner, J. Pat. US 2,589,707, 1952.
(292) *Azur Environ. MicrotoxOmniTM Softw. Wind. 95/98/NT. Carlsbad, CA, U.S.A.* **1999**.
(293) Marrero, J.; Gani, R. *Fluid Phase Equilib.* **2001**, *183–184* (0), 183–208.
(294) Queimada, A. J.; Mota, F. L.; Pinho, S. P.; Macedo, E. A. *J. Phys. Chem. B* **2009**, *113* (11), 3469–3476.
(295) Mota, F. L.; Queimada, A. J.; Pinho, S. P.; Macedo, E. A. *Ind. Eng. Chem. Res.* **2008**, *47* (15), 5182–5189.
(296) Lide, D. R.; Milne, G. W. A. *Handbook of data on organic compounds*, 3rd ed.; CRC Press: Boca Raton, Fla., 1994; Vol. Volume I.
(297) Klein, R.; Kellermeier, M.; Touraud, D.; Müller, E.; Kunz, W. *J. Colloid Interface Sci.* **2013**, *392* (0), 274–280.
(298) Klein, R.; Tiddy, G. J. T.; Maurer, E.; Touraud, D.; Esquena, J.; Tache, O.; Kunz, W. *Soft Matter* **2011**, *7* (15), 6973–6983.
(299) Hernández-Fernández, F. J.; Bayo, J.; Pérez de los Ríos, A.; Vicente, M. A.; Bernal, F. J.; Quesada-Medina, J. *Ecotoxicol. Environ. Saf.* **2015**, *116* (0), 29–33.
(300) Parvez, S.; Venkataraman, C.; Mukherji, S. *Environ. Int.* **2006**, *32* (2), 265–268.
(301) EU, Environmental Hazards 10 March 2011, http://www.unece.org/fileadmin/DAM/trans/danger/publi/ghs/ghs_rev01/English/04e_part4.pdf, (accessed 22.04.16).
(302) Passino, D. R. M.; Smith, S. B. *Environ. Toxicol. Chem.* **1987**, *6* (11), 901–907.
(303) Koshihara, Y.; Neichi, T.; Murota, S.; Lao, A.; Fujimoto, Y.; Tatsuno, T. *Biochim. Biophys. Acta - Lipids Lipid Metab.* **1984**, *792* (1), 92–97.
(304) Yang, W. S.; Jeong, D.; Yi, Y.-S.; Park, J. G.; Seo, H.; Moh, S. H.; Hong, S.; Cho, J. Y. *Mediators Inflamm.* **2013**, *2013*, 1–12.
(305) Búfalo, M. C.; Ferreira, I.; Costa, G.; Francisco, V.; Liberal, J.; Cruz, M. T.; Lopes, M. C.; Batista, M. T.; Sforcin, J. M. *J. Ethnopharmacol.* **2013**, *149* (1), 84–92.
(306) Chao, P. C.; Hsu, C. C.; Yin, M. C. *Nutr. Metab.* **2009**, *16*, 3–10.
(307) Barrera, G. *ISRN Oncol.* **2012**, *2012*, 1–21.
(308) Borges, A.; Ferreira, C.; Saavedra, M. J.; Simões, M. *Microb. Drug Resist.* **2013**, *19* (4), 256–265.

(309) Wang, K.; Zhu, X.; Zhang, K.; Zhu, L.; Zhou, F. *J. Biochem. Mol. Toxicol.* **2014**, *28* (9), 387–393.
(310) *Chirality* **1992**, *4* (5), 338–340.
(311) Jóźwiak, K.; Lough, W. J. (W. J.; Wainer, I. W. *Drug stereochemistry : analytical methods and pharmacology*; 2012.
(312) Schuur, B.; Verkuijl, B. J. V.; Minnaard, A. J.; de Vries, J. G.; Heeres, H. J.; Feringa, B. L. *Org. Biomol. Chem.* **2011**, *9* (1), 36–51.
(313) Pirkle, W. H.; Pochapsky, T. C. *Chem. Rev.* **1989**, *89* (2), 347–362.
(314) Keith E. Gutowski; Grant A. Broker; Heather D. Willauer; Jonathan G. Huddleston; Richard P. Swatloski; John D. Holbrey, A.; Rogers, R. D. *J. Am. Chem. Soc.* **2003**, *125*, 6632–6633.
(315) Earle, M. J.; McCormac, P. B.; Seddon, K. R. *Green Chem.* **1999**, *1* (1), 23–25.
(316) Weiliang Bao; Zhiming Wang, A.; Li, Y. *J. Org. Chem.* **2002**, *68*, 591–593.
(317) Bica, K.; Gaertner, P. *European J. Org. Chem.* **2008**, *2008* (19), 3235–3250.
(318) Payagala, T.; Armstrong, D. W. *Chirality* **2012**, *24* (1), 17–53.
(319) Santamarta, F.; Vilas, M.; Tojo, E.; Fall, Y. *RSC Adv.* **2016**, *6* (37), 31177–31180.
(320) Jayachandra, R.; Reddy, S. *RSC Adv.* **2016**, *6* (46), 39758–39761.
(321) Wu, H.; Yao, S.; Qian, G.; Yao, T.; Song, H. *J. Chromatogr. A* **2015**, *1418*, 150–157.
(322) Allen, C. R.; Richard, P. L.; Ward, A. J.; van de Water, L. G. A.; Masters, A. F.; Maschmeyer, T. *Tetrahedron Lett.* **2006**, *47* (41), 7367–7370.
(323) De Santis, S.; Masci, G.; Casciotta, F.; Caminiti, R.; Scarpellini, E.; Campetella, M.; Gontrani, L. *Phys. Chem. Chem. Phys.* **2015**, *17* (32), 20687–20698.
(324) Bhattacharjee, A.; Lopes-da-Silva, J. A.; Freire, M. G.; Coutinho, J. A. P.; Carvalho, P. J. *Fluid Phase Equilib.* **2015**, *400*, 103–113.
(325) Bhattacharjee, A.; Luís, A.; Santos, J. H.; Lopes-da-Silva, J. A.; Freire, M. G.; Carvalho, P. J.; Coutinho, J. A. P. *Fluid Phase Equilib.* **2014**, *381*, 36–45.
(326) Lee, S. Y.; Vicente, F. A.; Coutinho, J. A. P.; Khoiroh, I.; Show, P. L.; Ventura, S. P. M. *J. Chem. Eng. Data* **2016**, *61* (7), 2260–2268.
(327) ChemSpider database (accessed 06.01.17), http://www.chemspider.com.
(328) Fukami, T.; Tahara, S.; Yasuda, C.; Nakasone, K. *Int. J. Chem.* **2016**, *8* (2), 9–21.
(329) Tariq, M.; Forte, P. A. S.; Gomes, M. F. C.; Lopes, J. N. C.; Rebelo, L. P. N. *J. Chem. Thermodyn.* **2009**, *41* (6), 790–798.
(330) Hou, X.-D.; Liu, Q.-P.; Smith, T. J.; Li, N.; Zong, M.-H. *PLoS One* **2013**, *8* (3), e59145.
(331) Abiko, A.; Masamune, S. *Tetrahedron Lett.* **1992**, *33* (38), 5517–5518.
(332) Icke, R.; Wisegarver, B.; Alles, G. *Org. Synth.* **1945**, *25*, 89.
(333) Brunet, J.-J.; Chauvin, R.; Chiffre, J.; Huguet, S.; Leglaye, P. *J. Organomet. Chem.* **1998**, *566* (1), 117–123.
(334) Ianni, F.; Carotti, A.; Marinozzi, M.; Marcelli, G.; Di Michele, A.; Sardella, R.; Lindner, W.; Natalini, B. *Anal. Chim. Acta* **2015**, *885*, 174–182.
(335) Ianni, F.; Pataj, Z.; Gross, H.; Sardella, R.; Natalini, B.; Lindner, W.; Lämmerhofer, M. *J. Chromatogr. A* **2014**, *1363*, 101–108.
(336) Keunchkarian, S.; Padró, J. M.; Gotta, J.; Nardillo, A. M.; Castells, C. B. *J. Chromatogr. A* **2011**, *1218* (23), 3660–3668.
(337) Bicker, W.; Chiorescu, I.; Arion, V. B.; Lämmerhofer, M.; Lindner, W. *Tetrahedron: Asymmetry* **2008**, *19* (1), 97–110.

(338) Lindner, W.; LÄMMERHOFER, M.; Maier, N. Cinchonan based chiral selectors for separation of stereoisomers. PCT/EP97/02888, 1997.
(339) Piette, V.; Lindner, W.; Crommen, J. *J. Chromatogr. A* **2000**, *894* (1), 63–71.
(340) Gao, H.-S.; Hu, Z.-G.; Wang, J.-J.; Qiu, Z.-F.; Fan, F.-Q. *Aust. J. Chem.* **2008**, *61* (7), 521–525.
(341) Toda, F.; Tanaka, K. *Chem. Commun.* **1997**, *24* (12), 1087–1088.
(342) Zhao, J.; Zheng, M.-X.; Lin, Y.-J.; Chen, Y.-C.; Ruan, Y.-P.; Zhang, H. *Acta Physico-Chimica Sin.* **2010**, *26*, 1832–1836.
(343) Subbarao, C. V; Chakravarthy, I. P. K.; Sai Bharadwaj, A. V. S. L.; Prasad, K. M. M. *Chem. Eng. Technol.* **2012**, *35* (2), 225–237.
(344) Stanton, K.; Tibazarwa, C.; Certa, H.; Greggs, W.; Hillebold, D.; Jovanovich, L.; Woltering, D.; Sedlak, R. *Integr. Environ. Assess. Manag.* **2010**, *6* (1), 155–163.
(345) Neuberg, C. *Biochem. Z.* **1916**, *76*, 107–176.
(346) Hodgdon, T. K.; Kaler, E. W. *Curr. Opin. Colloid Interface Sci.* **2007**, *12* (3), 121–128.
(347) Roy, B. K.; Moulik, S. P. *Colloids Surfaces A Physicochem. Eng. Asp.* **2002**, *203* (1–3), 155–166.
(348) Subramanian, D.; Boughter, C. T.; Klauda, J. B.; Hammouda, B.; Anisimov, M. A. *Faraday Discuss.* **2013**, *167* (0), 217–238.
(349) Eastoe, J.; Hatzopoulos, M. H.; Dowding, P. J. *Soft Matter* **2011**, *7* (13), 5917–5925.
(350) Dhapte, V.; Mehta, P. *St. Petersbg. Polytech. Univ. J. Phys. Math.* **2015**, *1* (4), 424–435.
(351) Sanghvi, R.; Evans, D.; Yalkowsky, S. H. *Int. J. Pharm.* **2007**, *336* (1), 35–41.
(352) Hussain, M. A.; Diluccio, R. C.; Maurin, M. B. *J. Pharm. Sci.* **1993**, *82* (1), 77–79.
(353) Matero, A.; Mattsson, Å.; Svensson, M. *J. Surfactants Deterg.* **1998**, *1* (4), 485–489.
(354) Bauduin, P.; Renoncourt, A.; Kopf, A.; Touraud, D.; Kunz, W. *Langmuir* **2005**, *21* (15), 6769–6775.
(355) Lee, J.; Lee, S. C.; Acharya, G.; Chang, C.; Park, K. *Pharm. Res.* **2003**, *20* (7), 1022–1030.
(356) Neumann, M. G.; Schmitt, C. C.; Prieto, K. R.; Goi, B. E. *J. Colloid Interface Sci.* **2007**, *315* (2), 810–813.
(357) Booth, J. J.; Abbott, S.; Shimizu, S. *J. Phys. Chem. B* **2012**, *116* (51), 14915–14921.
(358) Shimizu, S.; Matubayasi, N. *J. Phys. Chem. B* **2014**, *118* (35), 10515–10524.
(359) Ferraz, R.; Branco, L. C.; Prudêncio, C.; Noronha, J. P.; Petrovski, Ž. *ChemMedChem* **2011**, *6* (6), 975–985.
(360) Hough, W. L.; Rogers, R. D. *Bull. Chem. Soc. Jpn.* **2007**, *80* (12), 2262–2269.
(361) Bica, K.; Rogers, R. D. *Chem. Commun.* **2010**, *46* (8), 1215–1217.
(362) Stoimenovski, J.; MacFarlane, D. R. *Chem. Commun.* **2011**, *47* (41), 11429–11431.
(363) Bica, K.; Rodríguez, H.; Gurau, G.; Andreea Cojocaru, O.; Riisager, A.; Fehrmann, R.; Rogers, R. D. *Chem. Commun.* **2012**, *48* (44), 5422–5424.
(364) Bica, K.; Rijksen, C.; Nieuwenhuyzen, M.; Rogers, R. D. *Phys. Chem. Chem. Phys.* **2010**, *12* (8), 2011–2017.
(365) Balk, A.; Wiest, J.; Widmer, T.; Galli, B.; Holzgrabe, U.; Meinel, L. *Eur. J. Pharm. Biopharm.* **2015**, *94*, 73–82.
(366) Sintra, T. E.; Luís, A.; Rocha, S. N.; Lobo Ferreira, A. I. M. C.; Gonçalves, F.; Santos, L. M. N. B. F.; Neves, B. M.; Freire, M. G.; Ventura, S. P. M.; Coutinho, J. A. P. *ACS*

Sustain. Chem. Eng. **2015**, *3* (10), 2558–2565.
(367) Claudio, A. F. M.; Neves, M. C.; Shimizu, K.; Canongia Lopes, J. N.; Freire, M. G.; Coutinho, J. A. P. *Green Chem.* **2015**, *17* (7), 3948–3963.
(368) Rengstl, D.; Kraus, B.; Van Vorst, M.; Elliott, G. D.; Kunz, W. *Colloids Surfaces B Biointerfaces* **2014**, *123*, 575–581.
(369) Williams, R. O.; Watts, A. B.; Miller, D. A. *Formulating Poorly Water Soluble Drugs*; Springer New York, 2011.
(370) Dahan, A.; Miller, J. M.; Amidon, G. L. *AAPS J.* **2009**, *11* (4), 740–746.
(371) e Silva, F. A.; Caban, M.; Stepnowski, P.; Coutinho, J. A. P.; Ventura, S. P. M. *Green Chem.* **2016**, *18* (13), 3749–3757.
(372) Yalkowsky, S. H.; Dannenfelser, R. M. *Coll. Pharmacy, Univ. Arizona, Tucson, AZ* **1992**.
(373) Shimizu, S.; Booth, J. J.; Abbott, S. *Phys. Chem. Chem. Phys.* **2013**, *15* (47), 20625–20632.
(374) Hopkins Hatzopoulos, M.; Eastoe, J.; Dowding, P. J.; Rogers, S. E.; Heenan, R.; Dyer, R. *Langmuir* **2011**, *27* (20), 12346–12353.
(375) Russo, J. W.; Hoffmann, M. M. *J. Chem. Eng. Data* **2011**, *56* (9), 3703–3710.
(376) Subramanian, D.; Ivanov, D. A.; Yudin, I. K.; Anisimov, M. A.; Sengers, J. V. *J. Chem. Eng. Data* **2011**, *56* (4), 1238–1248.
(377) Subramanian, D.; Anisimov, M. A. *Fluid Phase Equilib.* **2014**, *362*, 170–176.
(378) Rasool, A. A.; Hussain, A. A.; Dittert, L. W. *J. Pharm. Sci.* **1991**, *80* (4), 387–393.
(379) Mansur, C. R. E.; Spinelli, L. S.; Lucas, E. F.; González, G. *Colloids Surfaces A Physicochem. Eng. Asp.* **1999**, *149* (1–3), 291–300.
(380) Hopkins Hatzopoulos, M.; Eastoe, J.; Dowding, P. J.; Grillo, I.; Demé, B.; Rogers, S. E.; Heenan, R.; Dyer, R. *Langmuir* **2012**, *28* (25), 9332–9340.
(381) Kragl, U.; Eckstein, M.; Kaftzik, N. *Curr. Opin. Biotechnol.* **2002**, *13* (6), 565–571.
(382) Yang, Z.; Pan, W. *Enzyme Microb. Technol.* **2005**, *37* (1), 19–28.
(383) Zhang, G.-R.; Etzold, B. J. M. *J. Energy Chem.* **2016**, *25* (2), 199–207.
(384) Chinnappan, A.; Baskar, C.; Kim, H. *RSC Adv.* **2016**, *6* (68), 63991–64002.
(385) Eshetu, G. G.; Armand, M.; Ohno, H.; Scrosati, B.; Passerini, S. *Energy Environ. Sci.* **2016**, *9* (1), 49–61.
(386) Pal, A.; Yadav, S. *Fluid Phase Equilib.* **2016**, *412*, 71–78.
(387) Pino, V.; Yao, C.; Anderson, J. L. *J. Colloid Interface Sci.* **2009**, *333* (2), 548–556.
(388) Vaghela, N. M.; Sastry, N. V.; Aswal, V. K. *Colloids Surfaces A Physicochem. Eng. Asp.* **2011**, *373* (1), 101–109.
(389) Mester, P.; Wagner, M.; Rossmanith, P. *Sep. Purif. Technol.* **2012**, *97*, 211–215.
(390) Flieger, J.; Siwek, A.; Pizoń, M.; Czajkowska-Żelazko, A. *J. Sep. Sci.* **2013**, *36* (9-10), 1530–1536.
(391) Qiu, H.; Zhang, Q.; Chen, L.; Liu, X.; Jiang, S. *J. Sep. Sci.* **2008**, *31* (15), 2791–2796.
(392) Wiedmer, S. K.; King, A. W. T.; Riekkola, M.-L. *J. Chromatogr. A* **2012**, *1253*, 171–176.
(393) Rageh, A. H.; Pyell, U. *J. Chromatogr. A* **2013**, *1316*, 135–146.
(394) Ventura, S. P. M.; Santos, L. D. F.; Saraiva, J. A.; Coutinho, J. A. P. *Green Chem.* **2012**, *14* (6), 1620–1625.
(395) Pino, V.; Germán-Hernández, M.; Martín-Pérez, A.; Anderson, J. L. *Sep. Sci. Technol.*

2012, *47* (2), 264–276.
(396) Germán-Hernández, M.; Pino, V.; Anderson, J. L.; Afonso, A. M. *J. Chromatogr. A* **2012**, *1227*, 29–37.
(397) Smirnova, N. A.; Safonova, E. A. *Russ. J. Phys. Chem. A* **2010**, *84* (10), 1695–1704.
(398) Brown, P.; Butts, C.; Dyer, R.; Eastoe, J.; Grillo, I.; Guittard, F.; Rogers, S.; Heenan, R. *Langmuir* **2011**, *27* (8), 4563–4571.
(399) Engin Özdil, S.; Akbaş, H.; Boz, M. *J. Chem. Eng. Data* **2016**, *61* (1), 142–150.
(400) Bradaric, C. J.; Downard, A.; Kennedy, C.; Robertson, A. J.; Zhou, Y. *Green Chem.* **2003**, *5* (2), 143–152.
(401) Almeida, H. F. D.; Lopes-da-Silva, J. A.; Freire, M. G.; Coutinho, J. A. P. *J. Chem. Thermodyn.* **2013**, *57*, 372–379.
(402) Martins, M.; Wei, O. C.; Neves, M. C.; Pereira, J. F. B.; Coutinho, J. A. P.; Ventura, S. P. M. **2017**, (under preparation).
(403) Pérez-Rodríguez, M.; Prieto, G.; Rega, C.; Varela, L. M.; Sarmiento, F.; Mosquera, V. **1998**, *14* (16), 4422–4426.
(404) Mosquera, V.; del Río, J. M.; Attwood, D.; García, M.; Jones, M. N.; Prieto, G.; Suarez, M. J.; Sarmiento, F. *J. Colloid Interface Sci.* **1998**, *206* (1), 66–76.
(405) Muslim, A. Al; Ayyash, D.; Gujral, S. S.; Mekhail, G. M.; Rao, P. P. N.; Wettig, S. D.; Quagliotto, P.; Donofrio, G.; Różycka-Roszak, B.; Misiak, P.; Woźniak, E.; Sansone, F. *Phys. Chem. Chem. Phys.* **2017**, *19* (3), 1953–1962.
(406) Carvalho, P. J.; Ventura, S. P. M.; Batista, M. L. S.; Schröder, B.; Gonçalves, F.; Esperança, J.; Mutelet, F.; Coutinho, J. A. P. *J. Chem. Phys.* **2014**, *140* (6), 064505.
(407) Jing, B.; Lan, N.; Qiu, J.; Zhu, Y. *J. Phys. Chem. B* **2016**, *120* (10), 2781–2789.
(408) Łuczak, J.; Jungnickel, C.; Łącka, I.; Stolte, S.; Hupka, J. *Green Chem.* **2010**, *12* (4), 593–601.
(409) Gao, J.; Wang, J.-Q.; Song, Q.-W.; He, L.-N. *Green Chem.* **2011**, *13* (5), 1182–1186.
(410) Miao, C.-X.; Wang, J.-Q.; Yu, B.; Cheng, W.-G.; Sun, J.; Chanfreau, S.; He, L.-N.; Zhang, S.-J. *Chem. Commun.* **2011**, *47* (9), 2697–2699.
(411) Santos, E.; Albo, J.; Irabien, A. *RSC Adv.* **2014**, *4* (75), 40008–40018.
(412) Lee, S. H.; Ha, S. H.; You, C.-Y.; Koo, Y.-M. *Korean J. Chem. Eng.* **2007**, *24* (3), 436–437.
(413) Okuno, M.; Hamaguchi, H.; Hayashi, S. *Appl. Phys. Lett.* **2006**, *89* (13), 132506.
(414) Zhao, Q.; Herng, T. S.; Guo, C. X.; Zhao, D.; Ding, J.; Lu, X. *RSC Adv.* **2016**, *6* (19), 15731–15734.
(415) Clark, K. D.; Nacham, O.; Yu, H.; Li, T.; Yamsek, M. M.; Ronning, D. R.; Anderson, J. L. *Anal. Chem.* **2015**, *87* (3), 1552–1559.
(416) Bica, K.; Gaertner, P. *European J. Org. Chem.* **2008**, *2008* (20), 3453–3456.
(417) Chen, X.; Peng, Y. *Catal. Letters* **2007**, *122* (3), 310–313.
(418) Wang, H.; Yan, R.; Li, Z.; Zhang, X.; Zhang, S. *Catal. Commun.* **2010**, *11* (8), 763–767.
(419) Mohammad Fauzi, A. H.; Amin, N. A. S.; Mat, R. *Appl. Energy* **2014**, *114*, 809–818.
(420) Muraoka, J.; Kamiya, N.; Ito, Y. *J. Mol. Liq.* **2013**, *182*, 76–78.
(421) Zakrzewska, M. E.; Paninho, A. B.; Môlho, M. F.; Nunes, A. V. M.; Afonso, C. A. M.; Rosatella, A. A.; Lopes, J. M.; Najdanovic-Visak, V. *J. Chem. Thermodyn.* **2013**, *63*, 123–127.
(422) Zhuravlev, O. E.; Verolainen, N. V; Voronchikhina, L. I. *Russ. J. Appl. Chem.* **2011**, *84*

(7), 1158–1164.
(423) Dobbelin, M.; Jovanovski, V.; Llarena, I.; Claros Marfil, L. J.; Cabanero, G.; Rodriguez, J.; Mecerreyes, D. *Polym. Chem.* **2011**, *2* (6), 1275–1278.
(424) Kim, J.-Y.; Kim, J.-T.; Song, E.-A.; Min, Y.-K.; Hamaguchi, H. *Macromolecules* **2008**, *41* (8), 2886–2889.
(425) Akitsu, T.; Einaga, Y. *Inorg. Chem. Commun.* **2006**, *9* (11), 1108–1110.
(426) Branco, A.; Branco, L. C.; Pina, F. *Chem. Commun.* **2011**, *47* (8), 2300–2302.
(427) Guerrero-Sanchez, C.; Lara-Ceniceros, T.; Jimenez-Regalado, E.; Raşa, M.; Schubert, U. S. *Adv. Mater.* **2007**, *19* (13), 1740–1747.
(428) Guerrero-Sanchez, C.; Ortiz-Alvarado, A.; Schubert, U. S. *J. Phys. Conf. Ser.* **2009**, *149* (1), 12052.
(429) Hayashi, S.; Hamaguchi, H. *Chem. Lett.* **2004**, *33* (12), 1590–1591.
(430) Del Sesto, R. E.; Corley, C.; Robertson, A.; Wilkes, J. S. *J. Organomet. Chem.* **2005**, *690* (10), 2536–2542.
(431) Del Sesto, R. E.; McCleskey, T. M.; Burrell, A. K.; Baker, G. A.; Thompson, J. D.; Scott, B. L.; Wilkes, J. S.; Williams, P. *Chem. Commun.* **2008**, No. 4, 447–449.
(432) Santos, E.; Albo, J.; Rosatella, A.; Afonso, C. A. M.; Irabien, Á. *J. Chem. Technol. Biotechnol.* **2014**, *89* (6), 866–871.
(433) Yoshida, Y.; Otsuka, A.; Saito, G.; Natsume, S.; Nishibori, E.; Sakata, M.; Takata, M.; Takahashi, M.; Yoko, T. *Bull. Chem. Soc. Jpn.* **2005**, *78* (11), 1921–1928.
(434) Yoshida, Y.; Saito, G. *J. Mater. Chem.* **2006**, *16* (13), 1254–1262.
(435) Peppel, T.; Köckerling, M.; Geppert-Rybczyńska, M.; Ralys, R. V; Lehmann, J. K.; Verevkin, S. P.; Heintz, A. *Angew. Chemie Int. Ed.* **2010**, *49* (39), 7116–7119.
(436) Pitula, S.; Mudring, A.-V. *Chem. – A Eur. J.* **2010**, *16* (11), 3355–3365.
(437) Mallick, B.; Balke, B.; Felser, C.; Mudring, A.-V. *Angew. Chemie Int. Ed.* **2008**, *47* (40), 7635–7638.
(438) Nockemann, P.; Thijs, B.; Postelmans, N.; Van Hecke, K.; Van Meervelt, L.; Binnemans, K. *J. Am. Chem. Soc.* **2006**, *128* (42), 13658–13659.
(439) Frade, R. F. M.; Simeonov, S.; Rosatella, A. A.; Siopa, F.; Afonso, C. A. M. *Chemosphere* **2013**, *92* (1), 100–105.
(440) Daniel, C. I.; Vaca Chávez, F.; Feio, G.; Portugal, C. A. M.; Crespo, J. G.; Sebastião, P. J. *J. Phys. Chem. B* **2013**, *117* (39), 11877–11884.
(441) Zhang, S.; Zhang, Y.; Wang, Y.; Liu, S.; Deng, Y. *Phys. Chem. Chem. Phys.* **2012**, *14* (15), 5132–5138.
(442) Li, M.; De Rooy, S. L.; Bwambok, D. K.; El-Zahab, B.; DiTusa, J. F.; Warner, I. M. *Chem. Commun.* **2009**, No. 45, 6922–6924.
(443) Luis, P.; Albo, J.; Irabien, A.; Crespo, J.; Afonso, C.; Irabien, A. *Ecotoxicol. around Globe* **2011**, 359–372.
(444) Rosatella, A. A.; Siopa, F.; Frade, R. F. M.; Afonso, C. A. M. *New J. Chem.* **2016**, *40* (4), 3124–3129.
(445) Das, R. N.; Roy, K.; Popelier, P. L. A. *Ecotoxicol. Environ. Saf.* **2015**, *122*, 497–520.
(446) Das, R. N.; Sintra, T. E.; Coutinho, J. A. P.; Ventura, S. P. M.; Roy, K.; Popelier, P. L. A. *Toxicol. Res.* **2016**, *5* (5), 1388–1399.
(447) Irabien, Á.; Garea, A.; Luis, P. *Comput. Aided Chem. Eng.* **2009**, *26*, 63–67.
(448) Luis, P.; Ortiz, I.; Aldaco, R.; Irabien, A. *Ecotoxicol. Environ. Saf.* **2007**, *67* (3), 423–

429.
(449) Peric, B.; Sierra, J.; Martí, E.; Cruañas, R.; Garau, M. A. *Ecotoxicol. Environ. Saf.* **2015**, *115*, 257–262.
(450) Wang, C.; Wei, Z.; Wang, L.; Sun, P.; Wang, Z. *Ecotoxicol. Environ. Saf.* **2015**, *115*, 112–118.
(451) Ventura, S. P. M.; Gonçalves, A. M. M.; Sintra, T. E.; Pereira, J. L.; Gonçalves, F.; Coutinho, J. A. P. *Ecotoxicology* **2012**, *22* (1), 1–12.
(452) Denich, T. .; Beaudette, L. .; Lee, H.; Trevors, J. . *J. Microbiol. Methods* **2003**, *52* (2), 149–182.
(453) Zhang, Y.-M.; Rock, C. O. *Nat. Rev. Microbiol.* **2008**, *6* (3), 222–233.
(454) Montalbán, M. G.; Hidalgo, J. M.; Collado-González, M.; Díaz Baños, F. G.; Víllora, G. *Chemosphere* **2016**, *155*, 405–414.
(455) Ropel, L.; Belvèze, L. S.; Aki, S. N. V. K.; Stadtherr, M. A.; Brennecke, J. F. *Green Chem.* **2005**, *7* (2), 83–90.
(456) Wolterbeek, H. .; Verburg, T. . *Sci. Total Environ.* **2001**, *279* (1), 87–115.
(457) Li, Y.; Jiang, L.; Li, X.; Hu, Y.; Wen, J. *Chem. Res. Chinese Univ.* **2013**, *29* (3), 568–573.
(458) Welton, T. **1999**, *99*, 2071–2084.
(459) Rogers, R. D. *Nature* **2007**, *447* (7147), 917–918.
(460) Reeve, W.; Erikson, C. M.; Aluotto, P. F. *Can. J. Chem.* **1979**, *57* (20), 2747–2754.
(461) Ab Rani, M. A.; Brant, A.; Crowhurst, L.; Dolan, A.; Lui, M.; Hassan, N. H.; Hallett, J. P.; Hunt, P. A.; Niedermeyer, H.; Perez-Arlandis, J. M.; Schrems, M.; Welton, T.; Wilding, R. *Phys. Chem. Chem. Phys.* **2011**, *13* (37), 16831–16840.
(462) Pinkert, A.; Marsh, K. N.; Pang, S.; Staiger, M. P. *Chem. Rev.* **2009**, *109* (12), 6712–6728.
(463) Ohno, H.; Fukaya, Y. *Chem. Lett.* **2009**, *38* (1), 2–7.
(464) Zhu, S.; Wu, Y.; Chen, Q.; Yu, Z.; Wang, C.; Jin, S.; Ding, Y.; Wu, G. *Green Chem.* **2006**, *8* (4), 325–327.
(465) Zhao, Y.; Huang, Y.; Zhang, X.; Zhang, S. *Phys. Chem. Chem. Phys.* **2015**, *17* (5), 3761–3767.
(466) Roy, K.; Kar, S.; Das, R. N. *Understanding the basics of QSAR for applications in pharmaceutical sciences and risk assessment*; Academic Press, an imprint of Elsevier, 2015.
(467) Coutinho, J. A. P.; Carvalho, P. J.; Oliveira, N. M. C. *RSC Adv.* **2012**, *2* (19), 7322–7346.
(468) Yan, F.; Xia, S.; Wang, Q.; Shang, Q.; Ma, P. *Fluid Phase Equilib.* **2013**, *358*, 166–171.
(469) Fjodorava, N.; Novich, M.; Vrachko, M.; Smirnov, V.; Kharchevnikova, N.; Zholdakova, Z.; Novikov, S.; Skvortsova, N.; Filimonov, D.; Poroikov, V.; Benfenate, E. *J. Environ. Sci. Heal. Part C* **2008**, *26* (2), 201–236.
(470) *Current Approaches in the Statistical Analysis of Ecotoxicity Data*; OECD Series on Testing and Assessment; OECD Publishing, 2014.
(471) Pattard, M.; Moser, H. In *Ecotoxicological Characterization of Waste*; Springer New York: New York, NY, 2009; pp 105–115.
(472) Ledda, C.; Rapisarda, V.; Bracci, M.; Proietti, L.; Zuccarello, M.; Fallico, R.; Fiore, M.; Ferrante, M. *J. Occup. Med. Toxicol.* **2013**, *8* (1), 23.
(473) Cho, C.-W.; Ranke, J.; Arning, J.; Thöming, J.; Preiss, U.; Jungnickel, C.; Diedenhofen,

M.; Krossing, I.; Stolte, S. *SAR QSAR Environ. Res.* **2013**, *24* (10), 863–882.
(474) Das, R. N.; Roy, K. *Toxicol. Res. (Camb).* **2012**, *1* (3), 186–195.
(475) Luis, P.; Garea, A.; Irabien, A. *J. Mol. Liq.* **2010**, *152* (1), 28–33.
(476) Ventura, S. P. M.; Gardas, R. L.; Gonçalves, F.; Coutinho, J. A. P. *J. Chem. Technol. Biotechnol.* **2011**, *86* (7), 957–963.
(477) Ventura, S. P. M.; Gonçalves, A. M. M.; Gonçalves, F.; Coutinho, J. A. P. *Aquat. Toxicol.* **2010**, *96* (4), 290–297.
(478) Ventura, S. P. M.; Gurbisz, M.; Ghavre, M.; Ferreira, F. M. M.; Gonçalves, F.; Beadham, I.; Quilty, B.; Coutinho, J. A. P.; Gathergood, N. *ACS Sustain. Chem. Eng.* **2013**, *1* (4), 393–402.
(479) Roy, K.; Kar, S. In *Quantitative Structure-Activity Relationships in Drug Design, Predictive Toxicology, and Risk Assessment*; IGI Global, 1AD; pp 180–211.
(480) *Molecular Descriptors for Chemoinformatics*; Todeschini, R., Consonni, V., Eds.; Methods and Principles in Medicinal Chemistry; Wiley-VCH Verlag GmbH & Co. KGaA: Weinheim, Germany, 2009; Vol. 41.
(481) O'Brien, S. E.; Popelier, P. L. A. *J. Chem. Soc. Perkin Trans. 2* **2002**, No. 3, 478–483.
(482) and, U. A. C.; Popelier*, P. L. A. *J. Phys. Chem. A* **2003**, *107* (22), 4578–4582.
(483) Roy, K.; Popelier, P. L. A. *J. Mol. Liq.* **2014**, *200*, 223–228.
(484) Everitt, B.; Landau, S.; Leese, M.; Stahl, D. *Cluster Analysis*; Wiley, 2011.
(485) Snedecor, G. W.; Cochran, W. G. *Statistical methods*, 6th ed.; Iowa State University Press: Ames Iowa, 1967.
(486) Wold, S.; Sjöström, M.; Eriksson, L. *Chemom. Intell. Lab. Syst.* **2001**, *58* (2), 109–130.
(487) Rogers, D.; Hopfinger, A. J. *J. Chem. Inf. Model.* **1994**, *34* (4), 854–866.
(488) Darlington, R. B. *Regression and linear models*; McGraw-Hill, 1990.
(489) Gadaleta, D.; Mangiatordi, G.; Catto, M.; Carotti, A.; Nicolotti, O. *Int. J. Quant. Struct. Relationships* **2016**, *1*, 45–63.
(490) MarvinSketch, version 15.12.7, ChemAxon Ltd, 2016, accessible at http://www.chemaxon.com.
(491) Dragon, version 6, TALETE srl, Italy, 2010, accessible at http://www.talete.mi.it/products/dragon_description.htm.
(492) Yap, C. W. *J. Comput. Chem.* **2011**, *32* (7), 1466–1474.
(493) GaussView, 4.1, Semichem Inc.,Gaussian Inc., Pittsburgh, PA, USA, 2003.
(494) Frisch, M.; Trucks, G. W.; Schlegel, H. B.; Scuseria, G. E.; Robb, M. A.; Cheeseman, J. R.; Montgomery Jr., J. A.; Vreven, T.; Kudin, K. N.; Burant, J. C. Gaussian 03, revision D. 01, Gaussian Inc., Wallingford, CT, 2004, vol. 26.
(495) Popelier, P. L. A. *Comput. Phys. Commun.* **1996**, *93* (2), 212–240.
(496) SPSS, version 9.0.0, SPSS Inc., USA, 1998, accessible at http://www.spss.co.in/.
(497) Cerius2, version 4.10, Accelrys Inc., San Diego, CA, USA, 2005, accessible at http://accelrys.com/.
(498) Version 14.13, Minitab, Inc., USA, 2004, accessible at http://www.minitab.com/en-US/default.aspx.
(499) SIMCA-P, version 10.0, Umetrics, UMEA, Sweden, 2002, accessible at http://umetrics.com/.
(500) Lorenzo, M.; Vilas, M.; Verdia, P.; Villanueva, M.; Salgado, J.; Tojo, E. *RSC Adv.* **2015**,

5 (51), 41278–41284.
(501) Pernak, J.; Borucka, N.; Walkiewicz, F.; Markiewicz, B.; Fochtman, P.; Stolte, S.; Steudte, S.; Stepnowski, P. *Green Chem.* **2011**, *13* (10), 2901–2910.
(502) Roy, K.; Das, R. N.; Ambure, P.; Aher, R. B. *Chemom. Intell. Lab. Syst.* **2016**, *152*, 18–33.
(503) Topliss, J. G.; Edwards, R. P. *J. Med. Chem.* **1979**, *22* (10), 1238–1244.
(504) Roy, K.; Ambure, P.; Aher, R. B. *Chemom. Intell. Lab. Syst.* **2016**, (under review).
(505) Alexander, D. L. J.; Tropsha, A.; Winkler, D. A. *J. Chem. Inf. Model.* **2015**, *55* (7), 1316–1322.

Estes anexos só estão disponíveis para consulta através do CD-ROM.
Queira por favor dirigir-se ao balcão de atendimento da Biblioteca.

Serviços de Biblioteca, Informação Documental e Museologia
Universidade de Aveiro